AD-A043 716 ARMY MOBILITY EQUIPMENT RESEARCH AND DEVELOPMENT COMM--ETC F/G 13/2

PROCESS DESIGN FOR TREATING SHOWER WASTEWATER BY ULTRAFILTRATIO--ETC(U)

JUN 77 D S LENT

UNCLASSIFIED MERADCOM-2212 NL

1 OF 2

AD A043716

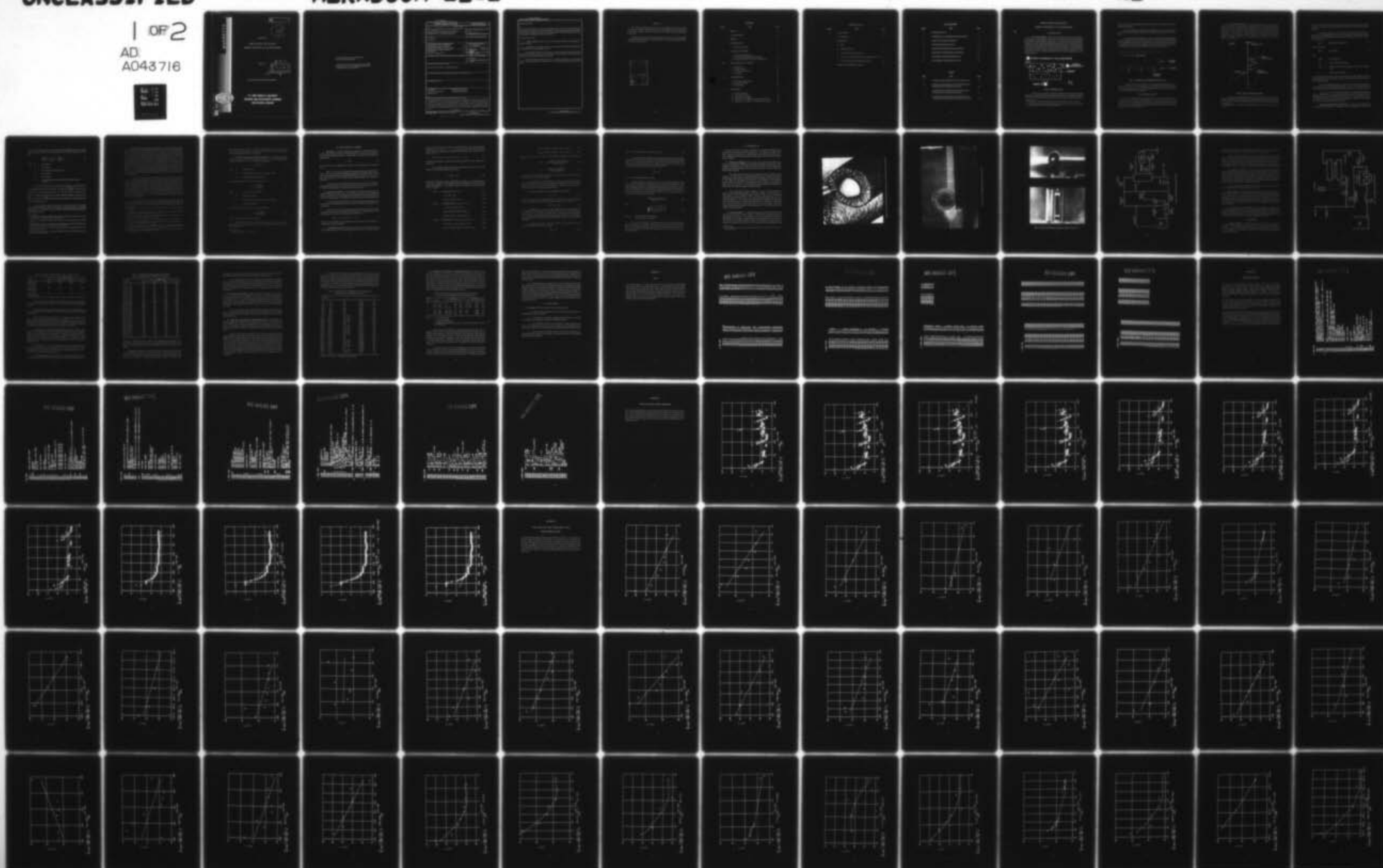

1.0 1.1 1.25 1.4 1.6 1.8 2.0 2.2 2.5 2.8 3.2 3.6 4.0 4.5 5.0 5.6

MICROCOPY RESOLUTION TEST CHART
NATIONAL BUREAU OF STANDARDS-1963-A

12

NW

Report 2212

# PROCESS DESIGN FOR TREATING SHOWER WASTEWATER BY ULTRAFILTRATION

June 1977





U.S. ARMY MOBILITY EQUIPMENT RESEARCH AND DEVELOPMENT COMMAND
FORT BELVOIR, VIRGINIA

UNCLASSIFIED

SECURITY CLASSIFICATION OF THIS PAGE (When Data Entered)

## REPORT DOCUMENTATION PAGE

READ INSTRUCTIONS BEFORE COMPLETING FORM

1. REPORT NUMBER: 2212 (14) MERADCOM-2212

2. GOVT ACCESSION NO.

3. RECIPIENT'S CATALOG NUMBER

4. TITLE (and Subtitle): (6) PROCESS DESIGN FOR TREATING SHOWER WASTEWATER BY ULTRAFILTRATION ,

5. TYPE OF REPORT & PERIOD COVERED: (9) Final rept.,

6. PERFORMING ORG. REPORT NUMBER

7. AUTHOR(s): (10) Daniel S. Lent

8. CONTRACT OR GRANT NUMBER(s)

9. PERFORMING ORGANIZATION NAME AND ADDRESS:
Sanitary Sciences Division, DRDME-GS
Energy & Water Resources Laboratory
MERADCOM, Fort Belvoir, Virginia 22060

10. PROGRAM ELEMENT, PROJECT, TASK AREA & WORK UNIT NUMBERS: (16) 1L762720D048-07 (17) 07

11. CONTROLLING OFFICE NAME AND ADDRESS:
MERADCOM
Fort Belvoir, Virginia 22060

12. REPORT DATE: (11) June 1977

13. NUMBER OF PAGES: 180 (12) 177p.

14. MONITORING AGENCY NAME & ADDRESS (if different from Controlling Office)

15. SECURITY CLASS. (of this report): Unclassified

15a. DECLASSIFICATION/DOWNGRADING SCHEDULE

16. DISTRIBUTION STATEMENT (of this Report)

Approved for public release; distribution unlimited.

17. DISTRIBUTION STATEMENT (of the abstract entered in Block 20, if different from Report)

18. SUPPLEMENTARY NOTES

19. KEY WORDS (Continue on reverse side if necessary and identify by block number)

Ultrafiltration
Concentration Polarization
Boundary Layer
Spiral-Wound Membranes
Hollow-Fiber Membranes

20. ABSTRACT (Continue on reverse side if necessary and identify by block number)

This report investigates curve fitting for the empirical explanation of shower wastewater treatment by ultrafiltration. A two-part model is proposed where, initially, the system is at unsteady state caused by the formation of the boundary layer. Later, the system comes to a steady state when the rates of boundary layer formation and decay reach constant values. The unsteady state portion is described by an exponential equation and the steady state portion is described by a linear equation.

(continued)

DD FORM 1 JAN 73 1473 EDITION OF 1 NOV 65 IS OBSOLETE

UNCLASSIFIED

SECURITY CLASSIFICATION OF THIS PAGE (When Data Entered)

403160

Block 20 (continued):

The model was evaluated on two separate ultrafiltration systems with each system utilizing a different membrane configuration. These configurations were the spiral-wound configuration which fit the model as stated and the hollow-fiber configuration which fit only the unsteady state portion of the model due to daily removal of the boundary layer.

The study concludes that:

a. A single, empirical equation cannot describe permeate production by ultrafiltration of shower wastewater.

b. A model based on unsteady and steady state phenomena of concentration polarization can empirically describe the ultrafiltration process.

c. The hollow-fiber system can be described by a single, empirical equation of exponential order because the system as studied was never allowed to reach steady state. Therefore, the unsteady state equation described the system's operation.

d. The spiral-wound membrane system can be described empirically by an exponential equation during the boundary layer formation and by a linear equation during steady state operation.

## PREFACE

This report was submitted to the Faculty of the College of Arts and Sciences of the American University, Washington, D.C., in partial fulfillment of the requirements for the degree of Master of Science in Chemistry. The material has been copyrighted by the author.

Computer time for this work was partially funded by project no. 1L762720D048, "Environmental Quality Research and Development," 07, "Wastewater Pollution Control," under work unit W-11.

## CONTENTS

CONTENTS (cont'd)

## ILLUSTRATIONS



## TABLES

PROCESS DESIGN FOR TREATING

SHOWER WASTEWATER BY ULTRAFILTRATION

## I. INTRODUCTION

1. **Previous Investigation.** Since the first description of the osmotic pressure phenomenon by Abbe Nollet in 1748, scientists and engineers have been intrigued by the properties of semipermeable membranes.[1] In the past few decades, membrane development has made membrane separation processes practical.[2] As might be expected, membrane processes, particularly the ultrafiltration process which is shown in Figure 1, are playing an increasing role in water and wastewater treatment. The ultrafiltration process depends upon a pressure driving force and a membrane permeable to a component (B) in a liquid solution and impermeable to the other component (A) in the solution (Figure 1).

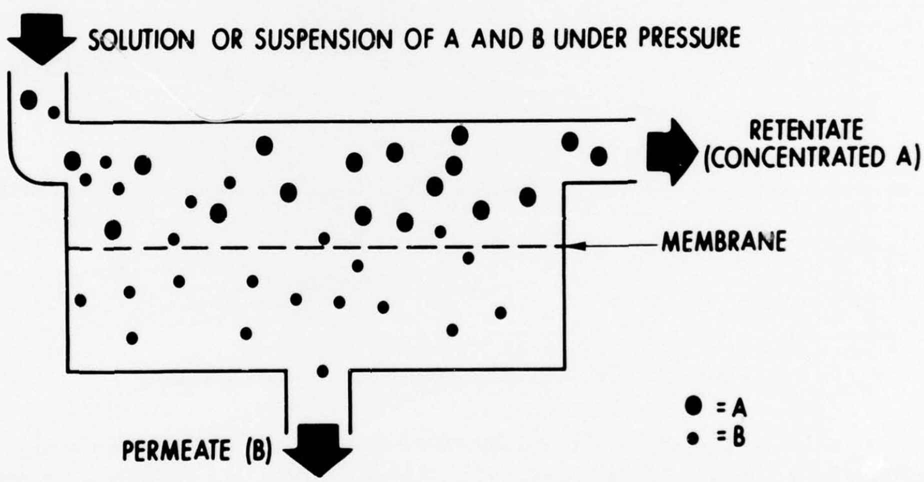


**Figure 1. Ultrafiltration process.**

When used for wastewater treatment, membranes are chosen that will retain impurities to be removed from the waste stream on one side of the membrane and collect water of desired quality from the other side. Therefore, the quality of effluent is

---

[1] F. Daniels and R. A. Alberty. *Physical Chemistry*, 3rd. Ed., John Wiley and Sons, Inc., New York, 1966.

[2] H. C. Gooding. "A Theoretical and Experimental Comparison of Unsteady and Steady State Ultrafiltration in Thin Horizontal Channels." M. S. Thesis, Clemson University, 1972.

fixed as a function of the membrane structure rather than as a function of the system operational parameters.

The most significant variable in the ultrafiltration process is water production expressed as flux with the units of flow (volume) per unit membrane area per unit time.

System optimization, therefore, is done by maximizing flux and minimizing the rate of decline of flux. This flux decline is due, in part, to a concentration buildup of the impermeable portion of the bulk solution at the membrane surface (concentration polarization). The system is configured as shown in Figure 2 with the bulk solution velocity parallel to the membrane surface, thus, reducing this buildup.

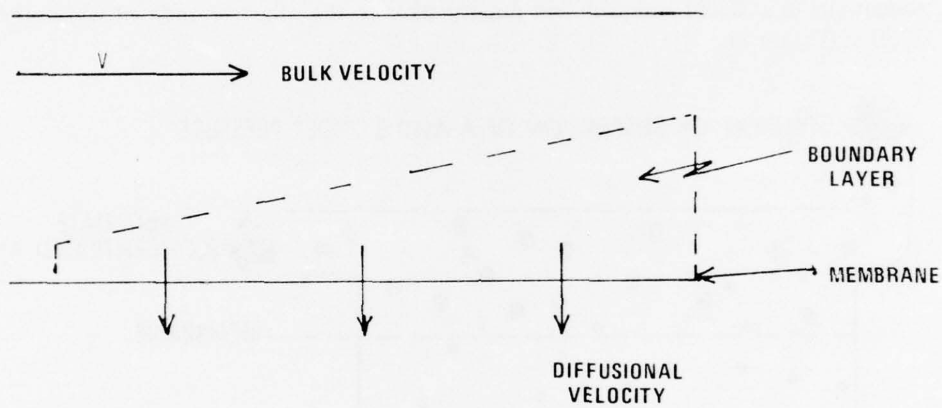


**Figure 2. Configuration of an ultrafiltration membrane system.**

The purpose of this investigation is to develop a mathematical model that describes the treatment of shower wastewater by ultrafiltration. The model is developed using transport principles for a general ultrafiltration system and is then used to evaluate actual ultrafiltration-system operation.

## II. LITERATURE REVIEW

The two membrane-separation processes that use a pressure gradient across a membrane are reverse osmosis and ultrafiltration. They differ in that the solute and solvent molecular dimensions in reverse osmosis are generally of the same order of magnitude; whereas, in ultrafiltration the solute molecular diameters are at least ten times greater than the solvent molecular size.

2. **Concentration Polarization.** In a continuous operation of reverse osmosis or ultrafiltration systems, a phenomenon commonly referred to as concentration polarization often represents the rate major/rate controlling step.[3] Concentration polarization is described as the accumulation of nontransferred solute in the boundary layer of the membrane as shown in Figure 3. This phenomenon is the result of the concentration of the solute at the membrane surface. As the solute concentrates, a concentration gradient is established resulting in a back diffusion of the solutes and reducing the transport of the solvent.

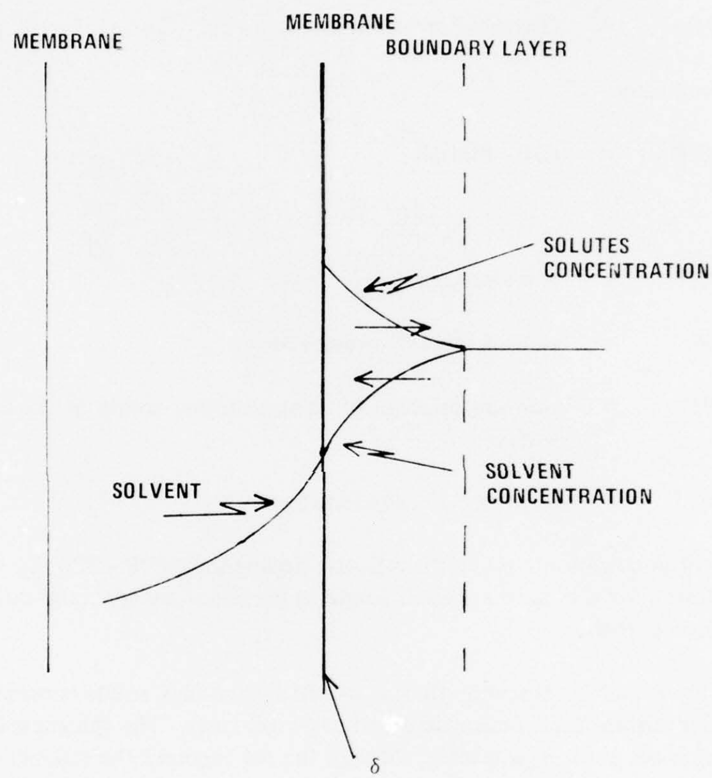


**Figure 3. Causes of concentration polarization.**

Solute may be transported away from the membrane surface by molecular diffusion perpendicular to the membrane (lateral direction) and by forced convection of the stream flow parallel to the membrane (axial direction). Eventually, steady state

---

3 N. Lakshiminarayanaiah. "Transport Phenomena in Artificial Membranes," *Chem. Reviews*, 65, No. 5, 491-565 (1965).

is achieved; and the rate of transport of solute to the membrane surface becomes equal to the rate of transport away from the surface if the process input variables remain unchanged.

Concentration polarization can have two detrimental effects on the mass-transfer rate in an ultrafiltration or a reverse osmosis system. The first detrimental effect is seen by considering the familiar equation relating mass-transfer rate, driving force, and resistance:

$$\text{Rate} = (\text{Driving Force})/(\text{Resistance}), \tag{1}$$

or, more specifically:

$$\text{MTR} = (\text{DP} - \text{PIM})/\text{R} \tag{2}$$

where:

MTR = mass-transfer rate

DP = transmembrane pressure drop

PIM = osmotic pressure of nontransferred solute at the membrane surface

R = resistance to mass transfer.

Concentration polarization reduces the effective driving force (DP – PIM) by increasing the concentration of the nontransferred solute in the boundary layer and thus increasing the osmotic pressure.

The second detrimental effect is caused by the high solute concentration at the membrane surface precipitating and forming a gel layer. The thickness of this gel layer will increase until mass transfer through the gel becomes the rate-limiting step.

In any event, once concentration polarization is controlling, increasing the pressure, or driving force, on the system will not increase the mass-transfer rate. The higher pressure causes a thicker layer of gel and, hence, a greater resistance to flow. The goal in process design is, therefore, to minimize the thickness of the boundary layer where concentration polarization takes place.

3. **Theoretical Studies of Mass-Transfer Rate.** In 1965, Brian developed a theoretical model for predicting the mass-transfer rate in a parallel-plate, reverse osmosis

system.[4] His model involved a numerical solution of a simplified version of the steady state equation of continuity of the nontransferred solute. Brian's equation is as follows:

$$\frac{\partial(U \cdot C)}{\partial X} + \frac{\partial}{\partial Y}\left(VC - \frac{D\partial C}{\partial Y}\right) = 0 \qquad (3)$$

where:

| | | | |
|---|---|---|---|
| | U | = | axial velocity |
| | X | = | axial distance |
| | C | = | concentration in the liquid stream |
| | Y | = | lateral distance |
| | V | = | lateral velocity |
| | D | = | effective diffusivity or reciprocal Peclet Number at initial conditions |

The terms in Equation (3) are in direct correspondence with the theory of concentration polarization discussed earlier. The first term, $\frac{\partial(U \cdot C)}{\partial X}$, represents forced convection of solute axially through the cell. The first part of the second term, $\frac{\partial}{\partial Y}(V \cdot C)$, indicates bulk convection of solute toward the membrane; and the second part of the second term, $\frac{D\partial C}{\partial Y}$, represents molecular diffusion of rejected solute away from the membrane surface.

In related studies, Brian,[5] Sherwood, *et al.*,[6] and Gill, *et al.*[7] [8] developed slightly different models modifying the boundary conditions and solution techniques of Equation (3). Unfortunately, none of the studies included experimental verification of the predicted results.

---

4 P. L. T. Brian. "Concentration Polarization in a Reverse Osmosis Desalination with Variable Flux and Incomplete Salt Rejection," *Ind. Eng. Chem. Fund.*, 4, 439-45 (1965).

5 P. L. T. Brian. "Concentration Polarization in a Reverse Osmosis System," *Ind. Eng. Chem. Fund.*, 5, 148-149 (1965).

6 T. K. Sherwood, P. L. T. Brian, R. E. Fisher, and L. Dresher. "SaH Concentration of Phase Boundaries in Desalination by Reverse Osmosis," *Ind. Eng. Chem. Fund.*, 4, 113-18 (1965).

7 W. N. Gill, C. Tien, and D. W. Zeh. "Boundary Layer Effects in Reverse Osmosis Desalination," *Ind. Eng. Chem. Fund.*, 5, 367-70 (1966).

8 W. N. Gill, C. Tien, and D. W. Zeh. "Concentration Polarization Effects in a Reverse Osmosis System," *Ind. Eng. Chem. Fund.*, 4, 433-39 (1965).

With the increasing interest in the application of membrane-separation processes, several theoretical and experimental methods of reducing concentration polarization effects have been studied. Sherwood, *et al.*[9] performed an experimental and theoretical investigation of a rotating, cylindrical, reverse osmosis apparatus for desalination and obtained partial confirmation of their previously developed theory.[10] Rotation of the membrane resulted in total flux increases of approximately 10 percent. Zeh and Gill[11] published a theoretical model of a rotating-disk system, implying but not quantitatively reporting the beneficial effects of rotation on the mass-transfer rate. Increased velocities in laminar flow are also known to decrease concentration polarization by creating greater shear rates, and turbulent flow adds the mechanism of eddy mixing. With the highly permeable membranes available today, the fluid velocities required to significantly reduce concentration polarization become very large, and energy consumption and fluid recirculation rates required to achieve reasonable recovery become prohibitive.[12]

Tien and Gill[13] theoretically investigated the use of impermeable "relaxation sections" to induce axial diffusion of the nontransferred solute, but their predictions indicated only a small increase in the steady state flux obtainable with an equivalent, entirely permeable area. Huffman[14] studied the effect of natural convection on concentration polarization by using a horizontal, parallel-plate ultrafilter. He operated a single membrane, first in the lower position and then in the upper position, and obtained semitheoretical correlations for his forced-only and forced-plus-natural convection data. The study demonstrated that natural convection effects can increase the steady state, mass-transfer rate by as much as 200 percent over comparable conditions with forced convection only.

In 1972, Gooding[15] experimentally validated his dynamic model of forced-convection ultrafiltration in thin, horizontal channels which requires a numerical solution of the unsteady state continuity equation for the nontransferred solute. He

---

9 T. K. Sherwood, P. L. T. Brian, and R. E. Fisher. "Desalination by Reverse Osmosis," *Ind. Eng. Chem. Fund.*, 6, 2-12 (1967).

10 T. K. Sherwood, P. L. T. Brian, R. E. Fisher, and L. Dresher. "Self Concentration of Phase Boundaries in Desalination by Reverse Osmosis," *Ind. Eng. Chem. Fund.*, 4, 113-18 (1965).

11 D. W. Zeh and W. N. Gill. "Convective Diffusion in Rotating Disk Systems with an Imperfect Semi-permeable Interface," *Amer. Inst. Chem. Eng. Journal*, 14, 715-19 (1968).

12 A. S. Michaels. "New Separation Technique for the CPI," *Chem. Eng. Prog.*, 64, No. 12, 31-43 (1968).

13 C. Tien and W. N. Gill. "The Relaxation of Concentration Polarization in a Reverse Osmosis Desalination System," *Amer. Inst. Chem. Eng. Journal*, 12, 722-27 (1966).

14 W. J. Huffman. "The Effect of Forced End Natural Convection During the Ultrafiltration of Protein-Saline Solutions in Thin, Horizontal Channels," *PhD Dissertation*. Clemson University Library, Clemson, S.C. (1970).

15 H. C. Gooding. "A Theoretical and Experimental Comparison of Unsteady and Steady State Ultrafiltration in Thin Horizontal Channels." *M.S. Thesis*, Clemson University (1972).

then used this model to study the possibility of improving mass transfer by using some form of unsteady state operation. Higher fluxes were predicted by the model but were not experimentally achieved in his investigation.

4. **Practical Considerations of Permeate Production.** The details of the derivation of the practical equation of concentration polarization control of ultrafiltrate flux have been worked out by others.[16] Simply, the relationship is:

$$F = K \ln (C_g/C_b) \tag{4}$$

where: $F$ = ultrafiltration flux

$C_g$ = concentration of the gel at the membrane surface

$C_b$ = concentration of the bulk stream

The mass-transfer coefficient is defined in laminar flow as:

$$K = \frac{V^{0.33}\ D^{0.67}}{h^{0.33}\ L^{0.33}} \tag{5}$$

where: $V$ = velocity along the membrane

$D$ = diffusivity of solvent

$h$ = height of the channel in which the fluid is flowing

$L$ = length of the channel.

In turbulent flow, the mass-transfer coefficient is defined as:

$$K = \frac{V^{0.75}\ D^{0.67}}{h^{0.25}\ \nu^{0.42}} \tag{6}$$

where $\nu$ = the kinematic viscosity of the fluid.

While these equations are useful in the predication of effects of channel height and length on flux, prediction of actual system operation for wastewater treatment is not possible.

---

[16] S. Messinger, "Ultrafiltration – A New Process Tool."

## III. DEVELOPMENT OF THEORY

5. **Background.** A mathematical function is defined as a relationship between a set of x values associated with the independent variable, x and a set of y values associated with the dependent variable, y. Symbolically, we described this mathematical relationship by:

$$y = f(x). \tag{7}$$

The function can also be displayed by a graph, or curve, depicting a set of data pairs (x, y).

When we are given a mathematical equation describing a relationship between x and y, a curve corresponding to this relationship can be easily plotted. On the other hand, when dealing with experimental information, the opposite is true. From a given set of points (x, y), we try to find a function which generates a curve fitting these data points.

For the purpose of this study, all functions are assumed to be continuous. This means that for every value of x in an interval (a, b) there is a unique value for $y = f(x)$ and that a small change in x produces only a small change in y.

6. **General Curve Fitting.** In technological applications, measurements are usually made of one quantity while a second quantity is varied with the results being plotted in graphical form. The problems lie in not being able to make measurements at every point of interest and the possibility of measurement error in the measurements.

To overcome these problems and to be able to represent the results in a compact manner, the experimenter often tries to fit the experimental measurements to a smooth curve.

The form of the curve selected will of course depend upon the type of measurements being made and the system under investigation. A standard function often used to represent a curve is a polynomial function of the form:

$$f(x) = a_o + a_1 x + a_2 x^2 + \ldots . a_u x^u. \tag{8}$$

The shape of the resulting curve depends both upon the value of the coefficients, a, and the degree of the polynomial, u.

7. **Least-Squares Curve Fit.** While trying to fit a curve to a set of data points, it is not possible to have the curve pass through each point. The most desirable condition

is the curve coming as close as possible to all the data points. If the set of data points is denoted as $(x_1, y_1), x_2, y_2), \ldots\ldots (x_v, y_v)$, where $x_i$ is the value of the independent variable when the measurement $y_i$ was made, then the distance of the i data point from the curve f(x) is:

$$d_i = y_i - f(x_i) = y_i - (a_0 + a_1 x_i + a_2 x_i^2 + \ldots a_u x_i^u. \tag{9}$$

This distance represents the "error" between the value given by the curve and the measured value.

The common formula that measures the difference between the curve and the data is the sum of the squared errors. That is:

$$C = \sum_{i-1}^{n} y_i - f(x_i)^2 . \tag{10}$$

To minimize the total error, the coefficients of a through $a_u$ are selected in such a manner as to minimize C. This function, having the smallest C value, is called a least-squares approximation. The conditions that must be satisfied are shown as follows for u = 1, 2, and 3:

Case 1: u = 1 Linear fit, $f(x) = a_0 + a_1 1x$: (11)

$$a_0 v + a_1 \Sigma x_i = \Sigma y_i \tag{12}$$

$$a_0 \Sigma x_i + a_1 \Sigma x_i^2 = \Sigma x_i y_i. \tag{13}$$

Case 2: u = 2 Quadratic fit, $f(x) = a_0 + a_i y_i + a_2 x_i^2$ (14)

$$a_0 + a_1 \Sigma x_i + a_2 \Sigma x_i^2 = \Sigma y_i \tag{15}$$

$$a_0 \Sigma x_i + a_1 \Sigma x_i^2 + a_2 \Sigma x_i^3 = \Sigma x_i y_i \tag{16}$$

$$a_0 \Sigma x_i^2 + a_1 \Sigma x_i^3 + a_2 \Sigma x_i^4 = \Sigma x_i^2 y_i \tag{17}$$

Case 3: u = 3 Cubic fit, $f(x) = a_0 + a_1 x_i + a_2 x_i^2 + a_3 x_i^3$ (18)

$$a_0 + a_1 \Sigma x_i + a_2 \Sigma x_i^2 + a_3 \Sigma x_i^3 = \Sigma y_i \tag{19}$$

$$a_0 \Sigma x_i, + a_1 \Sigma x_i^2 + a_x \Sigma x_i^3 + a_3 \Sigma x_i^4 = \Sigma x_i y_i \tag{20}$$

$$a_0 \Sigma x_i^2 + a_1 \Sigma x_i^3 + a_2 \Sigma x_i^4 + a_3 \Sigma x_i^5 = \Sigma x_i^2 y_i \tag{21}$$

$$a_0 \Sigma x_i^3 + a_1 \Sigma x_i^4 + a_2 \Sigma x_i^5 + a_3 \Sigma x_i^6 = \Sigma x_i^3 y_i . \tag{22}$$

These cases, in turn, can be solved for the different coefficients of a as shown in Case 1:

$$\text{Case 1:} \quad a_0 = \frac{(\Sigma y_i)(\Sigma x_i^2) - (\Sigma x_i y_i)(\Sigma x_i)}{(\Sigma x_i^2) - (\Sigma x_i^2)} , \tag{23}$$

$$\text{and} \quad a_1 = \frac{v(\Sigma x_i y_i) - (\Sigma x_i)(\Sigma y_i)}{(\Sigma x_i^2)(\Sigma x_i^2)} . \tag{24}$$

Or, more simply, the simultaneous equations can be solved directly by the method of elimination or by the use of determinants.

It can readily be seen that the higher the value of u the better the probable curve fit for nonlinear data. It can also be seen that the higher the value of u the more difficult it will be to solve for the coefficients of a. Therefore, other functions are tried and compared with results from polynomial fits.

One function considered is an exponential function as follows:

$$Y = ae^{bx} . \tag{25}$$

At first, this appears to be a difficult function to work with; however, by taking the $\ell n$ of both sides its form becomes a linear function similar to Case 1 as shown:

$$\ell n\, Y = \ell n\, a + b\, x . \tag{26}$$

8. **Correlation.** Once a curve or a line is fitted to the data, the next problem is to determine how well the data is actually fitted by the curve. A fair idea is gained by inspection of the curve and the data points; however, usually a more objective evaluation is required. In studying the data, an assessment must be made of the probability of random variables rather than the independent variable contributing to the variability of the data.

Essentially, the problem is analysis of variance; and the quantity to be analyzed, the total sum of the squares, is given by:

$$\sum_{i=1}^{n} (y_i - y)^2 \tag{27}$$

where: $y$ = the mean of the y values given by $\bar{y} = \sum_{i=1}^{n} y_i$. (28)

If the independent variable were the only thing that affected the dependent variable, the data points would all fall on a straight line assuming a linear relationship. Since this is rarely true, other factors do tend to affect the dependent variable. The variation caused by these other factors is usually measured by the sum of the squares of the vertical deviations from the point to the line given by:

$$\sum_{1=1}^{n}(y_i - y')^2 \tag{29}$$

where y = the individual, predicted y values.

This is identical to equation (10) or $f(x_i)$. The difference betweeen equations (27) and (29) measures the variation of the y's that can be attributed to x. This value divided by equation (27) gives the proportion of the total value of the y's, or dependent variable, that can be attributed to the relationship with x and is called the coefficient of determination. The square root is called the coefficient of correlation with the sign of this being the same as that of the coefficient, b, in the equation of the least-squares line. These equations are as follows:

$$r^2 = \frac{\Sigma(y_i) - y)^2 - \Sigma(y_i - y')^2}{\Sigma(y_i - \bar{y})}, \tag{30}$$

and

$$r = \sqrt{\frac{\Sigma(y_i - y)^2 - \Sigma(y_i - y')^2}{\Sigma(y_i - \bar{y})^2}} \tag{31}$$

where $r^2$ = the coefficient of determination

$r$ = the coefficient of correlation.

The value of r is the most widely used measure of the strength of the linear relationship between two variables. It indicates the goodness of fit of a line or curve fitted by the method of least squares and this, in turn, tells whether or not it is reasonable to say that a linear relationship (correlation) exists between the dependent and independent variables.

## IV. EXPERIMENTAL

Data for this study came from a Department of Transportation (DOT) report dealing with the renovation of shower wastewater.[17] The purpose of the DOT report was to evaluate the effectiveness of ultrafiltration for the renovation of shower wastewater. Different membranes and membrane configurations were utilized on the various treatment systems.

9. **Membrane Configuration.** The current study evaluated two different systems using two different membranes in two different membrane configurations. These membrane configurations were hollow-fiber and spiral-wound. Both configurations employ minimal channel height which according to equations (5) and (6) increases the mass-transfer coefficient.

The hollow-fiber membrane module contains 660 fibers of 0.045-inch bore diameter. Each fiber consists of a copolymer support with the noncellulosic membrane approximately 10.0 microns in thickness coated on the inside of this support (Figure 4). The fibers are encapsulated at both ends in a 3-inch-diameter by 25-inch-long, plastic cartridge. An end view of the cartridge is shown in Figure 5. The total membrane area is 15 square feet. The feed stream of raw wastewater flows through the inside of the fibers, and the permeate collects in the shell.

The spiral-wound membrane consists of a sheet 22 inches wide with a support backing and 0.030-inch-thick vexar spacer material. This entire system is then rolled in a jelly roll fashion around a permeate collection tube. Wastewater passes through the channel made by the vexar spacer material which also serves as a turbulence promoter. The permeate passes through the membrane and is channeled by the support material to the permeate collection tube. Wastewater, called waste brine, exits the end of the channel made by the vexar spacer material. The module contains approximately 30 square feet of membrane area. End and side views of the module are shown in Figure 6.

10. **System Description.** A simplified flow diagram of the hollow-fiber system operated in batch mode is shown in Figure 7. The wastewater is pumped from a feed tank through a bag prefilter. The ultrafiltration system is operated at a pressure of approximately 15 psig and an influent flow rate of 16 gallons per minute at a velocity of 6 feet per second. While permeate is collected in the shell of the module, the concentrate is recirculated to the feed tank. The system also had the capability of being

[17] D. S. Lent, "Renovation of Waste Shower Water by Membrane Filfration," Interim Report, U.S. Department of Transportation (1977).

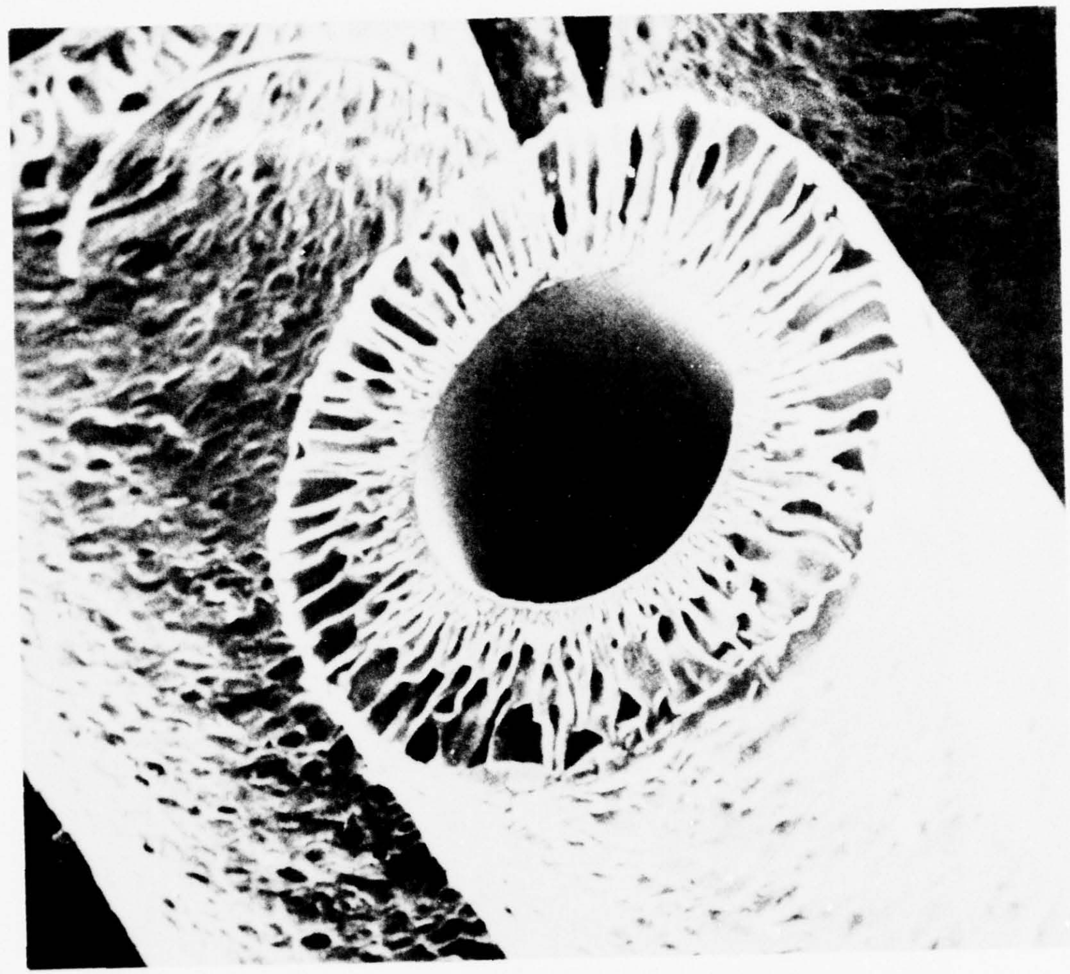

Figure 4. Photomicrograph of hollow fiber showing membrane coated on the inside of a porous support.

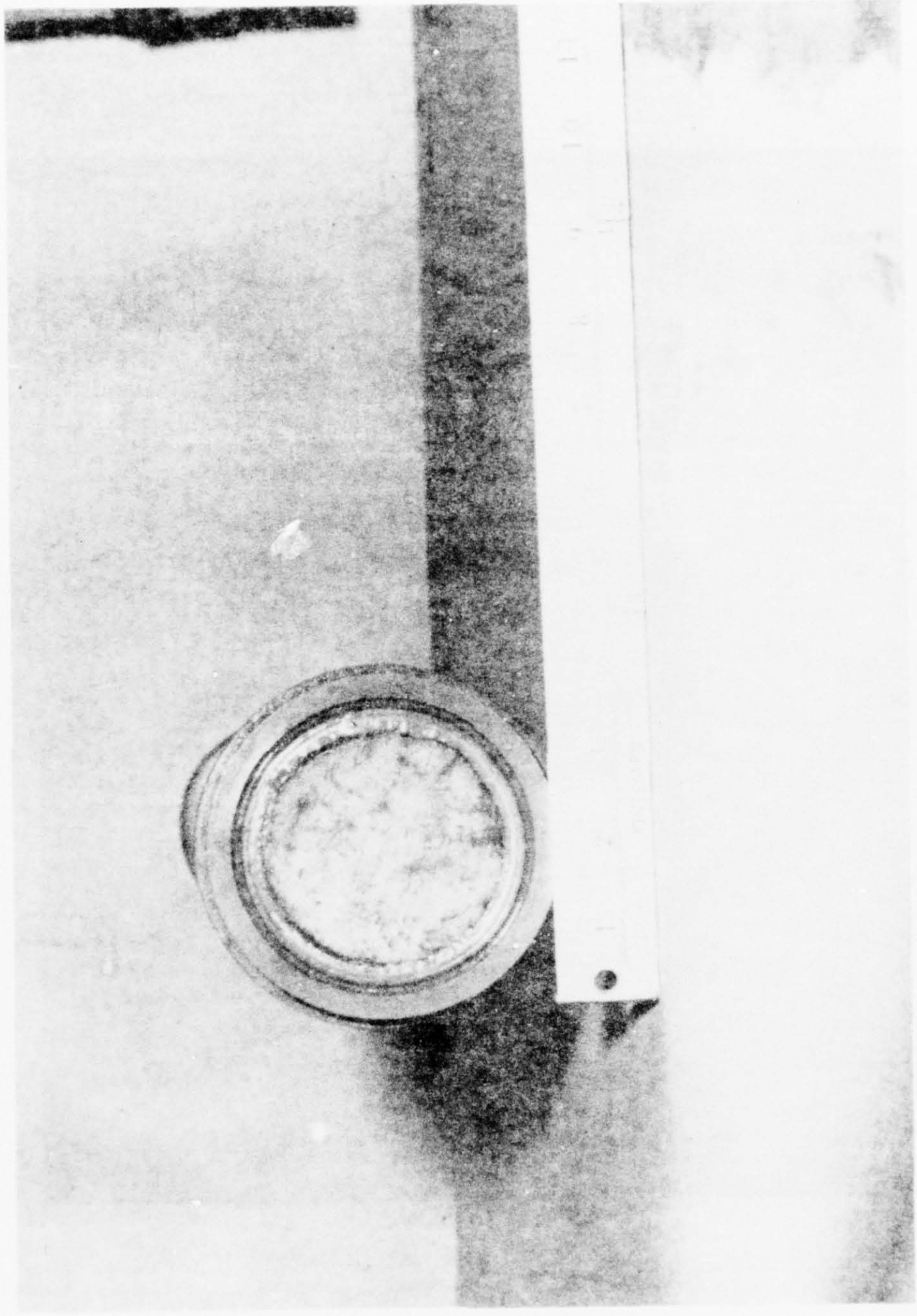

Figure 5. Hollow-fiber ultrafiltration membrane module (end view).

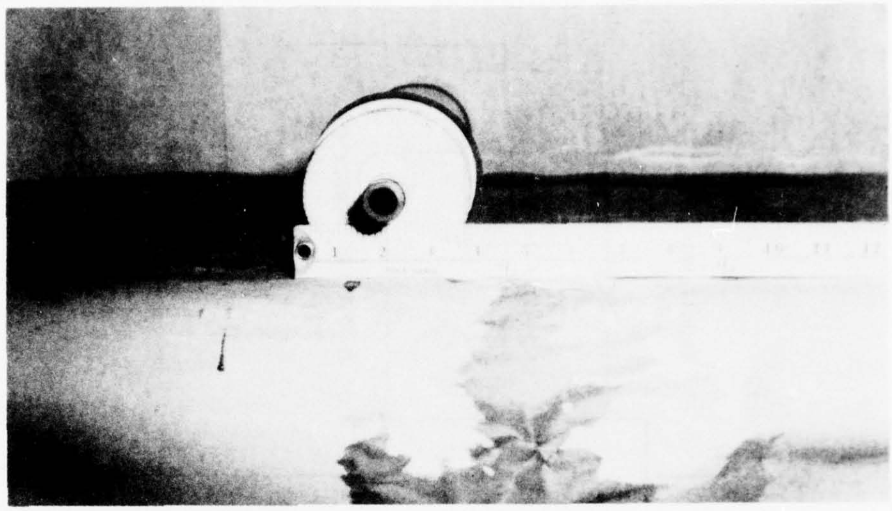

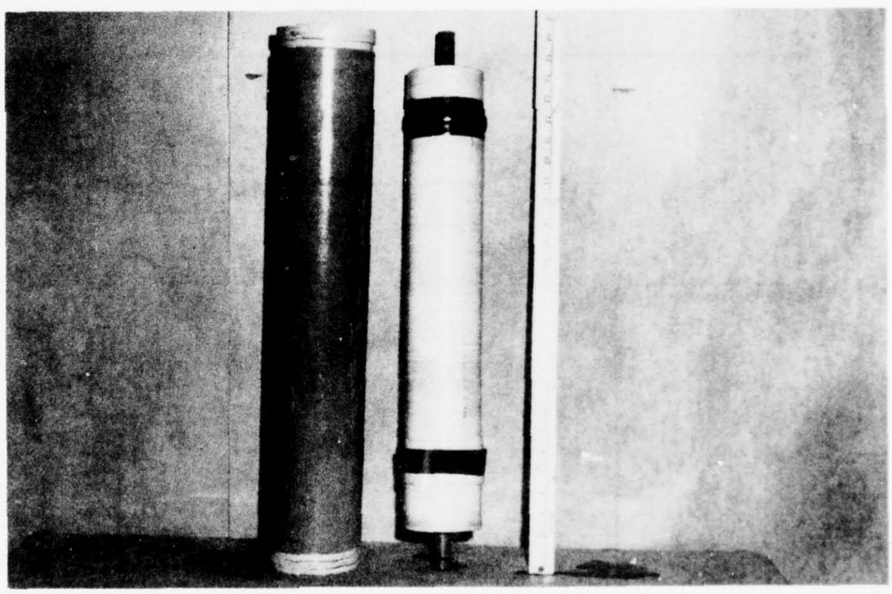

Figure 6. Spiral-wound ultrafiltration membrane module (end and side views).

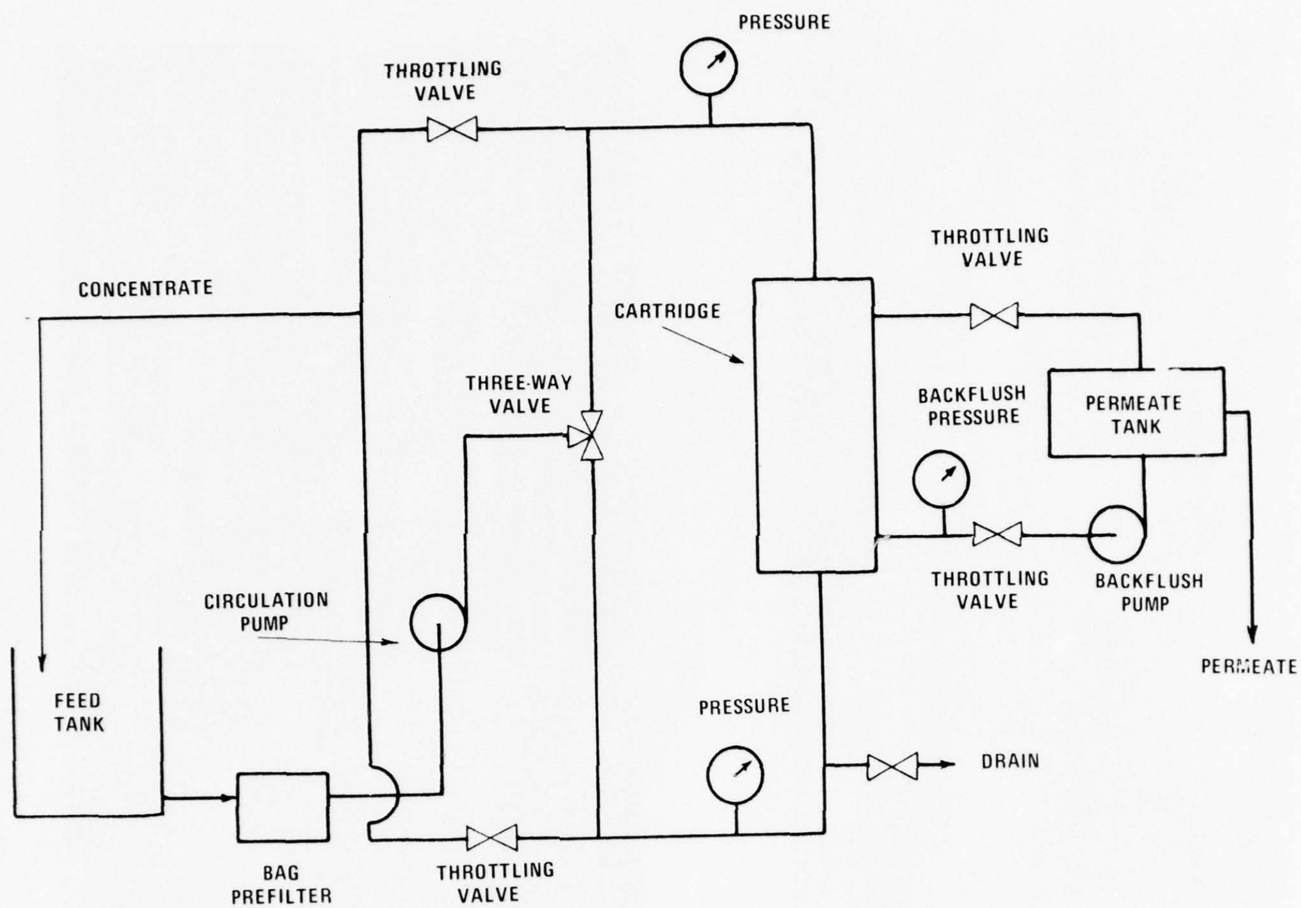


Figure 7. Flow diagram of the hollow-fiber system.

backflushed which allows the permeate to be pumped from the outside of the fiber to the inside, thus displacing any gel layer buildup on the membrane surface.

Daily operation consisted of 6 to 8 hours of continuous operation. Following the end of each day's run, the system was backflushed with about 20 gallons of permeate. On the following day, the direction of flow through the cartridge was reversed, thus eliminating any buildup of particulate material at the head or entrance, of the membrane module. The system concentrates a tank of waste to about 15 percent of its original volume. The tank is then dumped and refilled with fresh wastewater.

A simplified flow diagram of the system with the spiral-wound membrane configuration operated in feed and bleed mode is shown in Figure 8. Wastewater is pumped through two prefilters into the circulation pump which maintains the velocity in the circulation loop. Within the circulation loop, two membrane cartridges are connected in series. The flow rate in the loop is 10 to 15 gallons per minute. Concentrate from within the circulation loop is purged via a solenoid valve operated periodically to maintain the desired degree of concentration in the loop.

This system was also operated 6 to 8 hours daily. The degree of concentration maintained in the loop is approximately 98 percent.

11. **Data Analysis.** Two hundred and twenty-two hours of operational data for the hollow-fiber system and 118 hours of data for the spiral-wound system were analyzed. Data analysis was then performed on the first 118 hours of data from the hollow-fiber system to give an equal time base for system comparison. The data for the hollow-fiber system was then analyzed on a daily basis because at the end of each day's run the system was backflushed or cleaned causing a significant increase in permeate production.

The data analysis consists of first, second, and third-order polynomial curve fits and an exponential curve fit. The analysis was performed on a Control Data Corporation 6600 Computer using a Tektronix 4014 Graphics Terminal. The analysis consists of a scatter gram plot of the data, a curve generated to best fit the data, the equation of the curve, and the square of the multiple-correlation coefficient.

## V. DISCUSSION

12. **Analysis of Results.** Experimental values used in this study are shown in Appendix A. The computer program used for the data analysis is shown in Appendix B. Table 1 gives the coefficients of determination for various orders of fit. Table 2 gives the coefficients of determination for the time periods between backflushes for the hollow-fiber system.

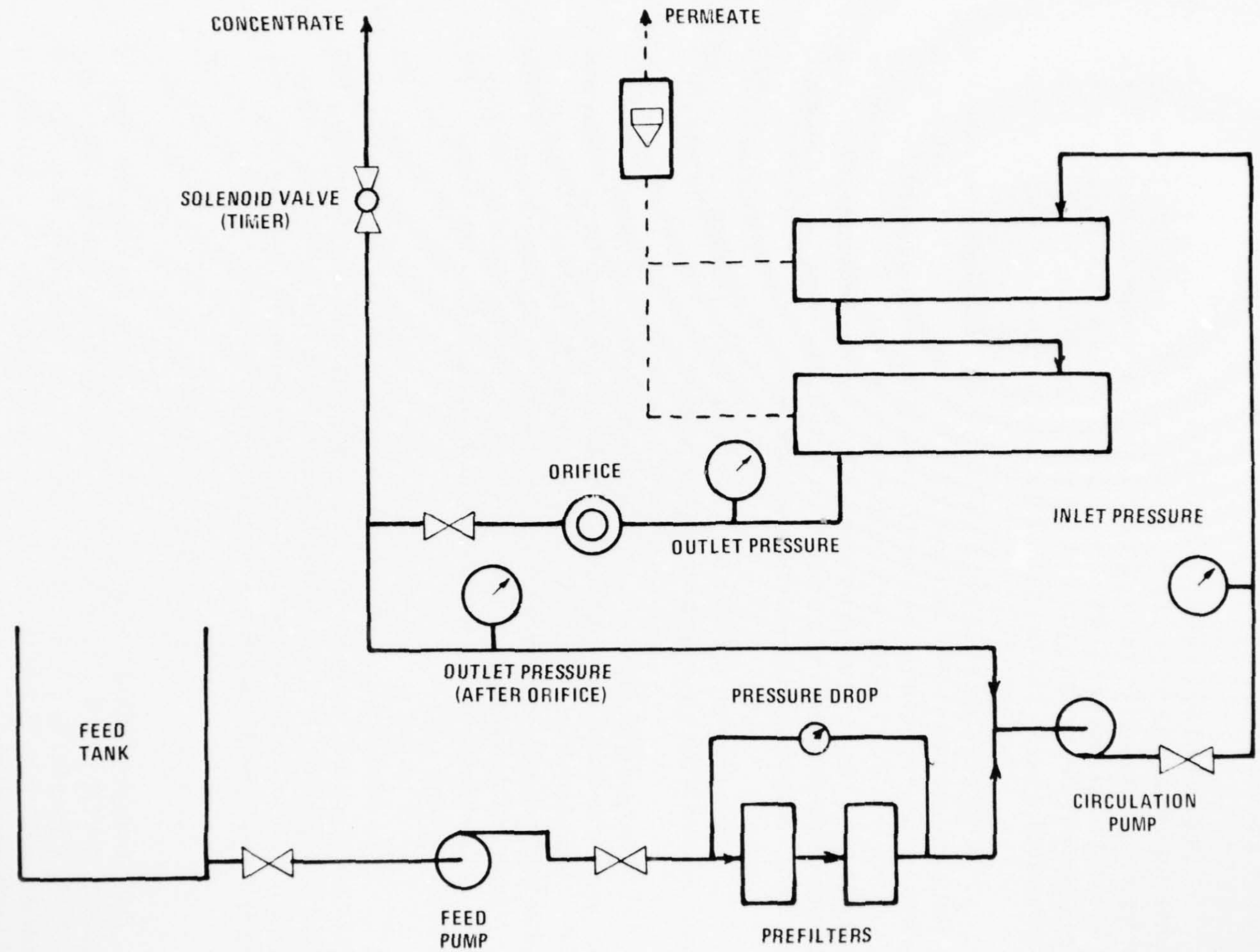

Figure 8. Flow diagram of the spiral-wound system.

Table 1. Coefficients of Determination for Various Orders of Fit

| System | Order of Fit | | | |
|---|---|---|---|---|
| | 1st | 2nd | 3rd | L |
| Hollow-Fiber, All (222 Hr) | .026 | .201 | .302 | .015 |
| Hollow-Fiber, Part (118 Hr) | .350 | .514 | :732 | .415 |
| Vexar Spiral-Wound (118 Hr) | .501 | .837 | .944 | .677 |

Results of the runs performed on the total data for both systems are shown in Appendix C along with the results for 118 hours of operation on the hollow-fiber system.

Appendix D contains the daily, segmented, or between-backflushing, data for the hollow-fiber system. Appendix E contains segmented, fitted data for the spiral-wound system.

Table 1 shows that the best curve fits are obtained with third-order polynomials. Thus, the general, best-fit equation is of the form $Y = a\,x^3 + b\,x^2 + c\,x + d$. This is further demonstrated in Table 2 where once again third-order polynomials give the best fit. The trend for best fits shows that second-order fits follow in fitting the data, followed by exponential fits, followed by a first-order, or linear, fit.

Examination of the graphs for the total data in Appendix C, however, shows that the curves generated by second- and third-order polynomials describe unrealistic results. The second-order fits in all cases show a maximum, a minimum, and then a maximum. This contradicts the phenomenon of concentration polarization described earlier in that the boundary-layer accumulation would have to increase to a point (causing a decrease in flux) then decrease at approximately the same rate (causing an increase in flux).

The third-order fits go one step further from the maximum/minimum/maximum and add a minimum. It is possible for the flux to decrease and increase; however, the rate of increase is always rapid and is achieved when the boundary gel layer is suddenly removed either naturally or by cleaning.

The empirical model, therefore, would be an equation of high order; thus, by having the predicted equation oscillate above and below the data enough times, the

Table 2. Coefficients of Determination for Time Periods Between Backflushings for the Hollow-Fiber System

| Segment | Order of Fit | | | |
|---|---|---|---|---|
| | 1st | 2nd | 3rd | L |
| 0 to 8.6 | .720 | .927 | .972 | .827 |
| 8.6 to 15.4 | .830 | .983 | .989 | .861 |
| 15.4 to 19.6 | .796 | .923 | .925 | .792 |
| 20.2 to 44.2 | .870 | .917 | .958 | .901 |
| 44.9 to 48.9 | .453 | .555 | .599 | .456 |
| 52.2 to 60.0 | .779 | .926 | .932 | .782 |
| 59.9 to 90.7 | .867 | .923 | .973 | .910 |
| 91.4 to 95.3 | .657 | .849 | .915 | .710 |
| 98.4 to 100.3 | .997 | 1.000 | 1.000 | 1.000 |
| 101.5 to 104.9 | .808 | .946 | .994 | .863 |
| 106.1 to 114.1 | .480 | .573 | .584 | .555 |
| 115.6 to 122.9 | .004 | .020 | .234 | .007 |
| 124.0 to 130.1 | .697 | .876 | .880 | .684 |
| 130.6 to 136.9 | .894 | .978 | .978 | .908 |
| 137.9 to 145.1 | .781 | .943 | .945 | .785 |
| 145.1 to 150.4 | .885 | .887 | .931 | .898 |
| 150.6 to 157.3 | .654 | .896 | .929 | .682 |
| 157.7 to 164.8 | .291 | .782 | .896 | .286 |
| 164.8 to 170.5 | .456 | .506 | .593 | .455 |
| 171.3 to 176.1 | .802 | .843 | .971 | .815 |
| 176.3 to 184.5 | .954 | .967 | .971 | .969 |
| 185.3 to 190.9 | .732 | .734 | .895 | .721 |
| 192.3 to 199.6 | .580 | .940 | .995 | .585 |
| 200.2 to 207.6 | .213 | .213 | .834 | .207 |
| 208.1 to 215.7 | .539 | .769 | .831 | .543 |
| 216.5 to 222.4 | .840 | .851 | .923 | .723 |

equation very nearly fits the line. However, the problems with this would be the large number of constants needed to define the equation and the computation of the constants. Therefore, without the data, prediction of any results would be purely arbitrary.

13. **Proposition of Theory.** Consideration of the actual system dictates that initially or early in the run the system is at unsteady state. This is true because at time zero there is no boundary layer present which is evident by observing the initial, rapid rate of flux decline which is proportional to the rate of buildup of boundary layer.

This buildup is directly proportional to the solute concentration because almost all of the solute removed from the waste stream is forming the boundary layer.

As the boundary layer develops, the transport of material from the boundary layer to the bulk solution begins to be the controlling factor for permeate production. The amount of this lateral diffusion is more proportional to the system's design and operational parameters than to the solute concentration. This, of course, is true only under the assumption that permeate production is proportional to the amount of boundary layer.

14. **Proposition of the Model.** Under this premise, a two-part model was tried. The first part would cover the unsteady state condition of rapid flux decline and the second part would cover the condition where diffusion away from the membrane is the controlling factor. A more detailed approach would also consider the transition period where permeate production is a function of both parts. However, since specific boundaries for this transition state would be very hard to establish, the two-part model was chosen.

The general procedure for using the model is to visually inspect the complete plots of the data and the data itself. Then, the data is separated into two portions which tentatively satisfy the conditions of the model and perform curve fits on both portions of the data.

15. ***Application of the Model to the Hollow-Fiber System.*** Examination of the plots and data of the hollow-fiber system in Appendices A and C fails to reveal the two parts described earlier. What the examination does reveal, however, are many segments, each exhibiting a rapid rate of flux decline with varying degrees of flux recovery between each segment. Therefore, it appears that this system's data does not fit the model.

However, when the daily operation of the system is considered, it is clear that the data does fit the model. This is true because each day the system was backflushed. This operation consisted of pumping permeate backward through the membrane thus removing the boundary layer. Since the boundary layer was removed each day, it never had a chance to build up enough to become the controlling factor in permeate production. Therefore, the system was always in an unsteady state condition, and only the first portion of the model should be applied to the system's data. Verification of the model consisted of segmenting the data into time periods between backflushes and then performing curve fits. The coefficients of determination for the fitted curves are shown in Table 2, and the actual, fitted curves are graphically shown in Appendix D.

A comparison of the coefficients of determination from the entire run and the first 118 hours of the run with the coefficients from the segmented data shows much better correlation with the segmented data. Review of the second- and third-order plots in Appendix D also shows these plots to be somewhat unrealistic because of their cyclic nature. First-order fits can also be eliminated since the trend in all cases is never linear. Therefore, the exponential fit best fits the segmented data for the hollow-fiber system. The coefficients as well as the coefficients of determination for the various segmented sections are given in Table 3.

Table 3. Exponential-Curve-Fit Coefficients and Coefficients of Determination for the Hollow-Fiber System

| Segment | a | b | $r^2$ |
|---|---|---|---|
| 0 – 8.6 | 79.0 | -0.104 | .827 |
| 8.6 – 15.4 | 102 | -0.070 | .861 |
| 15.4 – 19.6 | 172 | -0.098 | .792 |
| 20.2 – 44.2 | 43.9 | -0.024 | .901 |
| 44.9 – 48.9 | 60.6 | -0.022 | .456 |
| 52.2 – 60.0 | 56.0 | -0.018 | .782 |
| 59.9 – 90.7 | 51.1 | -0.014 | .910 |
| 91.4 – 95.3 | $1.35 \times 10^{4}$ | -0.063 | .710 |
| 98.4 – 100.3 | $2.47 \times 10^{11}$ | -0.230 | 1.000 |
| 101.5 – 104.9 | $1.42 \times 10^{8}$ | -0.151 | .863 |
| 106.1 – 114.1 | $3.15 \times 10^{4}$ | -0.069 | .555 |
| 115.6 – 122.9 | 18.1 | -0.003 | .007 |
| 124.0 – 130.1 | $1.61 \times 10^{7}$ | -0.109 | .684 |
| 130.6 – 136.9 | $1.74 \times 10^{4}$ | -0.050 | .908 |
| 137.9 – 145.1 | $3.28 \times 10^{3}$ | -0.035 | .785 |
| 145.1 – 150.4 | $4.40 \times 10^{4}$ | -0.201 | .898 |
| 150.6 – 157.3 | $3.87 \times 10^{7}$ | -0.0932 | .682 |
| 157.7 – 164.8 | 174 | -0.0115 | .286 |
| 164.8 – 170.5 | 169 | -0.0212 | .455 |
| 171.3 – 176.1 | $1.28 \times 10^{3}$ | -0.0225 | .815 |
| 176.3 – 184.5 | $3.09 \times 10^{5}$ | -0.0504 | .969 |
| 185.3 – 190.9 | $7.12 \times 10^{7}$ | -0.0800 | .721 |
| 192.3 – 199.6 | $1.67 \times 10^{-7}$ | -0.0936 | .585 |
| 200.2 – 207.6 | 417 | -0.0124 | .207 |
| 208.1 – 215.7 | $4.11 \times 10^{4}$ | -0.0341 | .543 |
| 216.5 – 222.4 | $1.85 \times 10^{17}$ | -0.165 | .723 |

where: $y = ae^{bx}$ and $r^2$ = coefficient of determination.

**16. Application of the Model to the Spiral-Wound System.** Examination of the graphs in Appendix C for this system reveals an initial, rapid rate of flux decline followed by an almost linear leveling out of the data. Therefore, this data appears to fit the proposed theory rather well. To test this, the data was segmented into two sections, and curve fits were performed on each section. The first segment was 531.9 to 555.3 and the second segment, the remainder of the data, 556.2 to 649.6. This was called Group 1 on which first-order and exponential curve fits were run. This process was continued for Groups 2 and 3, each of which segmented the data in a different place. These curve fits are shown in Appendix E. The resulting coefficients and coefficients of determination for the fits are shown in Table 4.

Table 4. First-Order and Exponential-Curve-Fit Coefficients and Coefficients of Determination for the Spiral-Wound System

| Group No. | Segment | 1st Order a | 1st Order b | 1st Order $r^2$ | Exponential *a | Exponential b | Exponential $r^2$ |
|---|---|---|---|---|---|---|---|
| 1 | 531.9 – 555.3 | -.13 | 76.8 | .910 | $3.4 \times 10^{14}$ | -.060 | .952 |
| 2 | 531.9 – 560.2 | -.12 | 66.2 | .900 | $6.8 \times 10^{13}$ | -0.057 | .963 |
| 3 | 531.9 – 575.0 | $-7.3 \times 10^{-2}$ | 42.3 | .800 | $2.5 \times 10^{10}$ | -0.43 | .909 |
| 1 | 556.2 – 649.6 | $-4.52 \times 10^{-3}$ | 3.29 | .543 | 38.0 | -0.007 | .535 |
| 2 | 561.1 – 649.6 | $-3.70 \times 10^{-3}$ | 2.77 | .480 | 19.7 | -0.006 | .463 |
| 3 | 576.0 – 649.6 | $-6.30 \times 10^{-4}$ | .864 | .067 | 1.02 | -0.001 | .057 |

Where: $y = ax + b$ for first order
$y = ae^{bx}$ for exponential
$r^2$ = coefficient of determination
* calculated using Hewlett Packard model 65 calculator with StatPack Exponential Curve Fit Program

Group 2 data for the initial, or unsteady state, gives the best fit. It is no surprise that the best fit comes from the exponential equation with a rather high coefficient of determination. As for the steady state, or latter portion, of the data, the optimum tends to be closer to Group 1. In this case, the first-order fit gives a better fit than the exponential fit. Examination of the daily operation data shows essentially constant daily permeate production; however, on different days this figure fluctuates. The coefficient of determination is low and appears to get worse as less data is considered.

The reason for this can be seen by comparing the curve fits for the total data found in Appendix C and the curve fits of the segmented data. Visual examination of the 560- to 650-hour range in the graph of the total data on this system reveals an almost linear area of the curve. Compare this with the 561.1- to 649.6-hour segmented

graph found in Appendix E. Since the permeate production is much less variable here than for the whole system, the y axis is greatly expanded here as compared to the whole system. Thus, the amount of error is expanded as less data is considered not only in the visual presentation but also as witnessed in the low value for the coefficient of determination.

The apparent discrepancy between Group 2 data best fitting the unsteady state condition and Group 1 data best fitting the steady state condition can be partly attributed to Group 1's steady state data being more voluminous and, therefore, having a better coefficient of determination. However, the main reason for the discrepancy could be the definition of the boundary conditions for steady and unsteady states. In actuality, the boundary conditions probably lie between the boundary conditions defined as Group 1 and those defined as Group 2; and, second, it is doubtful that there is a discrete boundary between the two states resulting in a third, or transition, state as pointed out earlier.

## VI. CONCLUSIONS

**17. Conclusions.** Based on the data, this study concludes that:

a. A single, empirical equation cannot describe permeate production by ultrafiltration of shower wastewater.

b. A model based on unsteady and steady state phenomena of concentration polarization can empirically describe the ultrafiltration process.

c. The hollow-fiber system can be described by a single, empirical equation of exponential order because the system as studied was never allowed to reach steady state. Therefore, the unsteady state equation described the system's operation.

d. The spiral-wound membrane system can be described empirically by an exponential equation during the boundary layer formation and by a linear equation during steady state operation.

# APPENDIX A

## DATA

The following pages are a computer listing of the data. Line numbers 100 through 2010 are the data from the hollow-fiber system. The first number is the line number and is followed by an equal sign. The second number is the time factor expressed in hours, and the third number is the flux expressed in gallons per square feet of membrane area per day. After Line 2010, the line numbers begin again at 100 and continue through 1380. This is the data from the spiral-wound system. Time, again, is expressed in hours; however, it is not normalized and, therefore, begins at 531.9. Flux, this time, is expressed in gallons per minute.

L,100 830

| | | | |
|---|---|---|---|
| 100=0.0 | 101.46 | 460=53.4 | 22.06 |
| 110=0.9 | 68.98 | 470=54.3 | 21.30 |
| 120=2.4 | 55.80 | 480=55.1 | 20.8 |
| 130=3.3 | 51.24 | 490=55.9 | 19.78 |
| 140=4.4 | 43.62 | 500=57.6 | 20.30 |
| 150=5.2 | 43.62 | 510=58.4 | 20.04 |
| 160=6.4 | 40.58 | 520=60. | 19.78 |
| 170=8.6 | 38.04 | 530=59.9 | 25.36 |
| 180=8.6 | 59.6 | 540=60.9 | 23.08 |
| 190=8.9 | 58.34 | 550=61.9 | 22.06 |
| 200=9.9 | 48.7 | 560=62.6 | 20.04 |
| 210=10.9 | 43.62 | 570=63.2 | 20.04 |
| 220=11.9 | 42.62 | 580=64.7 | 19.52 |
| 230=12.9 | 38.56 | 590=65.6 | 19.02 |
| 240=13.9 | 38.04 | 600=67.1 | 18.52 |
| 250=15.4 | 38.04 | 610=83.5 | 16.48 |
| 260=15.4 | 40.58 | 620=84.8 | 14.96 |
| 270=15.9 | 35. | 630=85.7 | 15.48 |
| 280=17.4 | 31.46 | 640=86.3 | 15.22 |
| 290=18.2 | 25.36 | 650=87.2 | 14.72 |
| 300=19.6 | 27.4 | 660=88.8 | 14.72 |
| 310=20.2 | 30.44 | 670=89.5 | 14.72 |
| 320=21.4 | 25.36 | 680=90.7 | 14.46 |
| 330=22.1 | 25.88 | 690=91.4 | 50.72 |
| 340=23.2 | 25.36 | 700=92.2 | 38.56 |
| 350=24.3 | 25.36 | 710=93.4 | 38.56 |
| 360=25.4 | 22.82 | 720=94.1 | 32.98 |
| 370=26.2 | 22.32 | 730=95.3 | 33.98 |
| 380=43.2 | 17.76 | 740=98. | 30.94 |
| 390=44.2 | 14.2 | 750=98.4 | 38.04 |
| 400=44.9 | 22.32 | 760=99.1 | 32.46 |
| 410=46.1 | 22.32 | 770=100.3 | 24.6 |
| 420=47.3 | 22.82 | 780=101.5 | 36.02 |
| 430=48. | 20.30 | 790=102. | 27.9 |
| 440=48.9 | 20.80 | 800=103. | 23.34 |
| 450=52.2 | 22.82 | 810=104.1 | 21.82 |
| | | 820=104.9 | 20.3 |
| | | 830=106.1 | 21.56 |

```
L,840 1570

  840-107.4     27.9
  850-107.6     16.24
  860-108.7     15.48
  870-109.7     14.72
  880-110.6     13.7
  890-111.9     13.7
  900-112.9     13.7
  910-114.1     13.7
  920-115.6     14.2
  930-116.4     12.68
  940-117.6     12.42
  950-117.9     12.42
  960-119.      14.2
  970-120.9     12.18
  980-122.2     14.96
  990-122.9     11.92
 1000-124.      24.08
 1010-124.9     21.82
 1020-125.9     14.2
 1030-126.9     16.74
 1040-127.9     12.7
 1050-128.9     10.9
 1060-130.1     13.94
 1070-130.6     27.9
 1080-131.1     25.88
 1090-132.      24.34
 1100-132.9     23.58
 1110-134.2     21.56
 1120-134.9     20.3
 1130-136.      20.8
 1140-136.9     20.3
 1150-137.9     27.4
 1160-138.9     26.12
 1170-140.      23.34
 1180-140.9     22.82
 1190-142.1     22.32
 1200-142.9     21.82
 1210-143.9     20.3
 1220-145.1     22.06
 1230-145.1     86.24
 1240-145.9     80.14
 1250-147.2     76.72
 1260-148.      44.12
 1270-149.1     39.06
 1280-150.4     32.98
 1290-150.6     35.5
 1300-151.1     36.02
 1310-152.3     21.3
 1320-153.5     20.66
 1330-154.1     20.3
 1340-154.9     20.04
 1350-156.2     19.52
 1360-157.3     19.28
 1370-157.7     30.44
 1380-158.1     28.4
 1390-158.9     26.64
 1400-160.1     26.12
 1410-161.5     26.88
 1420-162.      25.88
 1430-162.9     26.38
 1440-164.8     27.4
 1450-164.8     22.82
 1460-165.2     23.08
 1470-166.6     23.34
 1480-166.9     21.3
 1490-167.9     21.82
 1500-169.6     21.3
 1510-170.5     21.82
 1520-171.3     27.88
 1530-171.9     25.88
 1540-173.9     25.36
 1550-175.2     24.98
 1560-176.1     24.34
 1570-176.3     43.62
```

```
L,1580 2050

 1580-178.3     36.52
 1590-179.2     37.04
 1600-179.9     36.02
 1610-181.      33.98
 1620-182.3     30.94
 1630-182.9     30.44
 1640-184.5     28.4
 1650-185.3     26.38
 1660-185.9     25.88
 1670-186.9     18.76
 1680-187.9     20.3
 1690-189.2     21.3
 1700-190.1     20.8
 1710-190.9     16.48
 1720-192.      13.18
 1730-192.3     12.68
 1740-193.1     13.18
 1750-195.2     13.7
 1760-195.9     12.68
 1770-197.      13.18
 1780-199.6     28.92
 1790-200.2     31.7
 1800-201.      37.28
 1810-202.      36.26
 1820-203.1     34.5
 1830-204.3     31.7
 1840-205.1     31.46
 1850-205.9     31.2
 1860-207.6     33.22
 1870-208.1     38.42
 1880-209.4     30.44
 1890-210.2     33.48
 1900-211.3     27.4
 1910-212.1     27.64
 1920-213.2     28.92
 1930-214.2     29.16
 1940-215.7     27.64
 1950-216.5     48.2
 1960-217.4     39.56
 1970-218.4     39.06
 1980-219.5     32.22
 1990-220.2     30.44
 2000-221.5     31.46
 2010-222.4     13.18
..
```

BEST AVAILABLE COPY

L.100 830

| | | |
|---|---|---|
| 100- | 531.9000 | 5.0000 |
| 110- | 532.3000 | 4.0000 |
| 120- | 534.9000 | 3.0000 |
| 130- | 536.9000 | 3.0000 |
| 140- | 537.4000 | 3.0000 |
| 150- | 537.5000 | 3.0000 |
| 160- | 539.6000 | 3.0000 |
| 170- | 540.6000 | 3.0000 |
| 180- | 541.3000 | 3.0000 |
| 190- | 542.2000 | 2.8000 |
| 200- | 543.3000 | 2.5000 |
| 210- | 544.3000 | 2.4000 |
| 220- | 545.4000 | 2.0000 |
| 230- | 546.3000 | 1.8000 |
| 240- | 547.3000 | 1.8000 |
| 250- | 548.3000 | 1.6000 |
| 260- | 549.3000 | 1.5000 |
| 270- | 549.4000 | 1.5000 |
| 280- | 550.3000 | 1.4000 |
| 290- | 551.2000 | 1.3000 |
| 300- | 552.3000 | 1.3000 |
| 310- | 553.3000 | 1.3000 |
| 320- | 554.3000 | 1.1000 |
| 330- | 555.3000 | 1.1000 |
| 340- | 556.2000 | 1.0000 |
| 350- | 557.3000 | 1.0000 |
| 360- | 557.6000 | 1.0000 |
| 370- | 558.1000 | 1.0000 |
| 380- | 559.7000 | 1.0000 |
| 390- | 560.2000 | 1.0000 |
| 400- | 561.1000 | .8000 |
| 410- | 562.2000 | .8000 |
| 420- | 563.1000 | .8000 |
| 430- | 564.2000 | .8000 |
| 440- | 565.1000 | .8000 |
| 450- | 565.4000 | .8000 |
| 460- | 565.8000 | .8000 |
| 470- | 567.0000 | .8000 |
| 480- | 567.9000 | .8000 |
| 490- | 569.0000 | .8000 |
| 500- | 570.0000 | .8000 |
| 510- | 570.9000 | .8000 |
| 520- | 571.9000 | .8000 |
| 530- | 572.9000 | .8000 |
| 540- | 573.1000 | .8000 |
| 550- | 574.1000 | .8000 |
| 560- | 575.0000 | .8000 |
| 570- | 576.0000 | .6000 |
| 580- | 577.4000 | .6000 |
| 590- | 578.0000 | .6000 |
| 600- | 579.3000 | .6000 |
| 610- | 580.1000 | .5000 |
| 620- | 580.4000 | .5000 |
| 630- | 582.2000 | .5000 |
| 640- | 583.2000 | .5000 |
| 650- | 584.3000 | .5000 |
| 660- | 585.1000 | .5000 |
| 670- | 586.3000 | .5000 |
| 680- | 587.3000 | .5000 |
| 690- | 588.3000 | .5000 |
| 700- | 588.5000 | .5000 |
| 710- | 589.3000 | .5000 |
| 720- | 590.3000 | .5000 |
| 730- | 591.2000 | .5000 |
| 740- | 592.3000 | .5000 |
| 750- | 593.2000 | .5000 |
| 760- | 594.3000 | .5000 |
| 770- | 595.3000 | .5000 |
| 780- | 595.5000 | .5000 |
| 790- | 596.3000 | .4000 |
| 800- | 597.3000 | .4000 |
| 810- | 598.3000 | .5000 |
| 820- | 598.8000 | .5000 |
| 830- | 599.5000 | .5000 |

L,840 1570

| | | |
|---|---|---|
| 840- | 600.7000 | .5000 |
| 850- | 601.6000 | .5000 |
| 860- | 601.7000 | .5000 |
| 870- | 602.6000 | .5000 |
| 880- | 603.7000 | .5000 |
| 890- | 604.6000 | .5000 |
| 900- | 605.6000 | .5000 |
| 910- | 606.6000 | .5000 |
| 920- | 607.6000 | .5000 |
| 930- | 608.7000 | .5000 |
| 940- | 608.9000 | .5000 |
| 950- | 609.7000 | .5000 |
| 960- | 610.7000 | .4000 |
| 970- | 611.6000 | .4000 |
| 980- | 612.6000 | .4000 |
| 990- | 613.6000 | .4000 |
| 1000- | 614.6000 | .4000 |
| 1010- | 615.6000 | .4000 |
| 1020- | 616.3000 | .4000 |
| 1030- | 616.4000 | .4000 |
| 1040- | 617.4000 | .4000 |
| 1050- | 618.2000 | .4000 |
| 1060- | 619.4000 | .4000 |
| 1070- | 620.4000 | .4000 |
| 1080- | 621.4000 | .4000 |
| 1090- | 622.4000 | .4000 |
| 1100- | 623.2000 | .4000 |
| 1110- | 624.4000 | .4000 |
| 1120- | 624.5000 | .4000 |
| 1130- | 625.5000 | .5000 |
| 1140- | 626.6000 | .5000 |
| 1150- | 627.5000 | .5000 |
| 1160- | 628.5000 | .5000 |
| 1170- | 629.4000 | .5000 |
| 1180- | 630.5000 | .5000 |
| 1190- | 631.5000 | .5000 |
| 1200- | 631.8000 | .5000 |
| 1210- | 632.6000 | .5000 |
| 1220- | 633.6000 | .5000 |
| 1230- | 634.4000 | .5000 |
| 1240- | 635.5000 | .5000 |
| 1250- | 636.6000 | .5000 |
| 1260- | 637.4000 | .5000 |
| 1270- | 638.5000 | .4000 |
| 1280- | 639.3000 | .5000 |
| 1290- | 640.8000 | .5000 |
| 1300- | 641.7000 | .5000 |
| 1310- | 642.4000 | .5000 |
| 1320- | 643.6000 | .5000 |
| 1330- | 644.7000 | .5000 |
| 1340- | 645.7000 | .5000 |
| 1350- | 646.5000 | .5000 |
| 1360- | 647.5000 | .5000 |
| 1370- | 648.5000 | .5000 |
| 1380- | 649.6000 | .5000 |

..

# APPENDIX B

## COMPUTER PROGRAM

An interactive computer program was written in Fortran IV language for performing the curve fits. The subroutines for the graphics portion of the program are from the Tektronix Advanced Graphics Package. These include INITT, TERM, BINITT, MMX, BELL, SCURSR, DLIMX, DLIMY, ERASE, LINE, SYMBL, CHECK, DSPLAY, CPLOT, MOVABS, HSTRIN, VLABEL, AMMODE, and FINITT. The program was run on a Control Data Corporation 6000 Computer using a Tektronix 4014 Graphics Terminal.

The data was stored on a permanent disk file. The context editor was used to segment the data. This data was then saved as TAPE 1 without line numbers. TAPE 1 was rewound and the compiled version of the program was executed. Alternatively, data could be entered directly from the terminal by connecting TAPE 1 and entering the data when directed by the computer.

Upon execution, a scatter gram of zero-order fit is plotted. Options of E, R, L, or N can then be entered as explained in line numbers 580 through 610 for the graphical representation desired. The output consists of the order of fit, graphical data presentation, the titled curve, the equation of the curve, and the coefficient of determination expressed as SQ MULT CORR COEFF IS. In some cases, a coefficient of the equation is given by * * * * * * * * indicating insufficient storage capacity for the size number stored. The order of fit is not shown on the graphs because of margin limitations.

BEST AVAILABLE COPY

```
L 100 440                                   ..

   100=       PROGRAM CURFIT(TAPE1,INPUT,OUTPUT,TAPE5=INPUT,TAPE6=OUTPUT)
   110=       DIMENSION X(201),Y(201),YC(201),RES(201),C(11),SSR(5)
   120=       DIMENSION ITIT(12),IHT(9),IVT(5),YL(201)
   130=       DIMENSION FMT(6),JOD(11)
   140=       DATA FMT/7H(* Y= *,1H ,10H(F8.2 ,* X,9H *,3H** ,,9HI1,* + *
),7H F1
   150=      10.4)/
   160=       DATA ITIT/11,117B,122B,104B,105B,122B,40B,60B,40B,
   170=      1 106B,111B,124B/
   180=       DATA IHT/8,103B,125B,115B,40B,124B,111B,115B,105B/
   190=       DATA IVT/4,106B,114B,125B,130B/
   200=       DATA IASE/105B/,IASR/122B/,IASL/114B/
   210=       DATA C/11*0./
   220=       CALL CONNEC(5,2)
   230=       CALL CONNEC(6,2)
   240=       CALL INITT(30)
   250=       CALL TERM(3,1024)
   260=       CALL BINITT
   270=C
   280=C      INPUT THE DATA
   290=C
   300=8      CALL ERASE
   310=       I=0
   320=       CALL CONNEC(6,0)
   330=       WRITE(6,11)
   340=11     FORMAT(*  INPUT THE DATA*)
   350=       CALL CONNEC(6,2)
   360=9      READ(1,10) X(I+2),Y(I+2)
   370=10     FORMAT(2F10.4)
   380=       IF(EOF(1).NE.0) GO TO 20
   390=       I=I+1
   400=       IF(I.GE.200) GO TO 20
   410=       GO TO 9
   420=20     IF(I.LT.2) GO TO 99
   430=       X(1)=Y(1)=YC(1)=RES(1)=YL(1)=I
   440=C
```

BEST AVAILABLE COPY

```
L 450 800                                ..

C      DRAW THE DATA FIRST
C
200    CONTINUE
       IOPT=0
       CALL MNMX(Y,YMIN,YMAX)
       GO TO 31
C
C      GET THE OPTION
C
21     CALL BELL
       CALL SCURSR(IOPT,IX,IY)
C
C      TEST FOR OPTIONS ALLOWED
C      E END
C      R READ NEW DATA
C      L LOG FIT
C      N ORDER OF POLYNOMIAL TO FIT
C
       IF(IOPT.EQ.IASE) GO TO 99
       IF(IOPT.EQ.IASR) GO TO 8
       IF(IOPT.NE.IASL) GO TO 22
C
C      LOG FIT SECTION
C
       DO 23 J=1,I
23     YL(J+1)=ALOG(Y(J+1))
       CALL POLYFIT(X(2),YL(2),I,1,YC(2),RES(2),C,SSR)
       DO 24 J=1,I
24     YC(J+1)=EXP(YC(J+1))
       IOPT=IOPT-60B
       GO TO 25
22     CONTINUE
       IOPT=IOPT-60B
       IF(IOPT.LT. 0 .OR. IOPT .GT. 9) GO TO 99
       IF(IOPT.EQ.0) GO TO 200
C
```

```
L 810 1140                                    ..

  810-C       VALID CALL TO DO THE FIT
  820-C
  830-        CALL POLYFIT(X(2),Y(2),I,IOPT,YC(2),RES(2),C,SSR)
  840-25      CONTINUE
  850-        YMIN=AMIN1(Y(2),YC(2))
  860-        YMAX=AMAX1(Y(2),YC(2))
  870-        DO 30 J=2,I
  880-        IF(AMIN1(Y(J+1),YC(J+1)).LT.YMIN) YMIN=AMIN1(Y(J+1),YC(J+1)
)
  890-        IF(AMAX1(Y(J+1),YC(J+1)).GT.YMAX) YMAX=AMAX1(Y(J+1),YC(J+1)
)
  900-30      CONTINUE
  910-C
  920-C       DRAW THE GRAPH
  930-C
  940-31      CONTINUE
  950-        CALL DLIMX(X(2),X(I+1))
  960-        CALL DLIMY(YMIN,YMAX)
  970-C
  980-C       PLOT EXPR DATA
  990-C
 1000-        CALL ERASE
 1010-        CALL LINE(0)
 1020-        CALL SYMBL(2)
 1030-        CALL CHECK(X,Y)
 1040-        CALL DSPLAY(X,Y)
 1050-C
 1060-C       PLOT THE CURVE
 1070-C
 1080-        IF(IOPT.EQ.0) GO TO 32
 1090-        CALL SYMBL(0)
 1100-        CALL LINE(1)
 1110-        CALL CPLOT(X,YC)
 1120-C
 1130-C       ADD THE TITLES
 1140-C
```

BEST AVAILABLE COPY

```
L 1150 1470                                   ..

 1150=32    CONTINUE
 1160=      ITIT(8)=IOPT+60B
 1170=      CALL MOVABS(455,750)
 1180=      CALL HSTRIN(ITIT)
 1190=      CALL MOVABS(460,50)
 1200=      CALL HSTRIN(IHT)
 1210=      CALL MOVABS(50,500)
 1220=      CALL VLABEL(IVT(1),IVT(2))
 1230=C
 1240=C     EQUATION PLOT
 1250=C
 1260=      IF(IOPT.EQ.0) GO TO 320
 1270=      CALL MOVABS(75,50)
 1280=      CALL ANMODE
 1290=      CALL CONNEC(6,0)
 1300=      IF(ITIT(8).EQ.IASL) GO TO 300
 1310=C
 1320=C     REGULAR POLYNOMIAL
 1330=C
 1340=      ENCODE(10,305,FMT(2))IOPT
 1350= 305  FORMAT(I10)
 1360=      DO 330 JD=1,IOPT
 1370= 330  JOD(JD)=IOPT+1-JD
 1380=      WRITE(6,FMT)(C(JD),JOD(JD),JD=1,IOPT),C(IOPT+1)
 1385=      WRITE (6,315) SSR(4)
 1390=      GO TO 320
 1400= 300  CONTINUE
 1410=C
 1420=C     LOG SECTION
 1430=C
 1440=      C(2)=EXP(C(2))
 1450=      WRITE (6,310) C(2),C(1)
 1455=      WRITE (6,315) SSR(4)
 1460= 310  FORMAT(* Y = *,F10.3,* EXP( *,F10.3,* X)*)
 1465= 315  FORMAT( * SQ MULT CORR COEF IS *,2X,F10.3)
 1470= 320  CONTINUE
```

```
L 1480 1810                                      ..

 1480-      CALL CONNEC(6,2)
 1490-      GO TO 21
 1500-99    CALL FINITT(0,700)
 1510-      CALL DISCON(5)
 1520-      CALL DISCON(6)
 1530-      END
 1540-      SUBROUTINE POLYFIT(X,Y,N,M,YC,RES,C,SSR)
 1550-      DIMENSION A(11,12),B(20)
 1560-C   X,Y ARE INPUT ARRAYS
 1570-C   N IS THE NUMBER OF POINTS
 1580-C   M IS THE ORDER OF THE CURVE TO FIT
 1590-C   YC IS THE CALCULATED Y
 1600-C   RES IS THE RESIDUAL
 1610-C   C IS THE ARRAY OF COEFFICIENTS
 1620-C   SSR IS THE STATISTICS RETURN ARRRAY
 1630-      DIMENSION    X(200),Y(200),YC(200),RES(200),C(11),SSR(5)
 1640-      IF (N.LE.1) STOP
 1650-      IF (N.LE.200) GO TO 2
 1660-      PRINT 1100 , N
 1670- 1100 FORMAT(//5X18HNUMBER OF POINTS =,I5,2X19HEXCEEDS MAX. OF 50
0/
 1680-     C 5X18HPROGRAM ERROR STOP)
 1690-      STOP 10
 1700-    2 IF (M.GT.0) GO TO 3
 1710-      PRINT 1200 , M
 1720- 1200 FORMAT(//5X8HDEGREE =,I5,9H IN ERROR/5X18HPROGRAM ERROR STO
P)
 1730-      STOP 20
 1740-    3 IF (M.LE.10) GO TO 4
 1750-      PRINT 1300 , M
 1760- 1300 FORMAT(//5X8HDEGREE =,I5,2X,13HREDUCED TO 10)
 1770-      M = 10
 1780-4     CONTINUE
 1790-    5 MA = M + 1
 1800-      MB = M + 2
 1810-      M2 = M + M
```

```
L 1820 2170                                  ..

 1820-      DO 10 I = 1,M2
 1830-   10 B(I) = X(1)**I
 1840-      DO 20 I = 1,M2
 1850-      DO 20 J = 2,N
 1860-   20 B(I) = B(I) + X(J)**I
 1870-      A(1,MA) = N
 1880-      DO 30 I = 2,MA
 1890-   30 A(I,MA) = B(I-1)
 1900-      DO 40 I = 1,MA
 1910-      K = I - 1
 1920-      DO 40 J = 2,MA
 1930-      L = MA - J + 1
 1940-      K = K + 1
 1950-   40 A(I,L) = B(K)
 1960-      SUM = 0.0
 1970-      DO 50 I = 1,N
 1980-   50 SUM = SUM - Y(I)
 1990-      DO 60 I = 1,M
 2000-   60 B(I) = -Y(1)*X(1)**I
 2010-      DO 70 I = 1,M
 2020-      DO 70 J = 2,N
 2030-   70 B(I) = B(I) - Y(J)*X(J)**I
 2040-      A(1,MB) = SUM
 2050-      DO 80 I = 2,MA
 2060-   80 A(I,MB) = B(I-1)
 2070-      DO 100 K = 1,M
 2080-      L = K + 1
 2090-      DO 90 I = K,MA
 2100-      AB = A(I,K)
 2110-      DO 90 J = K,MB
 2120-   90 A(I,J) = A(I,J)/AB
 2130-      DO 100 I = L,MA
 2140-      DO 100 J = K,MB
 2150-  100 A(I,J) = A(K,J) - A(I,J)
 2160-      A(MA,MB) = A(MA,MB)/A(MA,MA)
 2170-      DO 110 I = 1,MA
```

```
L 2180 2410

  2180-  110 C(I) = -A(I,MB)
  2190-      DO 120 J = 2,MA
  2200-      K = MA - J + 2
  2210-      L = K - 1
  2220-      DO 120 I = 1,L
  2230-  120 C(I) = C(I) - A(I,K)*C(K)
  2240-      SUM = 0.0
  2250-      SY = 0.0
  2260-      SZ = 0.0
  2270-      DO 150 I = 1,N
  2280-      P = X(I)
  2290-      Q = P*C(1)
  2300-      IF(M.EQ.1) GO TO 145
  2310-      DO 140 J = 2,M
  2320-  140 Q = P*(Q+C(J))
  2330-  145 YC(I) = Q + C(MA)
  2340-      RES(I) = Y(I) - YC(I)
  2350-      SUM = SUM + RES(I)**2
  2360-      SY = SY + Y(I)
  2370-  150 SZ = SZ + Y(I)**2
  2380-      SZ = SZ - SY*SY/FLOAT(N)
  2390-      SSR(4) = 1.0 - SUM/SZ
  2400-      RETURN
  2410-      END
..
```

# APPENDIX C

## CURVE FITS FOR SYSTEM OPERATION

The first four graphs represent the total data for the hollow-fiber membrane system. The next four graphs represent the first 118 hours of operation of the hollow-fiber system. These are included for comparison of the two systems on an equal-time basis. The last four graphs represent the total data for the spiral-wound membrane system. The specific order of the graphs is first-, second-, and third-order followed by the exponential curve fit.

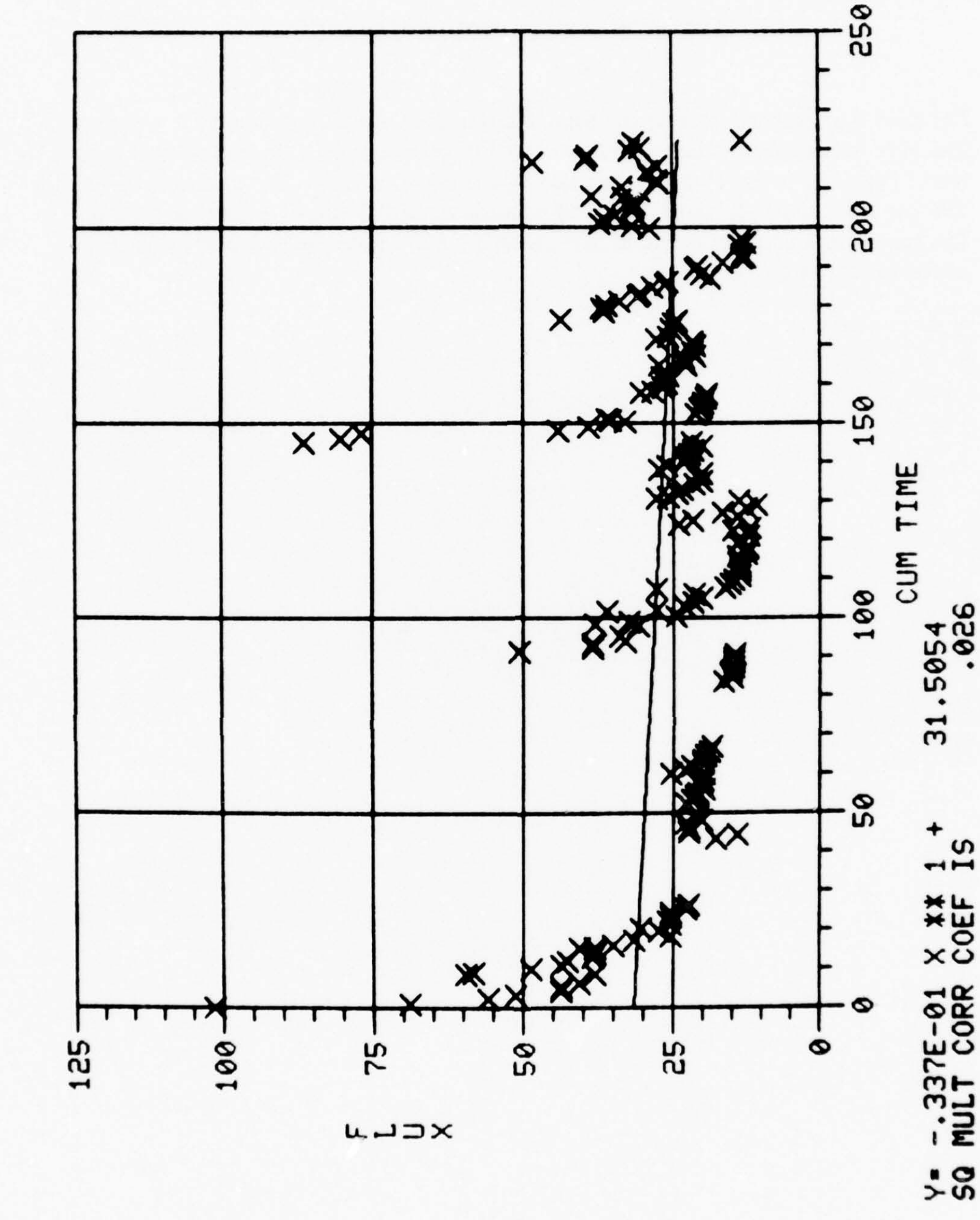
FLUX
CUM TIME
125
100
75
50
25
0
0
50
100
150
200
250
Y= -.337E-01 X ** 1 + 31.5054
SQ MULT CORR COEF IS .026

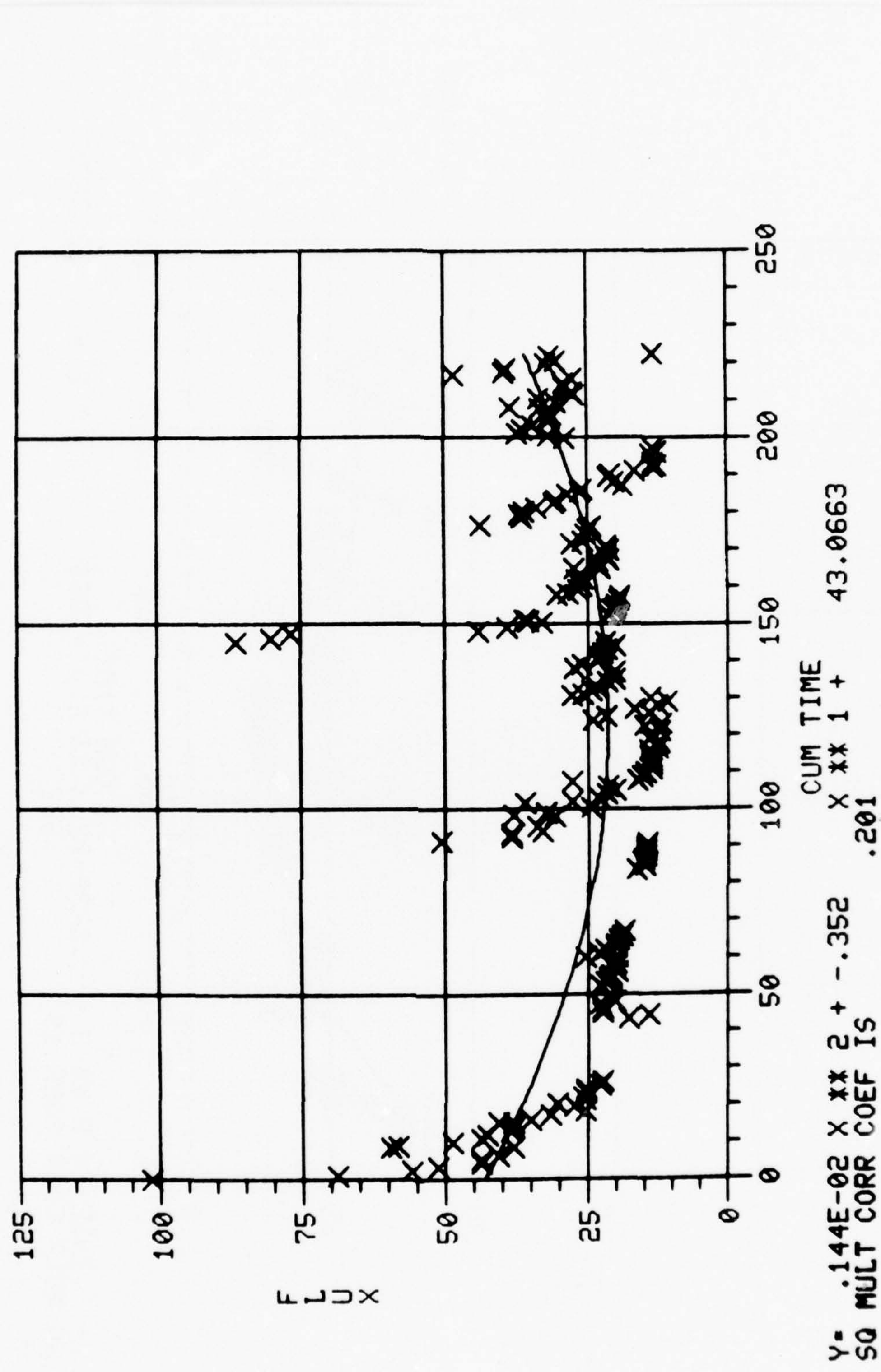
FLUX
125
100
75
50
25
0
0
50
100
150
200
250
CUM TIME
Y= .144E-02 X ** 2 + -.352 X ** 1 + 43.0663
SQ MULT CORR COEF IS .201

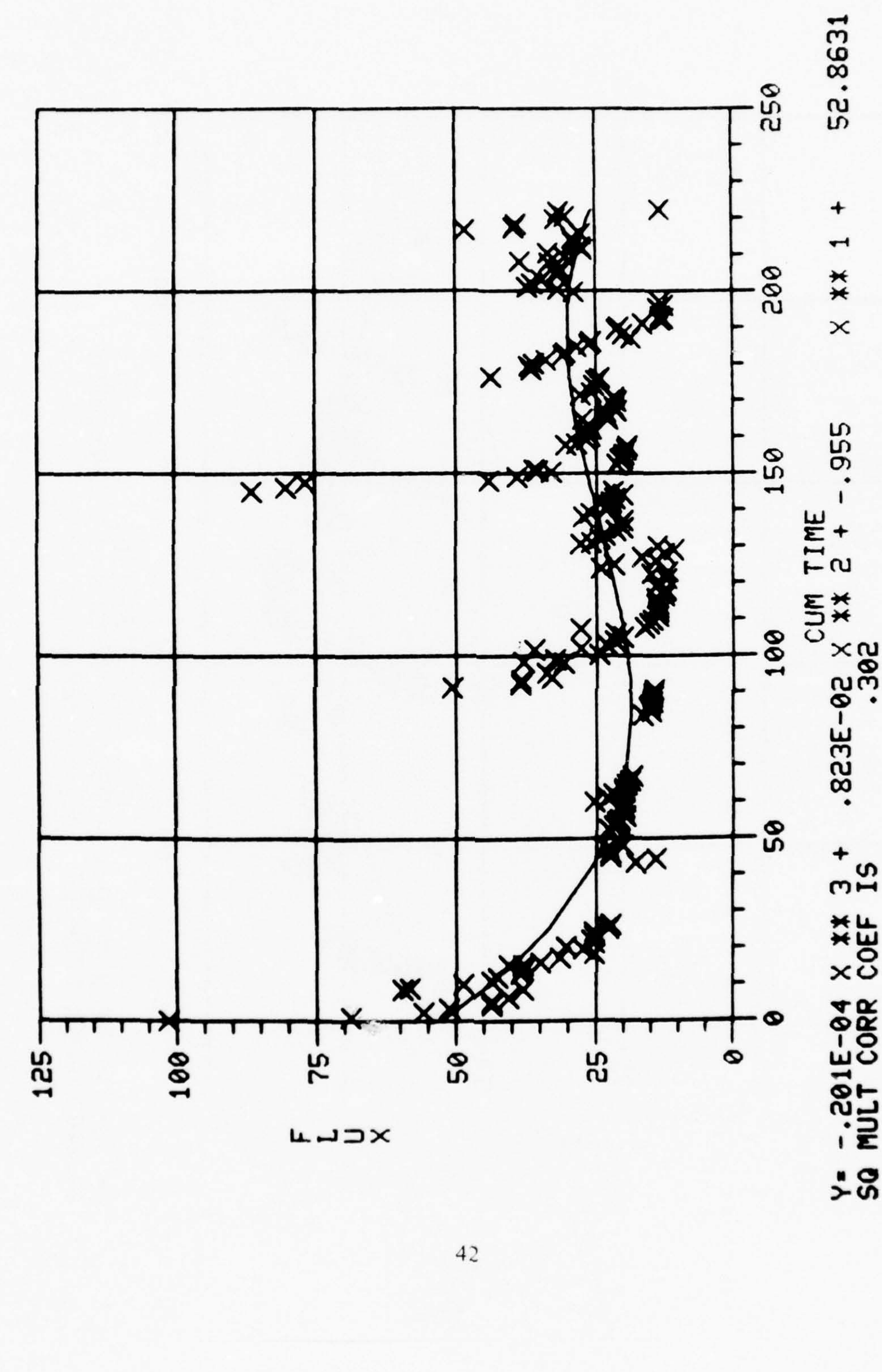
FLUX
125
100
75
50
25
0
0
50
100
150
200
250
CUM TIME
Y= -.201E-04 X ** 3 + .823E-02 X ** 2 + -.955 X ** 1 + 52.8631
SQ MULT CORR COEF IS .302

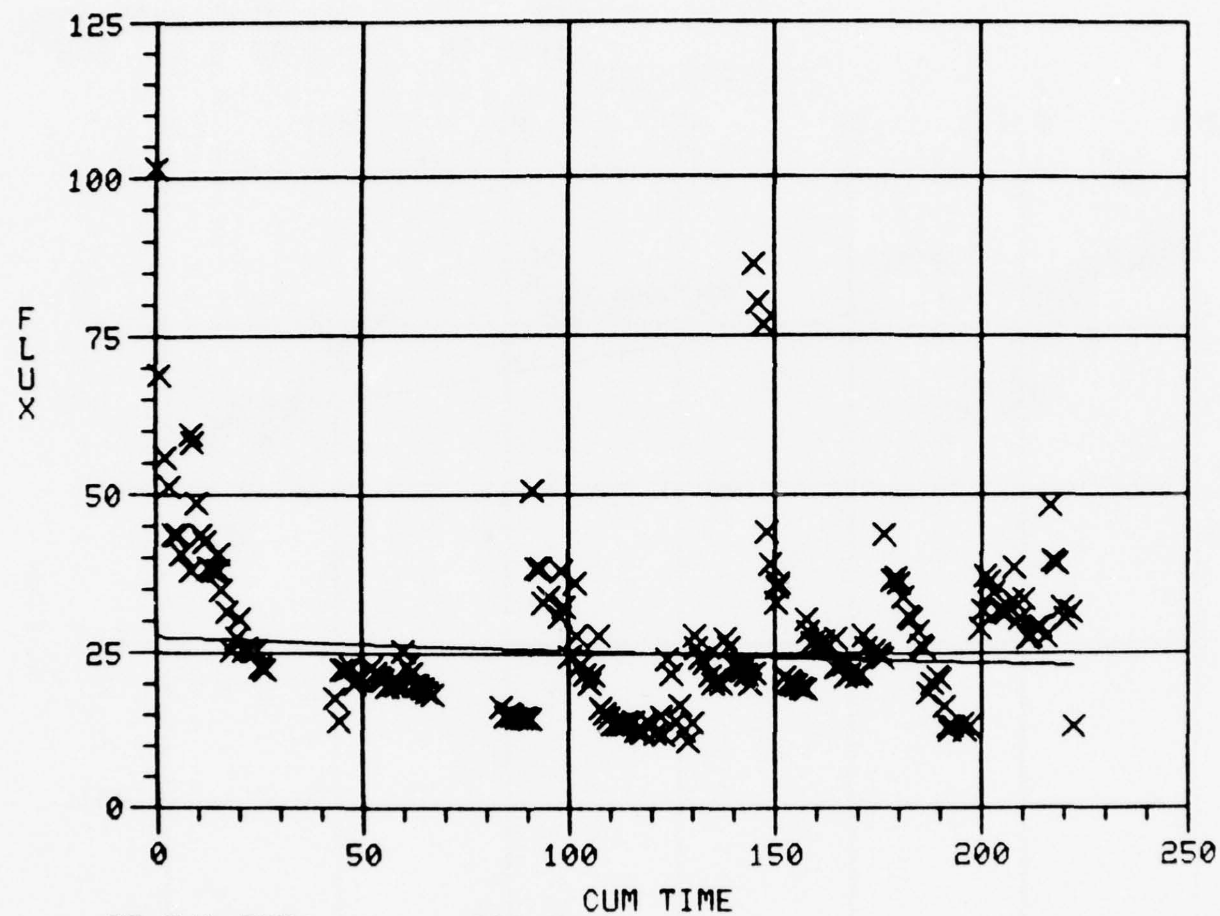


Y = 27.540 EXP( -.001 X)
SQ MULT CORR COEF IS .015

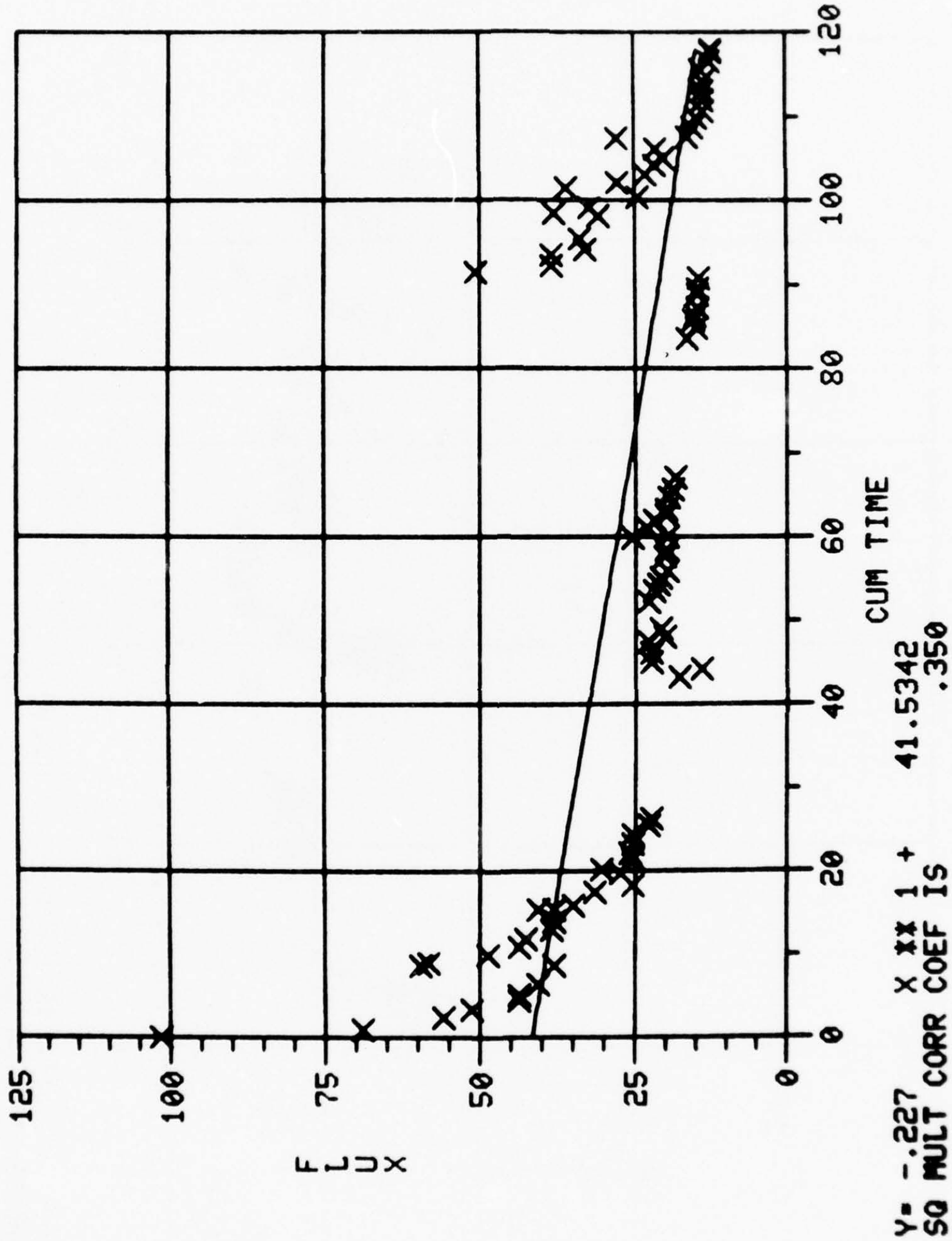

FLUX
125
100
75
50
25
0
0
20
40
60
80
100
120
CUM TIME
Y= -.227 X ** 1 + 41.5342
SQ MULT CORR COEF IS .350

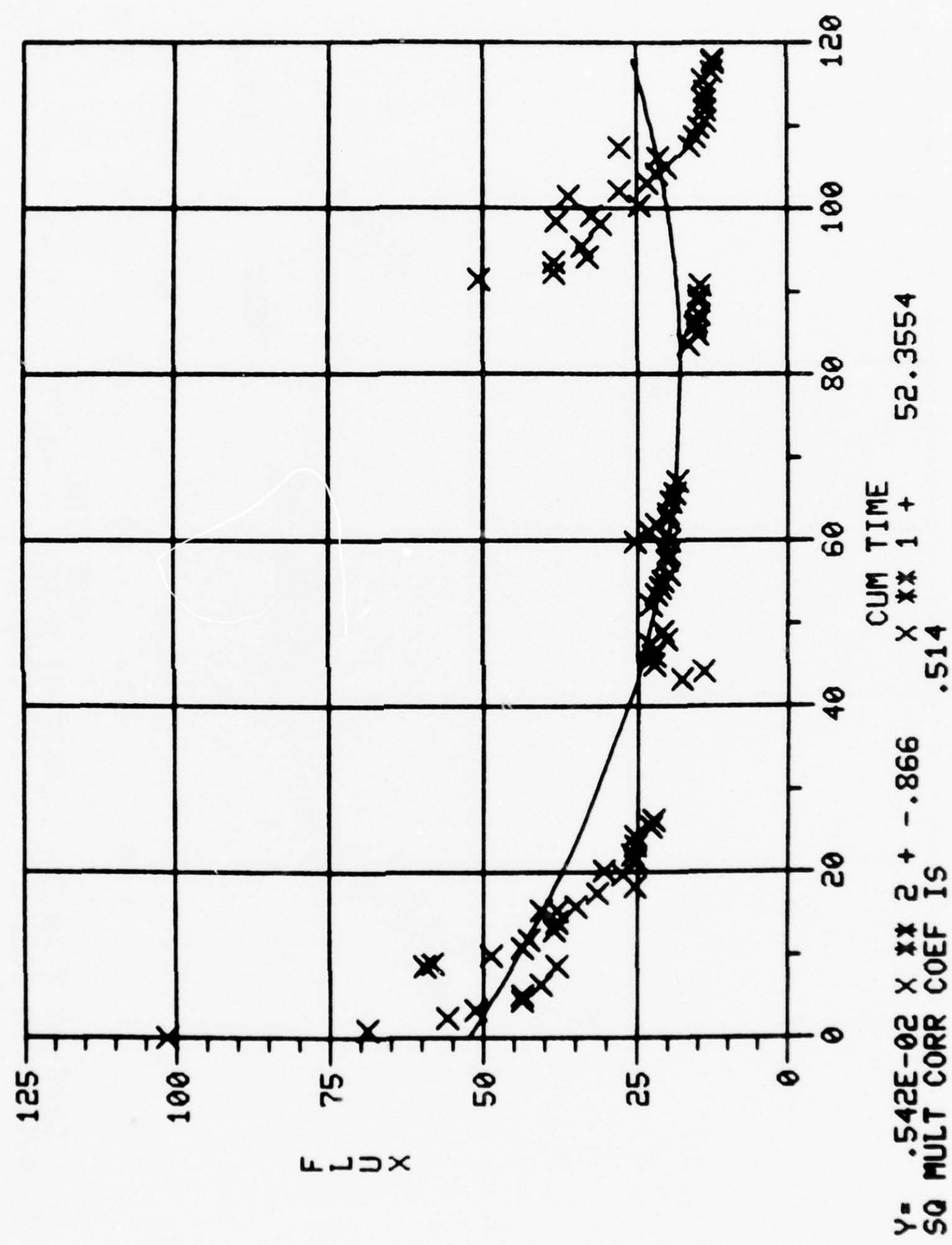

FLUX
125
100
75
50
25
0
0
20
40
60
80
100
120
CUM TIME
Y= .542E-02 X ** 2 + -.866 X ** 1 + 52.3554
SQ MULT CORR COEF IS .514

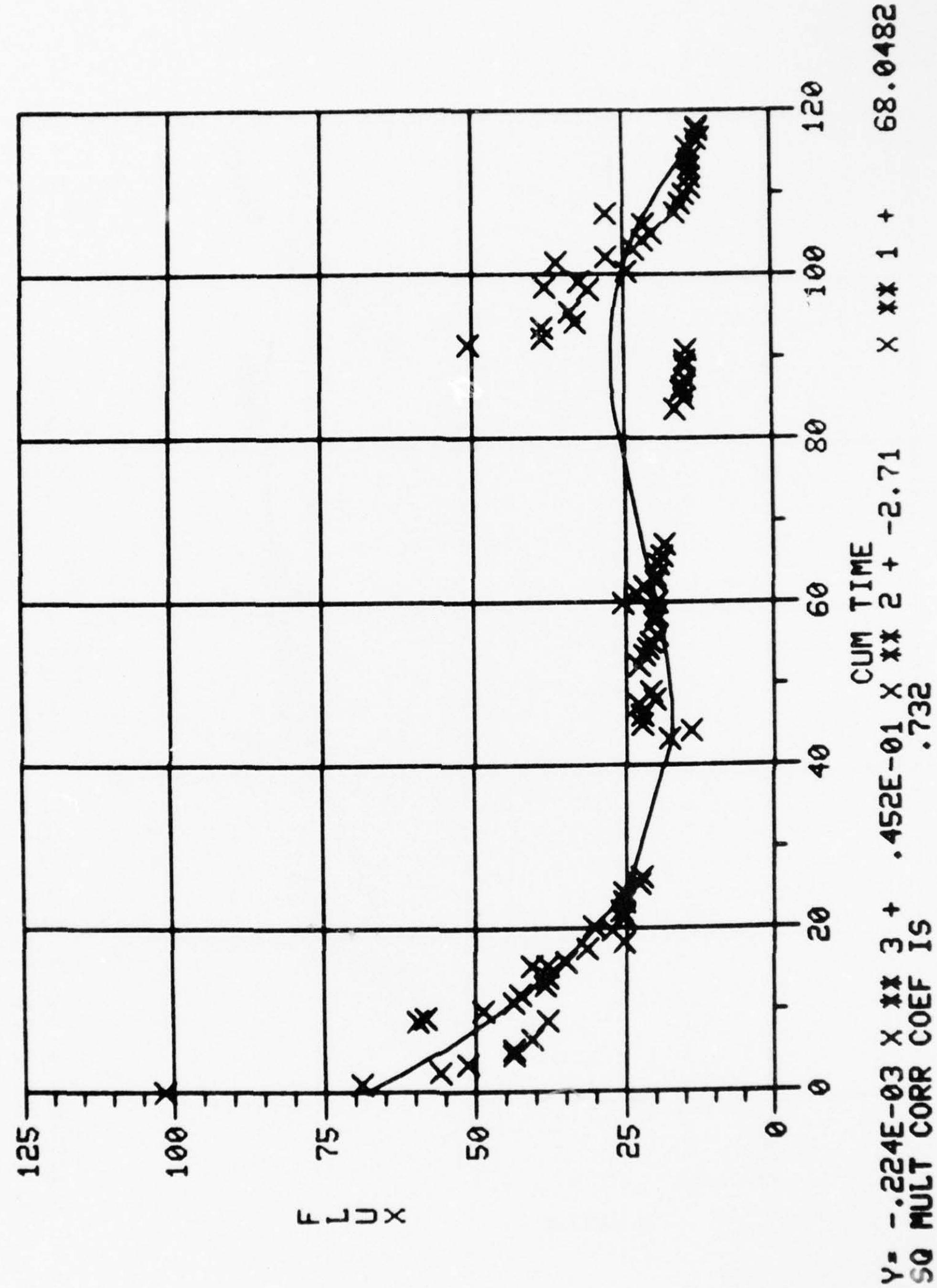

FLUX
125
100
75
50
25
0
0
20
40
60
80
100
120
CUM TIME
Y= -.224E-03 X ** 3 + .452E-01 X ** 2 + -2.71 X ** 1 + 68.0482
SQ MULT CORR COEF IS .732

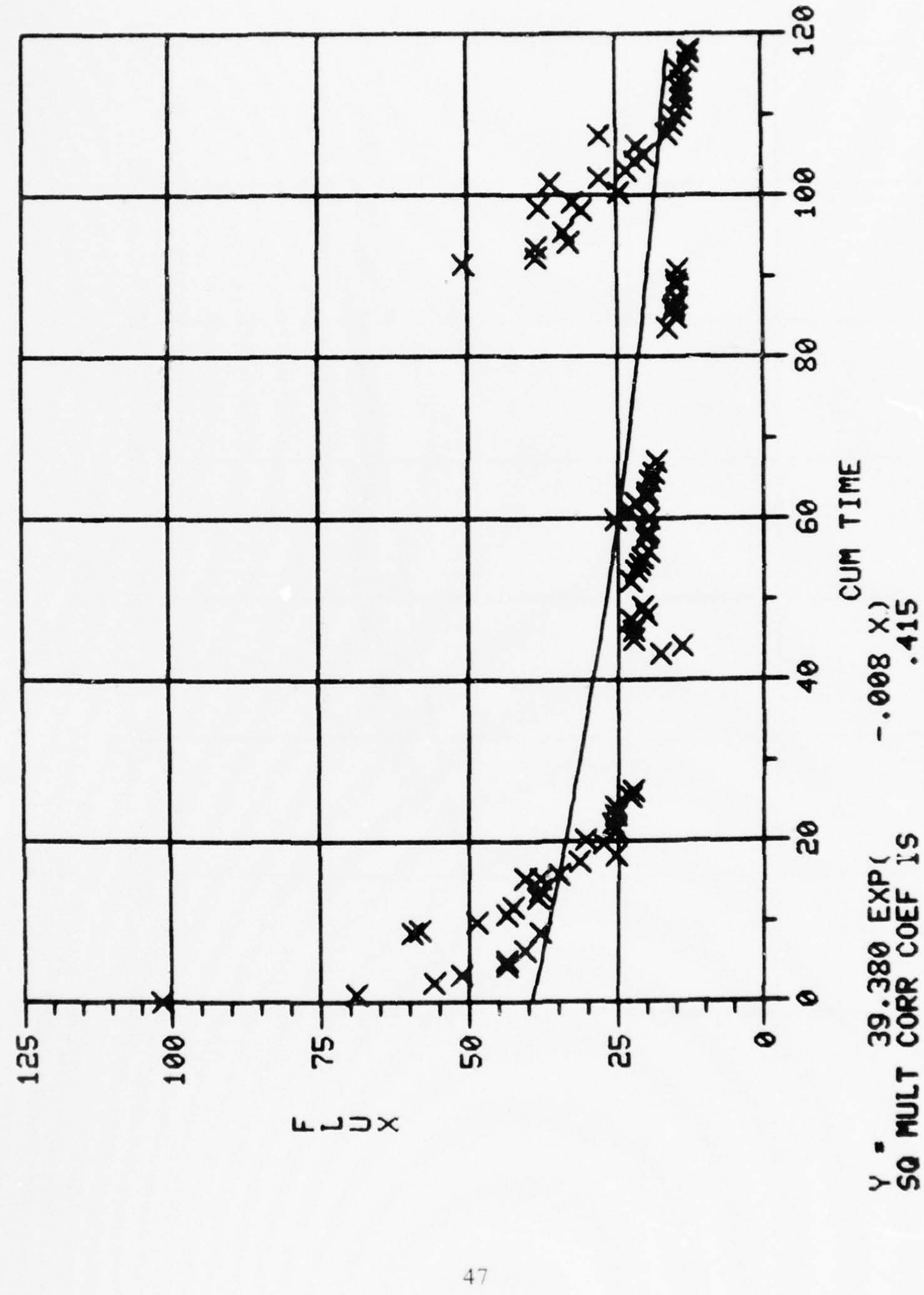

FLUX
125
100
75
50
25
0
0
20
40
60
80
100
120
CUM TIME
Y = 39.380 EXP( -.008 X)
SQ MULT CORR COEF IS .415

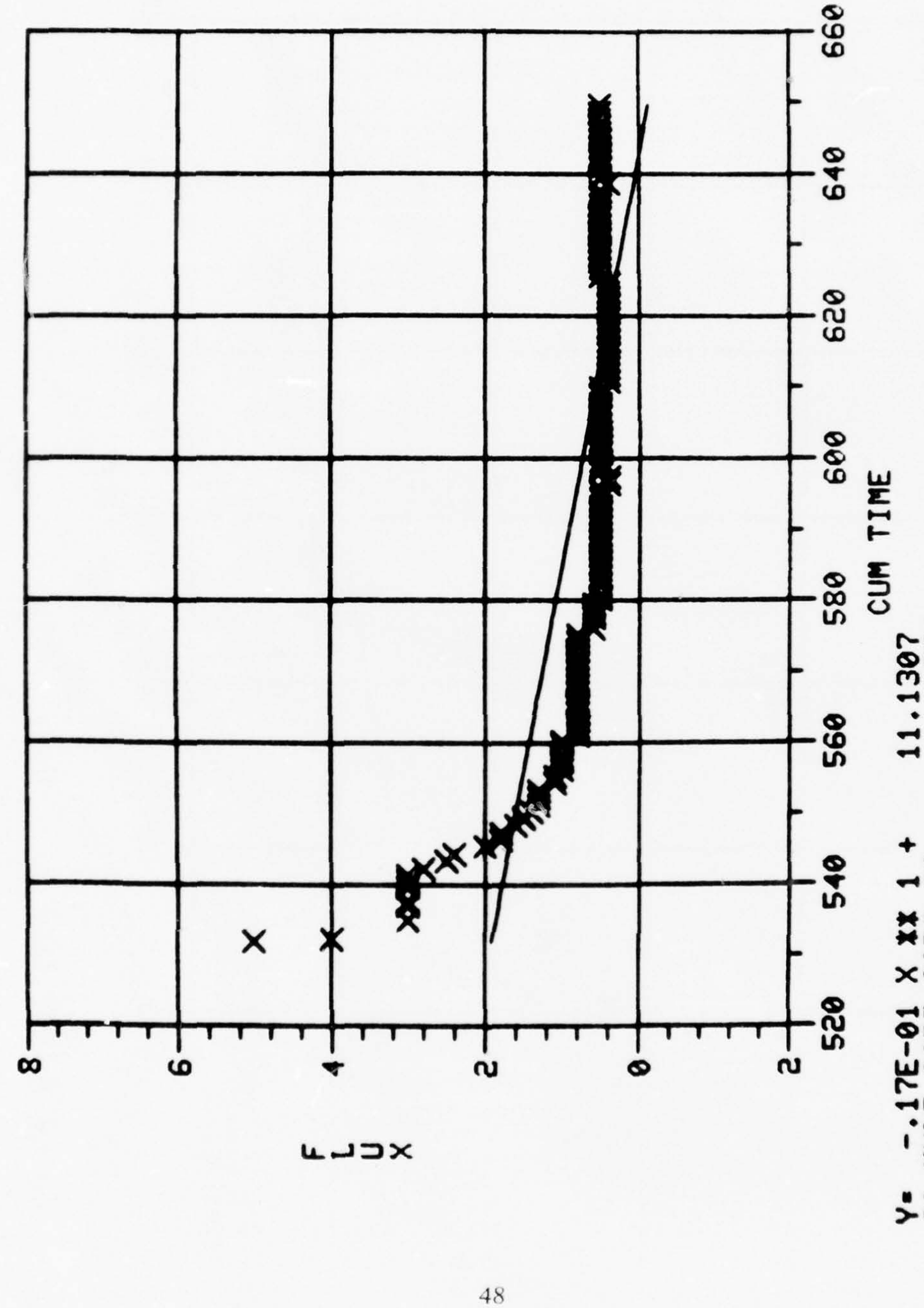
FLUX
8
6
4
2
0
2
520
540
560
580
600
620
640
660
CUM TIME
Y= -.17E-01 X XX 1 + 11.1307
SQ MULT CORR COEF IS .501

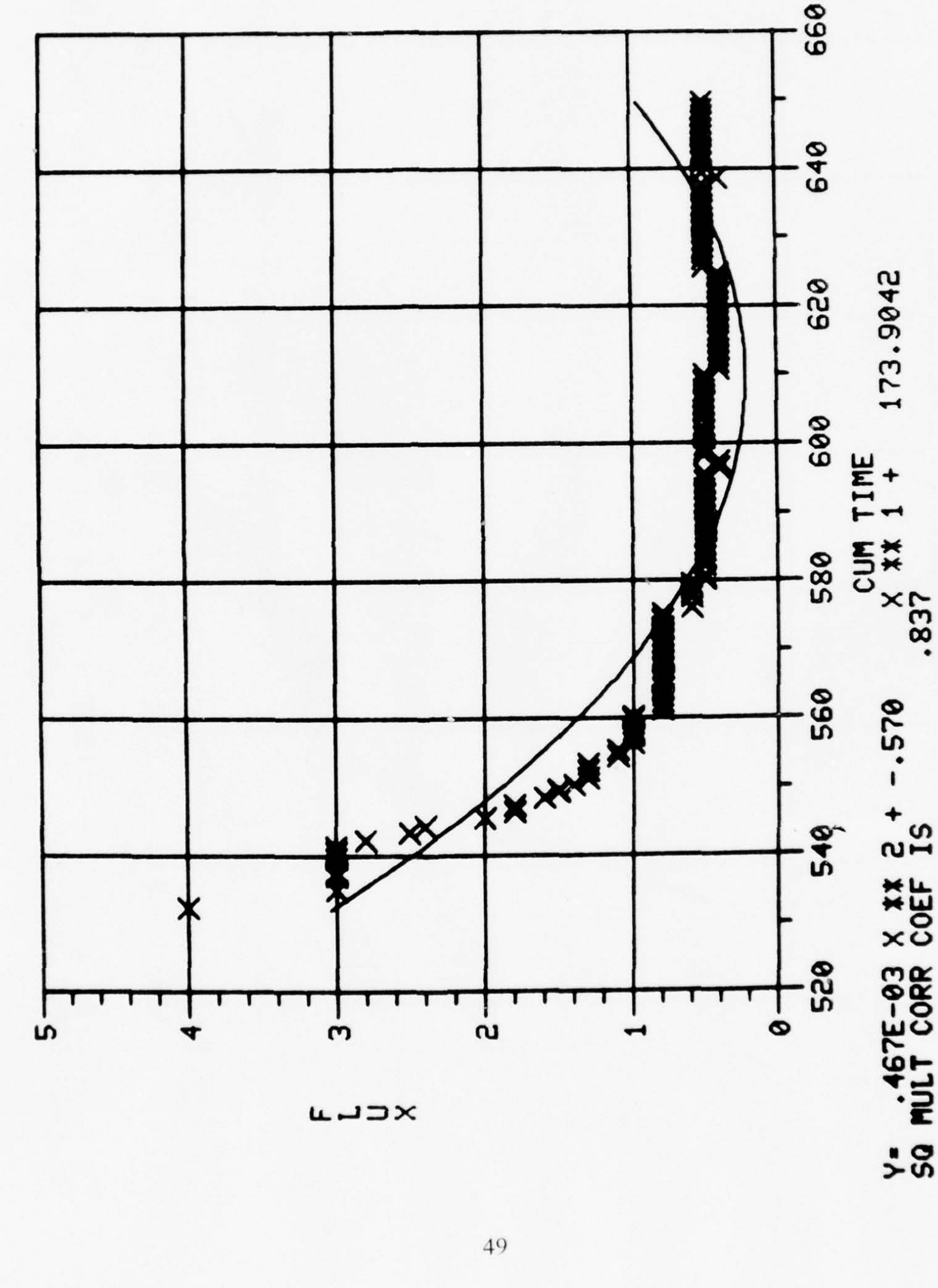
FLUX
0
1
2
3
4
5
520
540
560
580
600
620
640
660
CUM TIME
Y= .467E-03 X ** 2 + -.570 X ** 1 + 173.9042
SQ MULT CORR COEF IS .837

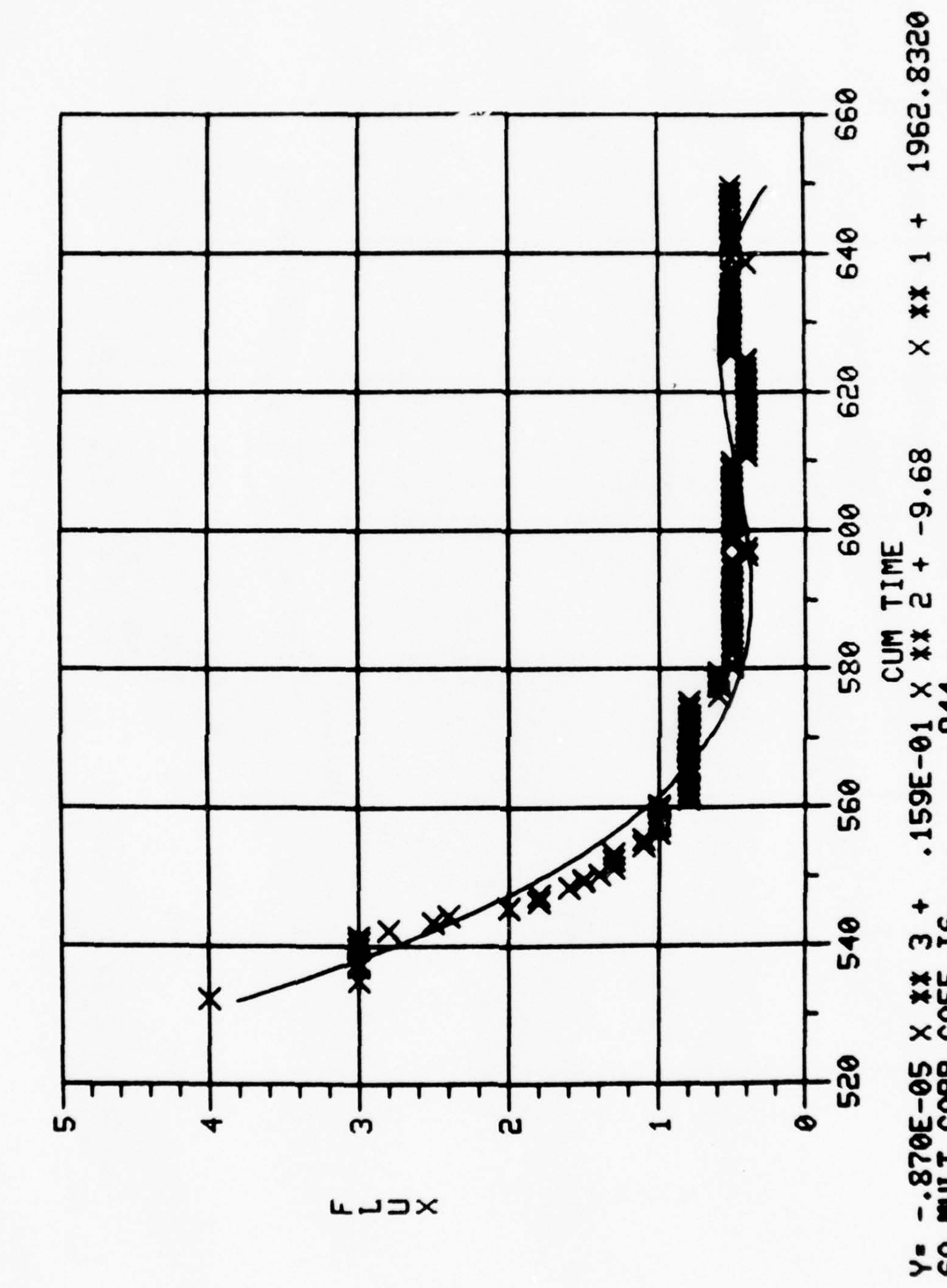
FLUX
CUM TIME
0
1
2
3
4
5
520
540
560
580
600
620
640
660
Y= -.870E-05 X ** 3 + .159E-01 X ** 2 + -9.68 X ** 1 + 1962.8320
SQ MULT CORR COEF IS .944

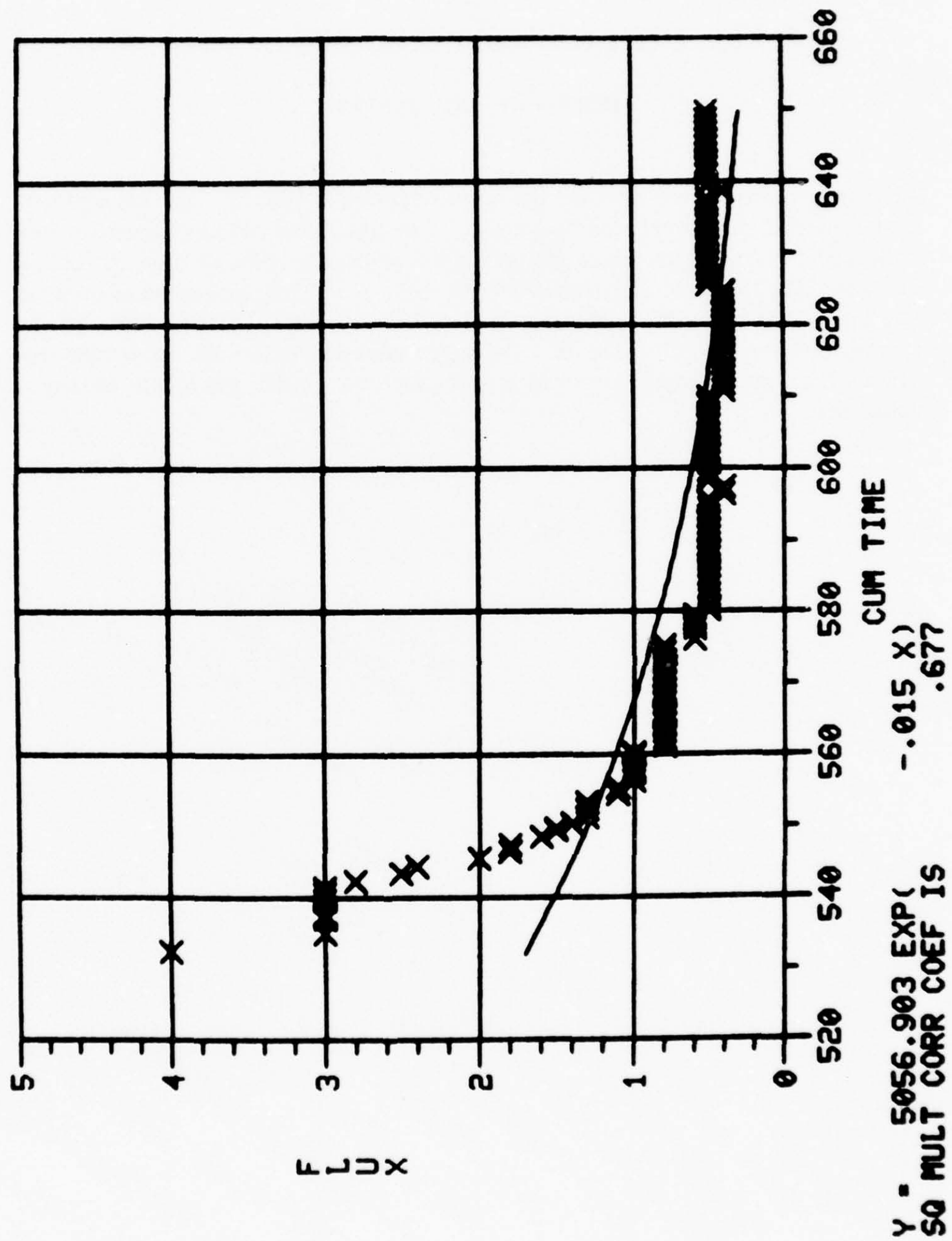
FLUX
0
1
2
3
4
5
520
540
560
580
600
620
640
660
CUM TIME
Y = 5056.903 EXP( -.015 X)
SQ MULT CORR COEF IS .677

# APPENDIX D

## CURVE FITS FOR DAILY OPERATION OF THE HOLLOW-FIBER SYSTEM

The graphs in this section represent the segments shown in Table 2. Each segment represents the time period between backflushes. The usual length of time covered is 5 to 8 hours. However, in some cases, the system was allowed to continue running through the night. The length of these runs could be from 24 to 32 hours depending on what time the following day the system was backflushed. A total of 26 segments or graphs is considered for each fit. The first 26 graphs represent first-order fits for the segments. These are followed in turn by second-order, third-order, and finally, the exponential fits.

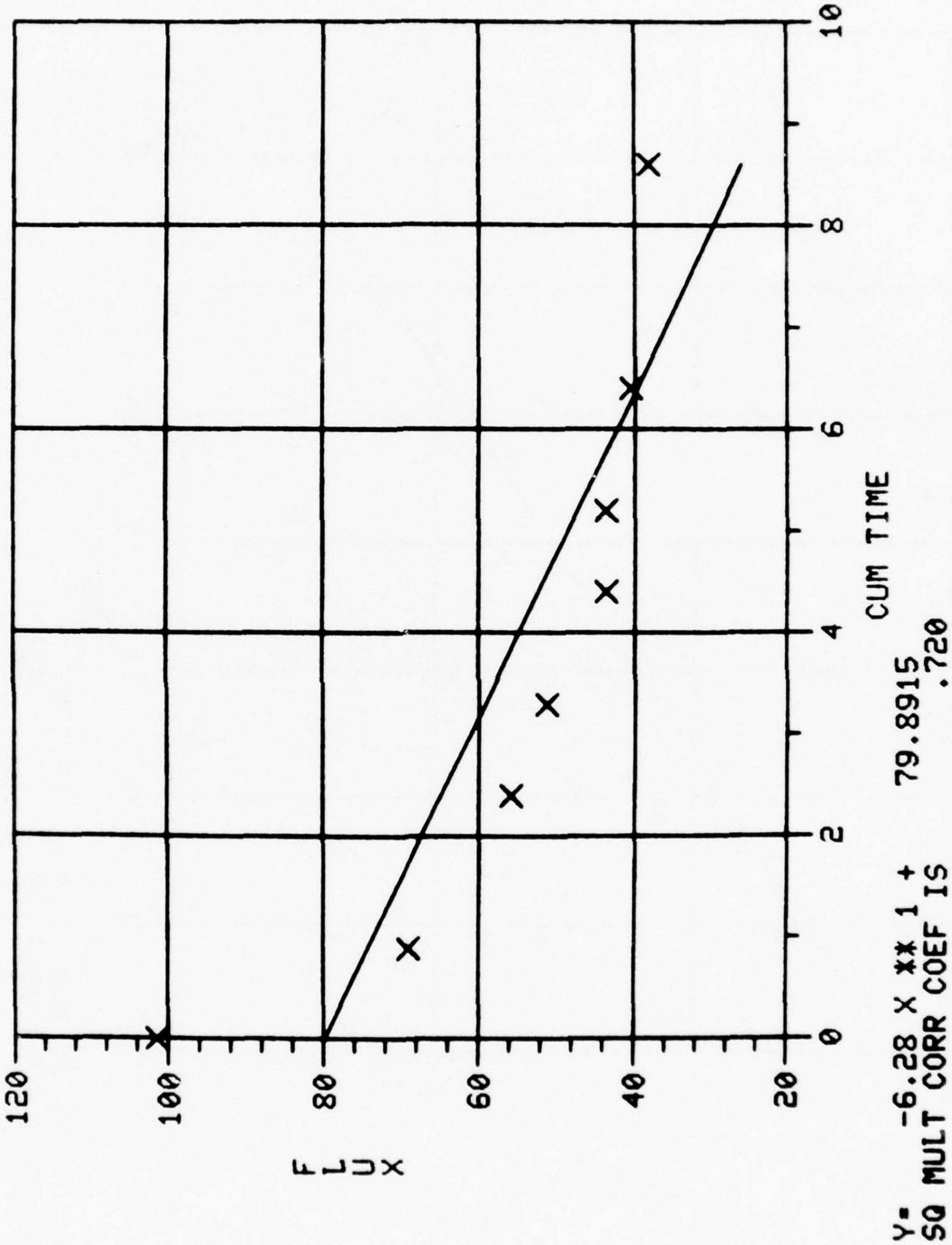
FLUX
CUM TIME
120
100
80
60
40
20
0
2
4
6
8
10
Y= -6.28 X ** 1 + 79.8915
SQ MULT CORR COEF IS .720

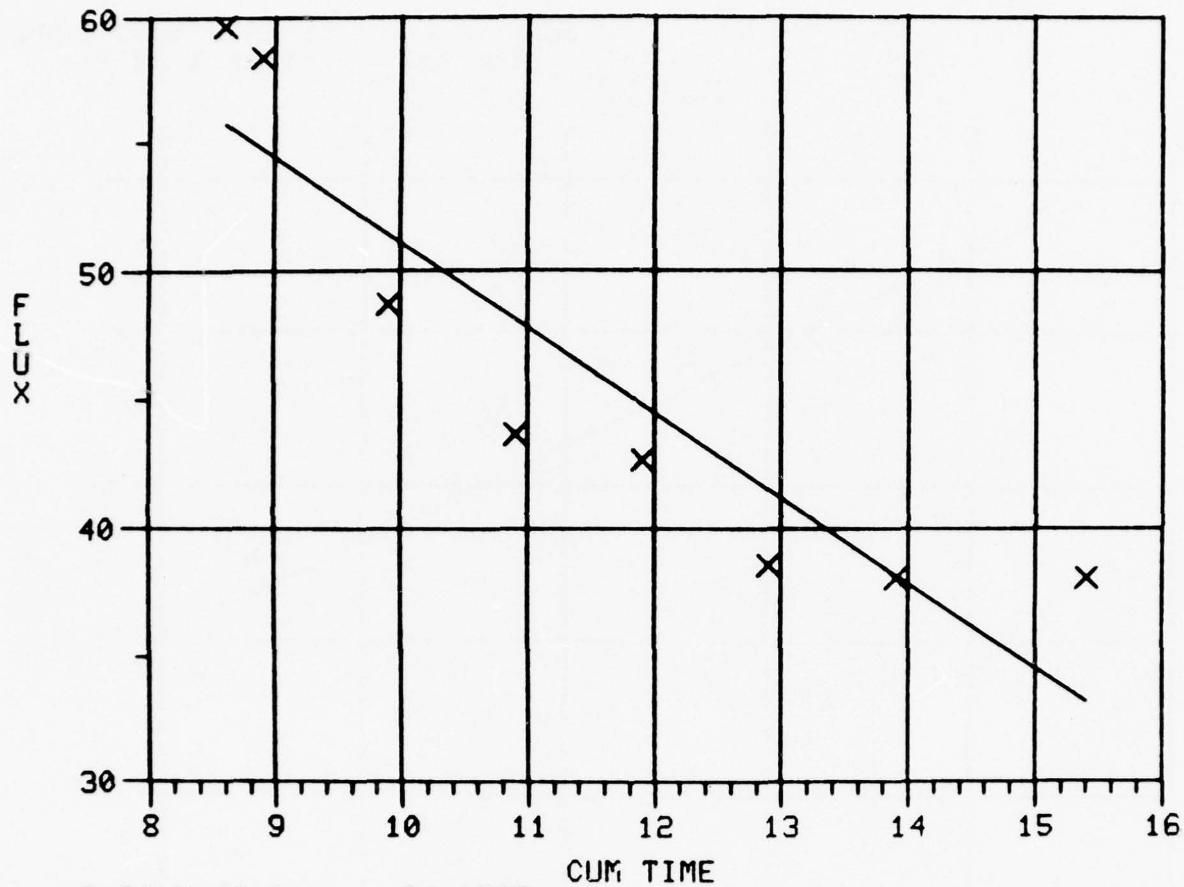


Y= -3.31 X ** 1 + 84.1897
SQ MULT CORR COEF IS .830

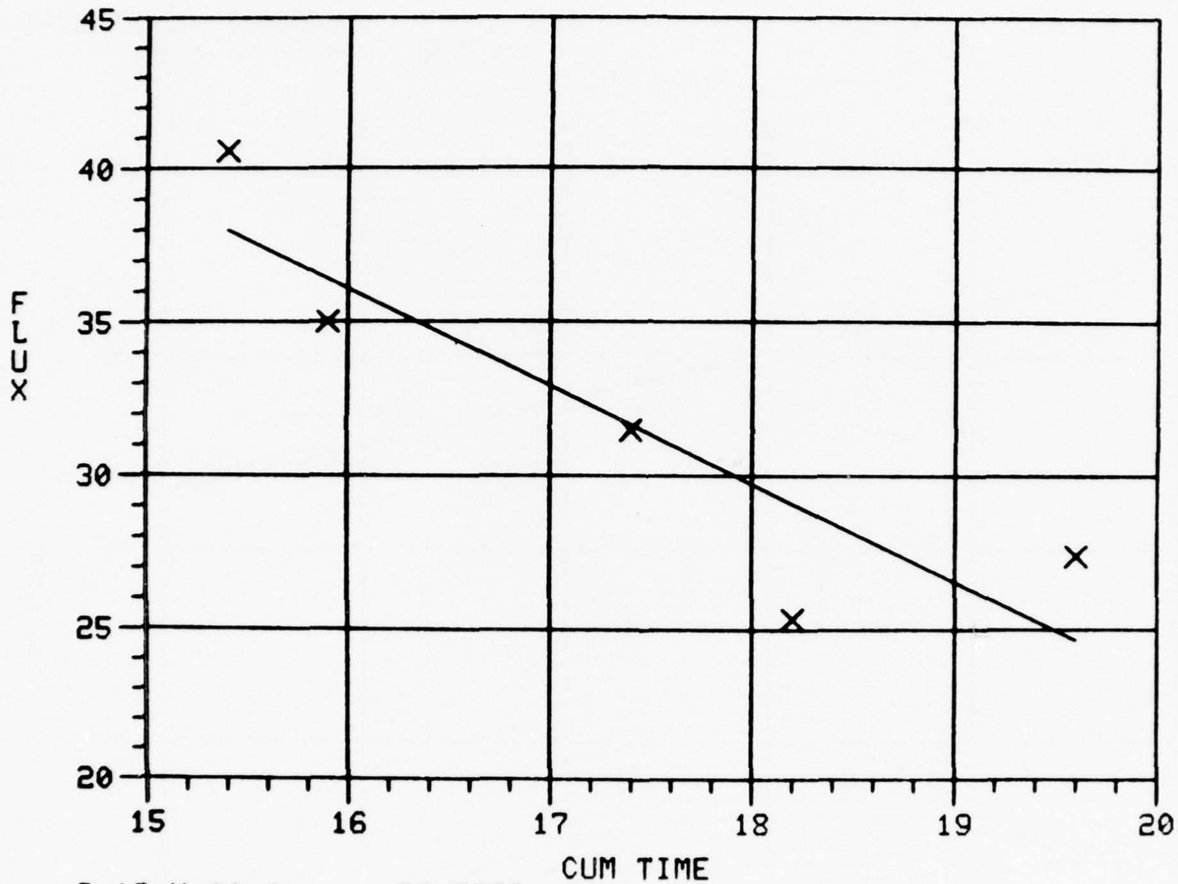


Y= -3.18 X ** 1 + 86.9290
SQ MULT CORR COEF IS .796

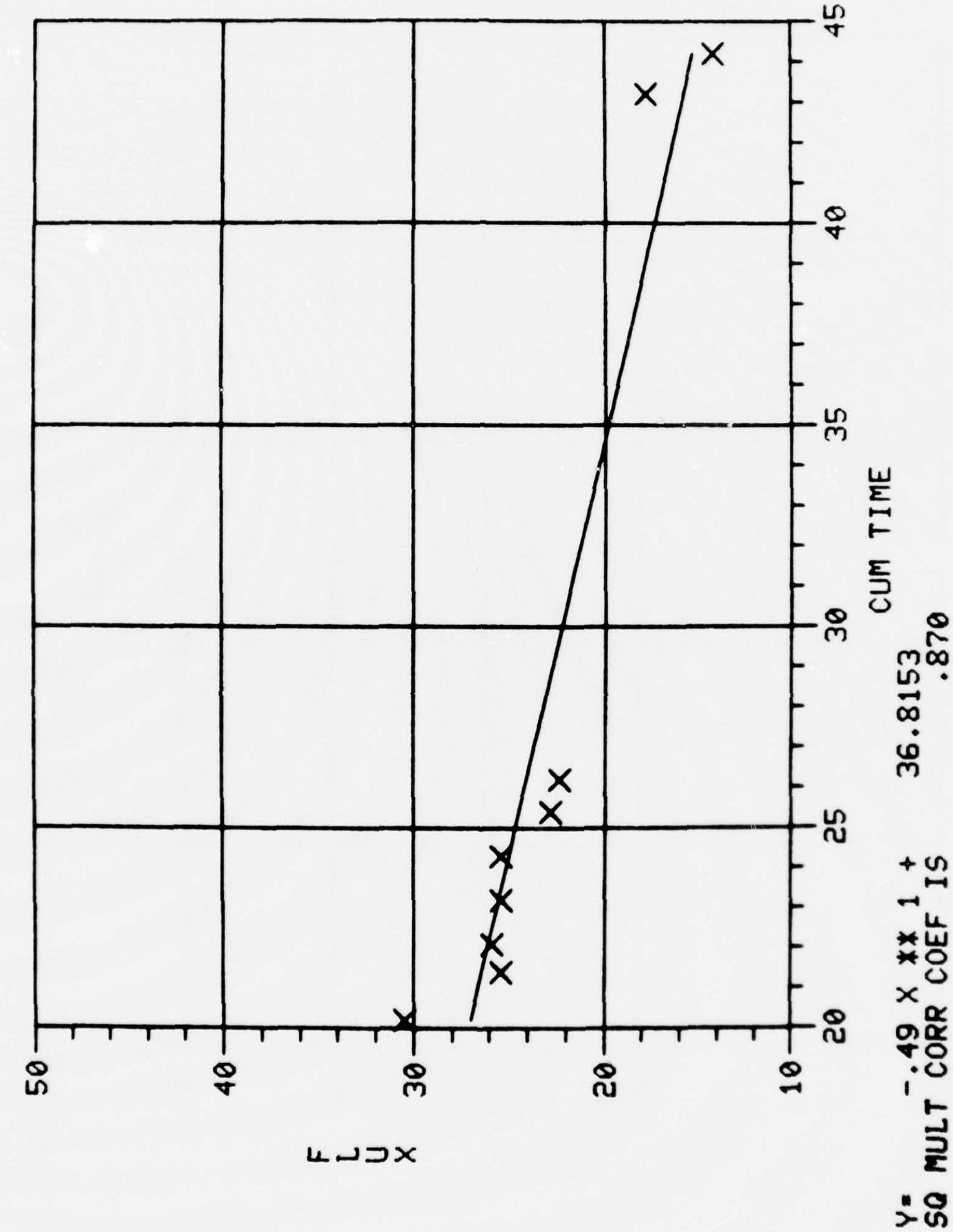
FLUX
CUM TIME
50
40
30
20
10
20
25
30
35
40
45
Y= -.49 X ** 1 + 36.8153
SQ MULT CORR COEF IS .870

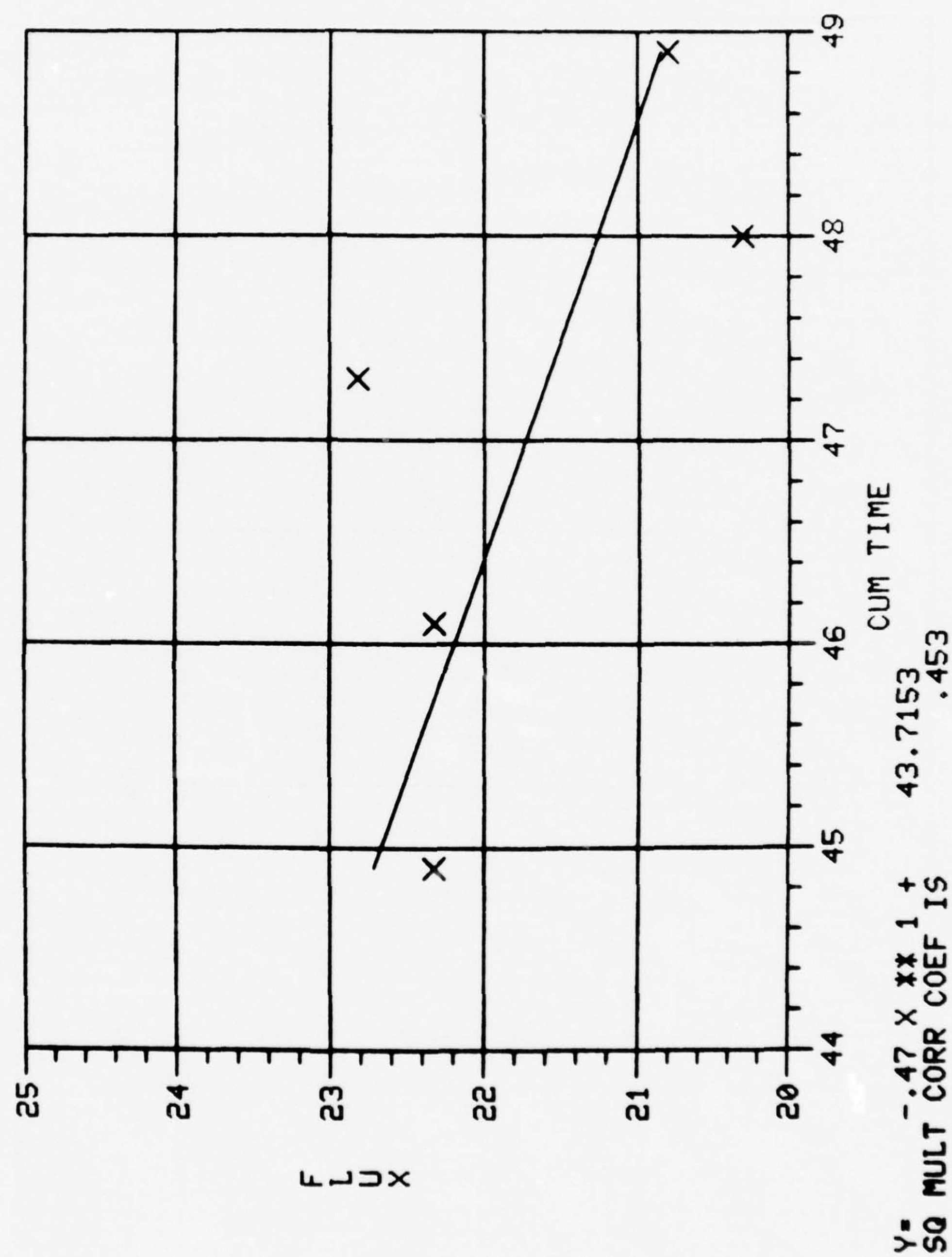
FLUX
25
24
23
22
21
20
44
45
46
47
48
49
CUM TIME
Y= -.47 X ** 1 + 43.7153
SQ MULT CORR COEF IS .453

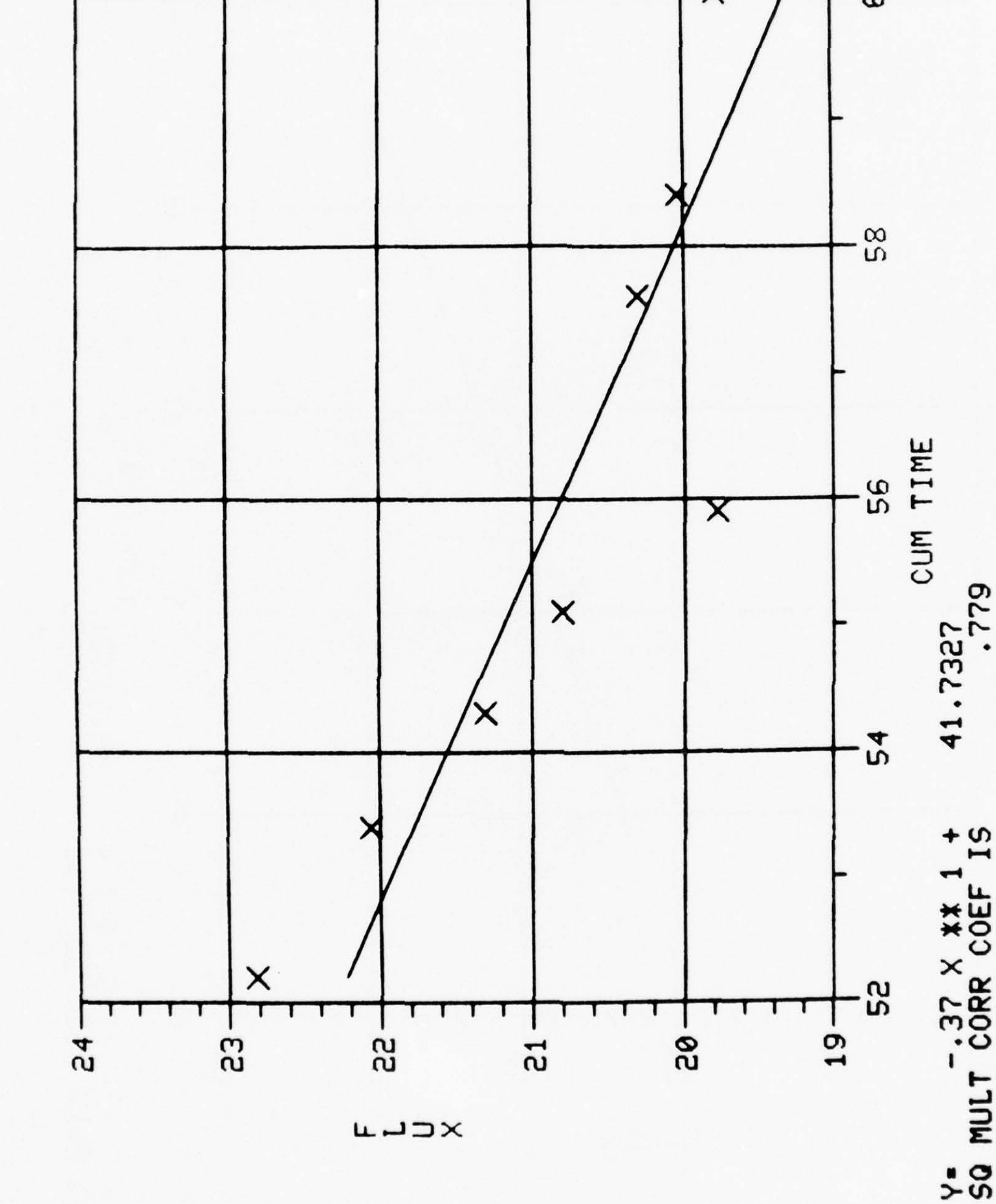
FLUX
CUM TIME
24
23
22
21
20
19
52
54
56
58
60
Y= -.37 X ** 1 + 41.7327
SQ MULT CORR COEF IS .779

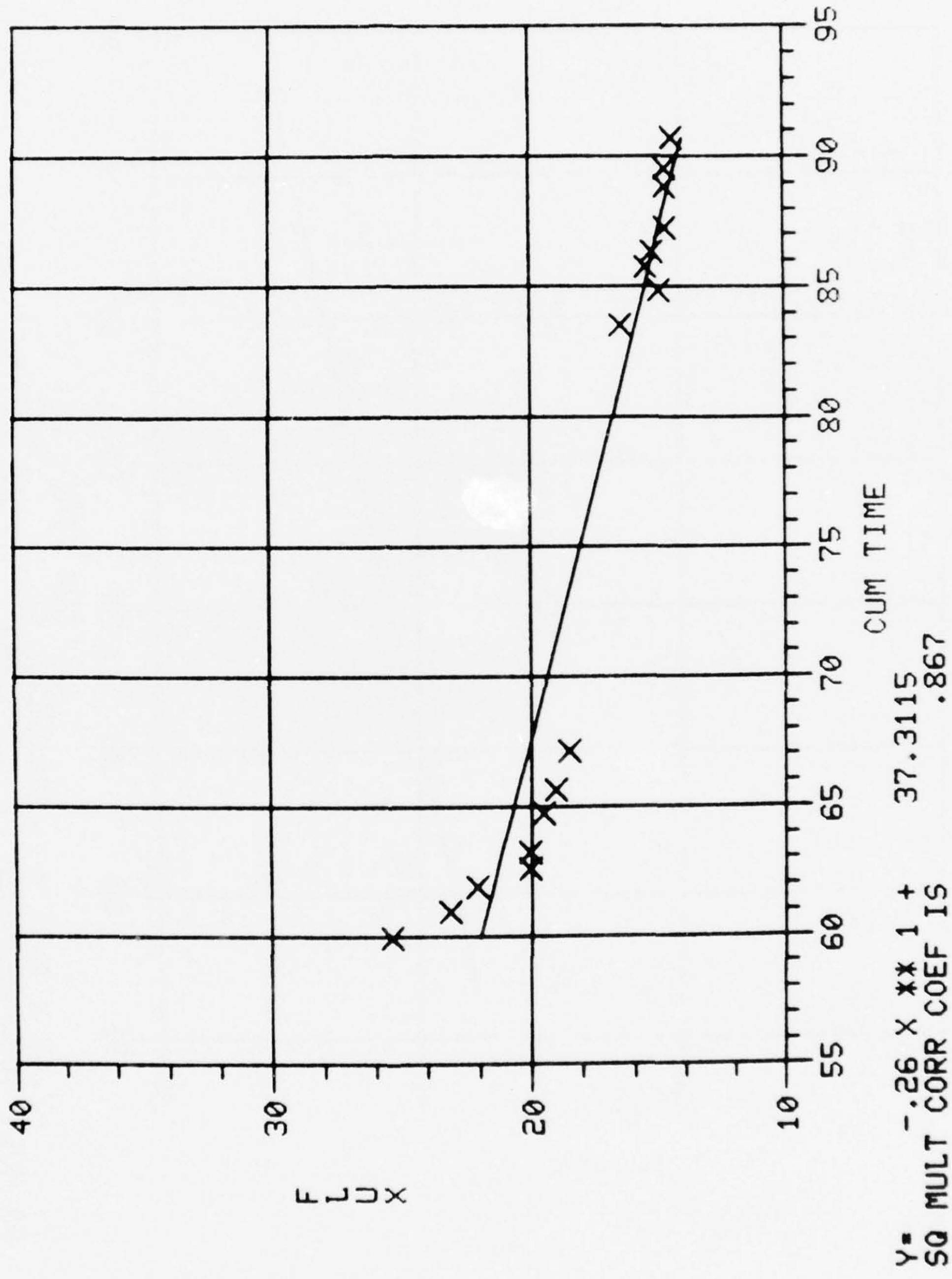
FLUX
CUM TIME
40
30
20
10
55
60
65
70
75
80
85
90
95
Y= -.26 X ** 1 + 37.3115
SQ MULT CORR COEF IS .867

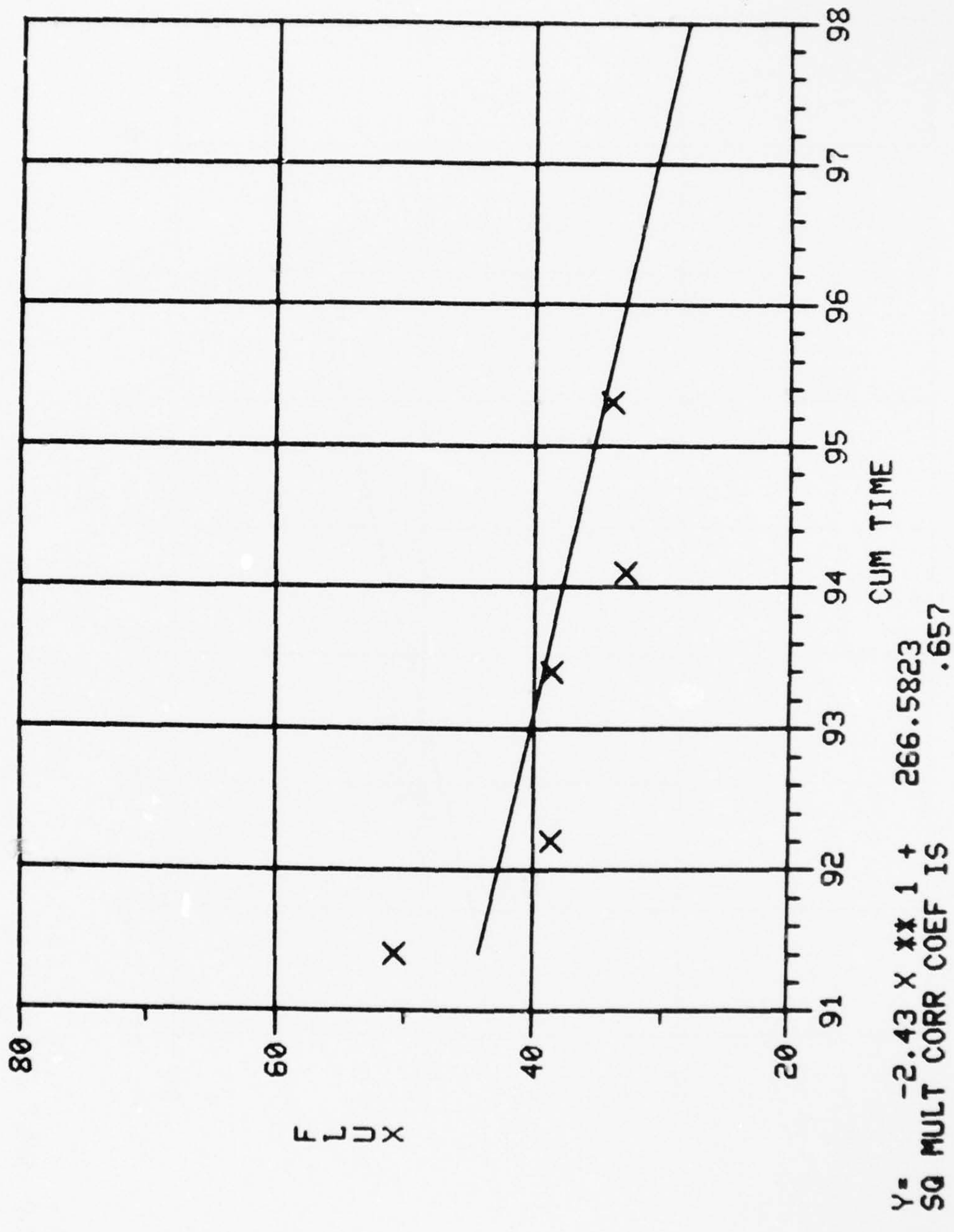
FLUX
80
60
40
20
91
92
93
94
95
96
97
98
CUM TIME
Y= -2.43 X ** 1 + 266.5823
SQ MULT CORR COEF IS .657

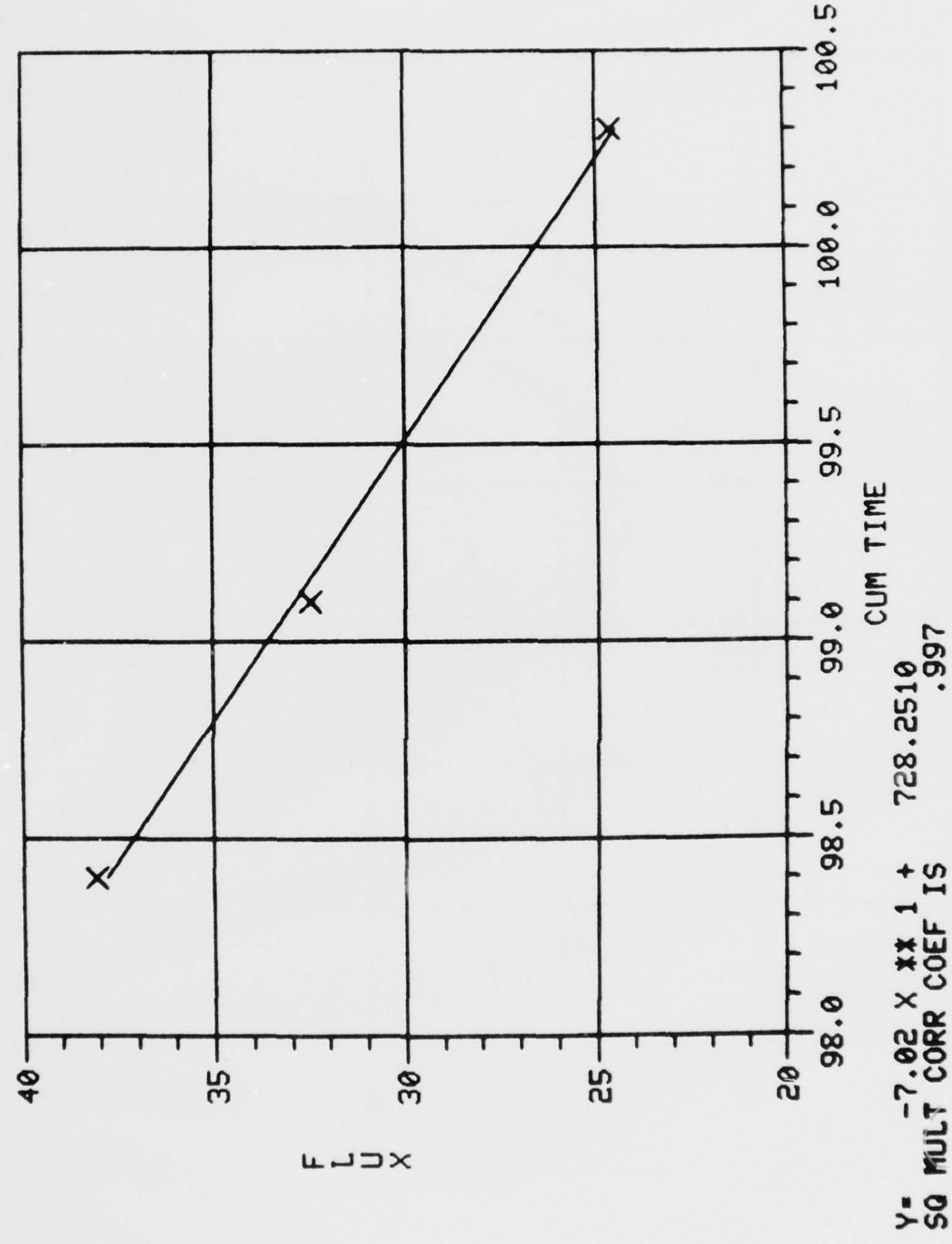

FLUX
CUM TIME
40
35
30
25
20
98.0
98.5
99.0
99.5
100.0
100.5
Y= -7.02 X ** 1 + 728.2510
SQ MULT CORR COEF IS .997

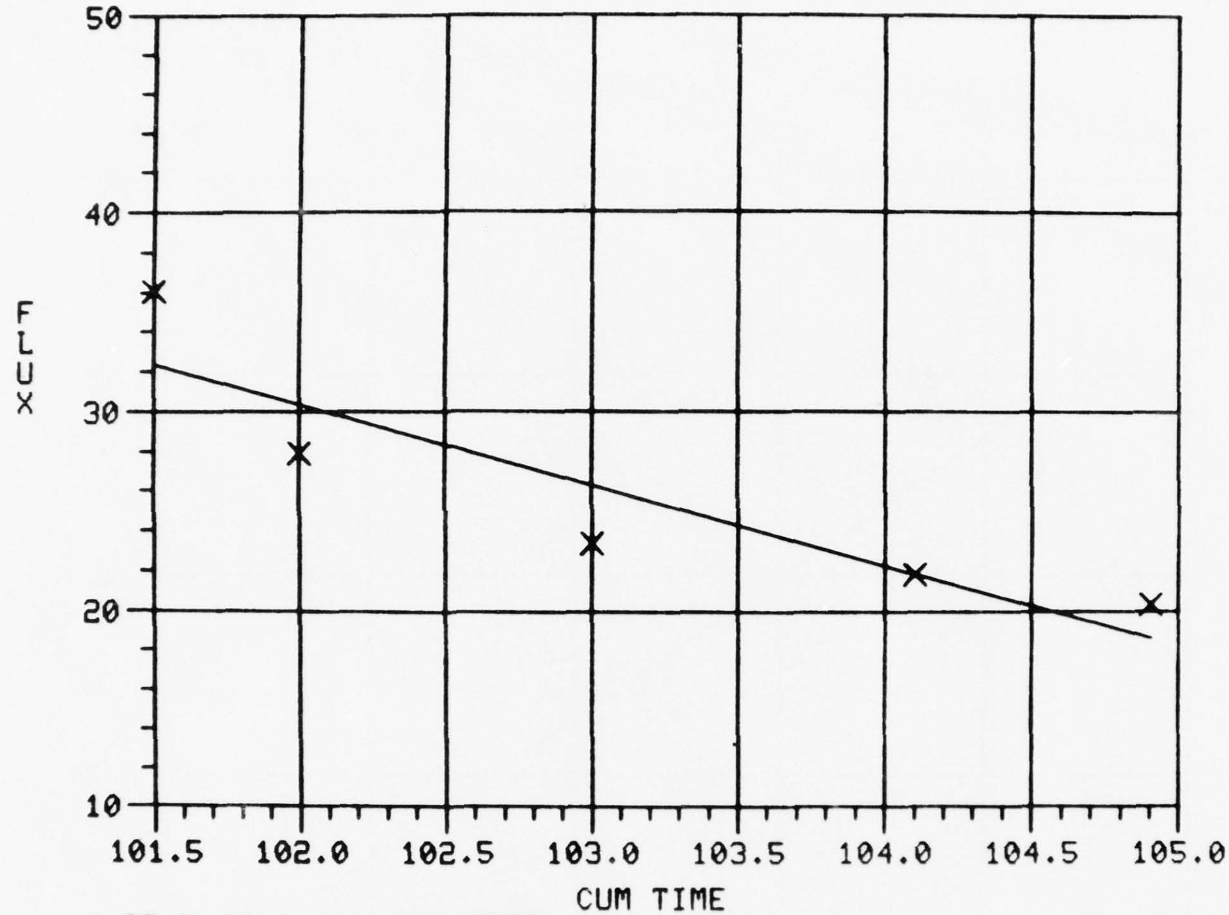


Y= -4.03 X ** 1 + 441.0528
SQ MULT CORR COEF IS .808

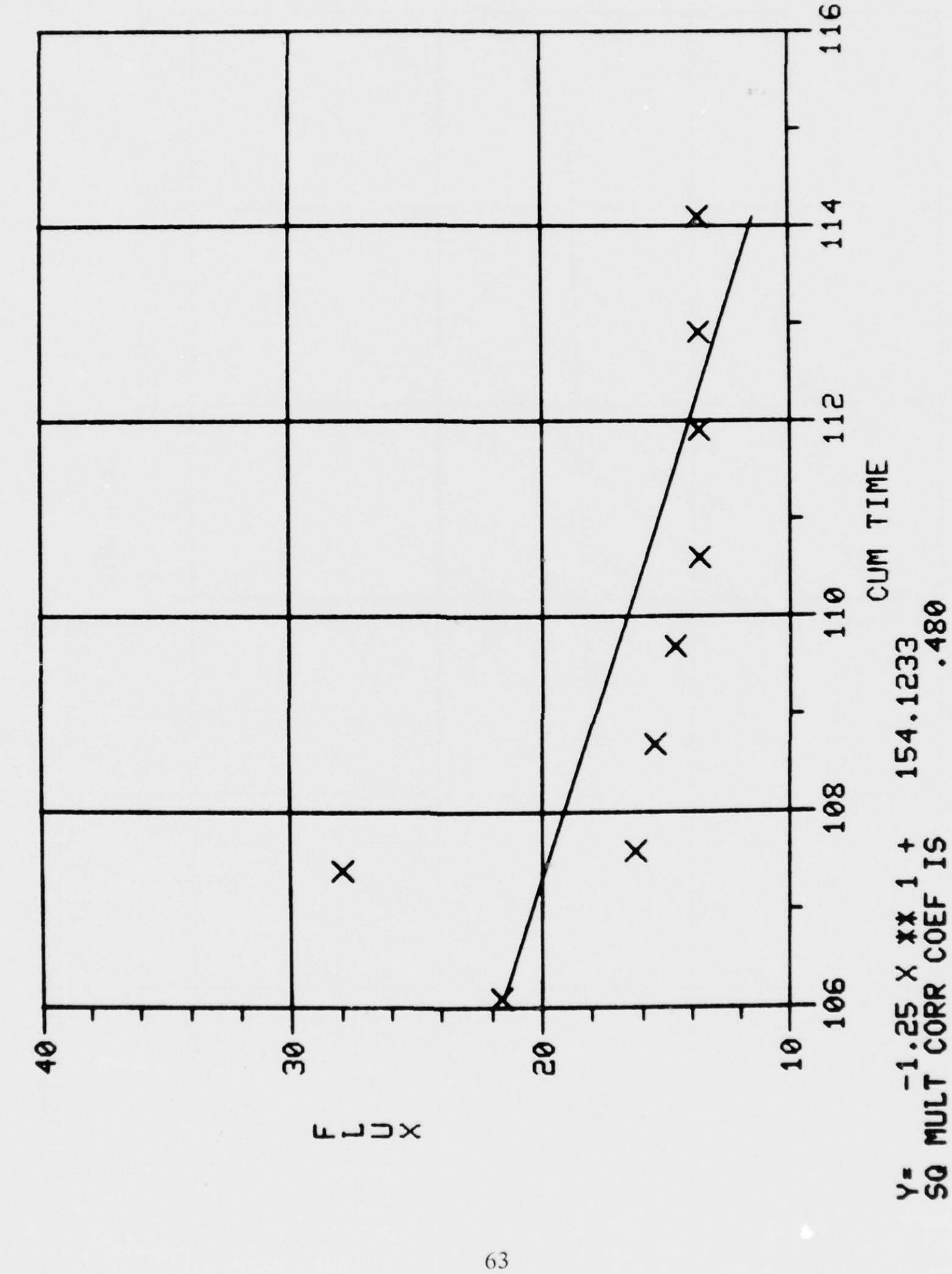
FLUX
40
30
20
10
106
108
110
112
114
116
CUM TIME
Y= -1.25 X ** 1 + 154.1233
SQ MULT CORR COEF IS .480

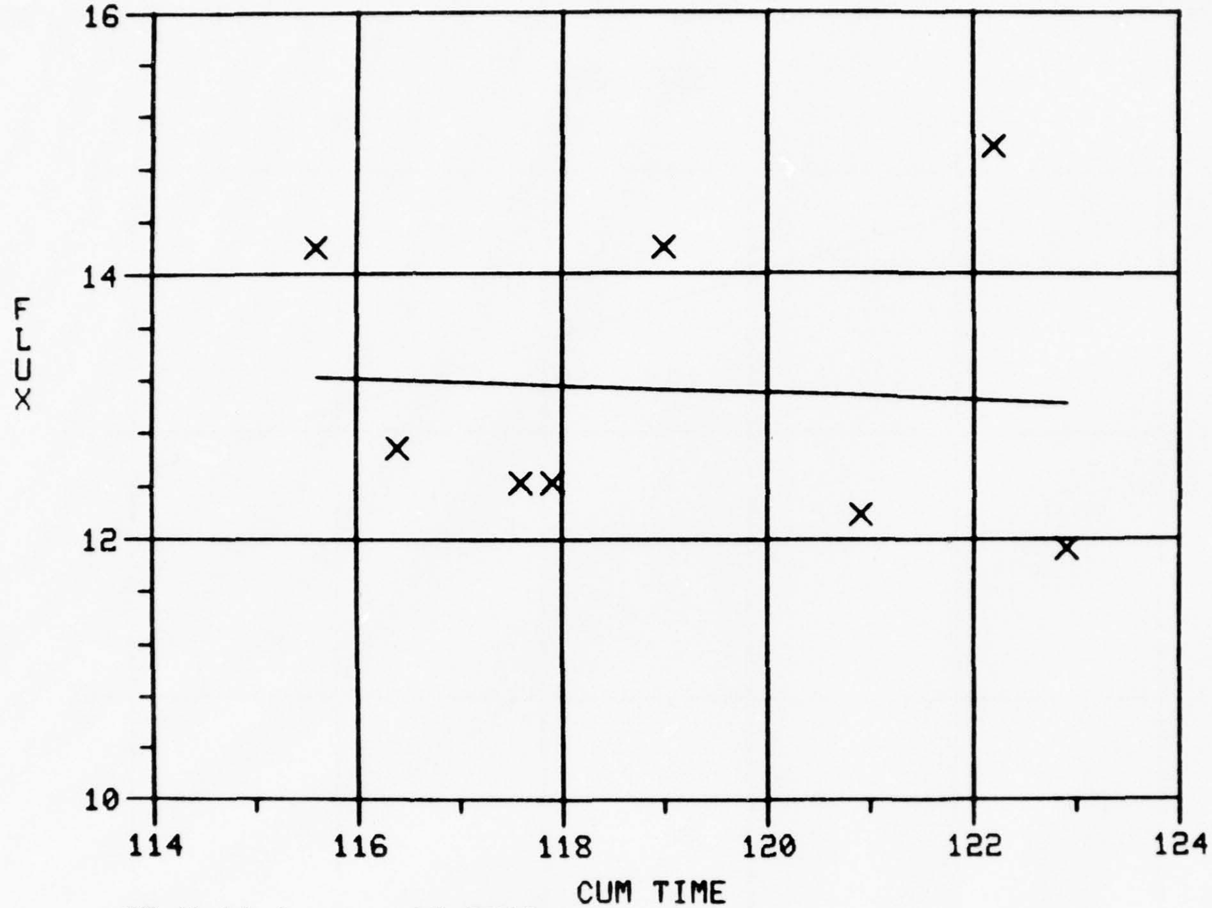


Y= -.03 X ** 1 + 16.3213
SQ MULT CORR COEF IS .004

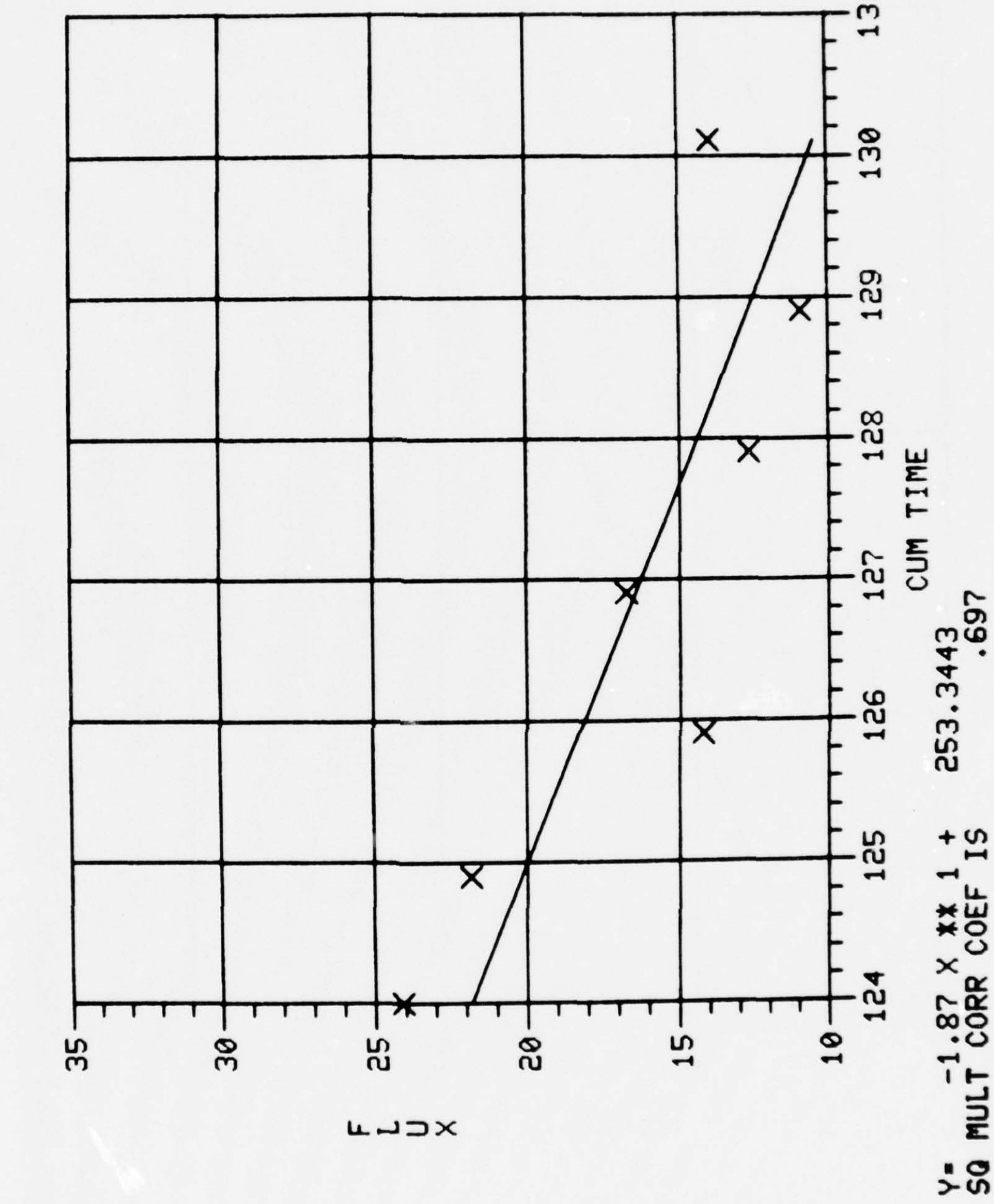
FLUX
35
30
25
20
15
10
124
125
126
127
128
129
130
131
CUM TIME
Y= -1.87 X ** 1 + 253.3443
SQ MULT CORR COEF IS .697

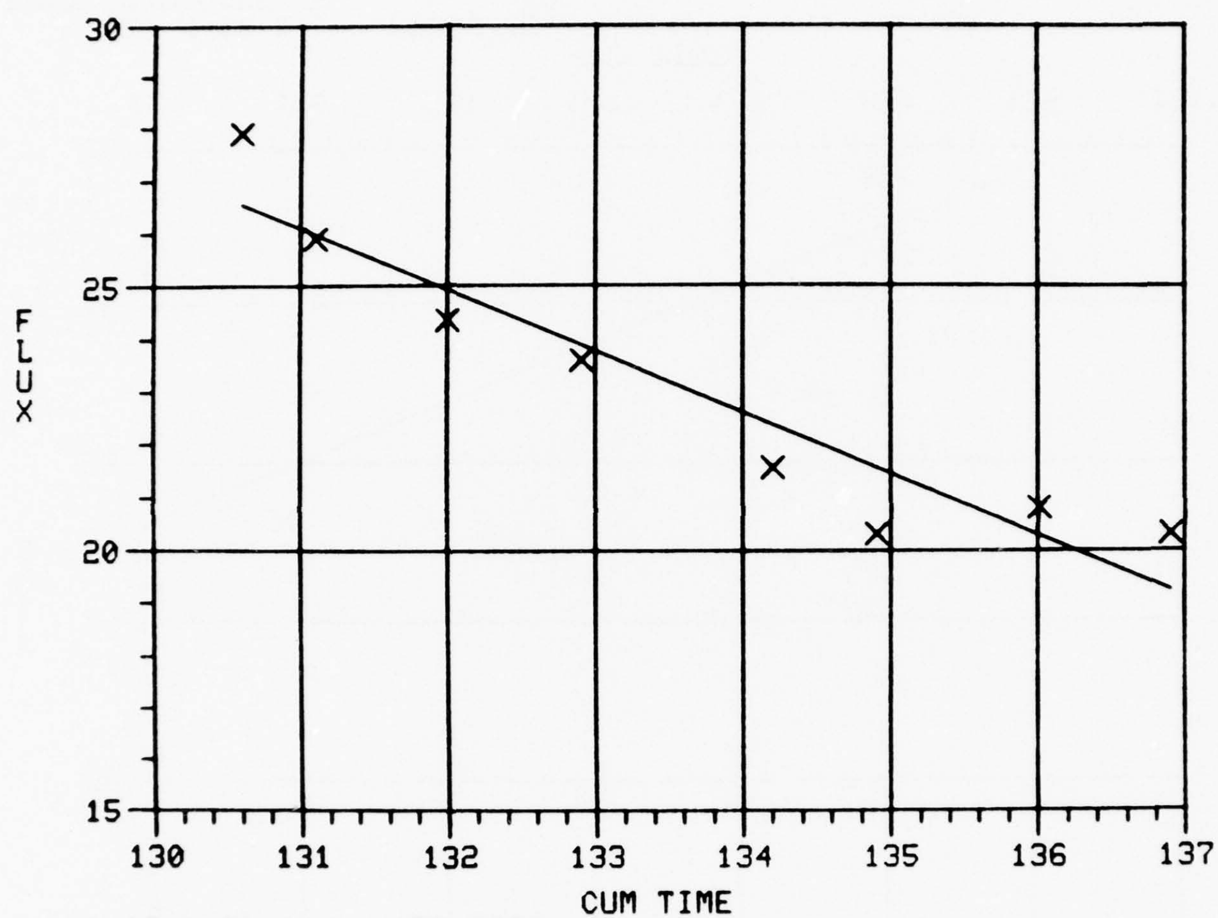


Y= -1.16 X ** 1 + 178.3303
SQ MULT CORR COEF IS .894

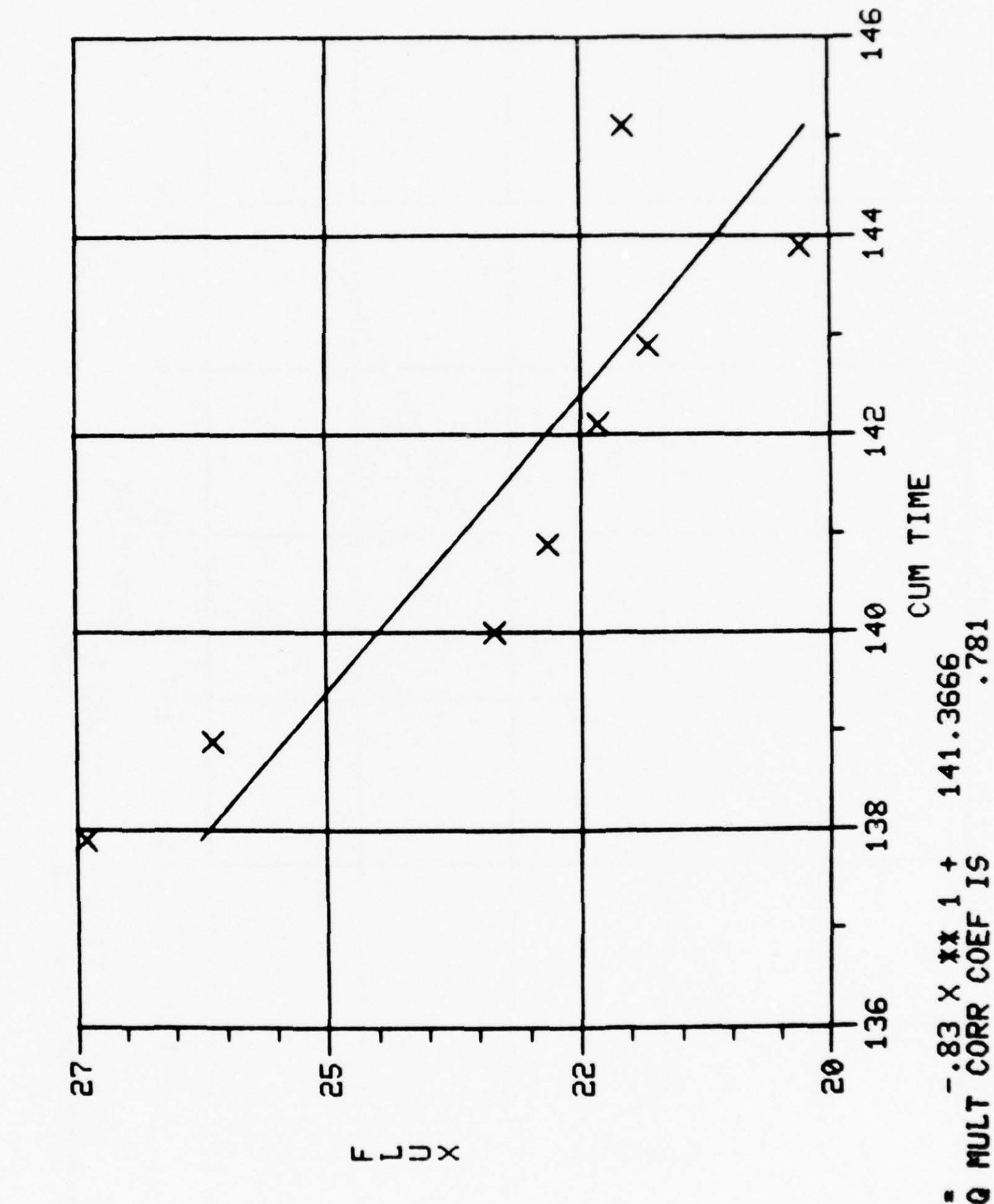
FLUX
CUM TIME
27
25
22
20
136
138
140
142
144
146
Y= -.83 X ** 1 + 141.3666
SQ MULT CORR COEF IS .781

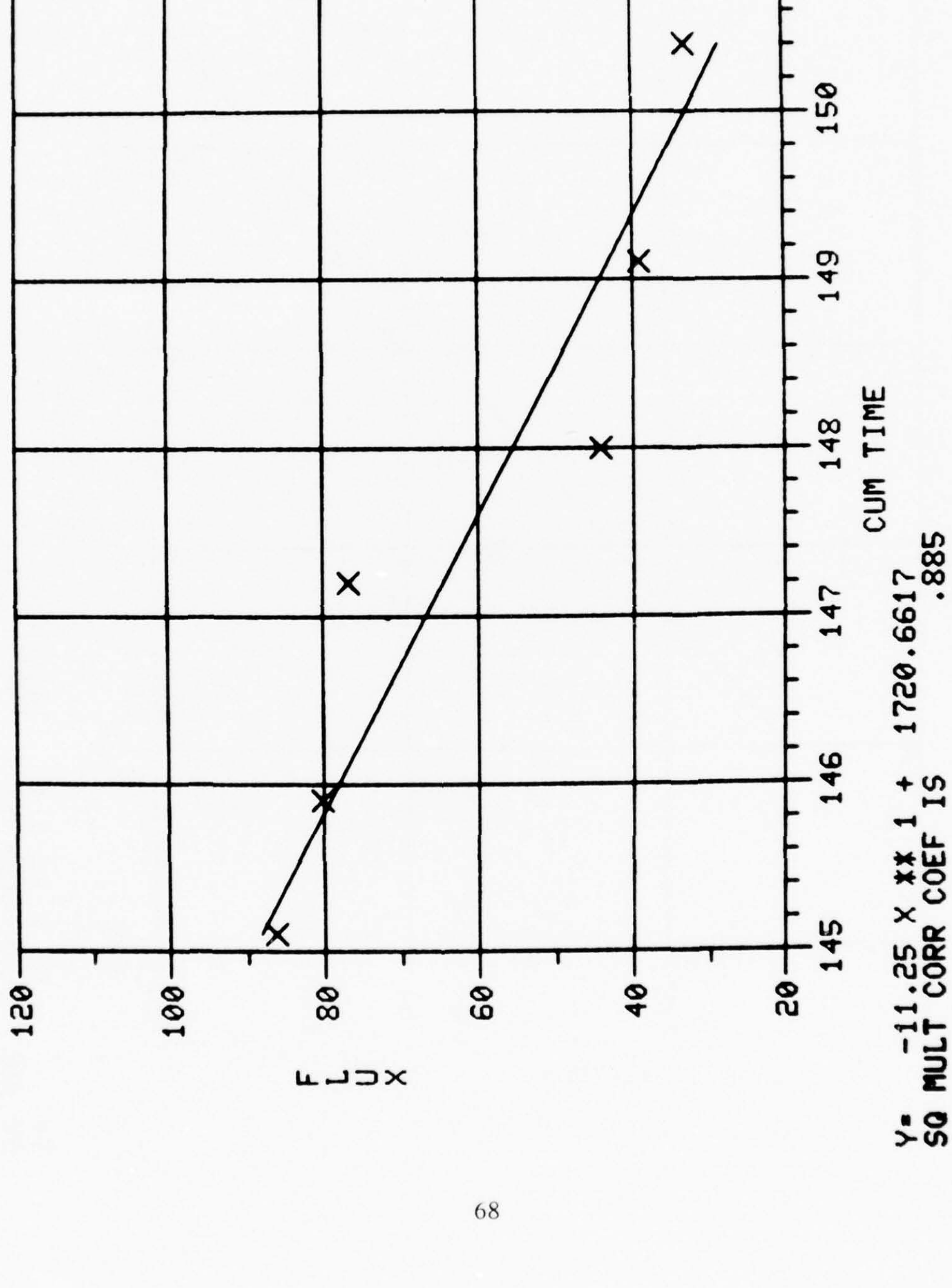
FLUX
CUM TIME
120
100
80
60
40
20
145
146
147
148
149
150
151
Y= -11.25 X ** 1 + 1720.6617
SQ MULT CORR COEF IS .885

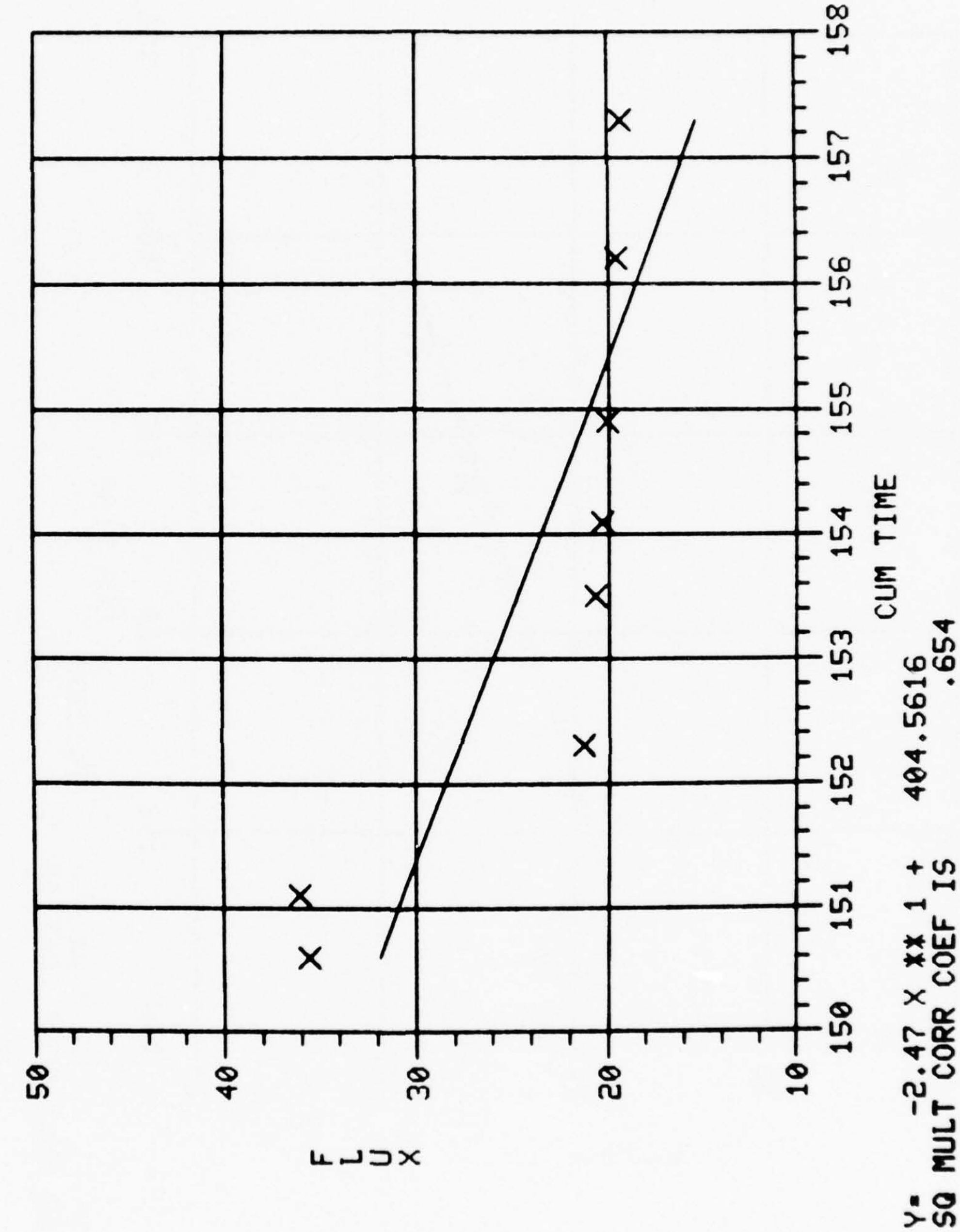
FLUX
50
40
30
20
10
150
151
152
153
154
155
156
157
158
CUM TIME
Y= -2.47 X ** 1 + 404.5616
SQ MULT CORR COEF IS .654

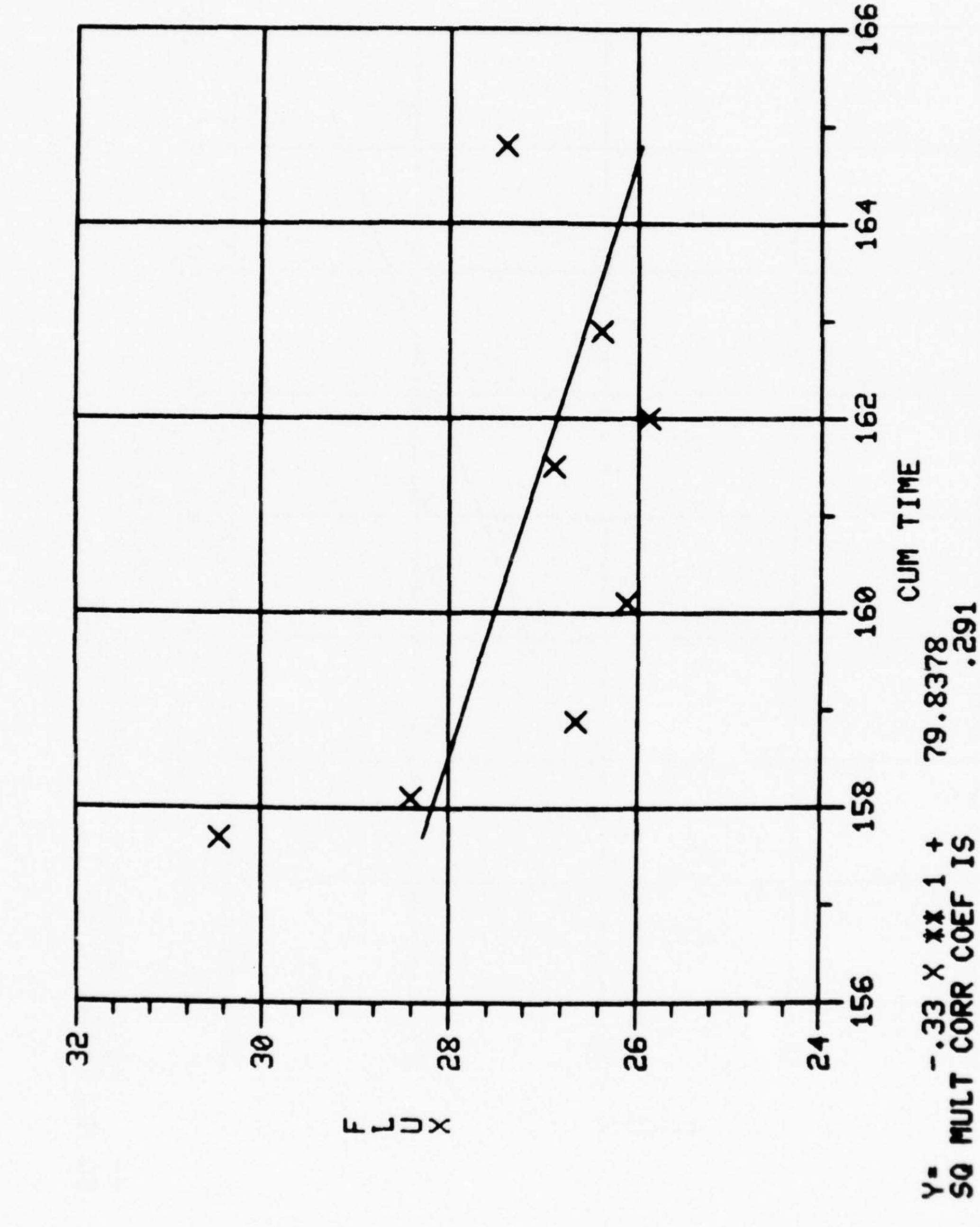
FLUX
32
30
28
26
24
156
158
160
162
164
166
CUM TIME
Y= -.33 X ** 1 + 79.8378
SQ MULT CORR COEF IS .291

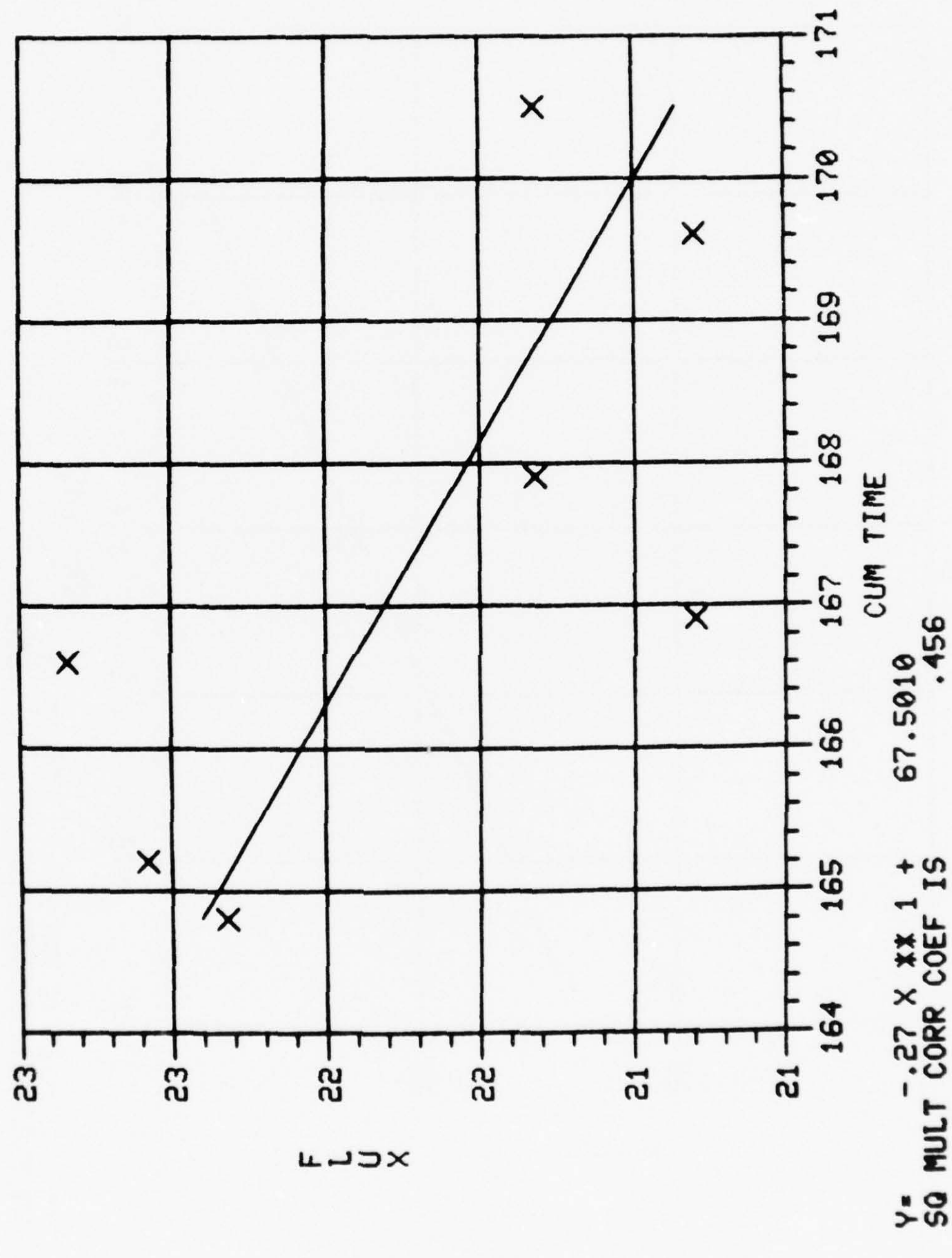
FLUX
CUM TIME
164
165
166
167
168
169
170
171
23
23
22
22
21
21
Y= -.27 X ** 1 + 67.5010
SQ MULT CORR COEF IS .456

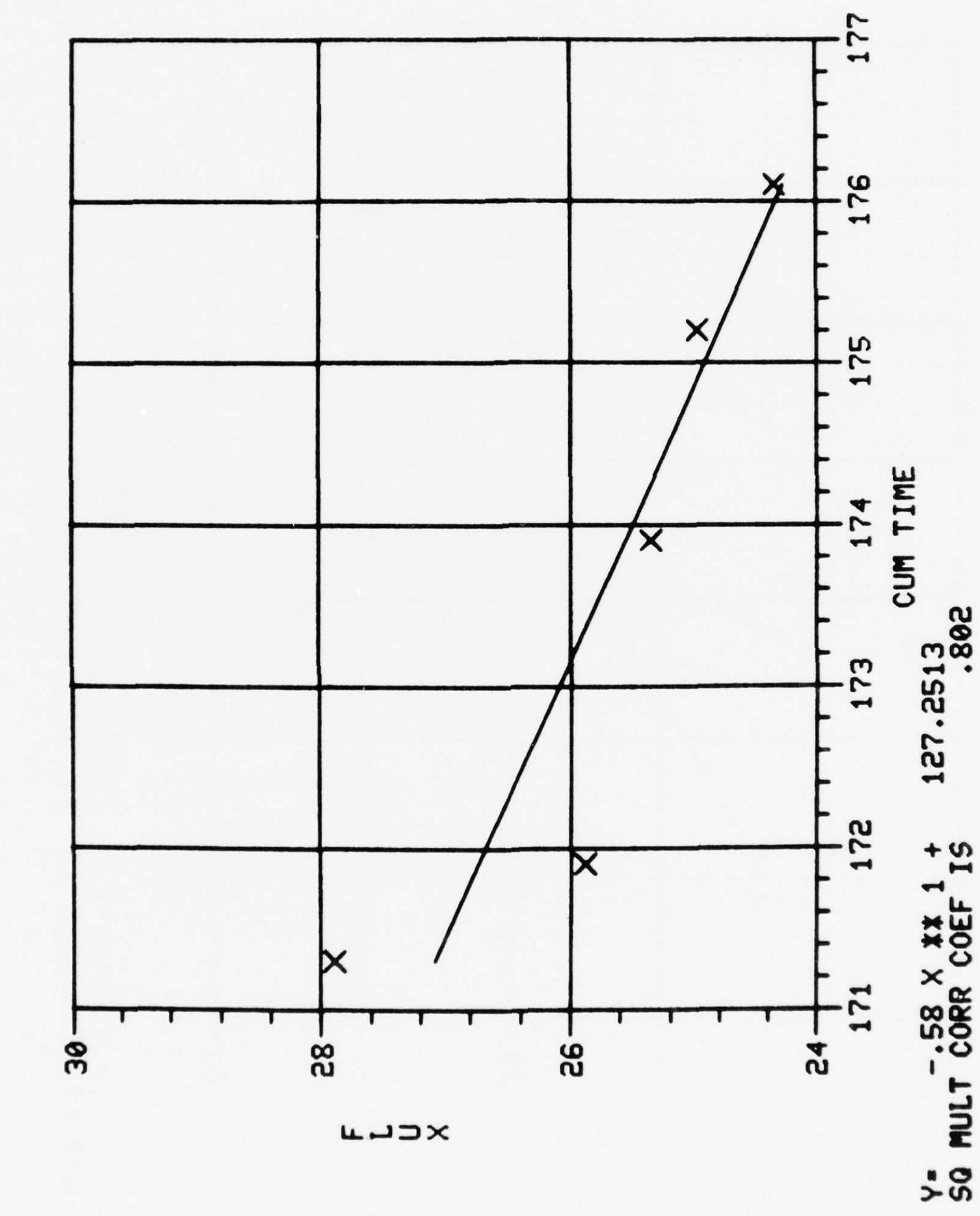
FLUX
30
28
26
24
171
172
173
174
175
176
177
CUM TIME
Y= -.58 X ** 1 + 127.2513
SQ MULT CORR COEF IS .802

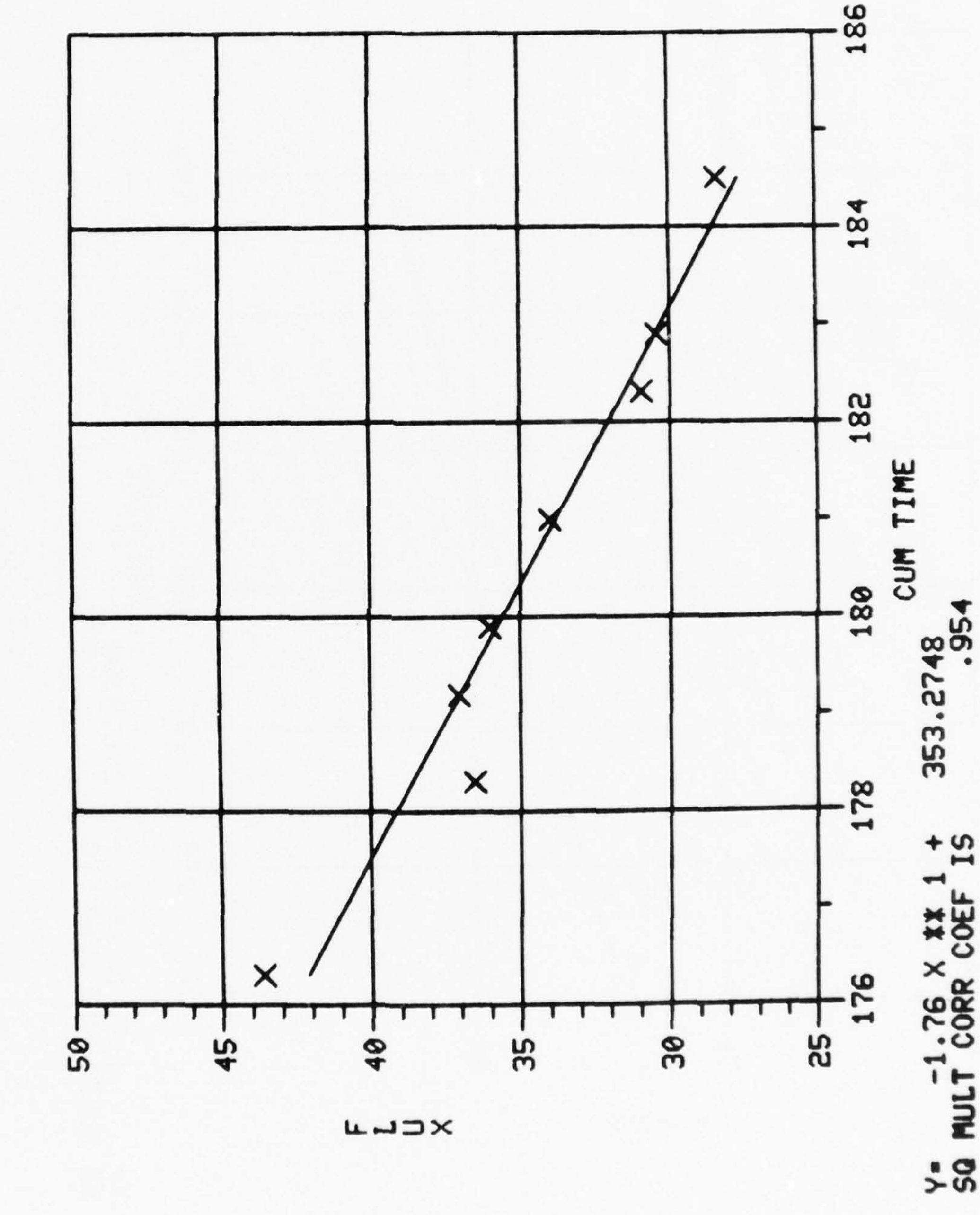
FLUX
50
45
40
35
30
25
176
178
180
182
184
186
CUM TIME
Y= -1.76 X XX 1 + 353.2748
SQ MULT CORR COEF IS .954

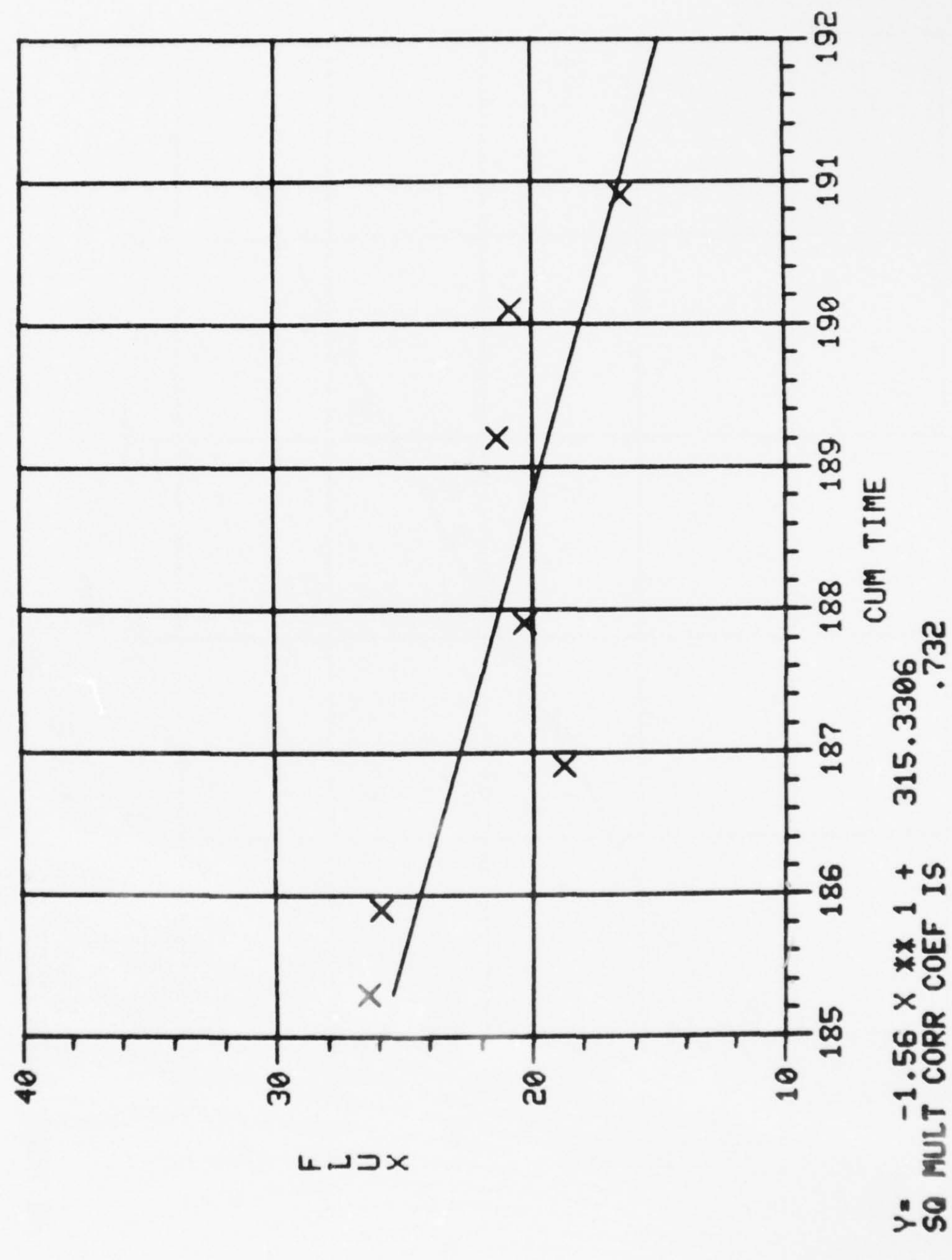
FLUX
40
30
20
10
185
186
187
188
189
190
191
192
CUM TIME
Y= -1.56 X ** 1 + 315.3306
SQ MULT CORR COEF IS .732

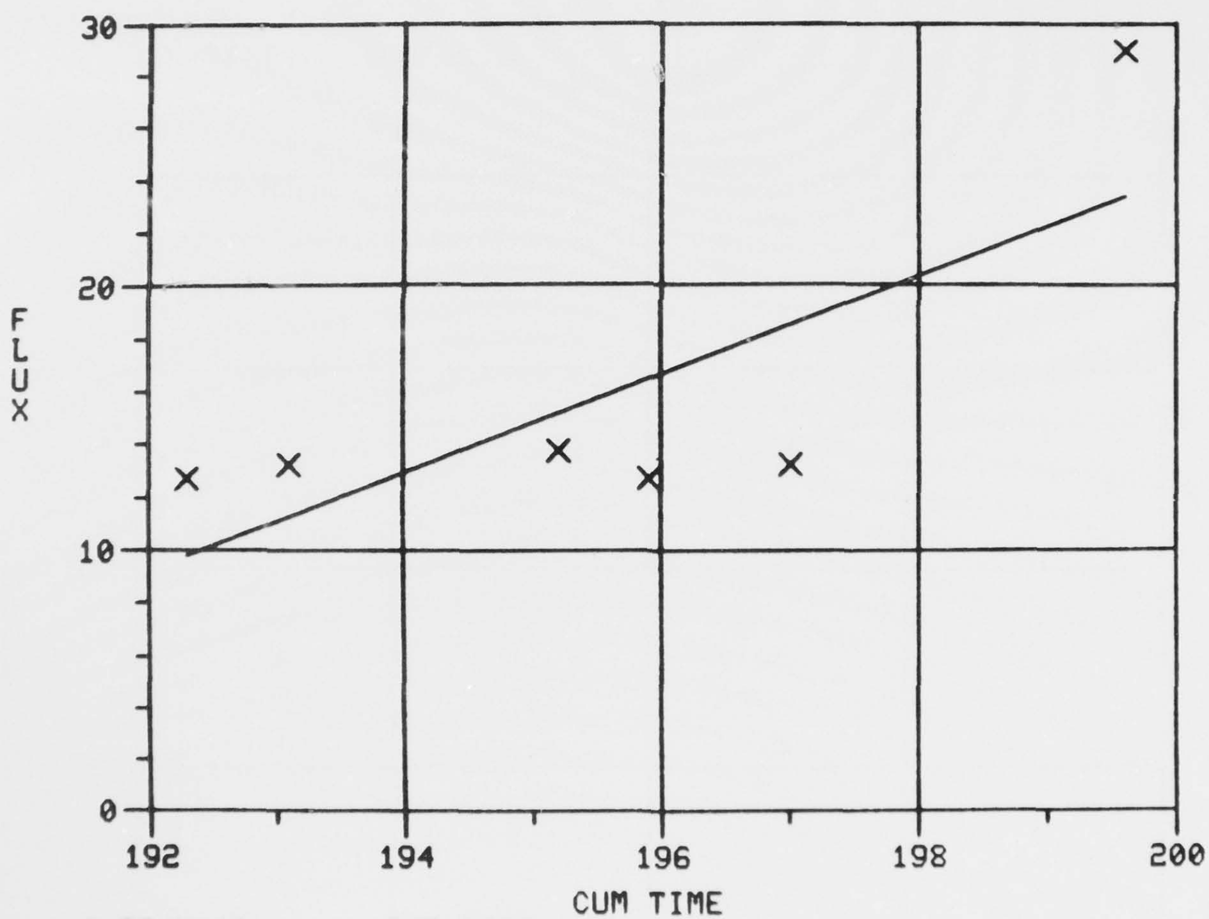


Y= 1.86 X ** 1 + -347.1080
SQ MULT CORR COEF IS .580

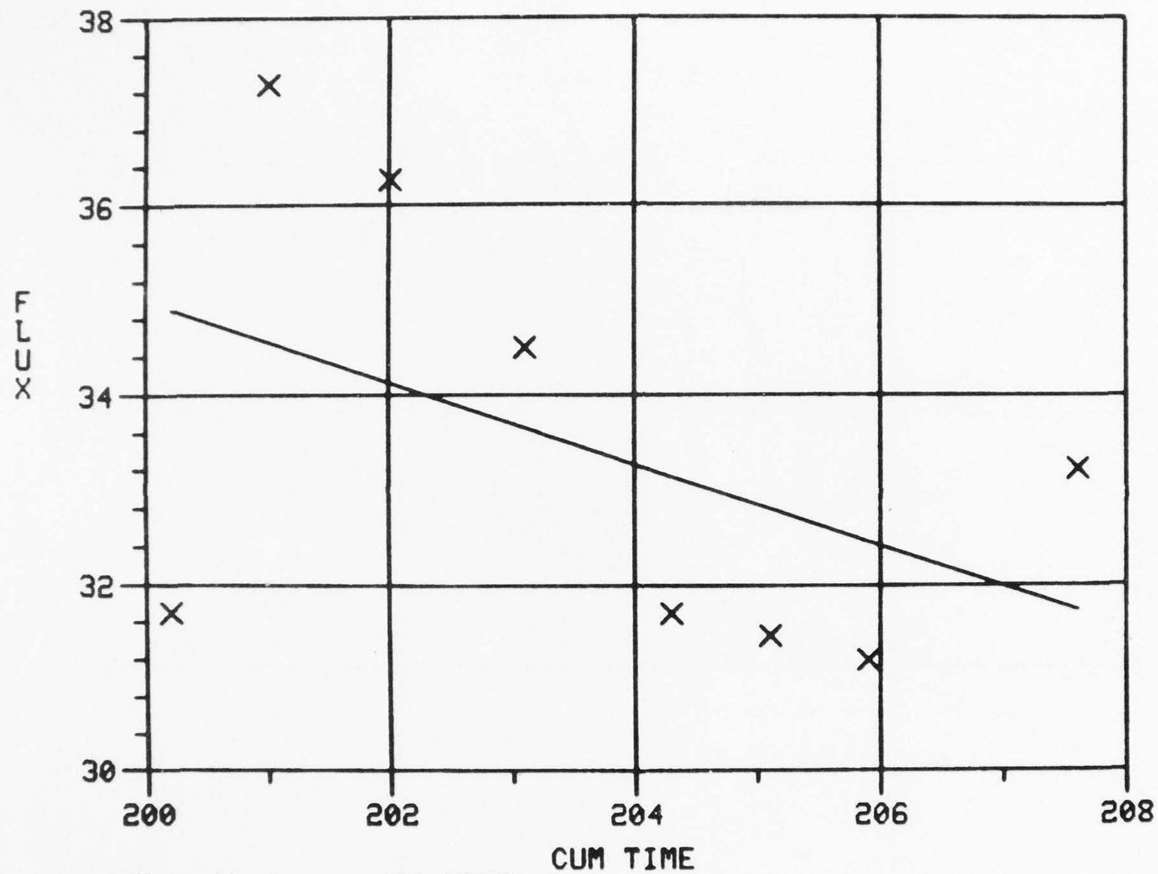


Y=      -.43 X ** 1 +    120.5776
SQ MULT CORR COEF IS          .213

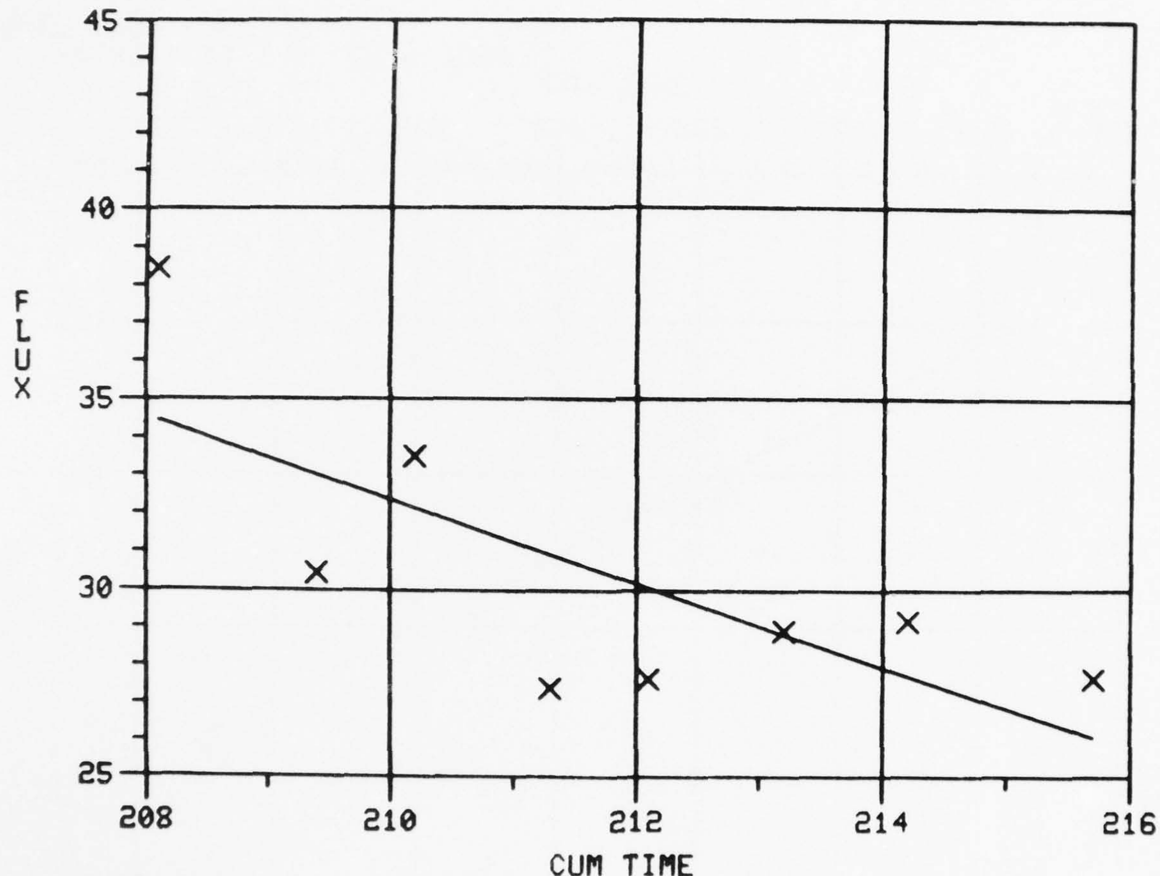


Y= -1.10 X ** 1 + 263.5177
SQ MULT CORR COEF IS .539

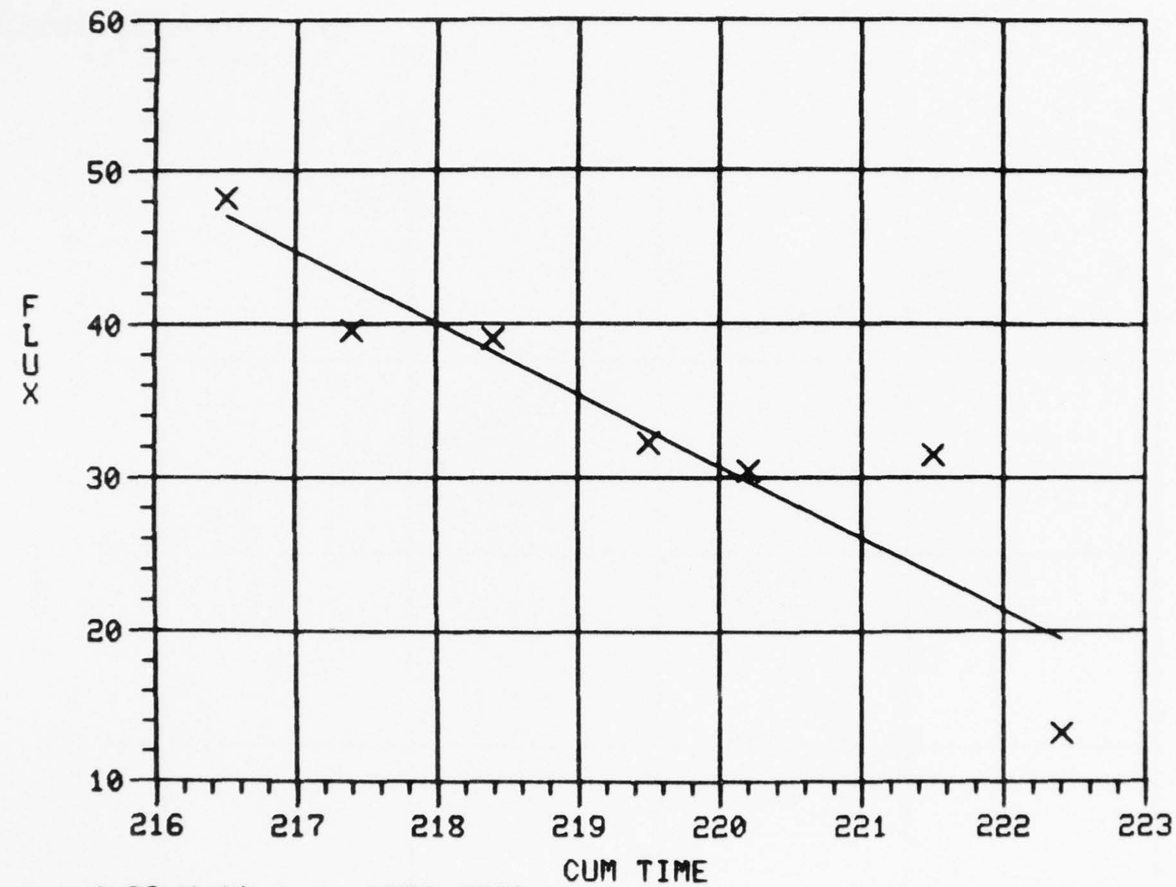


Y= -4.66 X ** 1 + 1056.8830
SQ MULT CORR COEF IS .840

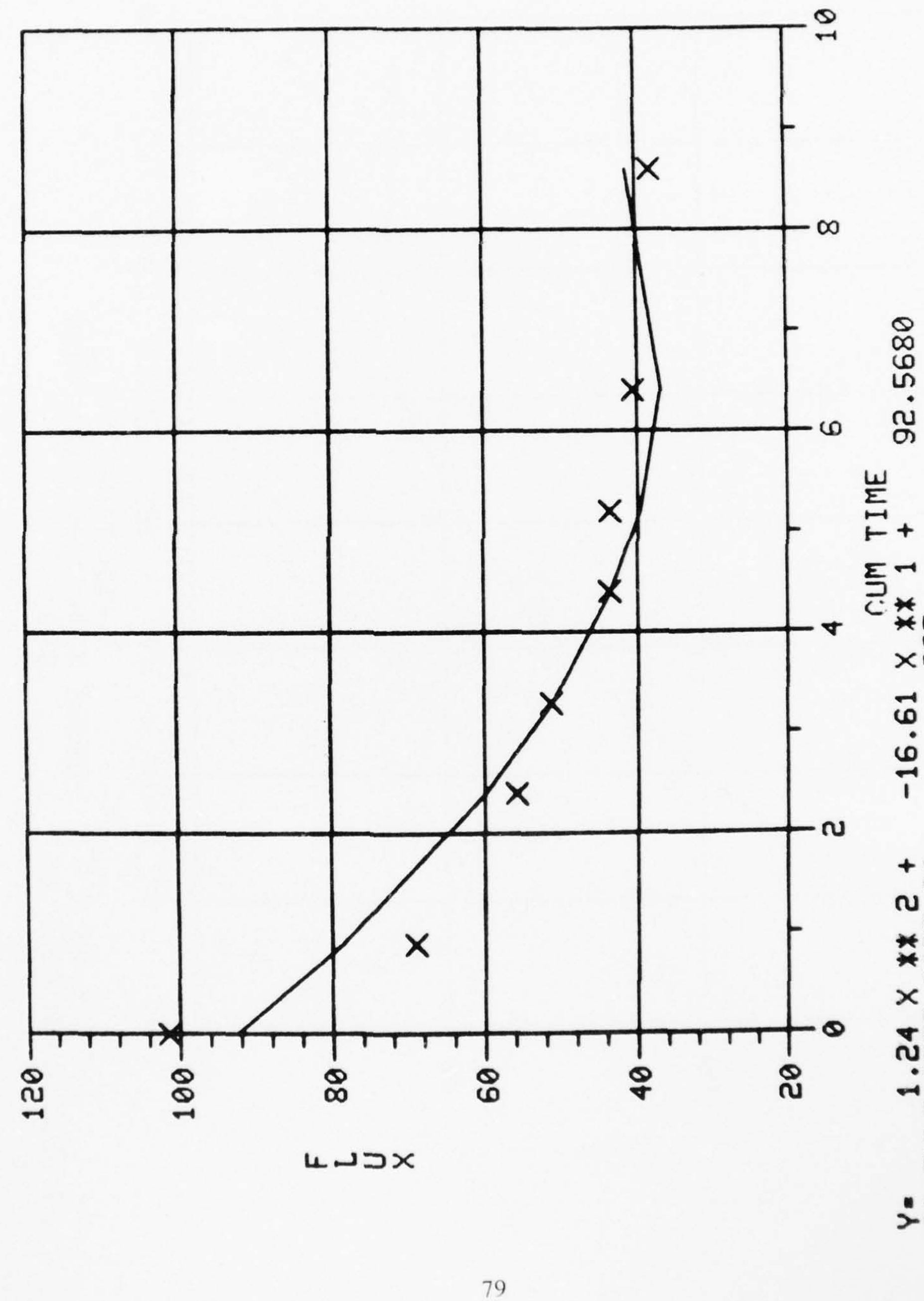
FLUX
CUM TIME
120
100
80
60
40
20
0
2
4
6
8
10
Y= 1.24 X ** 2 + -16.61 X ** 1 + 92.5680
SQ MULT CORR COEF IS .927

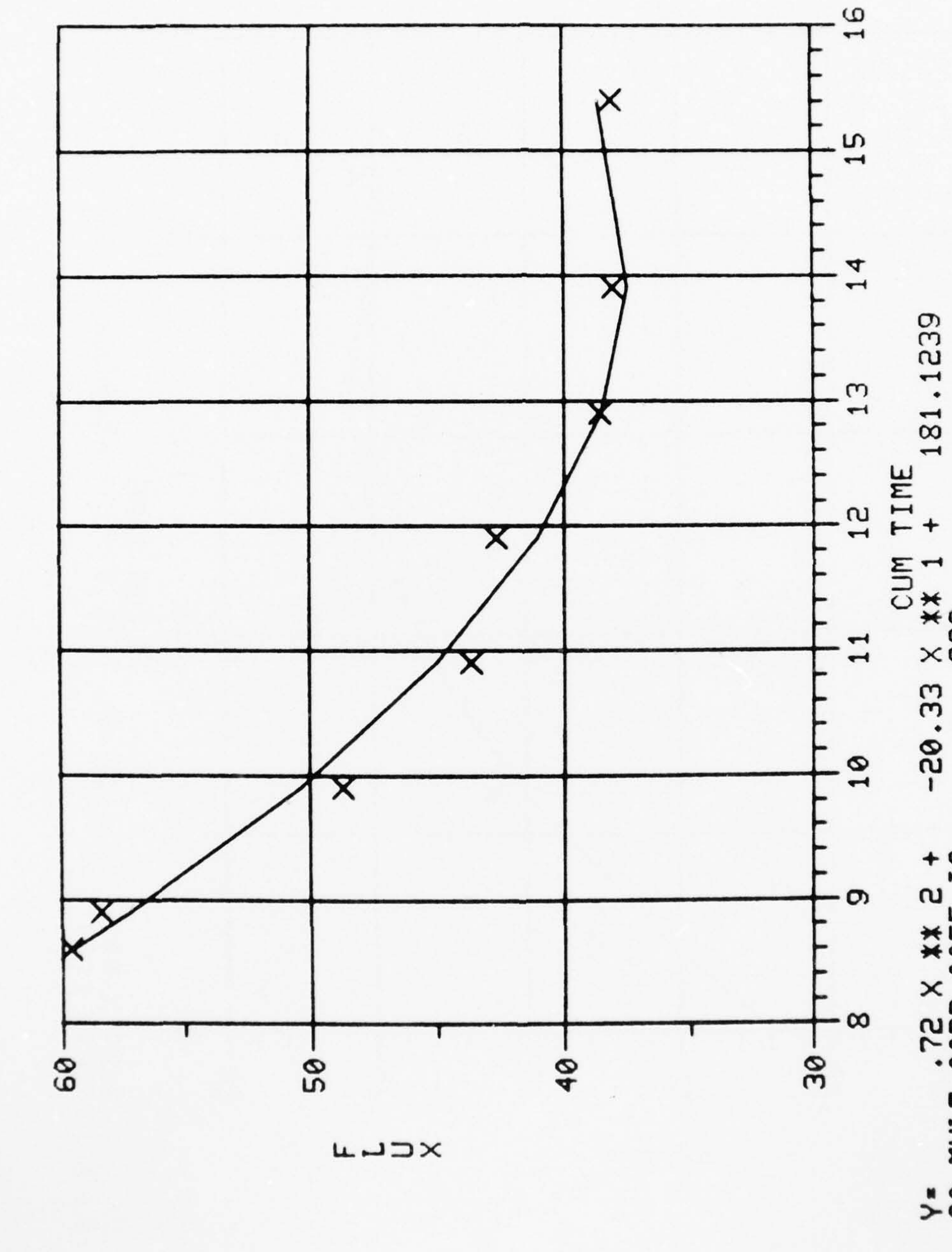
FLUX
60
50
40
30
8
9
10
11
12
13
14
15
16
CUM TIME
Y= .72 X ** 2 + -20.33 X ** 1 + 181.1239
SQ MULT CORR COEF IS .983

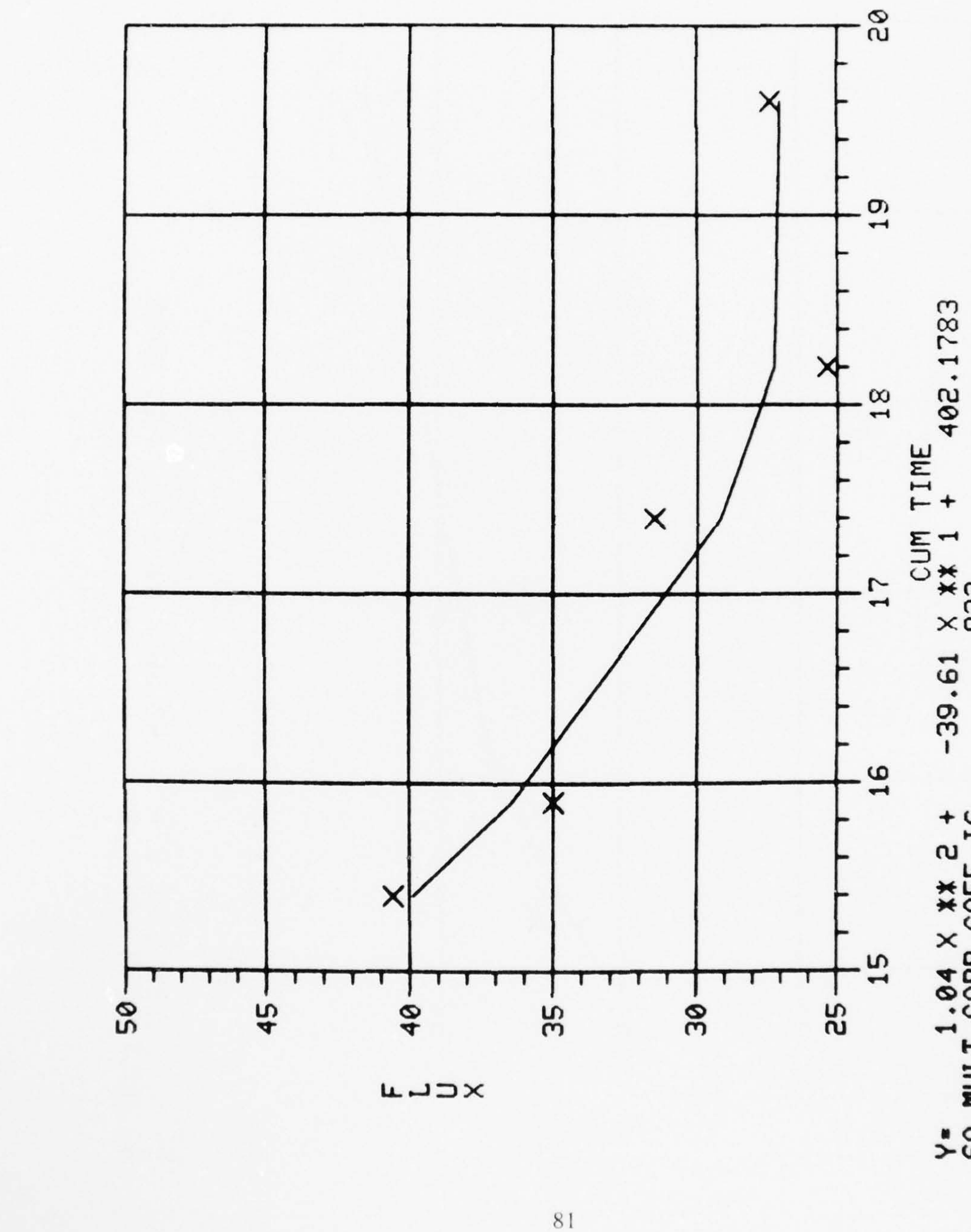
F
L
U
X
50
45
40
35
30
25
15
16
17
18
19
20
CUM TIME
Y= 1.04 X ** 2 + -39.61 X ** 1 + 402.1783
SQ MULT CORR COEF IS .923

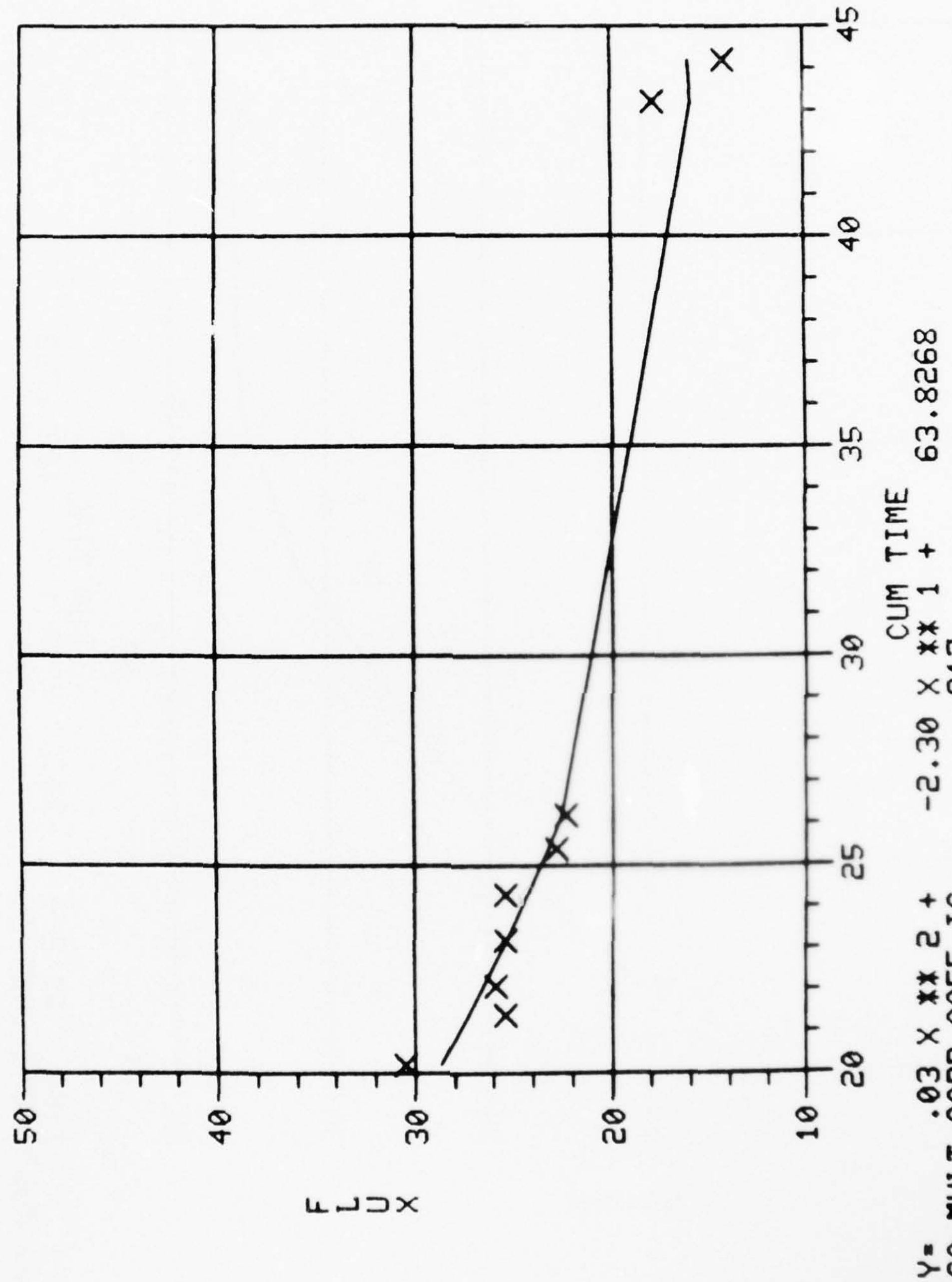

FLUX
50
40
30
20
10
20
25
30
35
40
45
CUM TIME
Y= .03 X ** 2 + -2.30 X ** 1 + 63.8268
SQ MULT CORR COEF IS .917

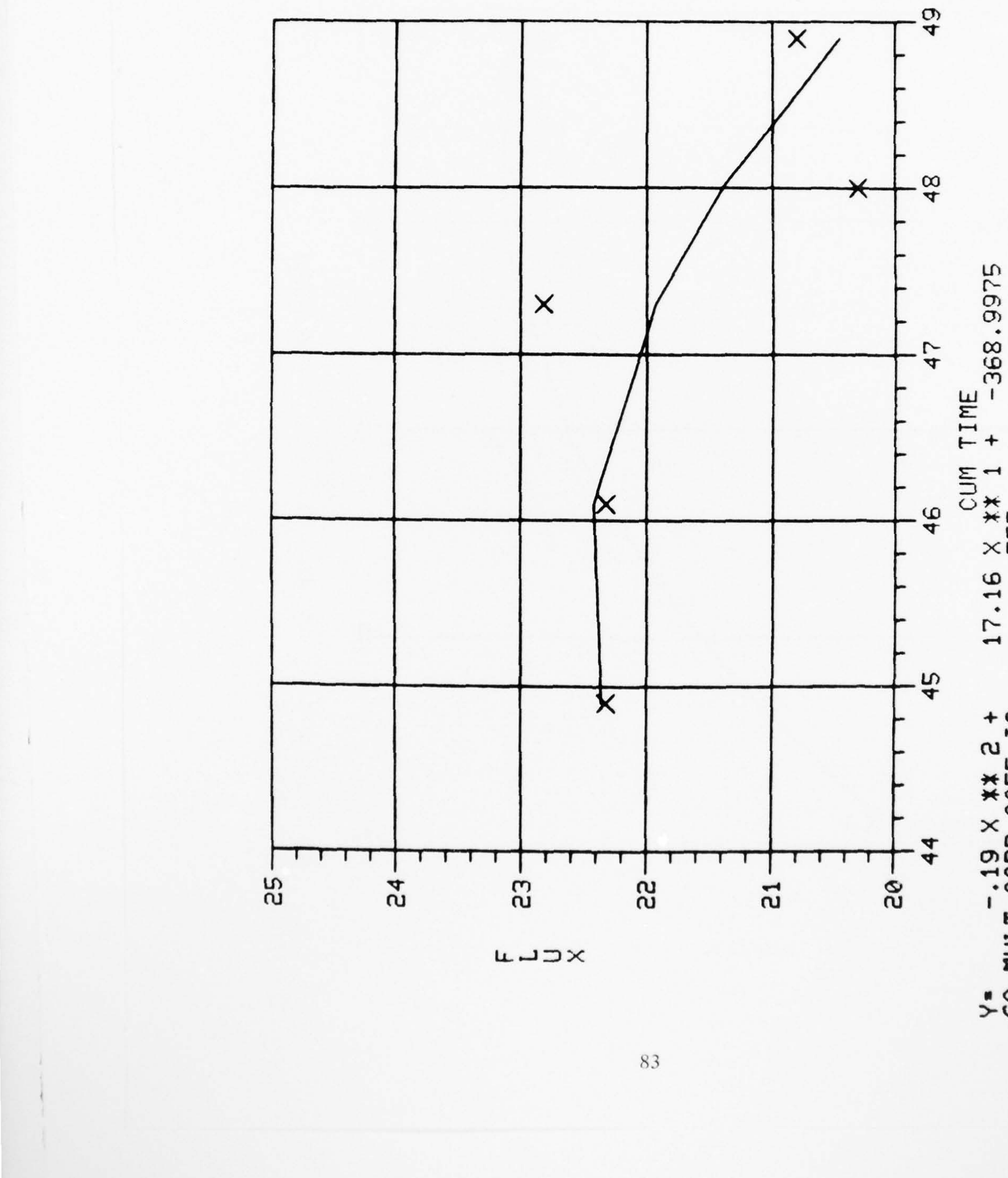

FLUX
25
24
23
22
21
20
44
45
46
47
48
49
CUM TIME
Y= -.19 X ** 2 + 17.16 X ** 1 + -368.9975
SQ MULT CORR COEF IS .555

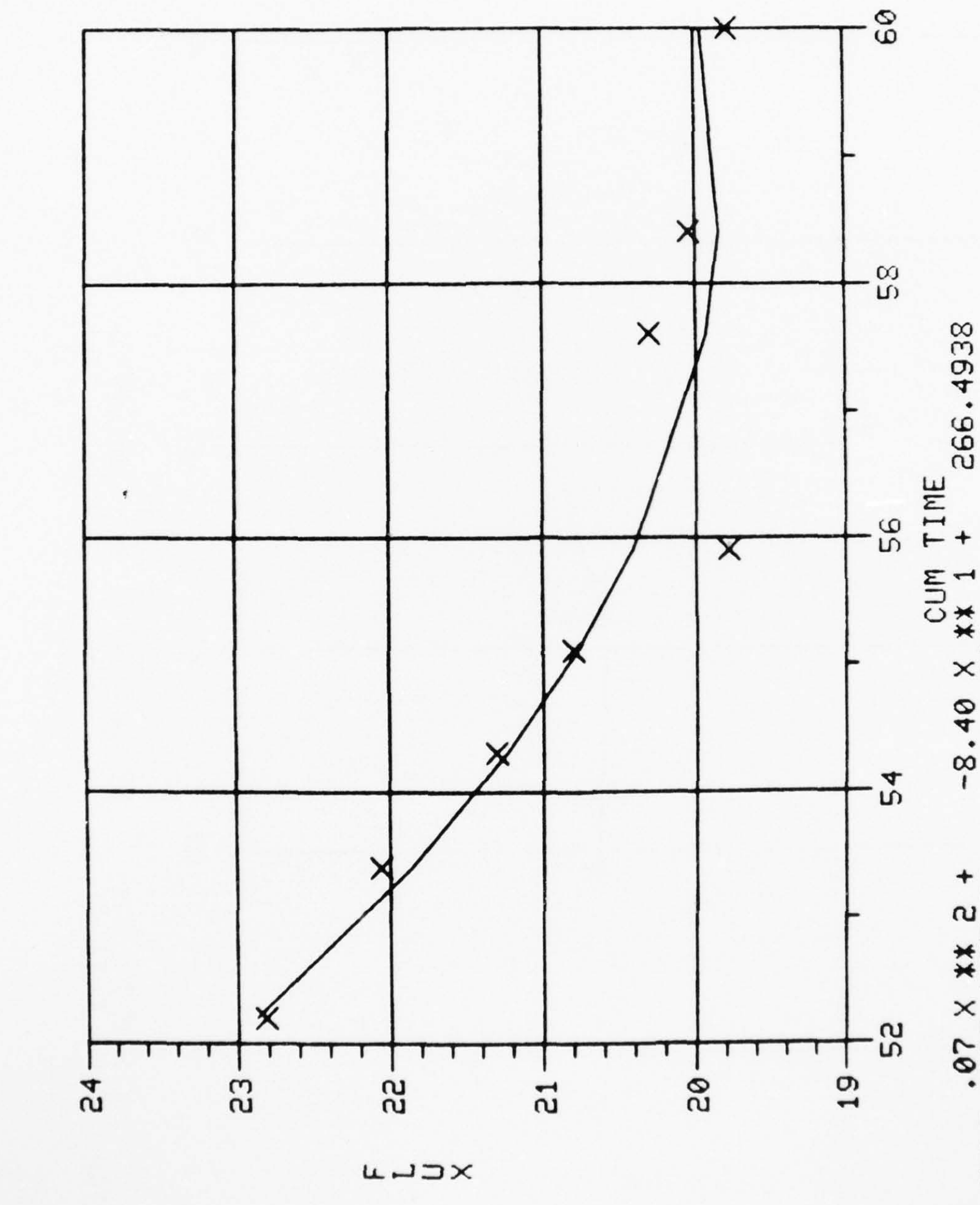

FLUX
24
23
22
21
20
19
52
54
56
58
60
CUM TIME
Y= .07 X ** 2 + -8.40 X ** 1 + 266.4938
SQ MULT CORR COEF IS .926

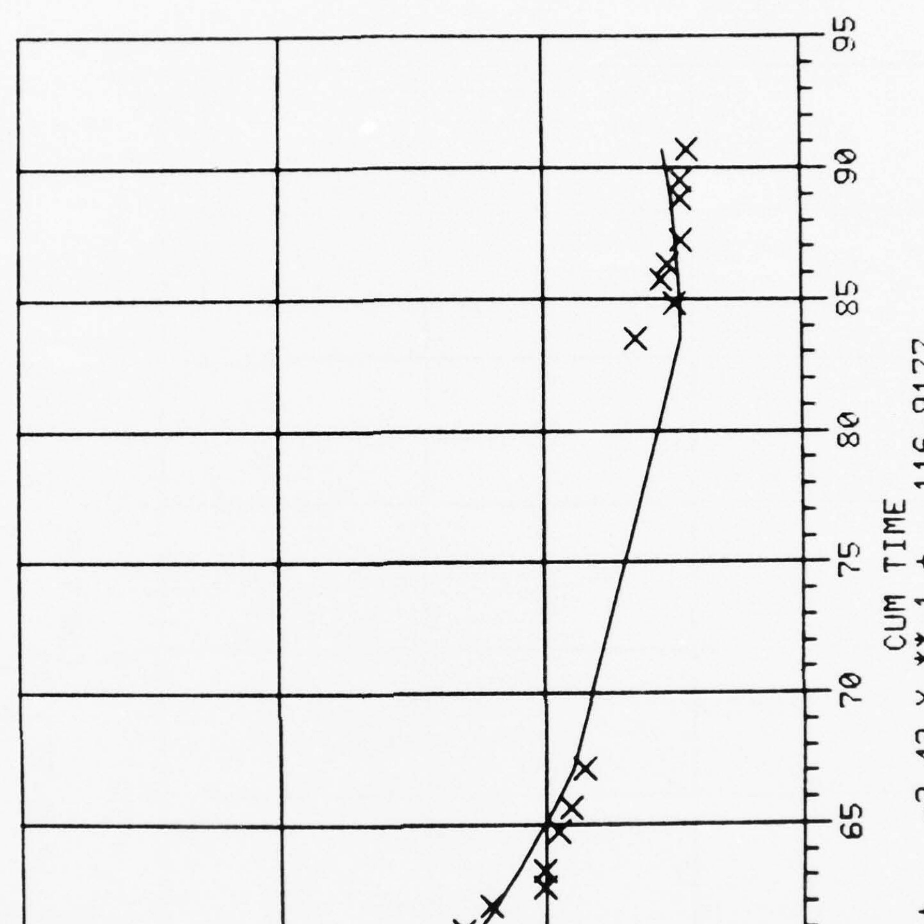
FLUX
40
30
20
10
55
60
65
70
75
80
85
90
95
CUM TIME
Y= .01 X ** 2 + -2.43 X ** 1 + 116.9177
SQ MULT CORR COEF IS .923

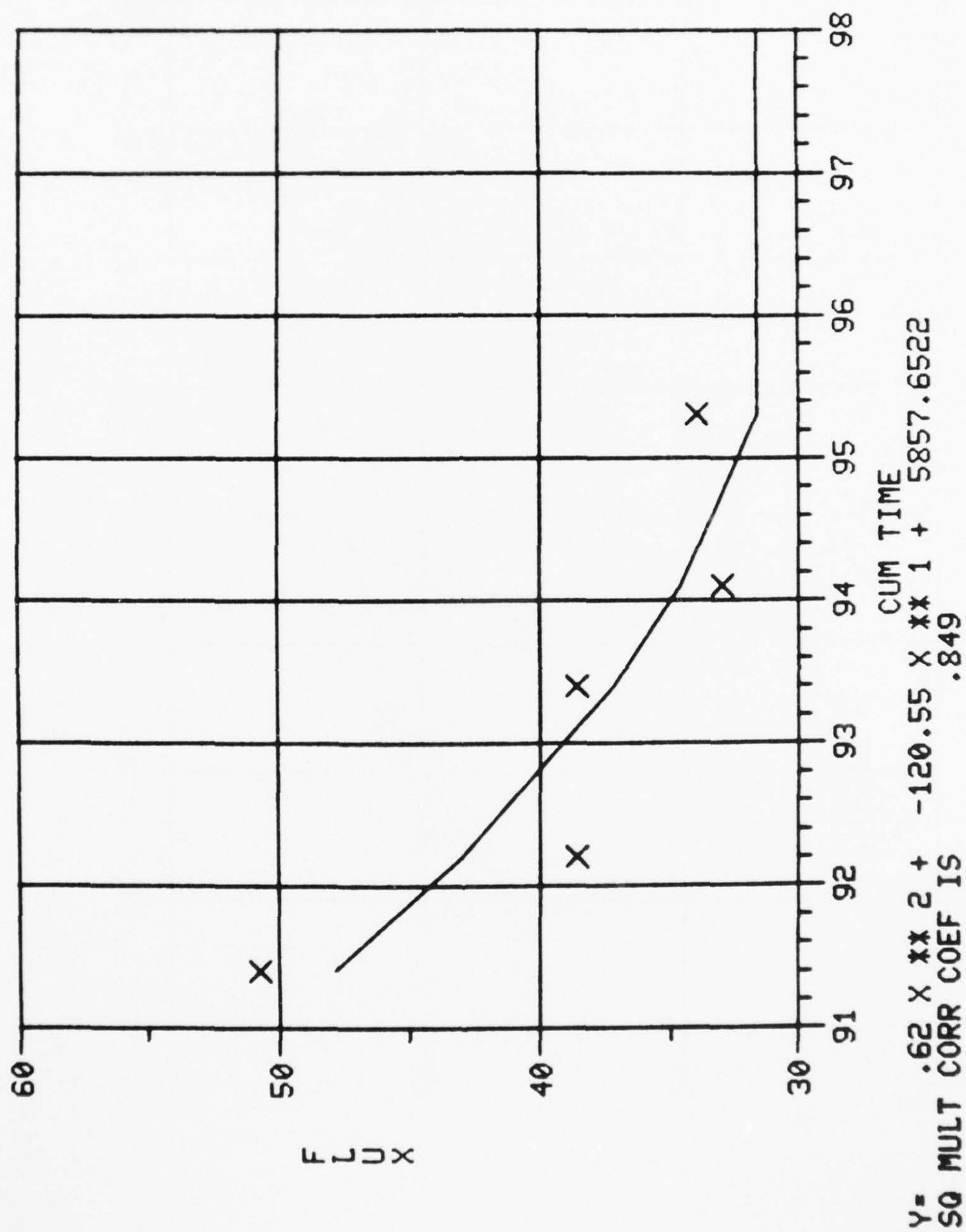
FLUX
60
50
40
30
91
92
93
94
95
96
97
98
CUM TIME
Y= .62 X ** 2 + -120.55 X ** 1 + 5857.6522
SQ MULT CORR COEF IS .849

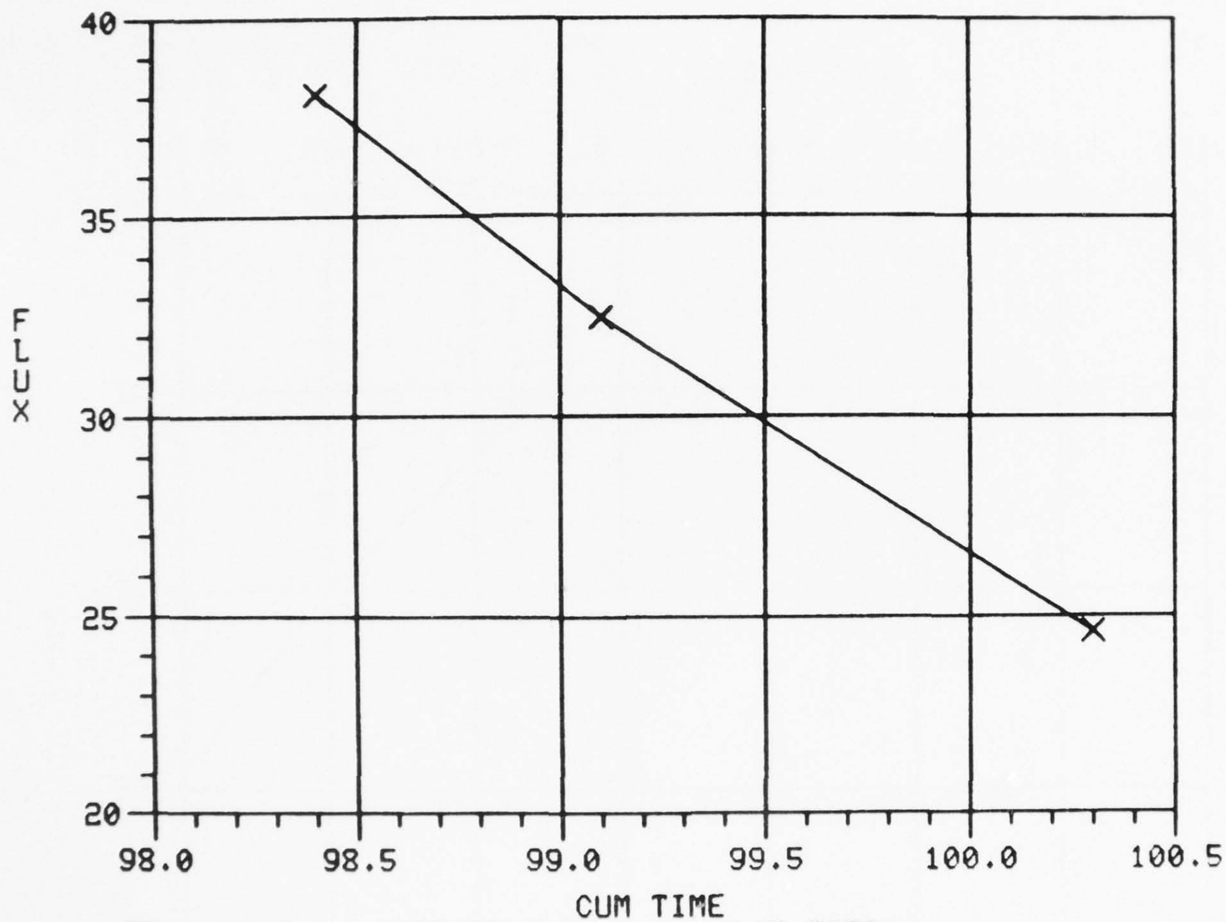


Y= .75 X ** 2 + -155.73 X ** 1 + 8117.7090
SQ MULT CORR COEF IS 1.000

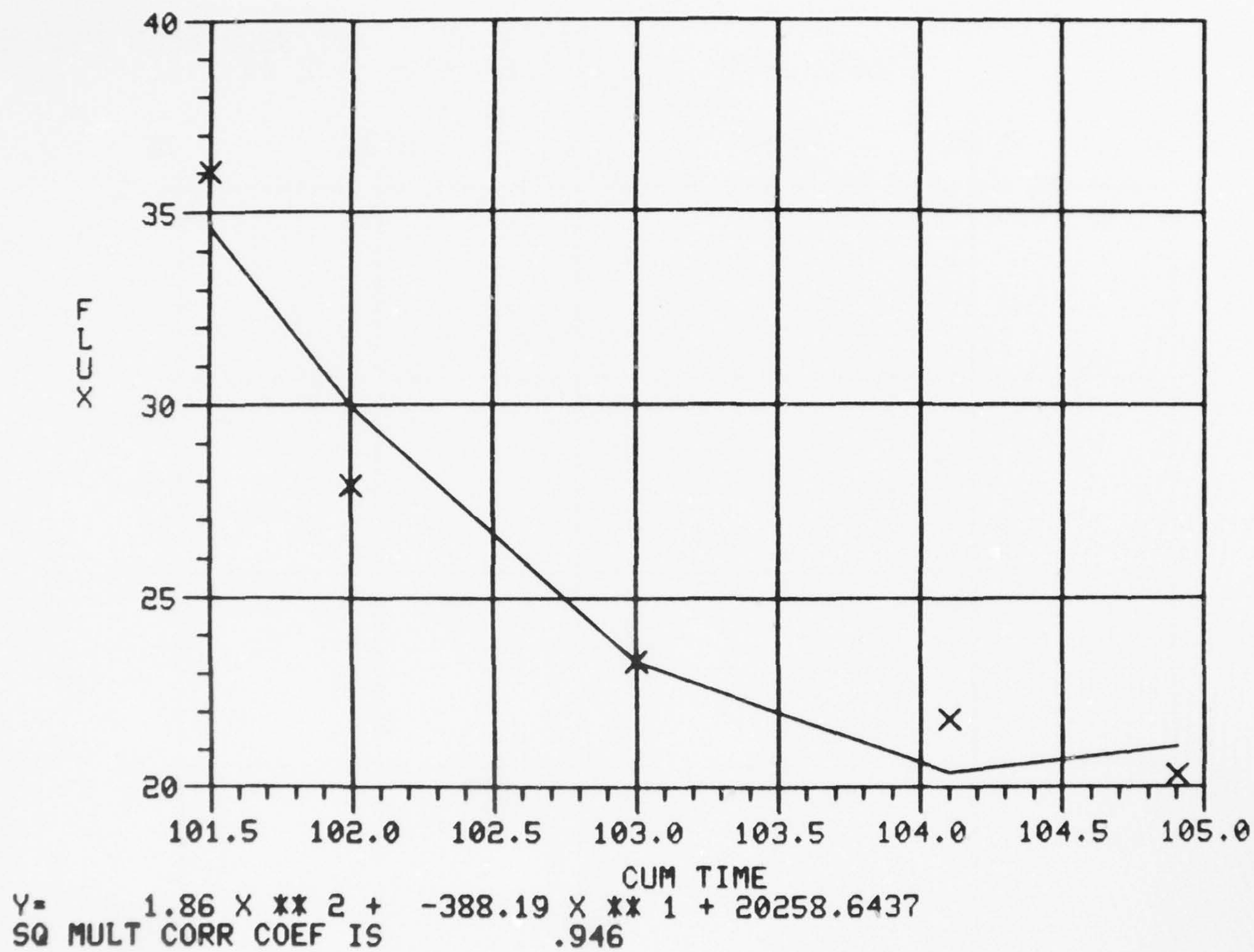
FLUX
40
35
30
25
20
101.5
102.0
102.5
103.0
103.5
104.0
104.5
105.0
CUM TIME
Y= 1.86 X ** 2 + -388.19 X ** 1 + 20258.6437
SQ MULT CORR COEF IS .946

AD-A043 716 ARMY MOBILITY EQUIPMENT RESEARCH AND DEVELOPMENT COMM--ETC F/G 13/2
PROCESS DESIGN FOR TREATING SHOWER WASTEWATER BY ULTRAFILTRATIO--ETC(U)
JUN 77 D S LENT
UNCLASSIFIED MERADCOM-2212 NL

2 OF 2
AD
A043716

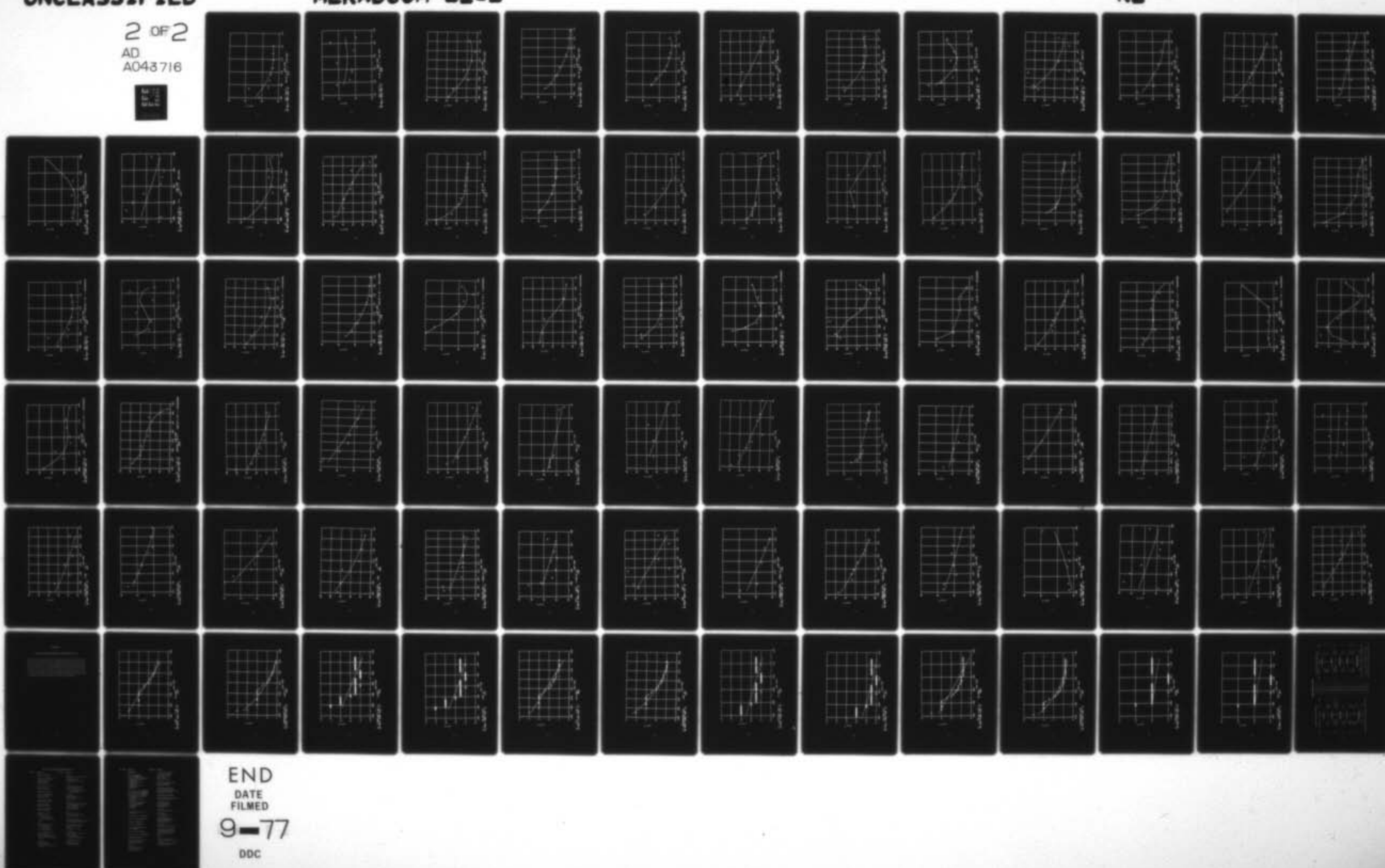

END
DATE
FILMED
9-77
DDC

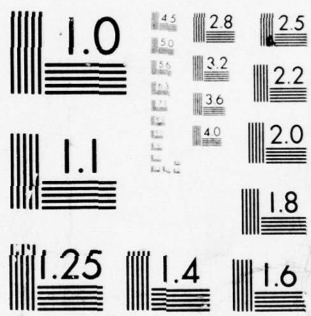


MICROCOPY RESOLUTION TEST CHART
NATIONAL BUREAU OF STANDARDS-1963-A

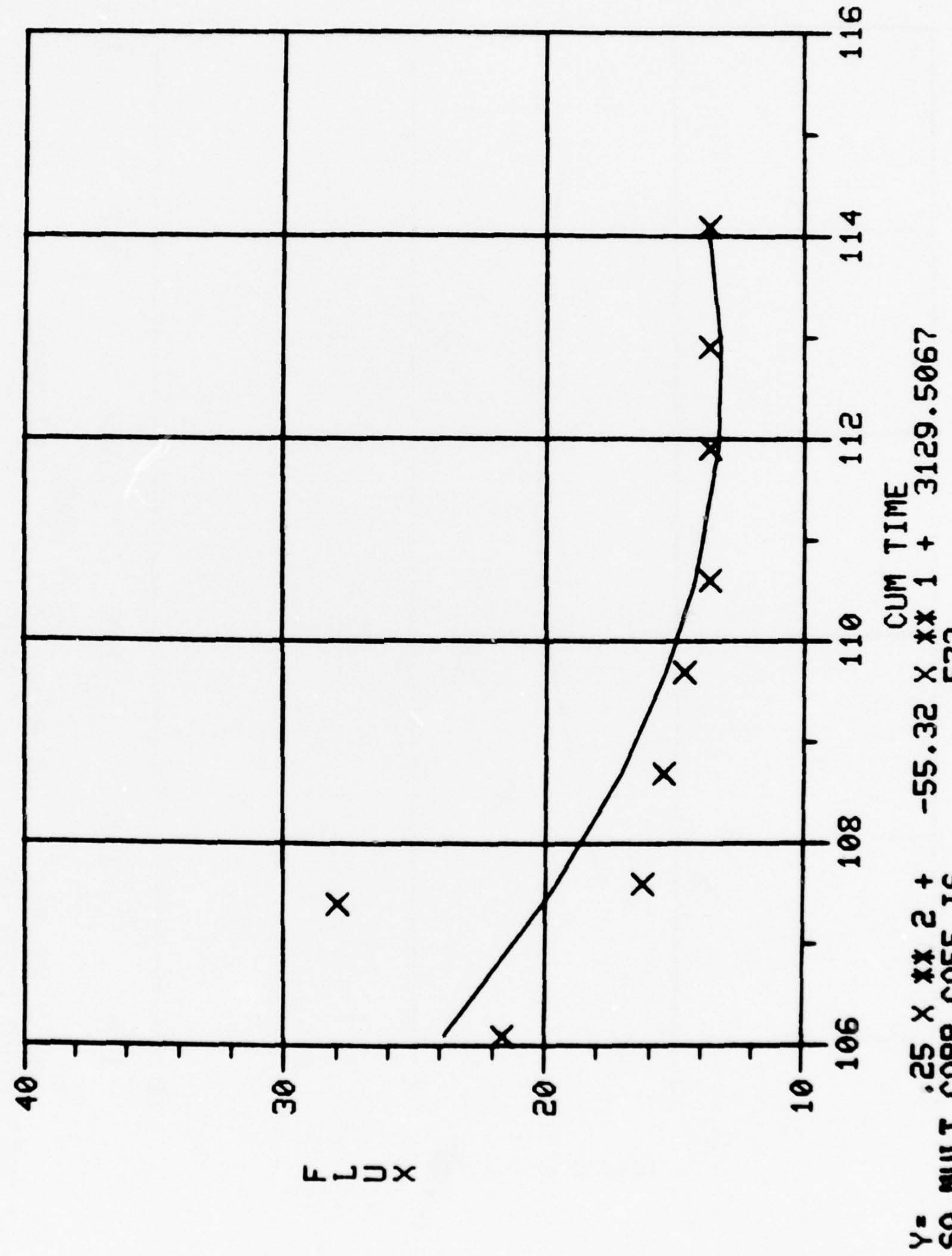
FLUX
40
30
20
10
106
108
110
112
114
116
CUM TIME
Y= .25 X ** 2 + -55.32 X ** 1 + 3129.5067
SQ MULT CORR COEF IS .573

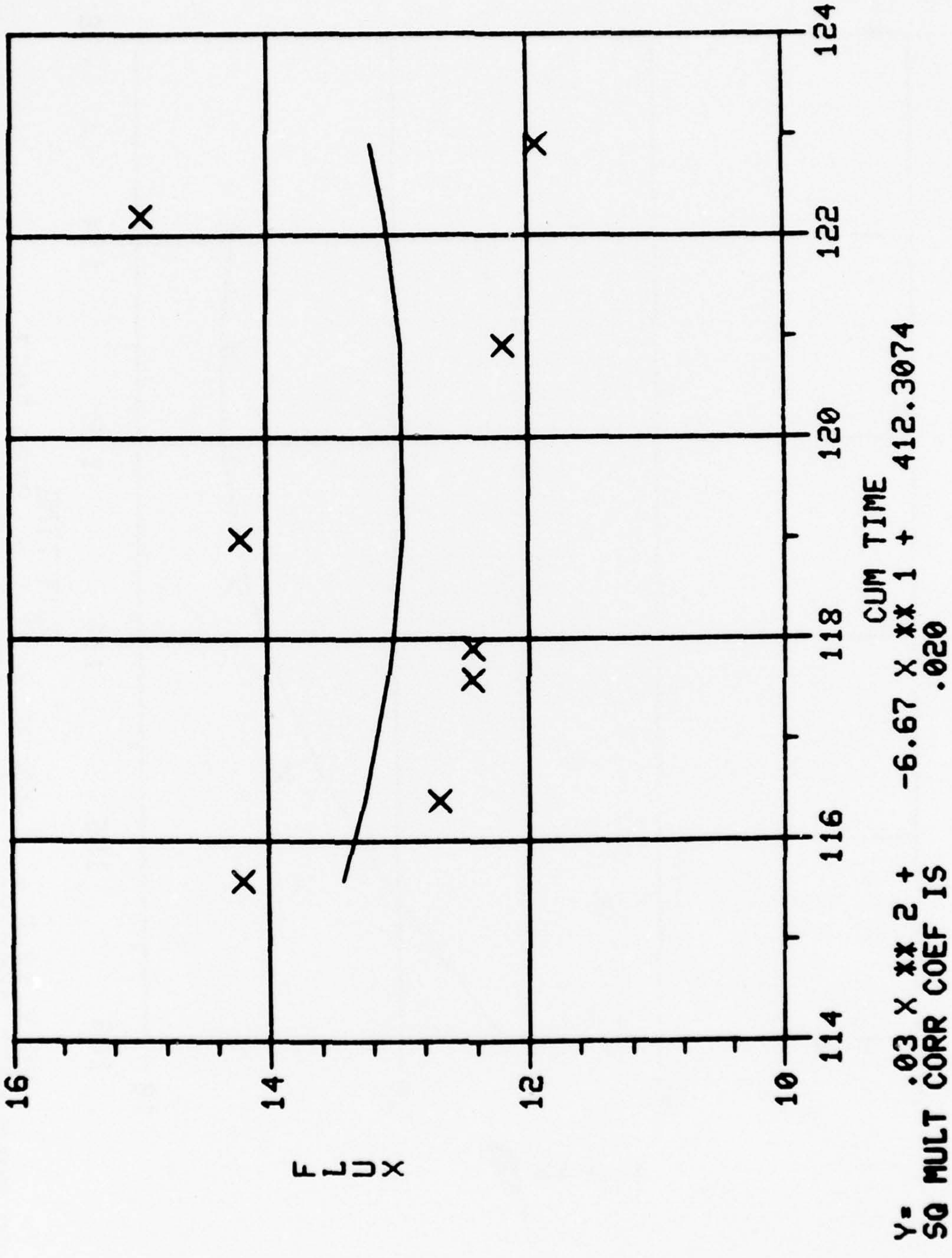
FLUX
16
14
12
10
114
116
118
120
122
124
CUM TIME
Y= .03 X XX 2 + -6.67 X XX 1 + 412.3074
SQ MULT CORR COEF IS .020

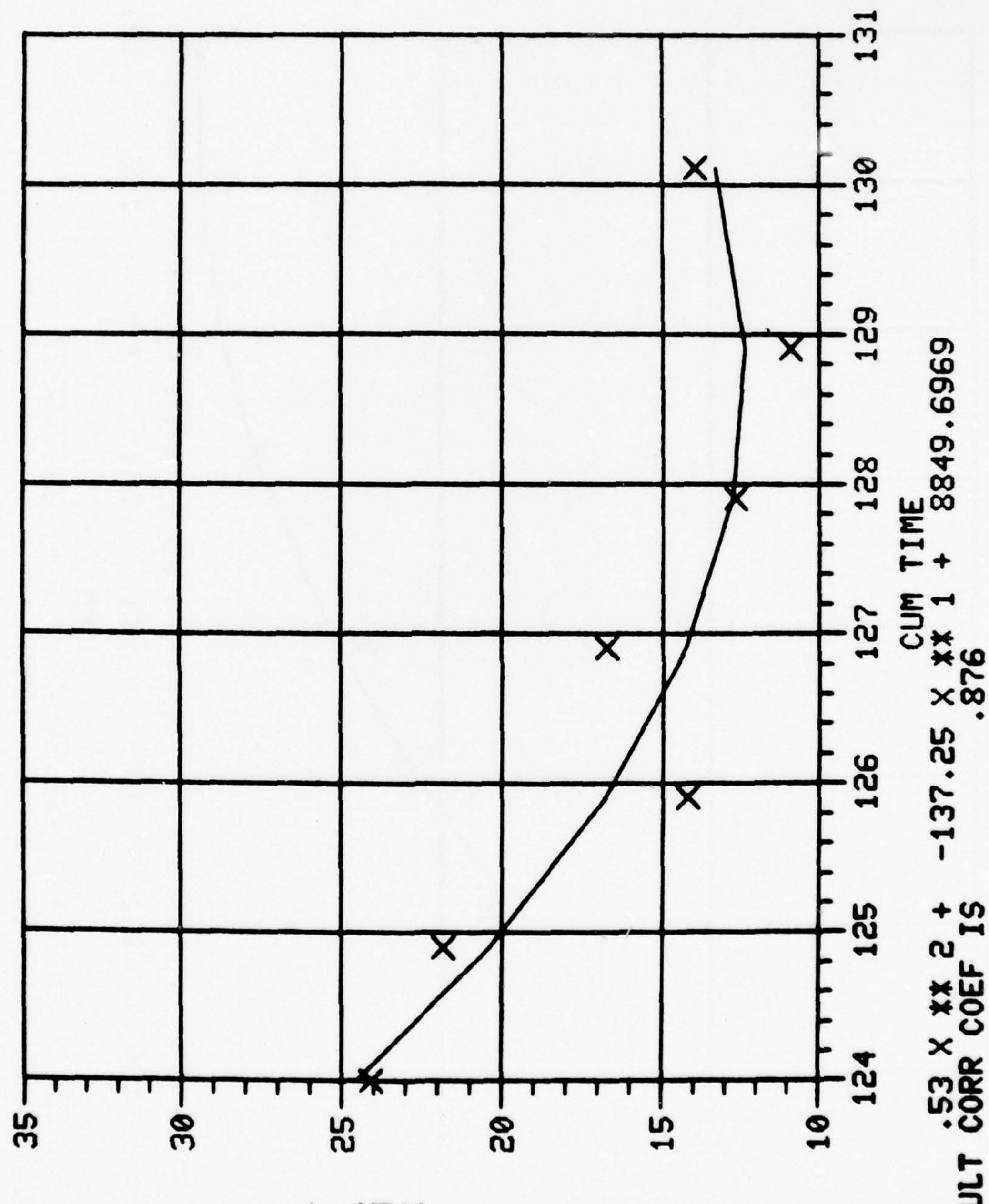
FLUX
35
30
25
20
15
10
124
125
126
127
128
129
130
131
CUM TIME
Y= .53 X ** 2 + -137.25 X ** 1 + 8849.6969
SQ MULT CORR COEF IS .876

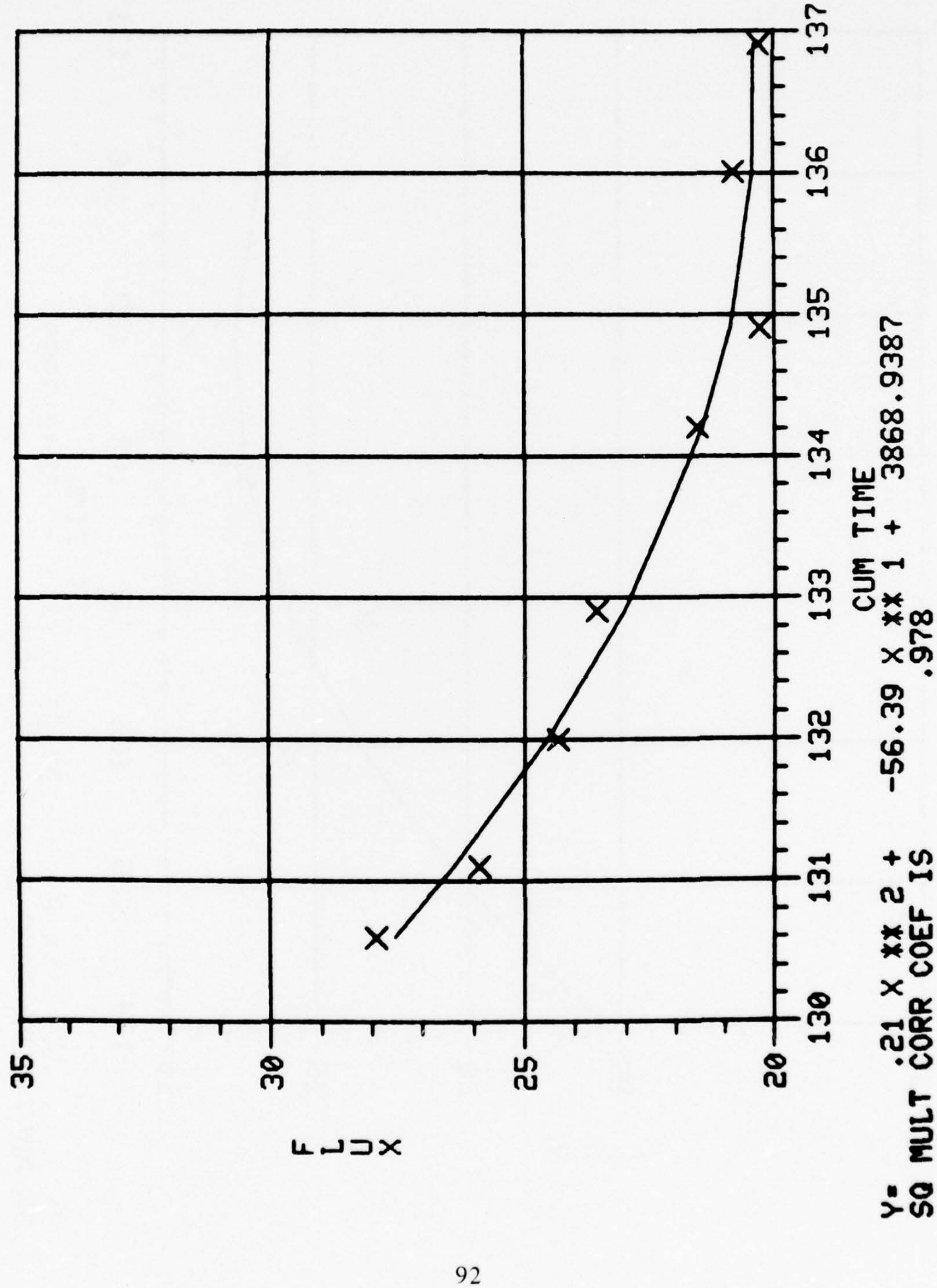

FLUX
CUM TIME
35
30
25
20
130
131
132
133
134
135
136
137
Y= .21 X ** 2 + -56.39 X ** 1 + 3868.9387
SQ MULT CORR COEF IS .978

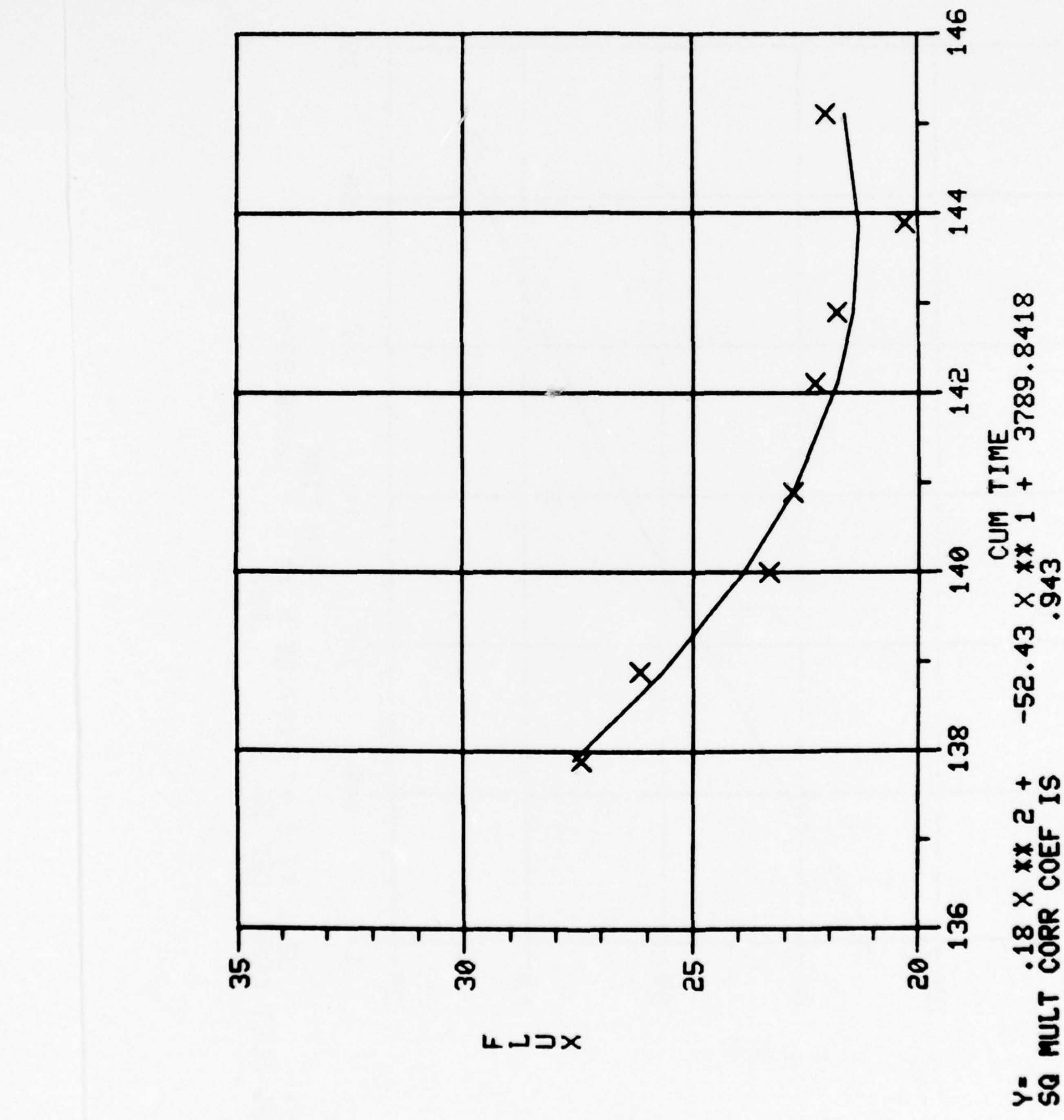

FLUX
35
30
25
20
136
138
140
142
144
146
CUM TIME
Y= .18 X XX 2 + -52.43 X XX 1 + 3789.8418
SQ MULT CORR COEF IS .943

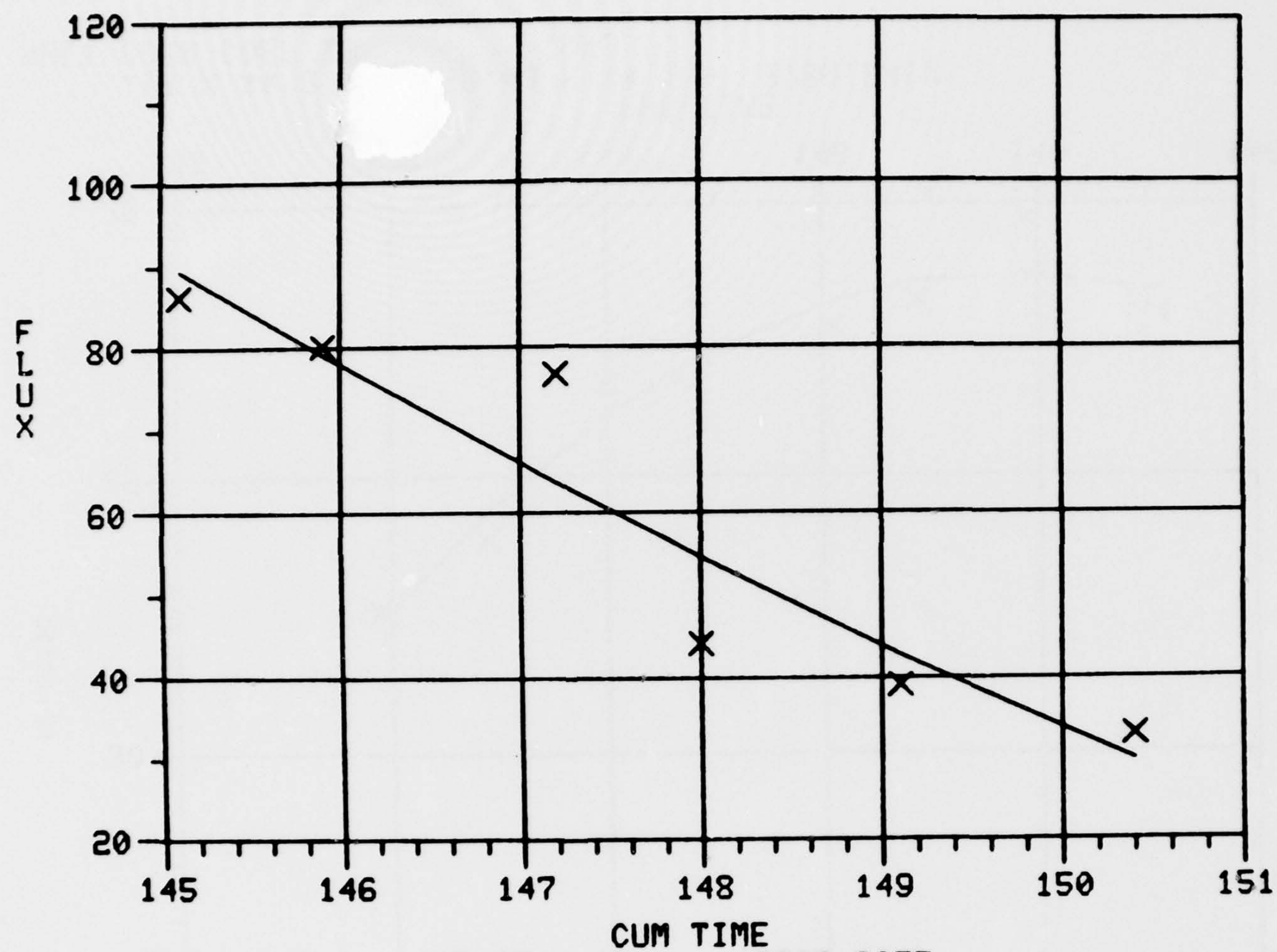


Y= .32 X ** 2 + -107.25 X ** 1 + 8809.9075
SQ MULT CORR COEF IS .887

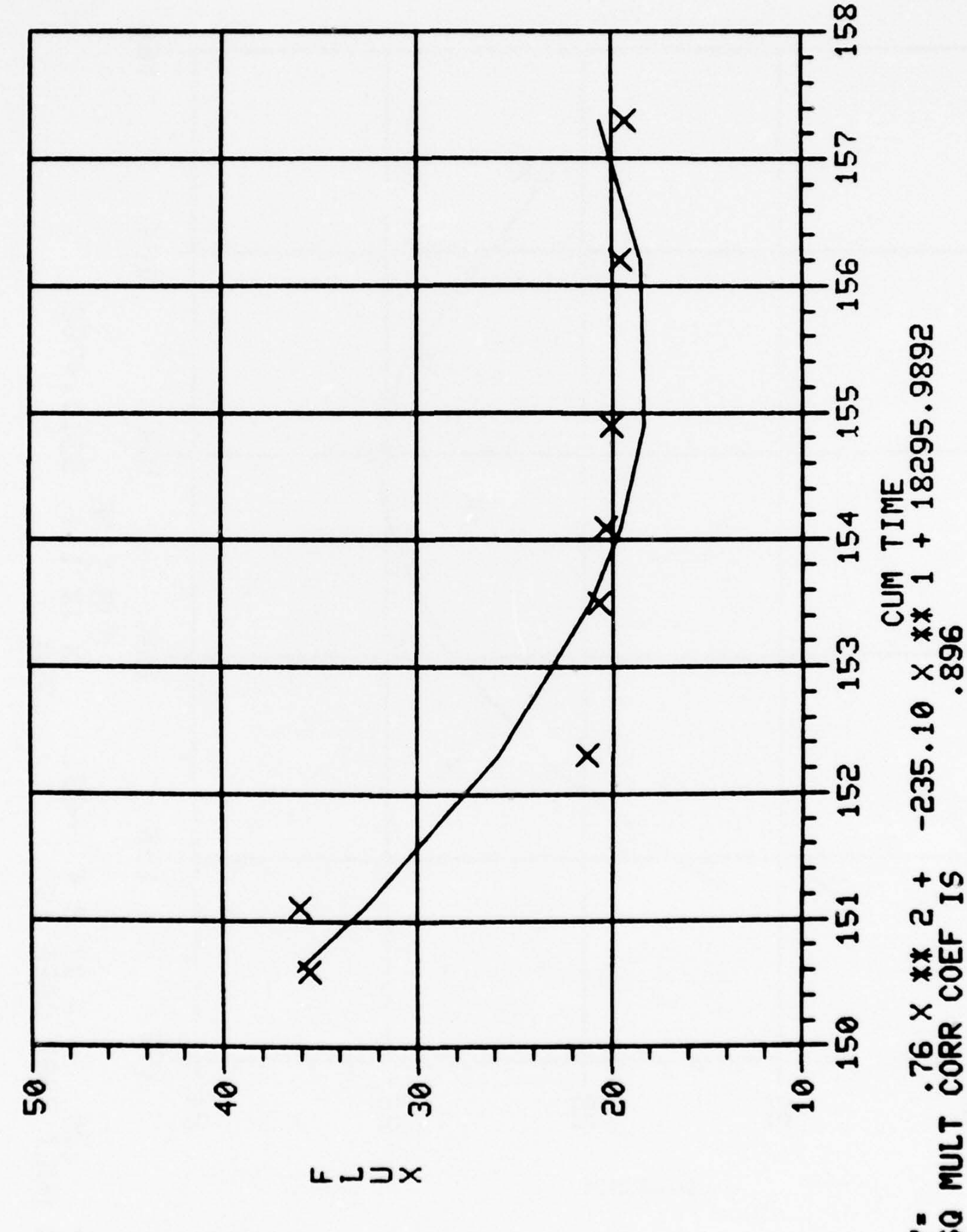
FLUX
CUM TIME
Y= .76 X ** 2 + -235.10 X ** 1 + 18295.9892
SQ MULT CORR COEF IS .896
50
40
30
20
10
150
151
152
153
154
155
156
157
158

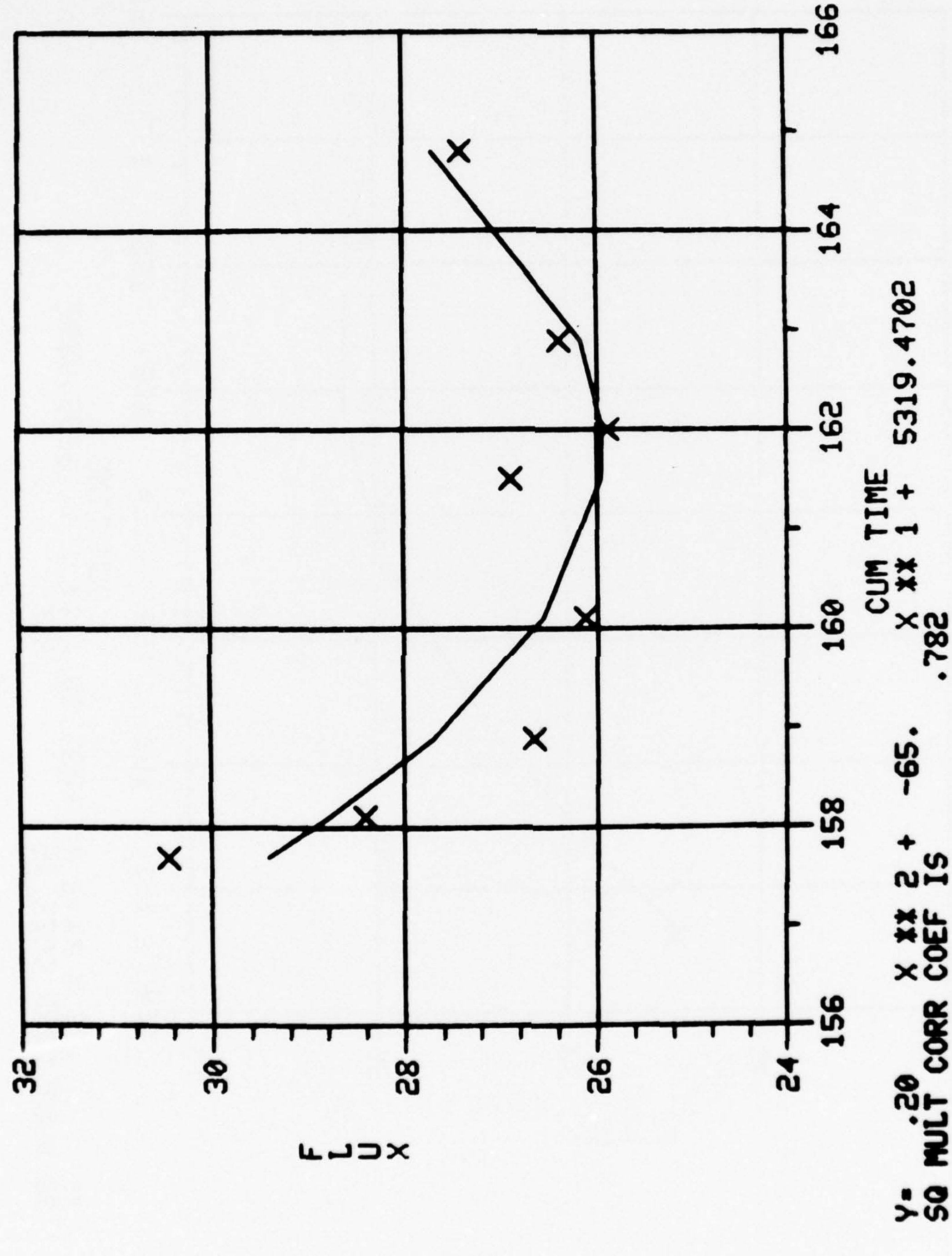
FLUX
32
30
28
26
24
156
158
160
162
164
166
CUM TIME
Y= .20 X XX 2 + -65. X XX 1 + 5319.4702
SQ MULT CORR COEF IS .782

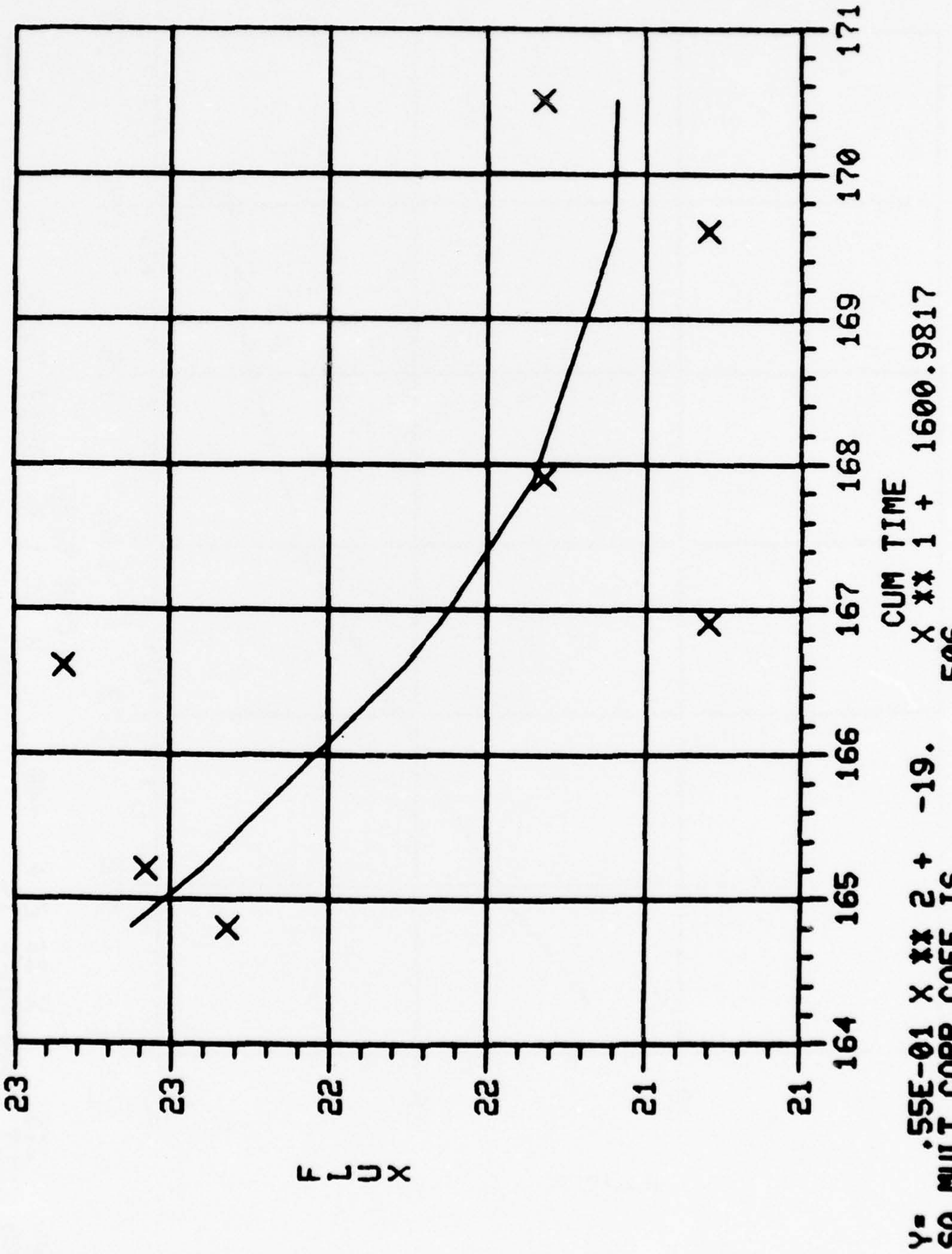
FLUX
23
23
22
22
21
21
164
165
166
167
168
169
170
171
CUM TIME
Y= .55E-01 X XX 2 + -19. X XX 1 + 1600.9817
SQ MULT CORR COEF IS .506

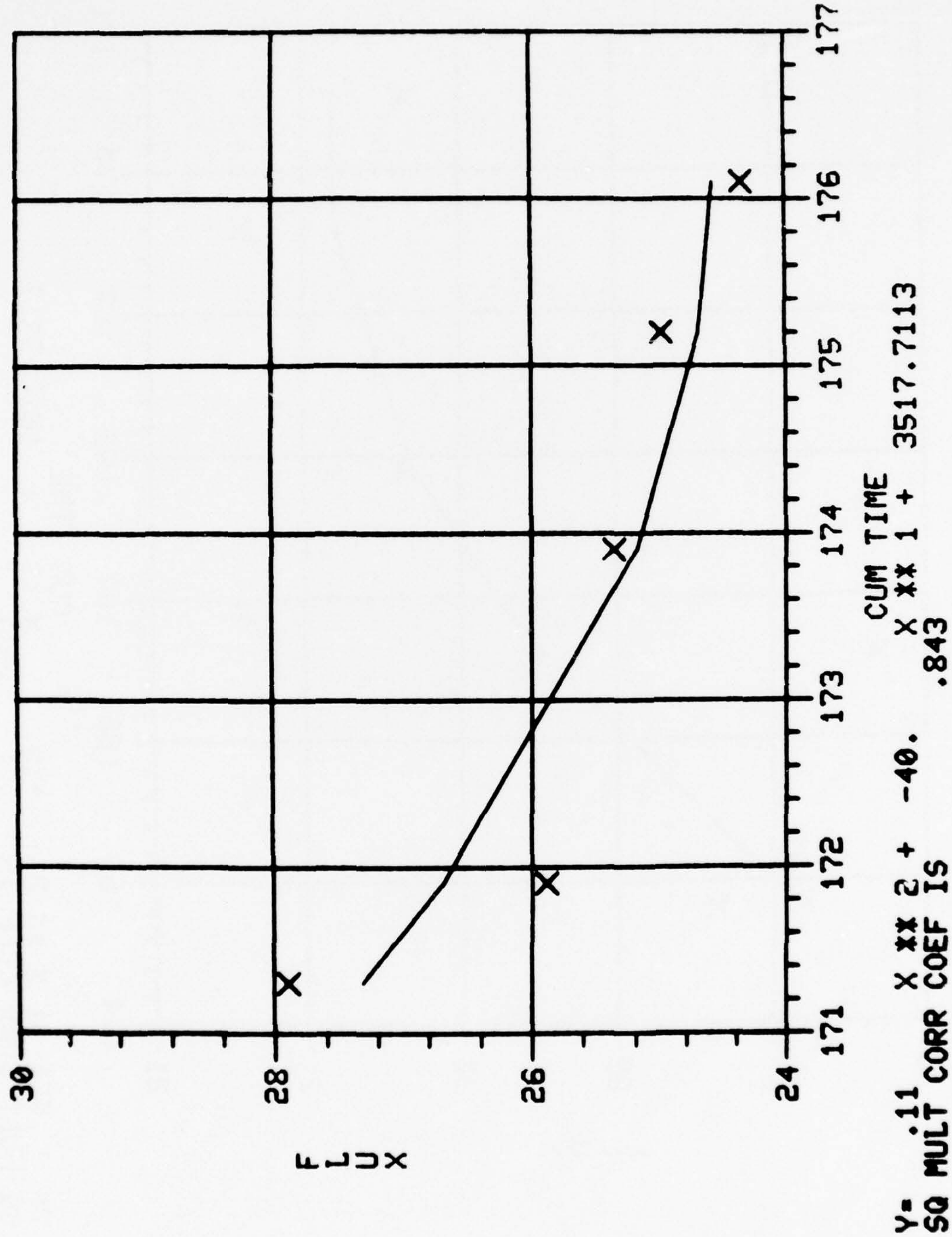
FLUX
30
28
26
24
171
172
173
174
175
176
177
CUM TIME
Y= .11 X ** 2 + -40. X ** 1 + 3517.7113
SQ MULT CORR COEF IS .843

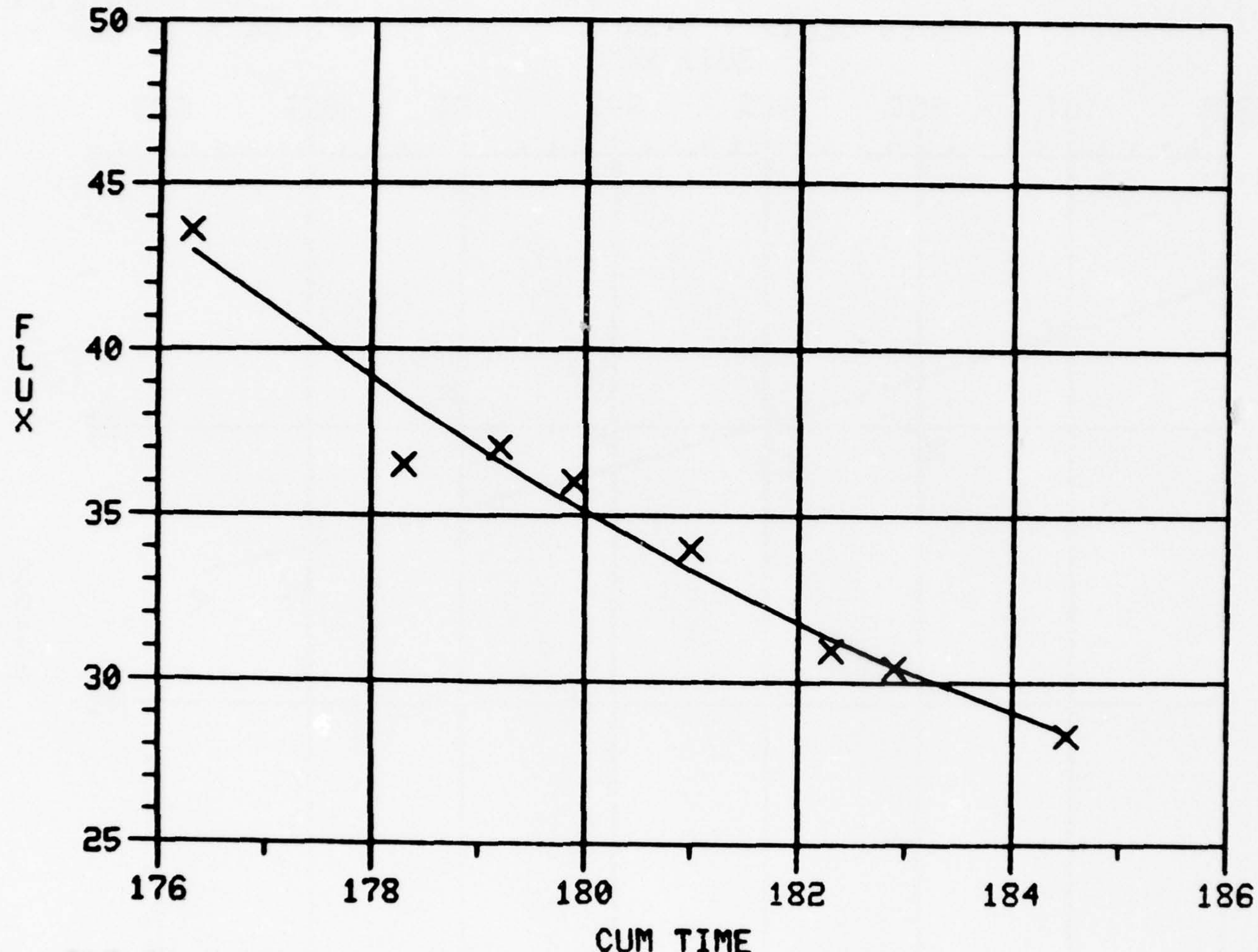


Y= .81E-01 X ** 2 + -31. X ** 1 + 2995.6225
SQ MULT CORR COEF IS .967

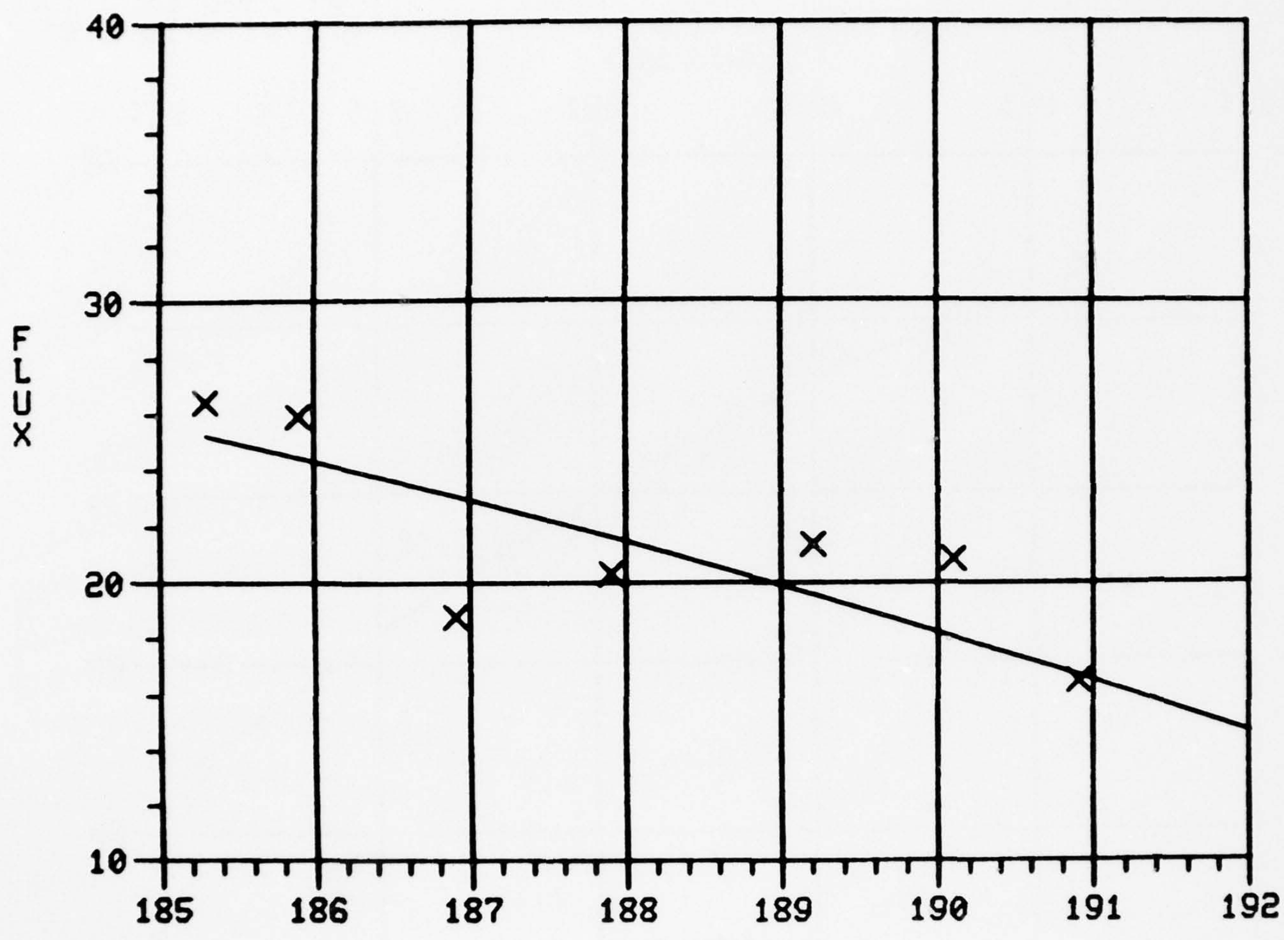


Y= -.47E-01 X ** 2 + 16. X ** 1 + -1339.8305
SQ MULT CORR COEF IS .734

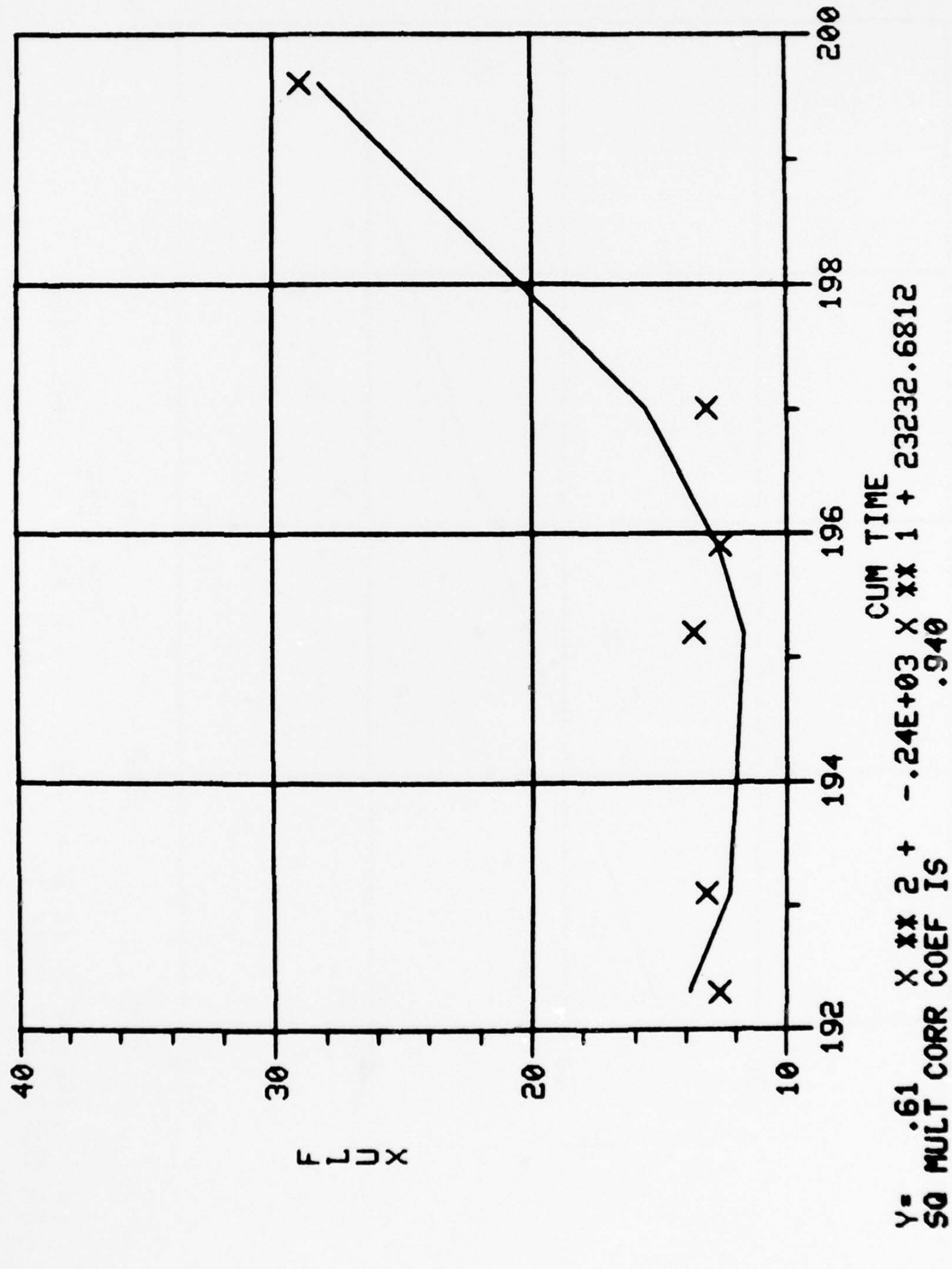

FLUX
40
30
20
10
192
194
196
198
200
CUM TIME
Y= .61 X ** 2 + -.24E+03 X ** 1 + 23232.6812
SQ MULT CORR COEF IS .940

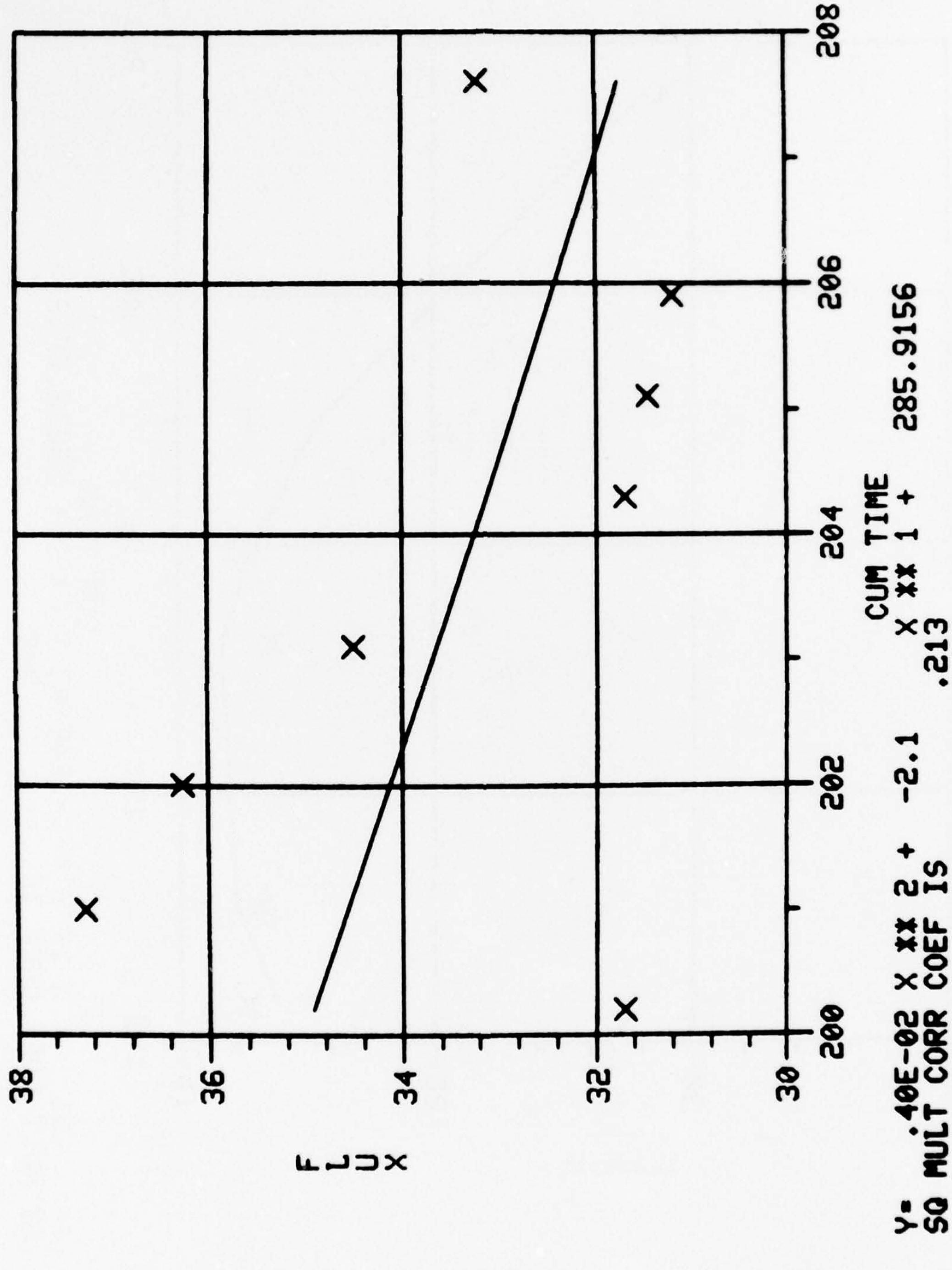
FLUX
38
36
34
32
30
200
202
204
206
208
CUM TIME
Y= .40E-02 X XX 2 + -2.1 X XX 1 + 285.9156
SQ MULT CORR COEF IS .213

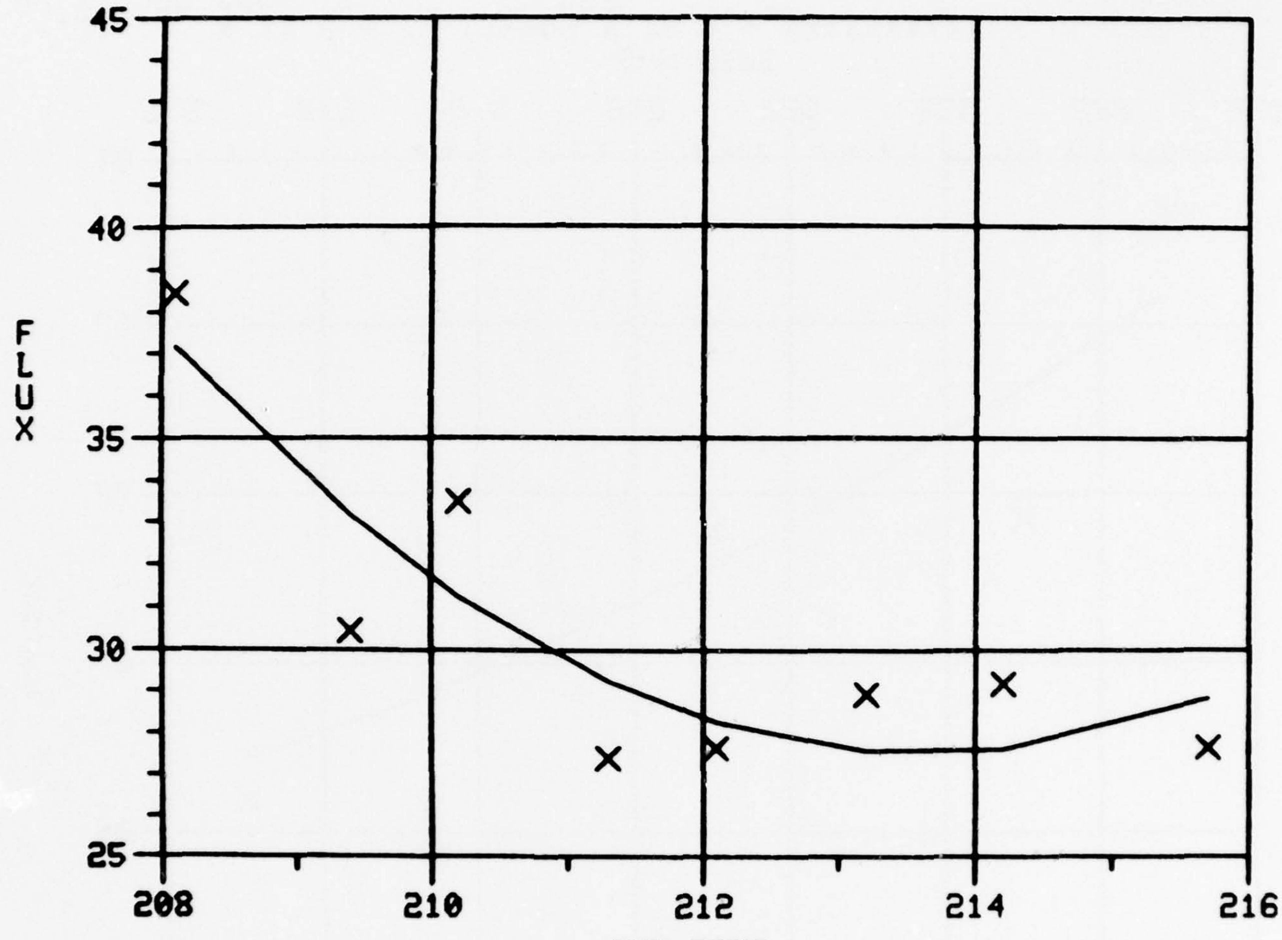


Y= .31 X ** 2 + -.13E+03 X ** 1 + 14357.5229
SQ MULT CORR COEF IS .769

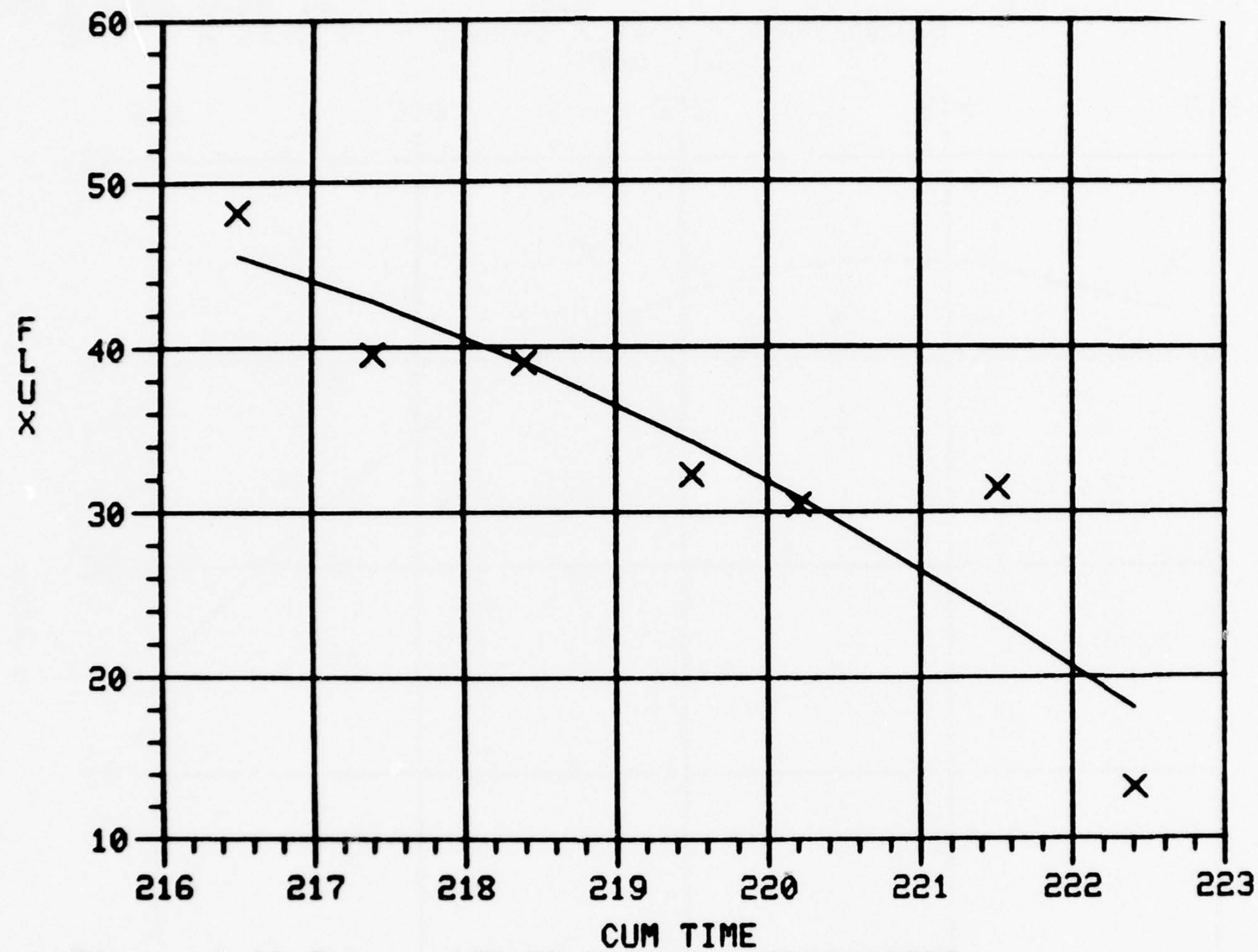


Y= -.31 X ** 2 + .13E+03 X ** 1 + **********
SQ MULT CORR COEF IS .851

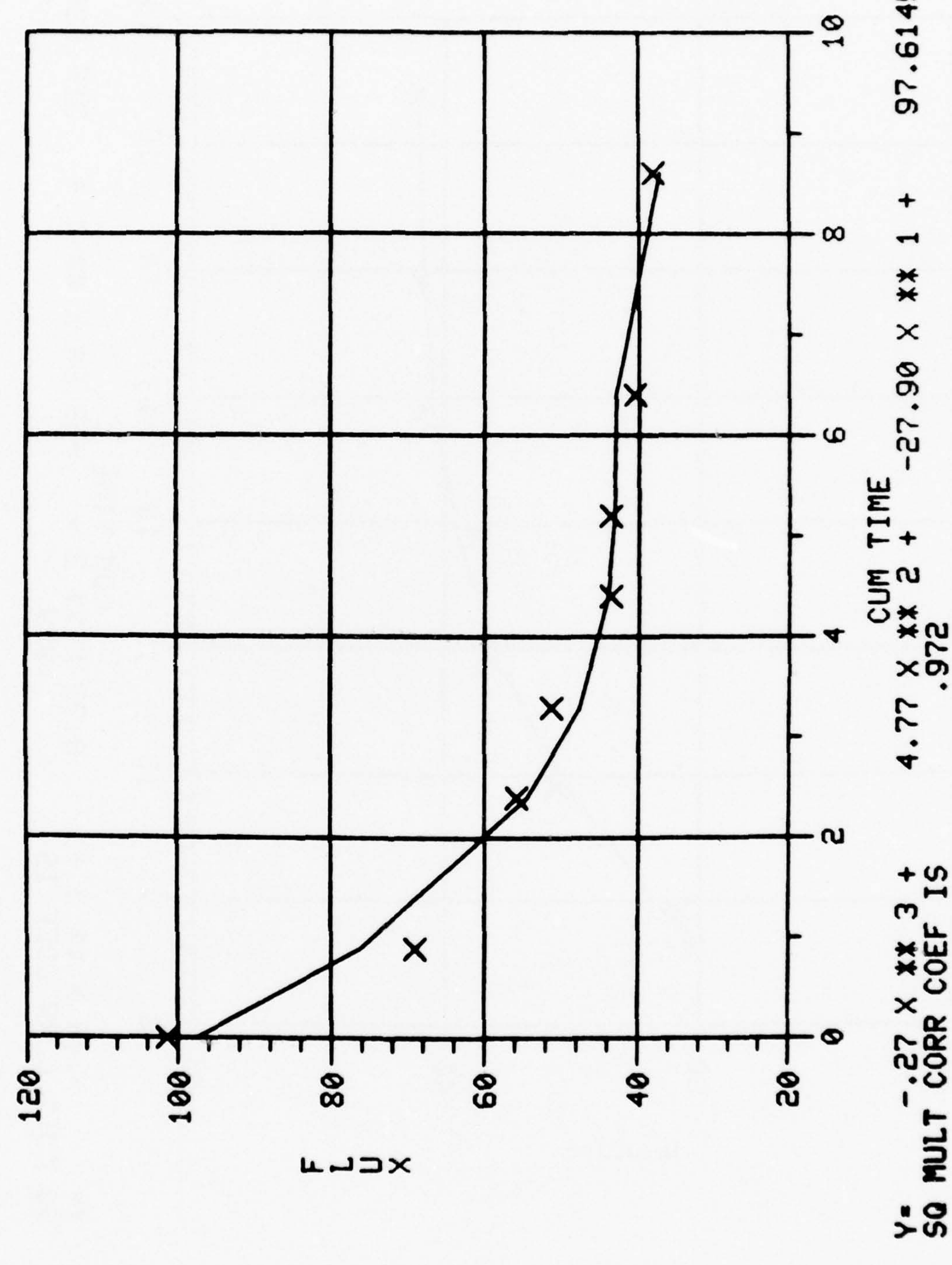
FLUX
120
100
80
60
40
20
0
2
4
6
8
10
CUM TIME
Y= -.27 X ** 3 + 4.77 X ** 2 + -27.90 X ** 1 + 97.6145
SQ MULT CORR COEF IS .972

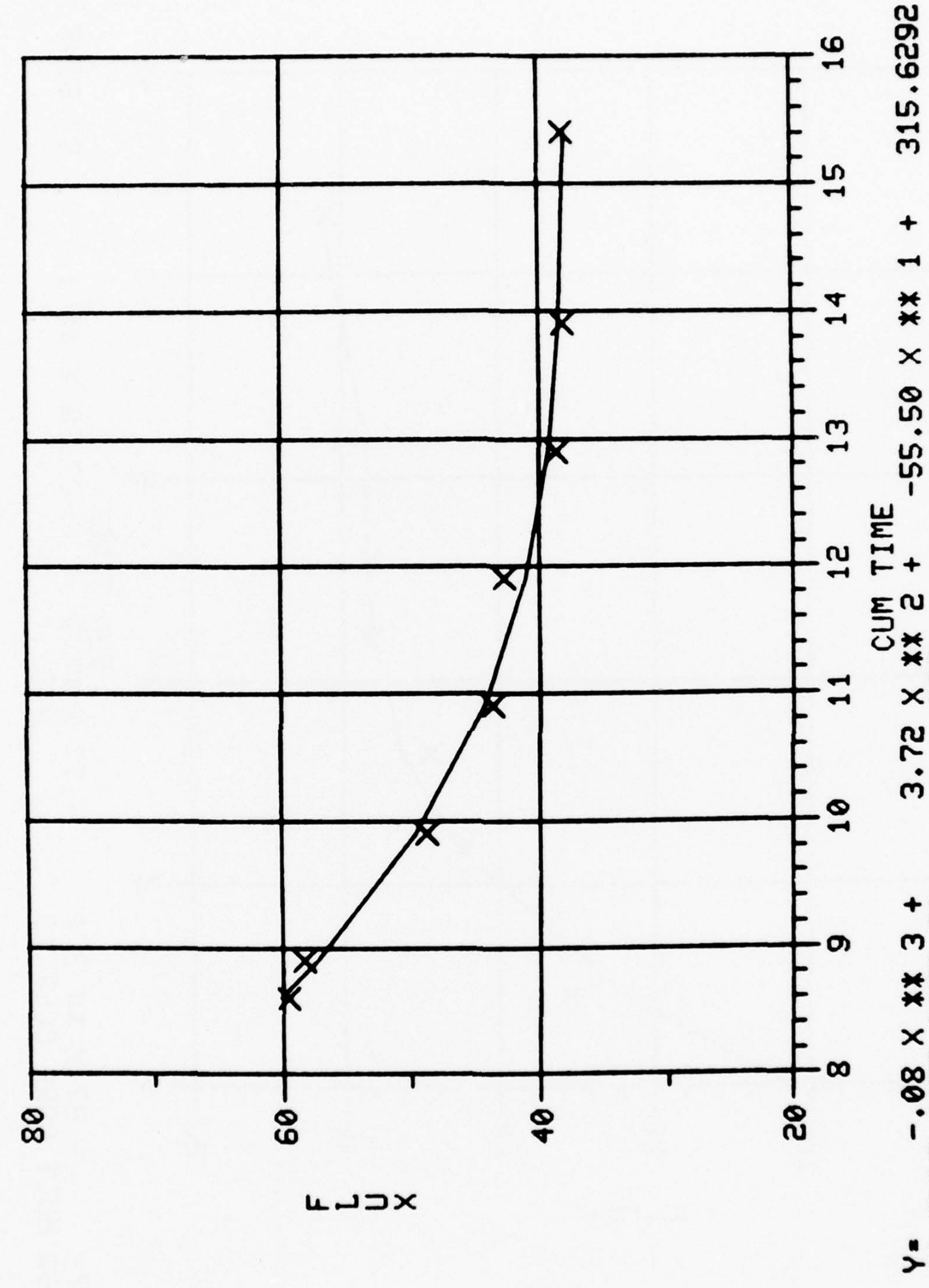
FLUX
80
60
40
20
8
9
10
11
12
13
14
15
16
CUM TIME
Y= -.08 X ** 3 + 3.72 X ** 2 + -55.50 X ** 1 + 315.6292
SQ MULT CORR COEF IS .989

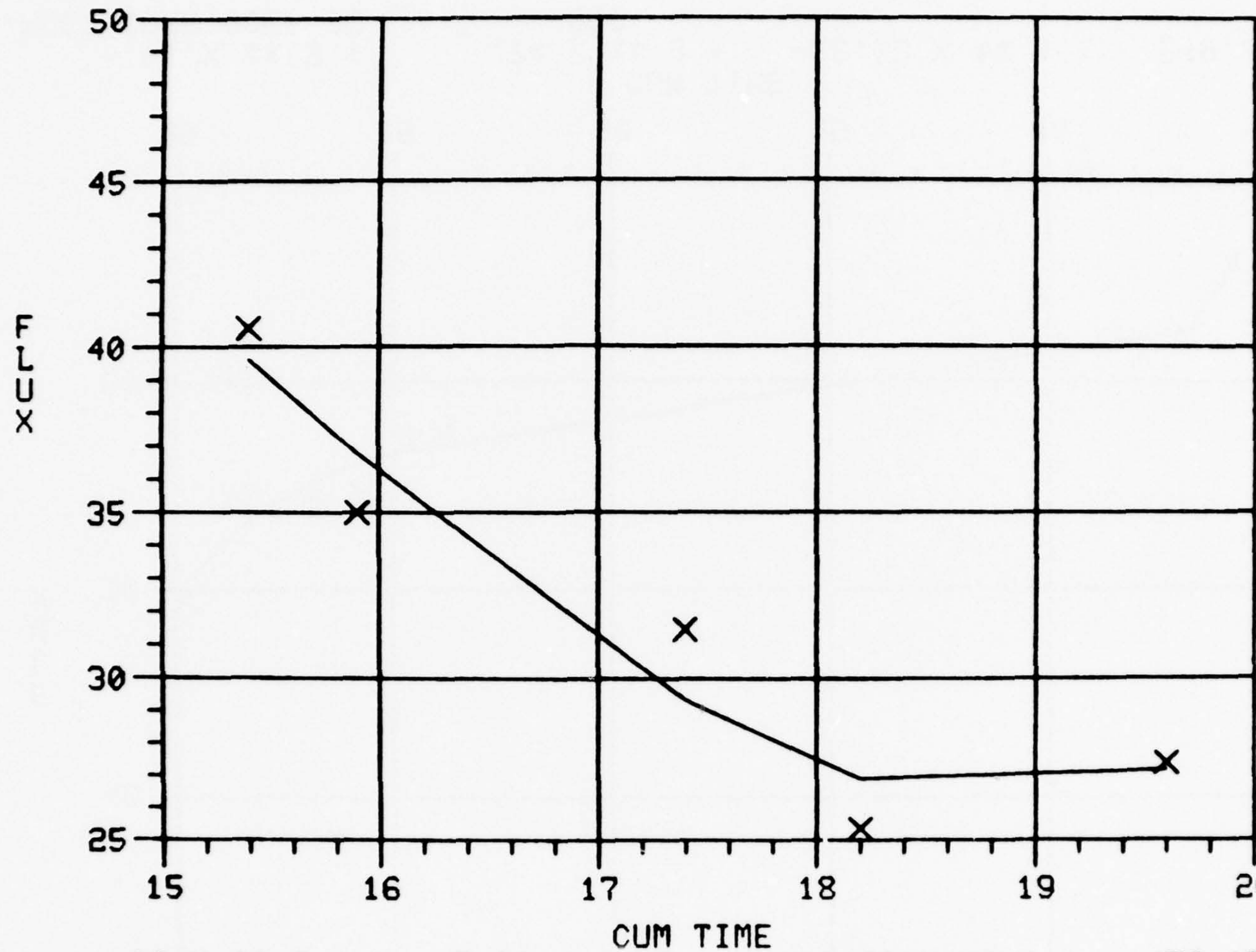


Y= .16 X ** 3 + -7.60 X ** 2 + 111.60 X ** 1 + -476.1777
SQ MULT CORR COEF IS .925

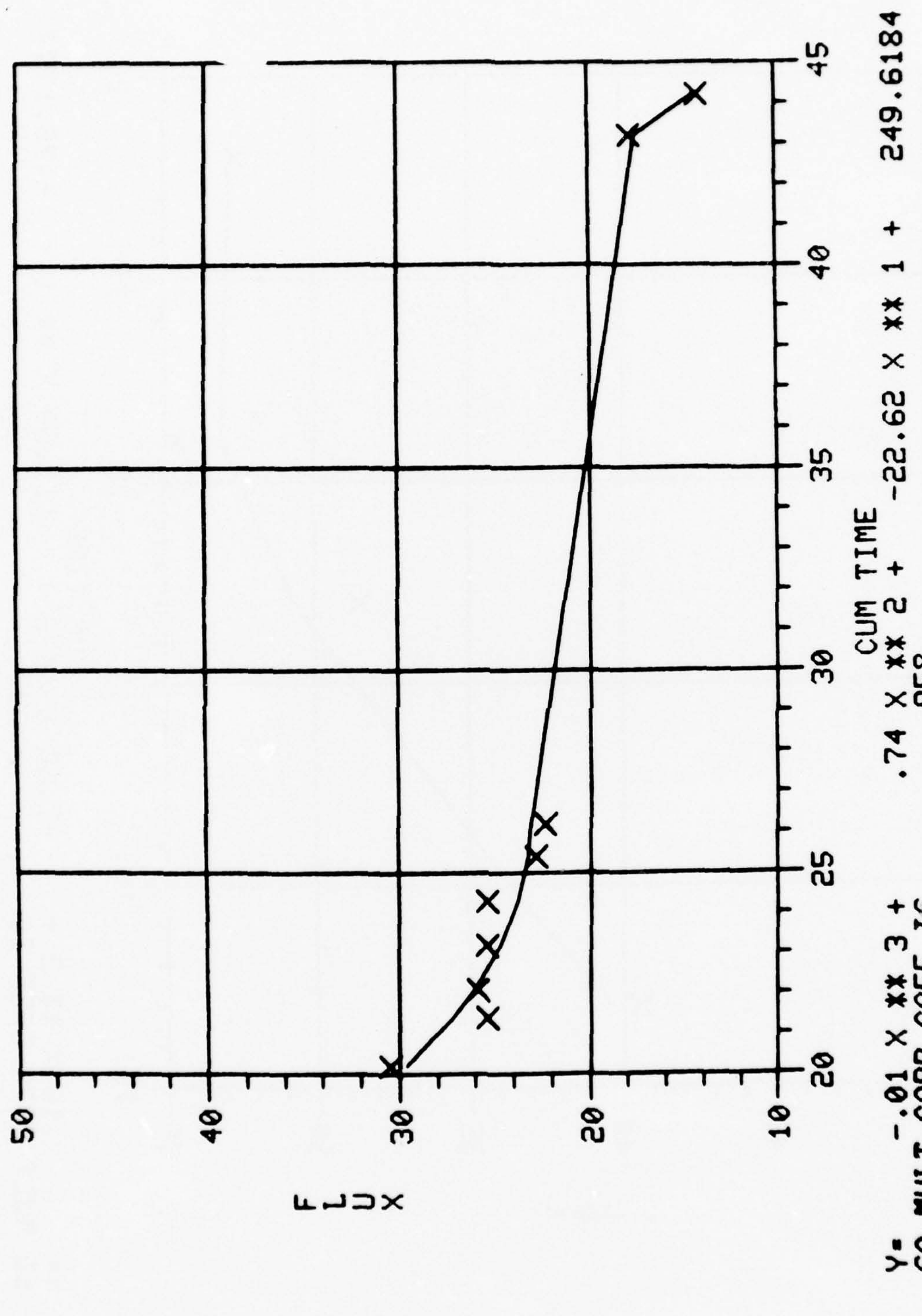
FLUX
50
40
30
20
10
20
25
30
35
40
45
CUM TIME
Y= -.01 X ** 3 + .74 X ** 2 + -22.62 X ** 1 + 249.6184
SQ MULT CORR COEF IS .958

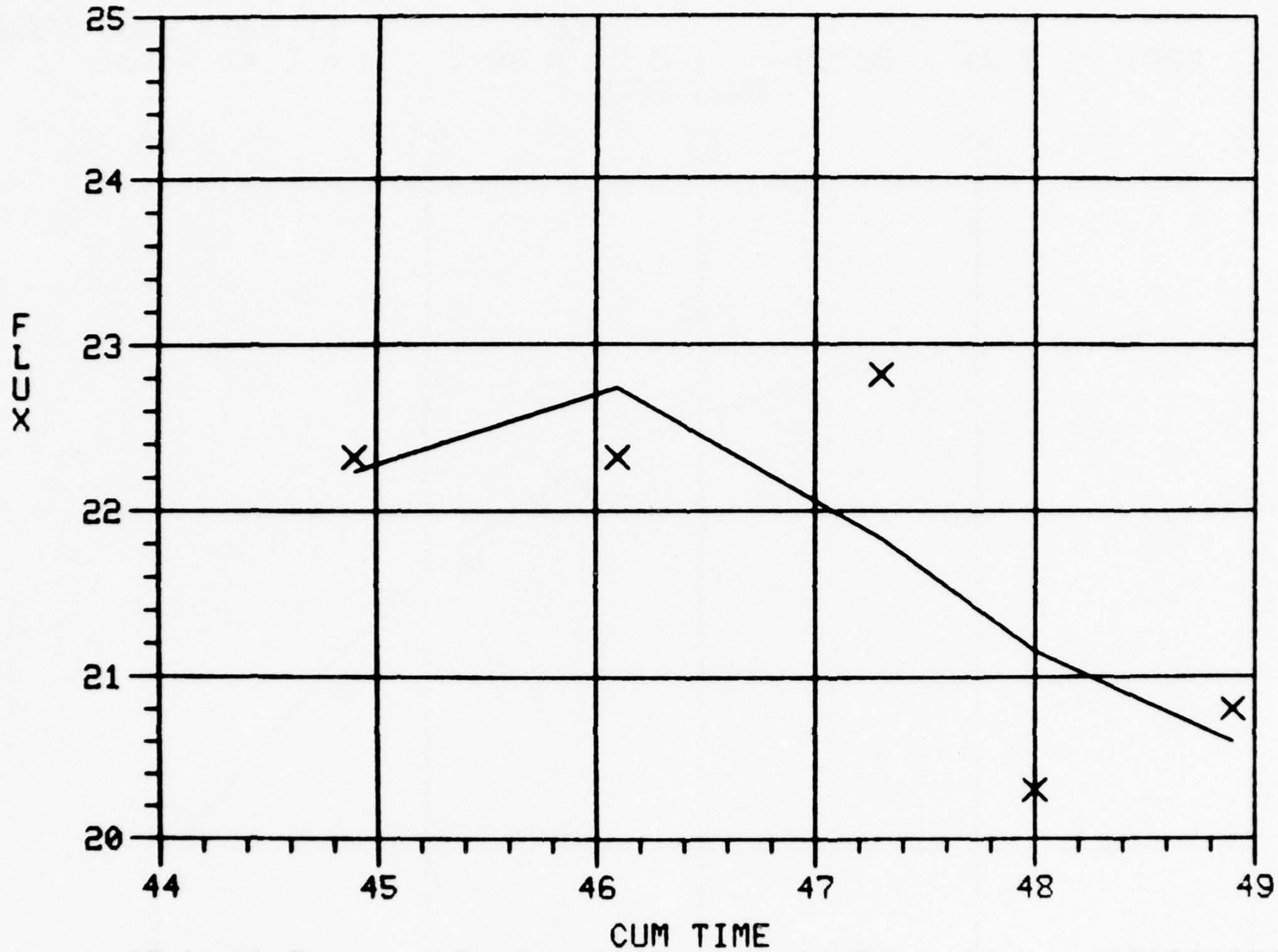


Y= .12 X ** 3 + -17.10 X ** 2 + 810.56 X ** 1 + **********
SQ MULT CORR COEF IS .599

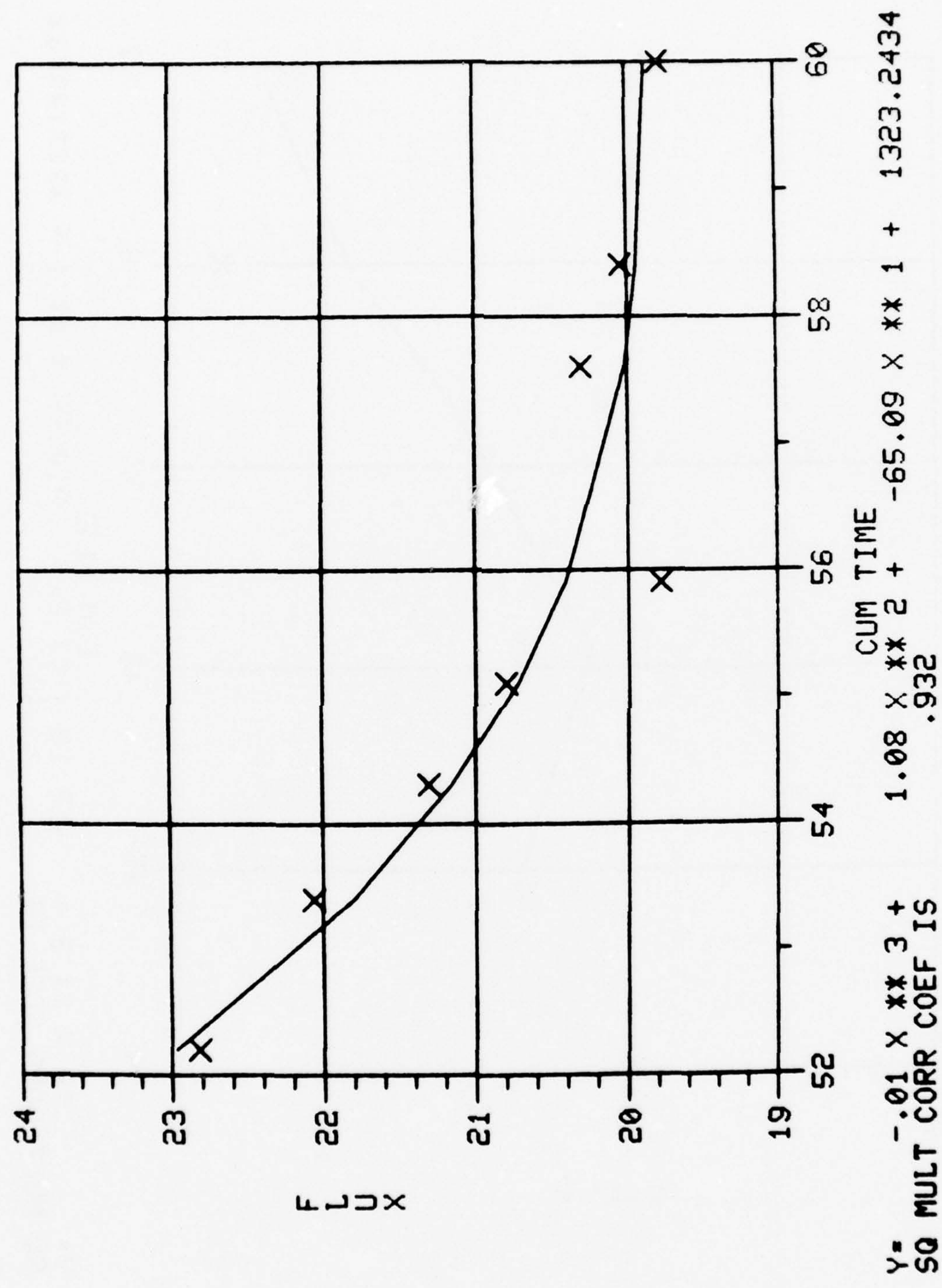
FLUX
24
23
22
21
20
19
52
54
56
58
60
CUM TIME
Y= -.01 X ** 3 + 1.08 X ** 2 + -65.09 X ** 1 + 1323.2434
SQ MULT CORR COEF IS .932

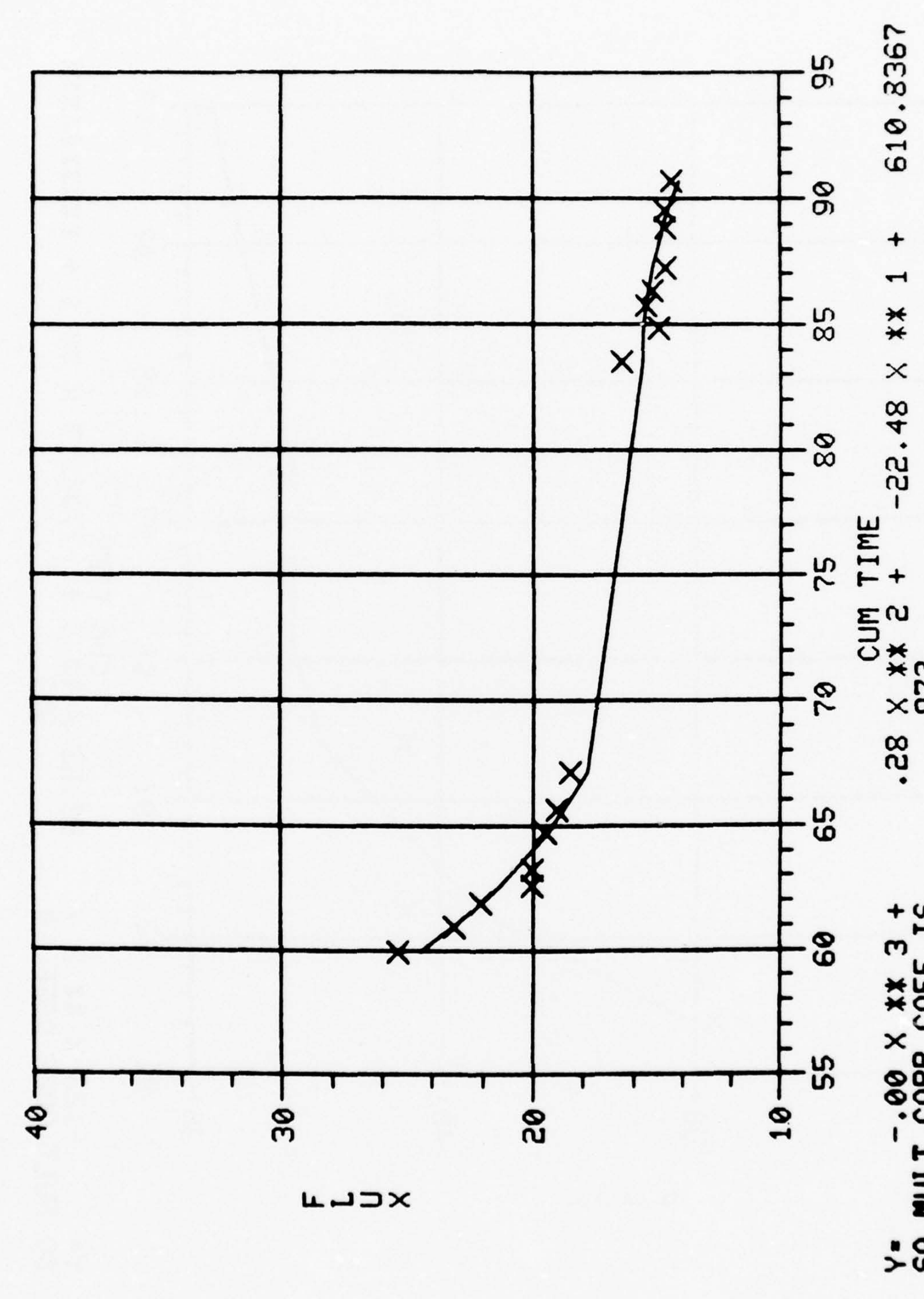
FLUX
40
30
20
10
55
60
65
70
75
80
85
90
95
CUM TIME
Y= -.00 X ** 3 + .28 X ** 2 + -22.48 X ** 1 + 610.8367
SQ MULT CORR COEF IS .973

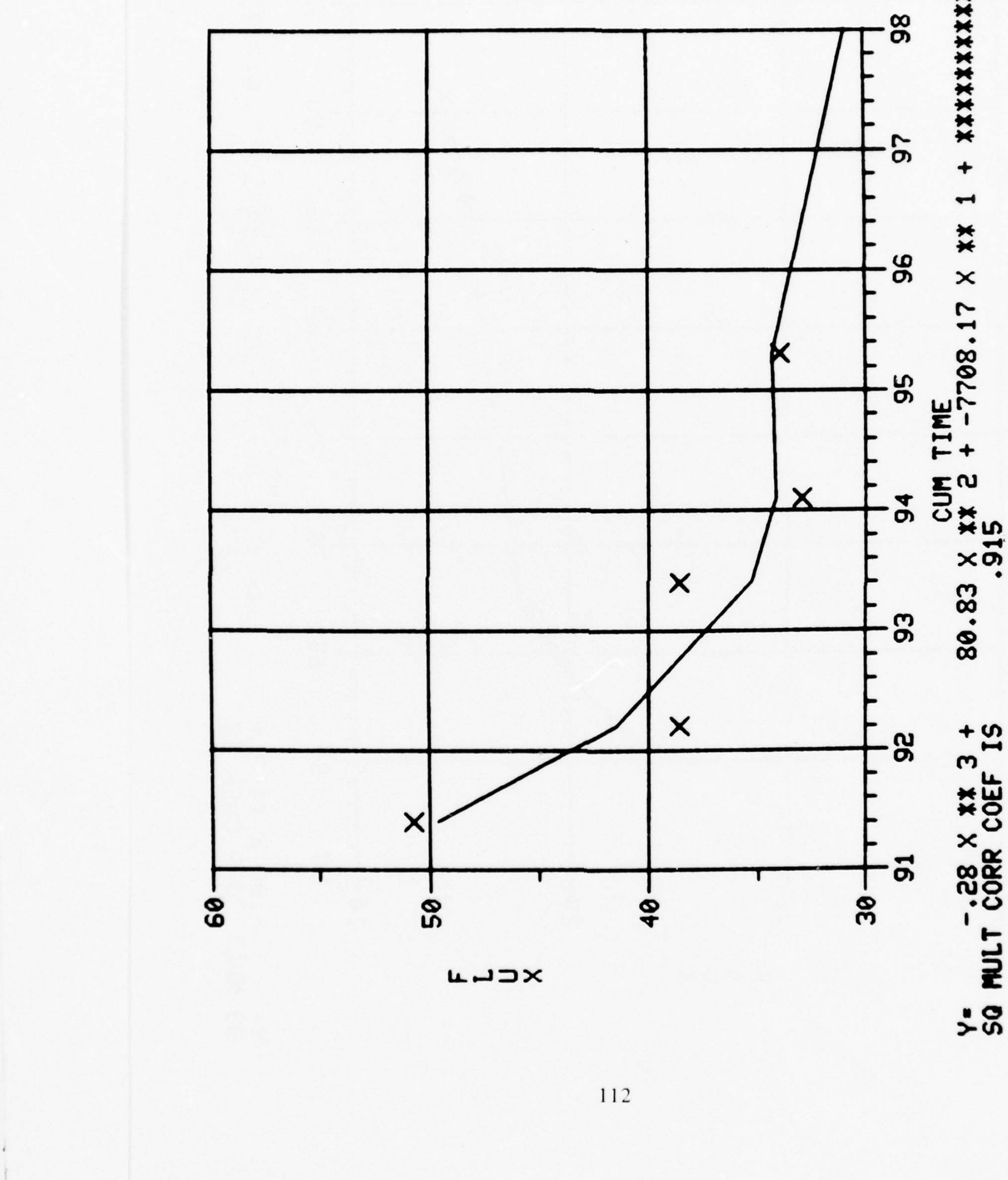
FLUX
60
50
40
30
91
92
93
94
95
96
97
98
CUM TIME
Y= -.28 X XX 3 + 80.83 X XX 2 + -7708.17 X XX 1 + XXXXXXXXX
SQ MULT CORR COEF IS .915

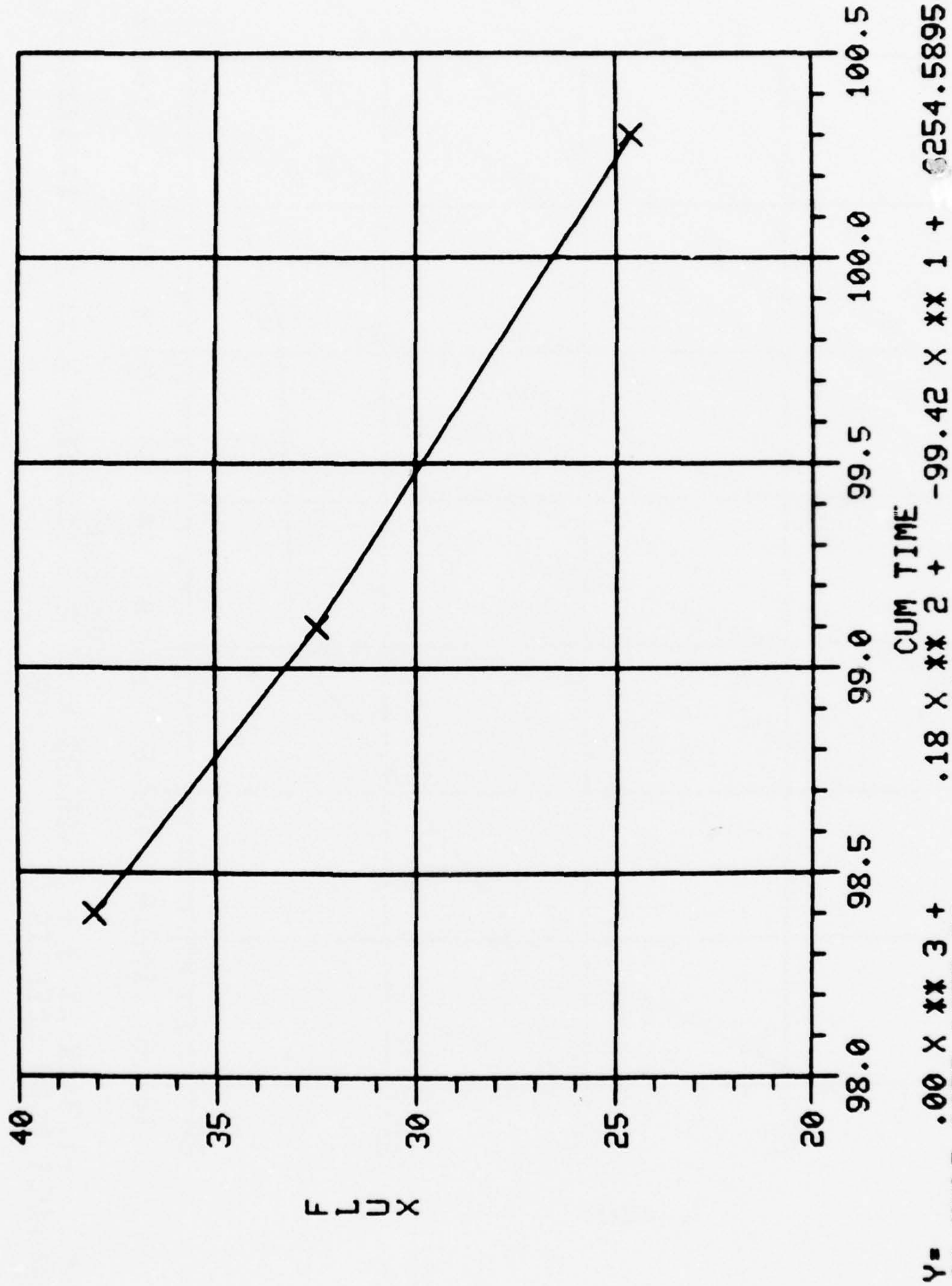

FLUX
40
35
30
25
20
98.0
98.5
99.0
99.5
100.0
100.5
CUM TIME
Y= .00 X ** 3 + .18 X ** 2 + -99.42 X ** 1 + 254.5895
SQ MULT CORR COEF IS 1.000

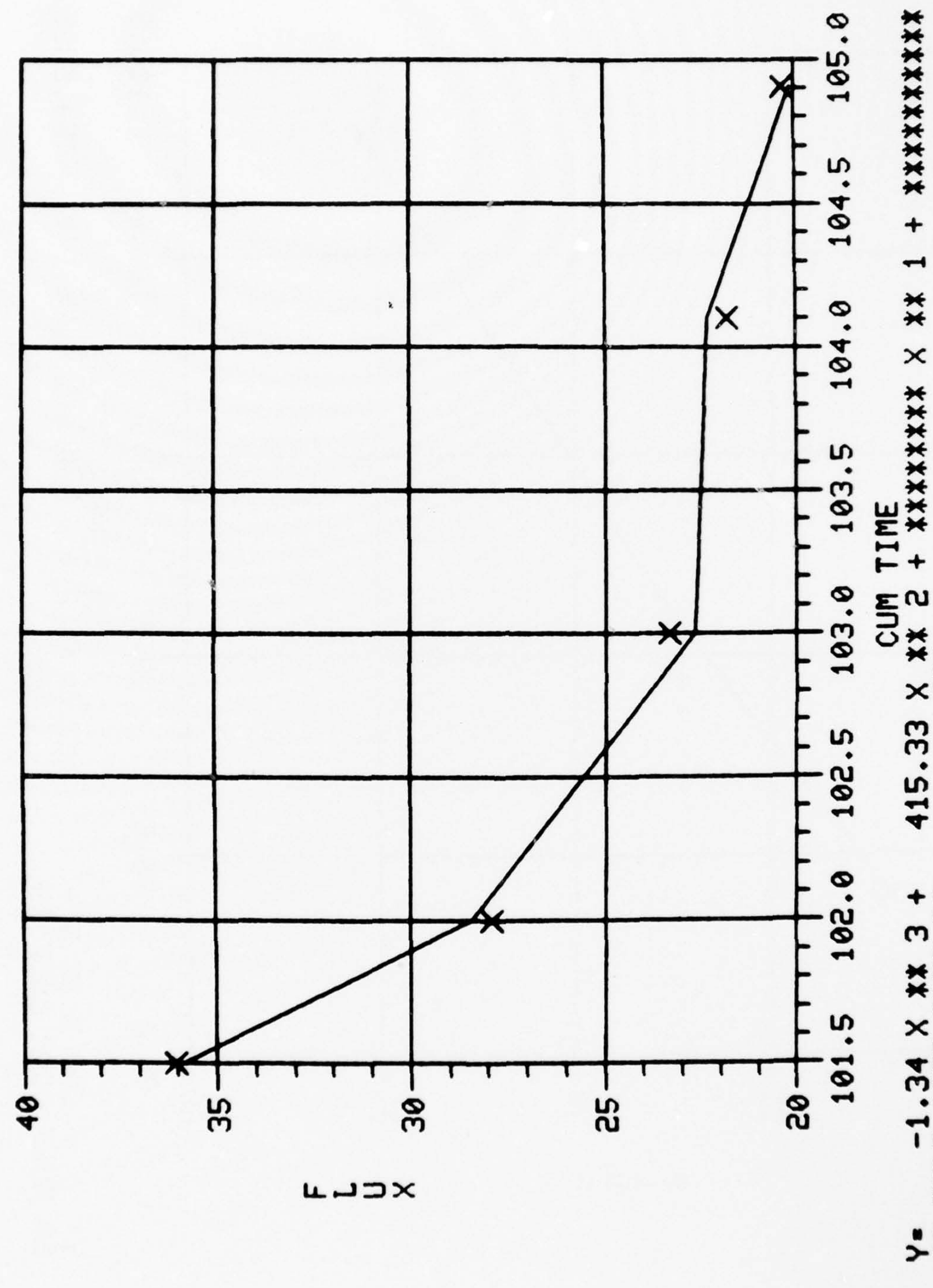
FLUX
40
35
30
25
20
101.5
102.0
102.5
103.0
103.5
104.0
104.5
105.0
CUM TIME
Y= -1.34 X ** 3 + 415.33 X ** 2 + ********* X ** 1 + *********
SQ MULT CORR COEF IS .994

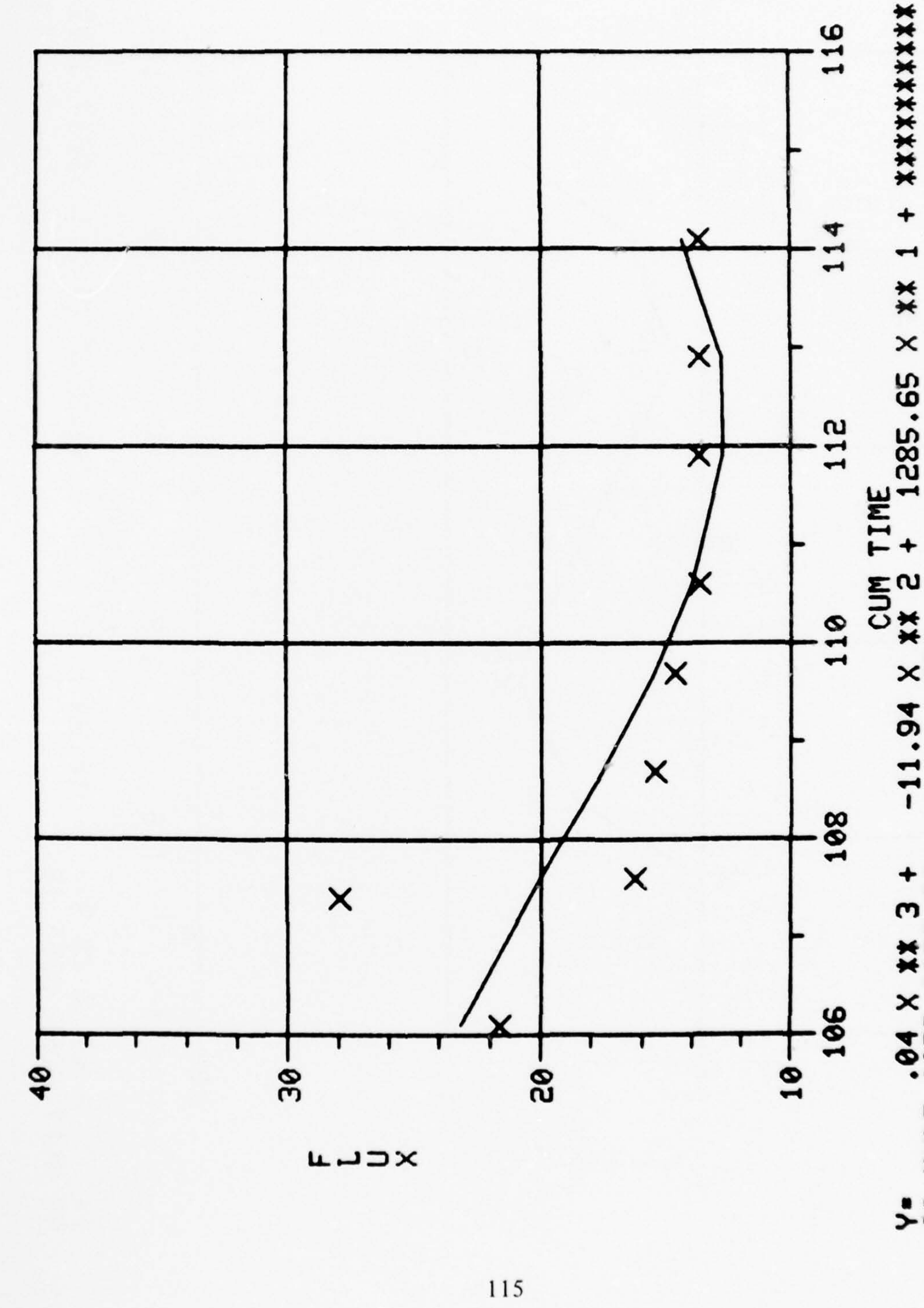
FLUX
40
30
20
10
106
108
110
112
114
116
CUM TIME
Y= .04 X ** 3 + -11.94 X ** 2 + 1285.65 X ** 1 + **********
SQ MULT CORR COEF IS .584

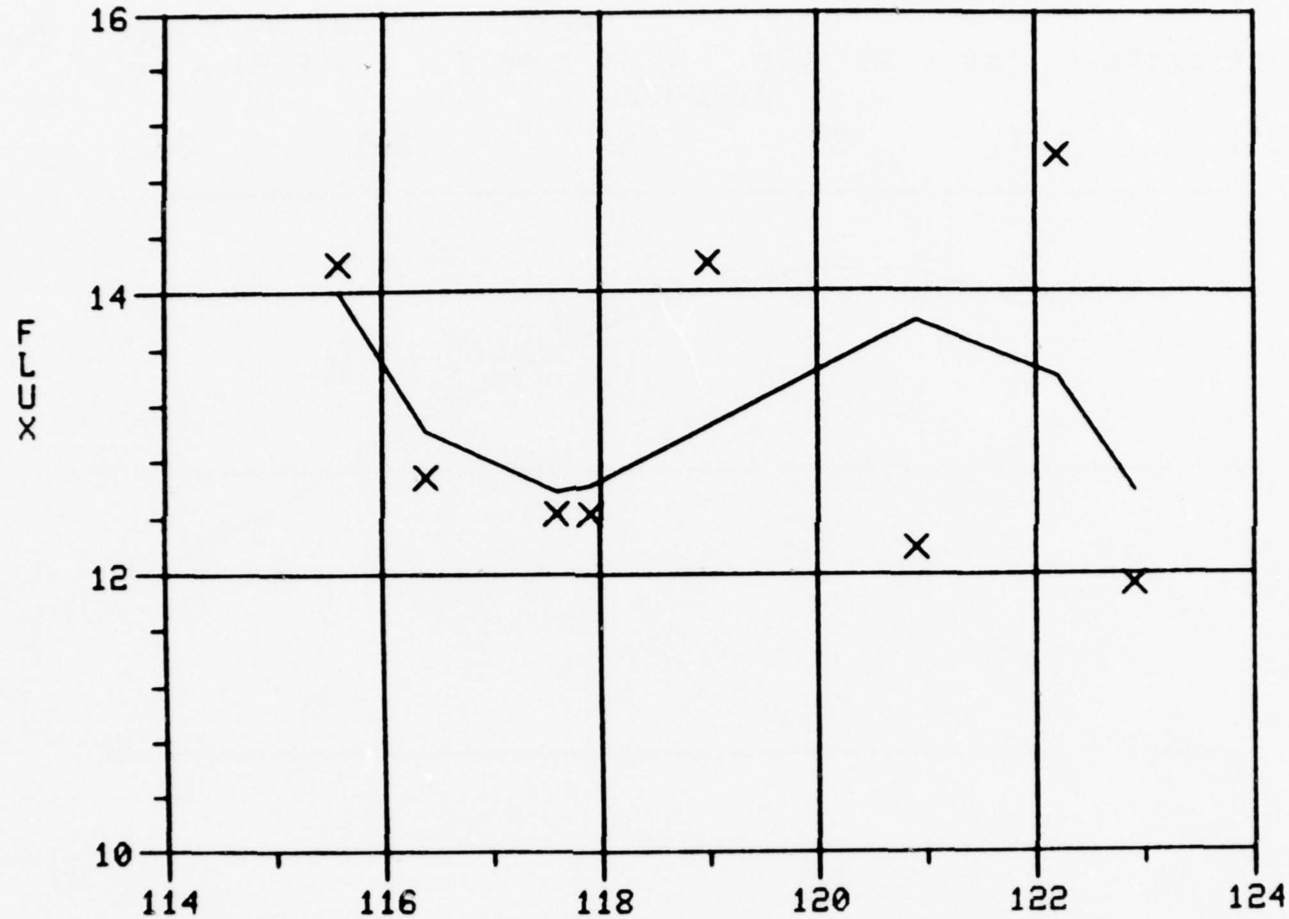


Y= -.05 X ** 3 + 18.94 X ** 2 + -2259.65 X ** 1 + 89837.3507
SQ MULT CORR COEF IS .234

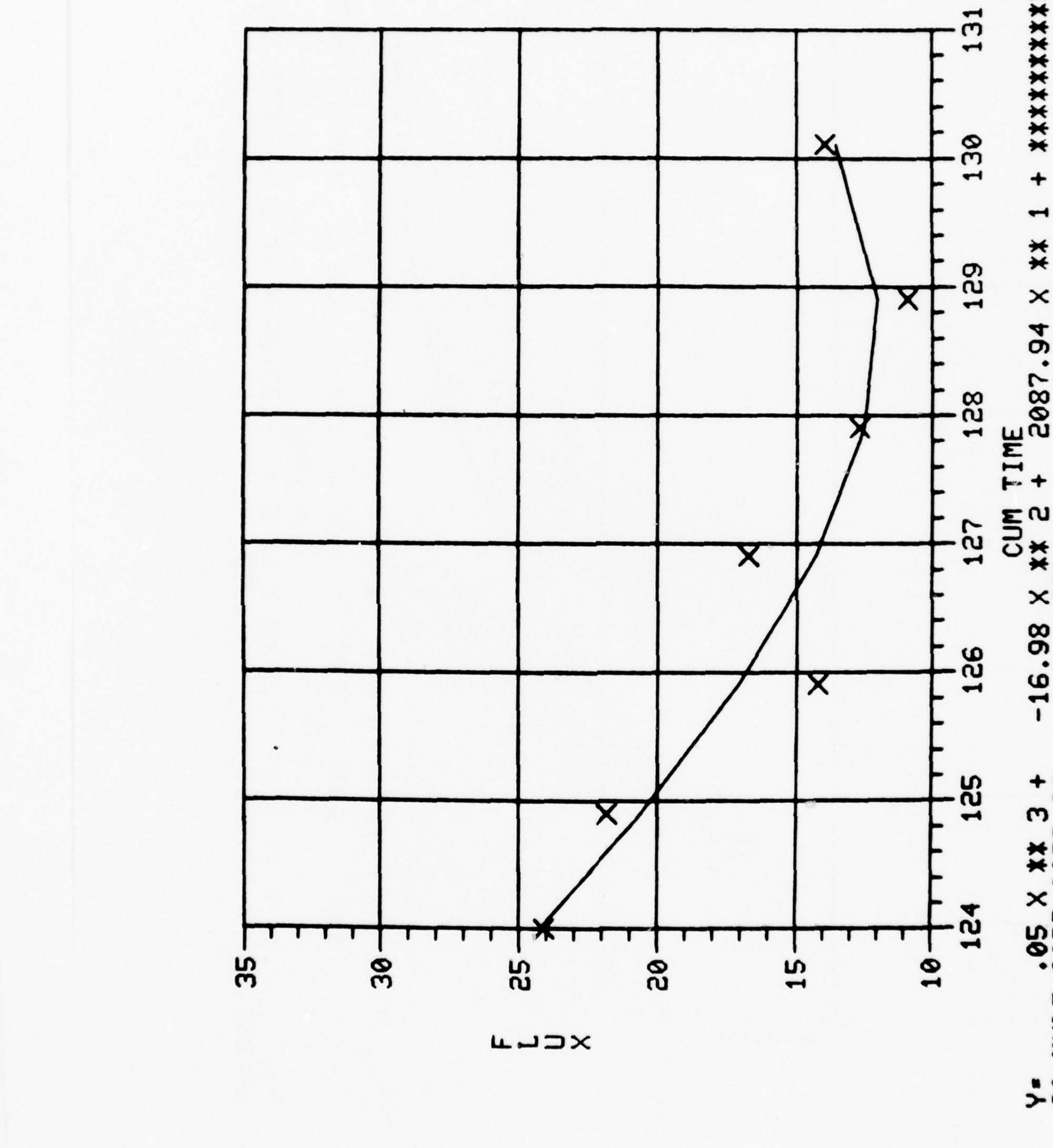
FLUX
CUM TIME
35
30
25
20
15
10
124
125
126
127
128
129
130
131
Y= .05 X ** 3 + -16.98 X ** 2 + 2087.94 X ** 1 + **********
SQ MULT CORR COEF IS .880

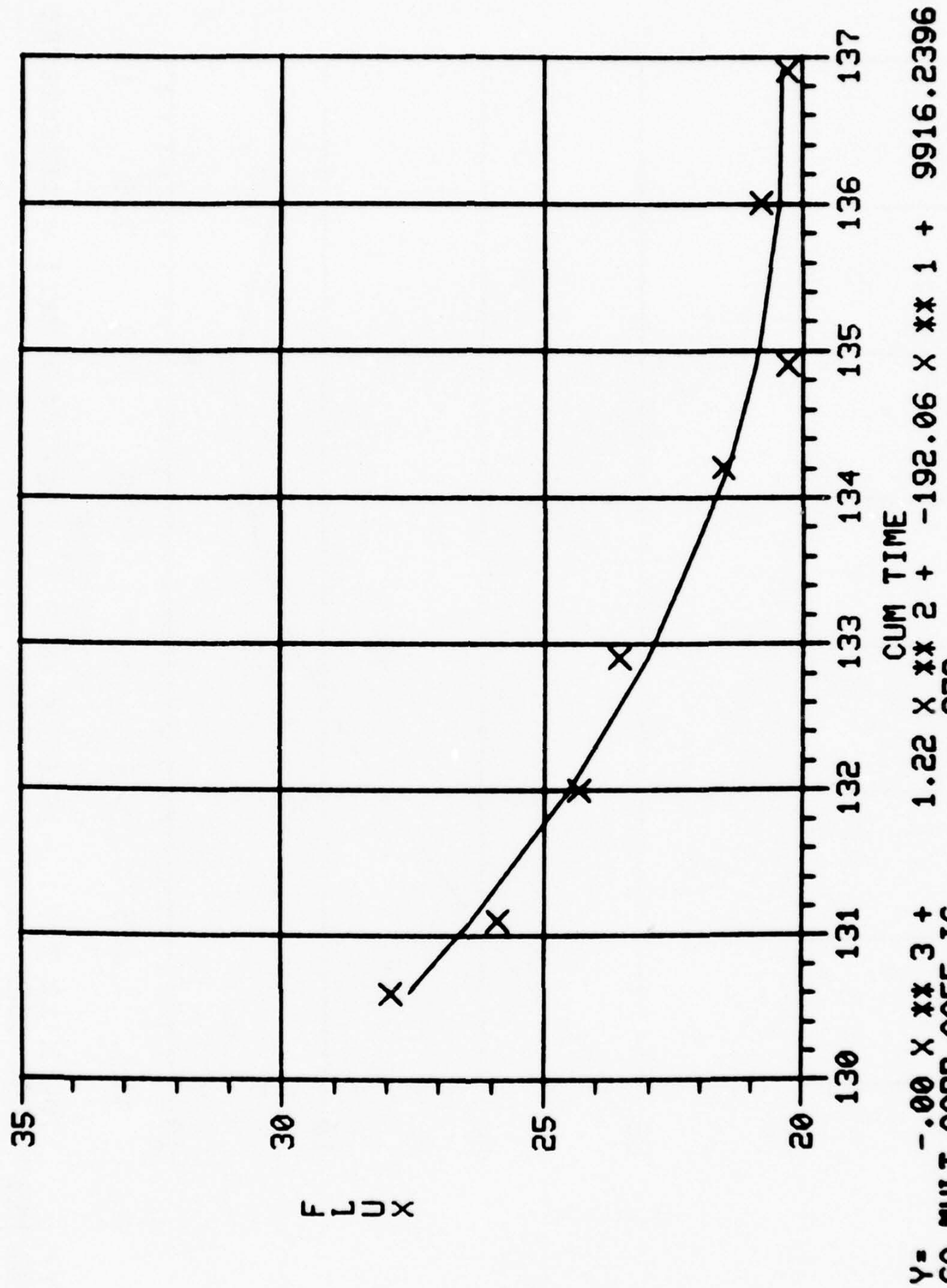
FLUX
35
30
25
20
130
131
132
133
134
135
136
137
CUM TIME
Y= -.00 X ** 3 + 1.22 X ** 2 + -192.06 X ** 1 + 9916.2396
SQ MULT CORR COEF IS .978

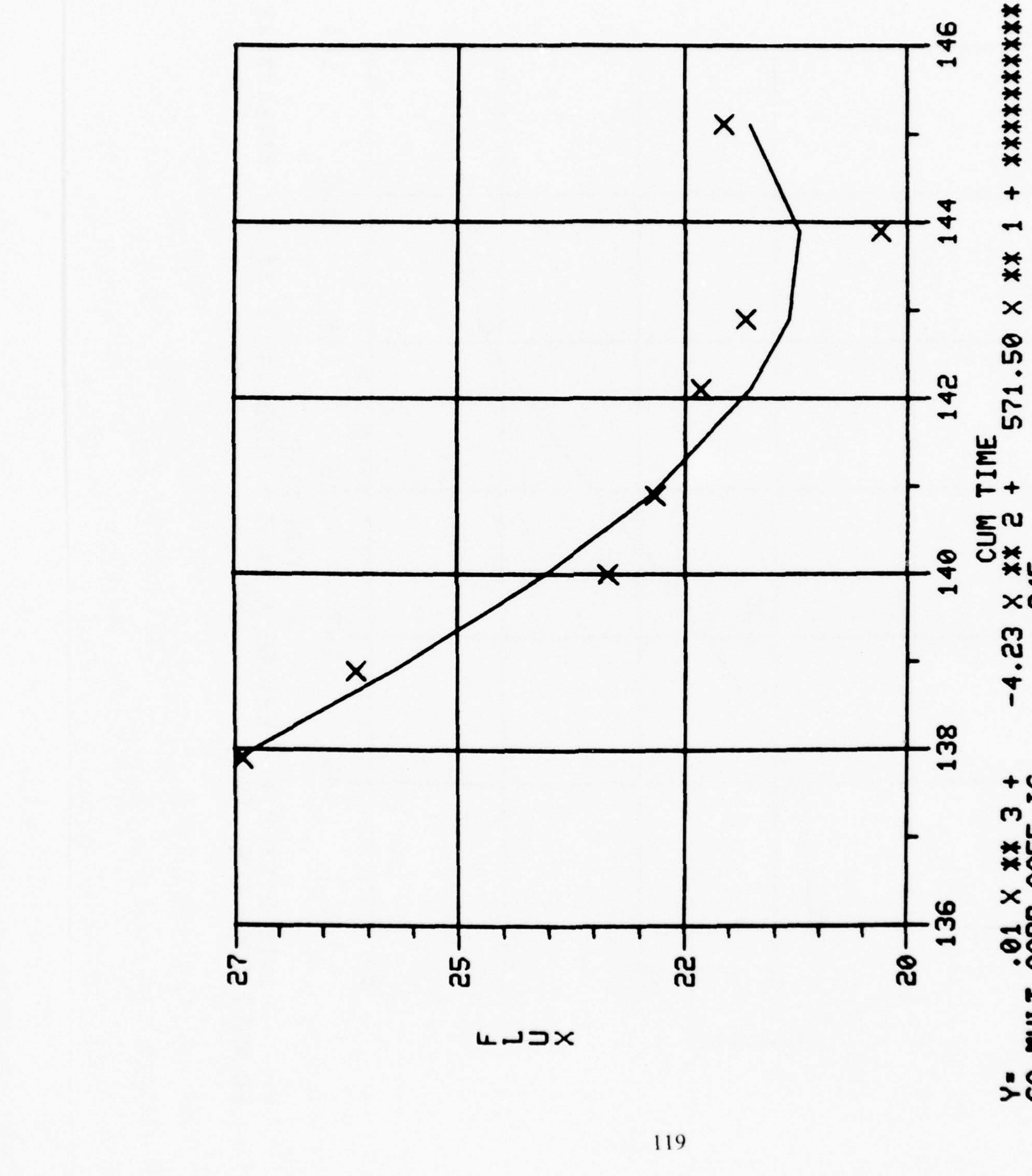

FLUX
CUM TIME
27
25
22
20
136
138
140
142
144
146
Y= .01 X ** 3 + -4.23 X ** 2 + 571.50 X ** 1 + XXXXXXXXX
SQ MULT CORR COEF IS .945

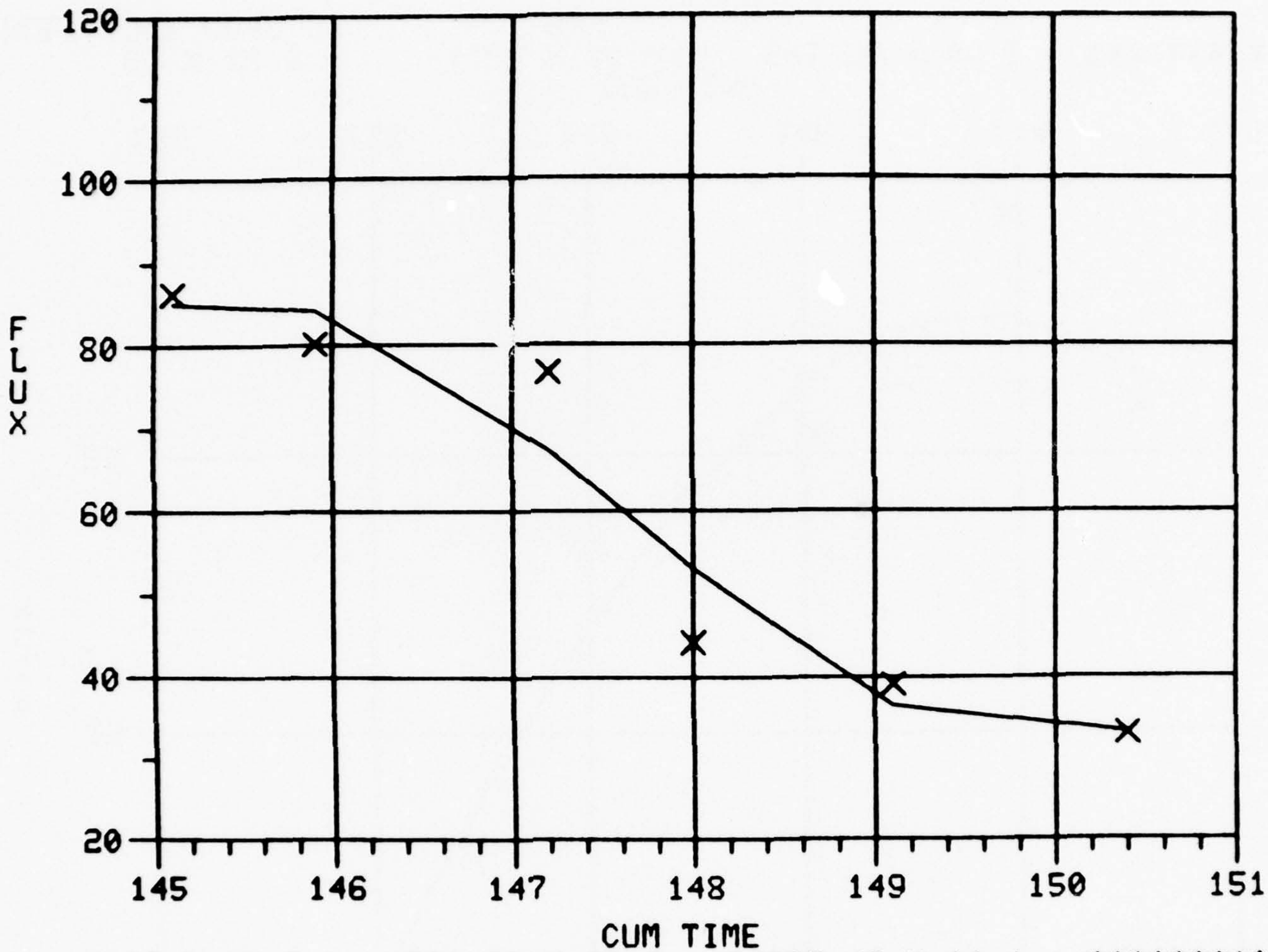

Y= 1.18 X ** 3 + -521.65 X ** 2 + 77022.49 X ** 1 + **********
SQ MULT CORR COEF IS .931

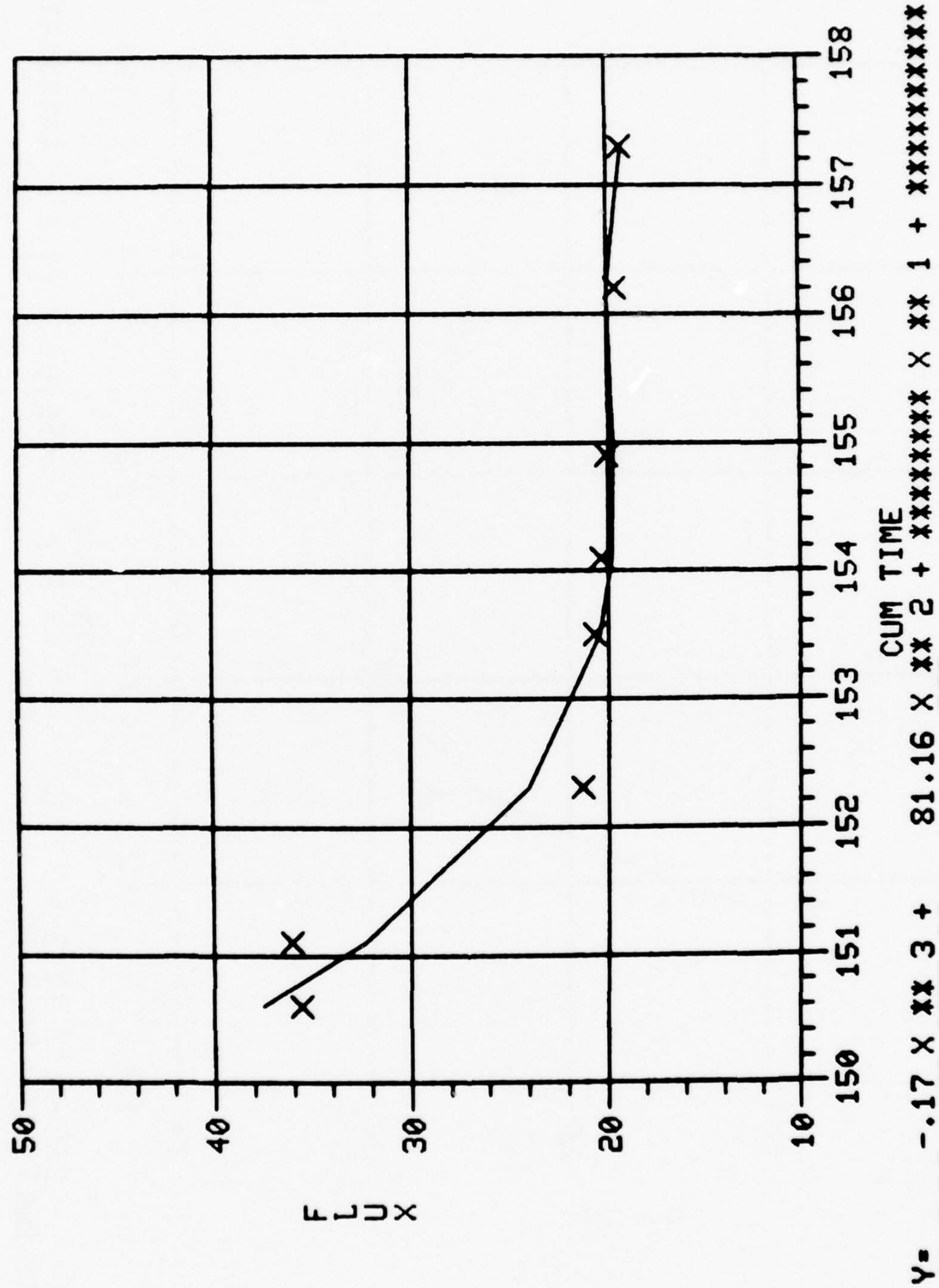
FLUX
CUM TIME
50
40
30
20
10
150
151
152
153
154
155
156
157
158
Y= -.17 X XX 3 + 81.16 X XX 2 + XXXXXXXX X XX 1 + XXXXXXXXXX
SQ MULT CORR COEF IS .929

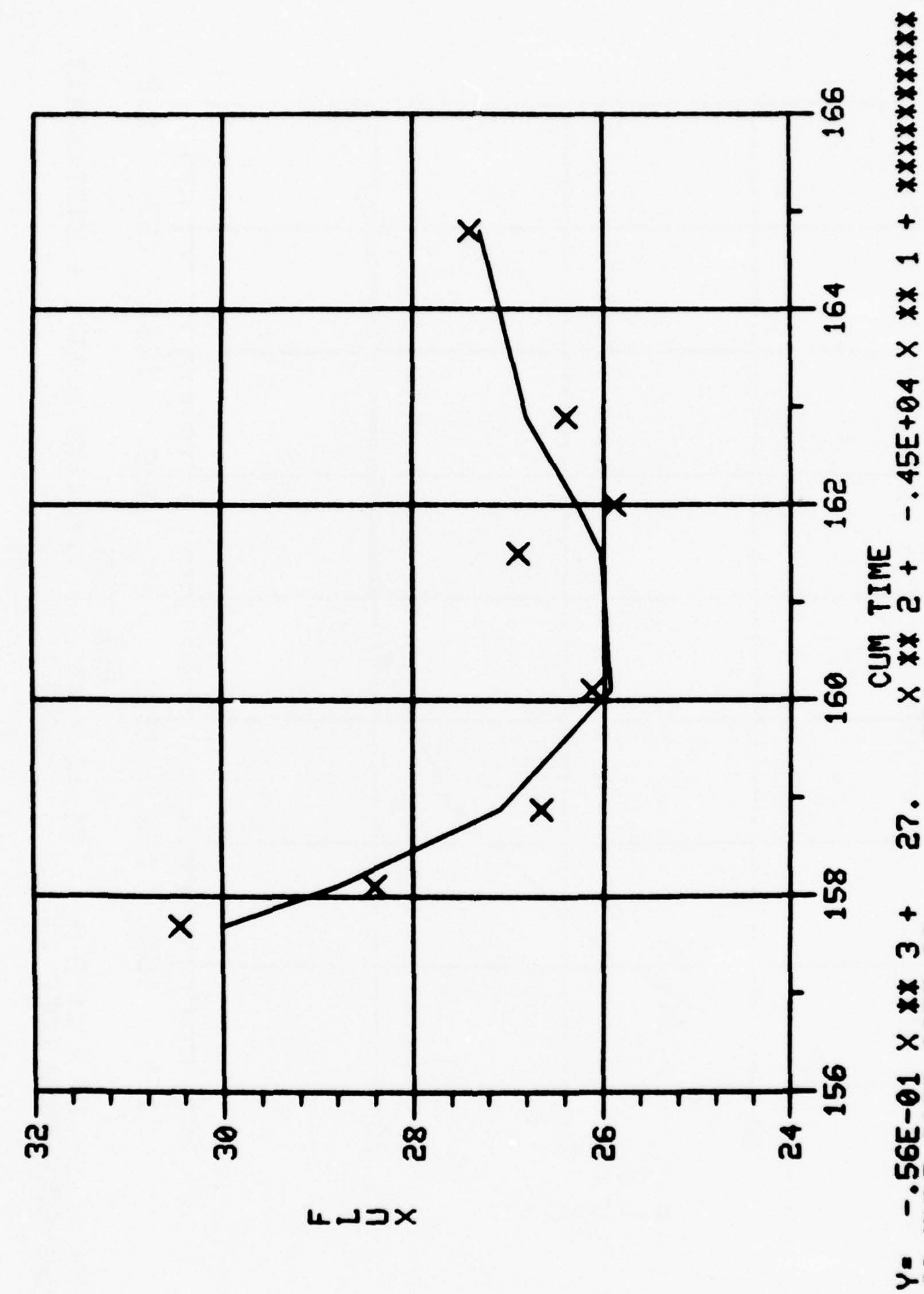
FLUX
32
30
28
26
24
156
158
160
162
164
166
CUM TIME
Y= -.56E-01 X ** 3 + 27. X ** 2 + -.45E+04 X ** 1 + **********
SQ MULT CORR COEF IS .896

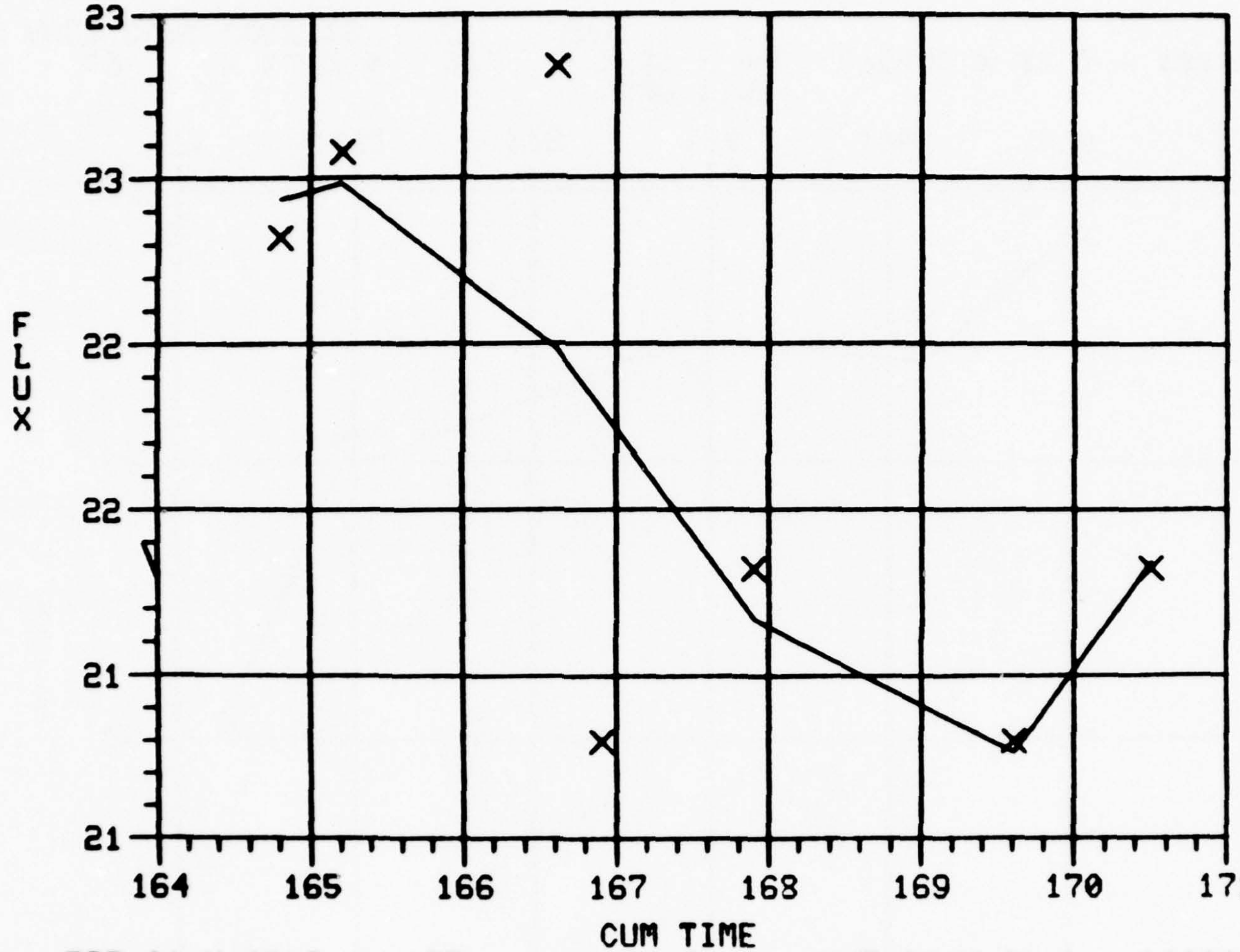


Y= .53E-01 X ** 3 + -27. X ** 2 + .44E+04 X ** 1 + **********
SQ MULT CORR COEF IS .593

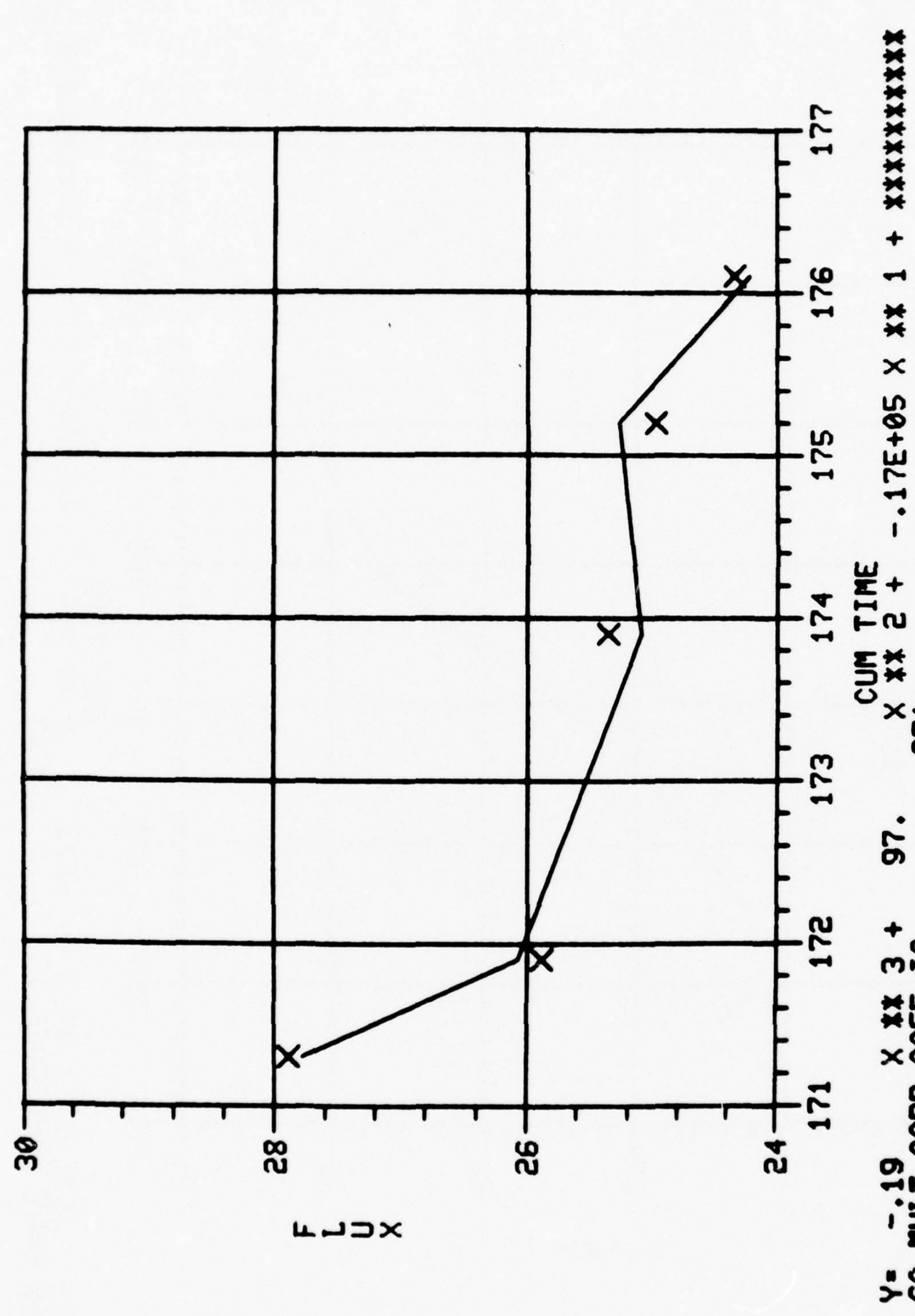
FLUX
30
28
26
24
171
172
173
174
175
176
177
CUM TIME
Y= -.19 X ** 3 + 97. X ** 2 + -.17E+05 X ** 1 + *********
SQ MULT CORR COEF IS .971

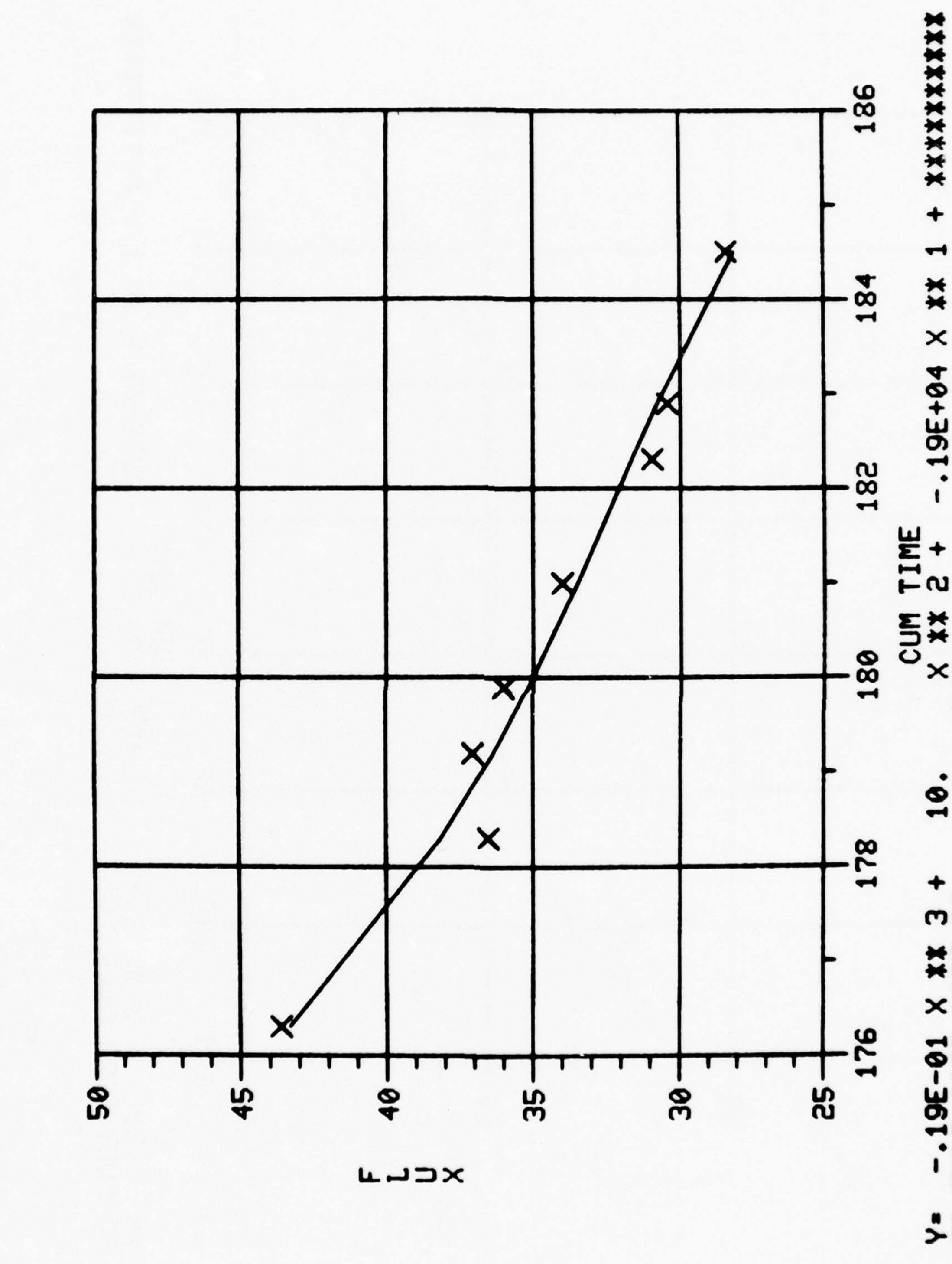
FLUX
50
45
40
35
30
25
176
178
180
182
184
186
CUM TIME
Y= -.19E-01 X ** 3 + 10. X ** 2 + -.19E+04 X ** 1 + XXXXXXXXXX
SQ MULT CORR COEF IS .971

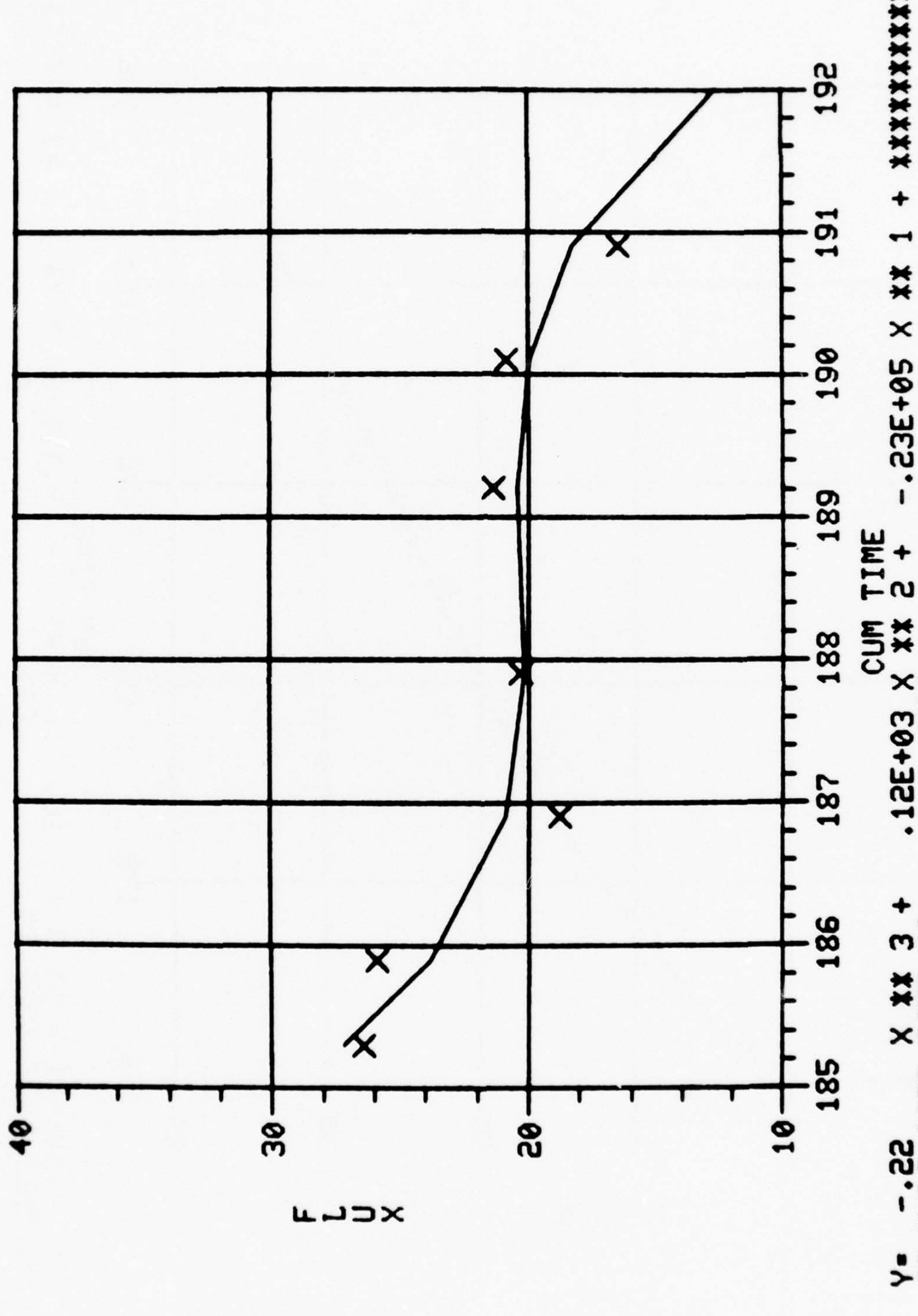
FLUX
CUM TIME
40
30
20
10
185
186
187
188
189
190
191
192
Y= -.22 X ** 3 + .12E+03 X ** 2 + -.23E+05 X ** 1 + *********
SQ MULT CORR COEF IS .895

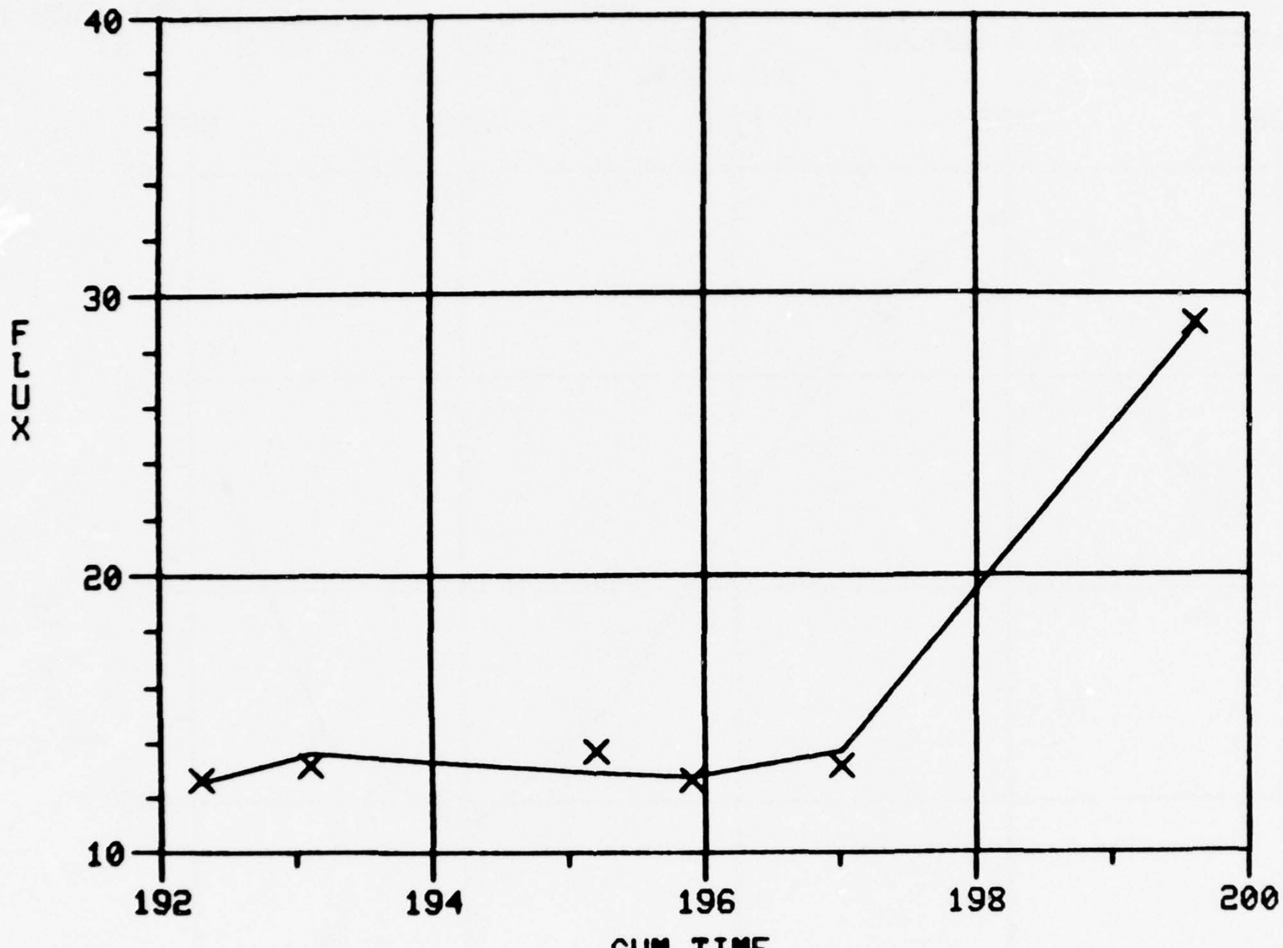


Y= .16 X ** 3 + -92. X ** 2 + .18E+05 X ** 1 + **********
SQ MULT CORR COEF IS .995

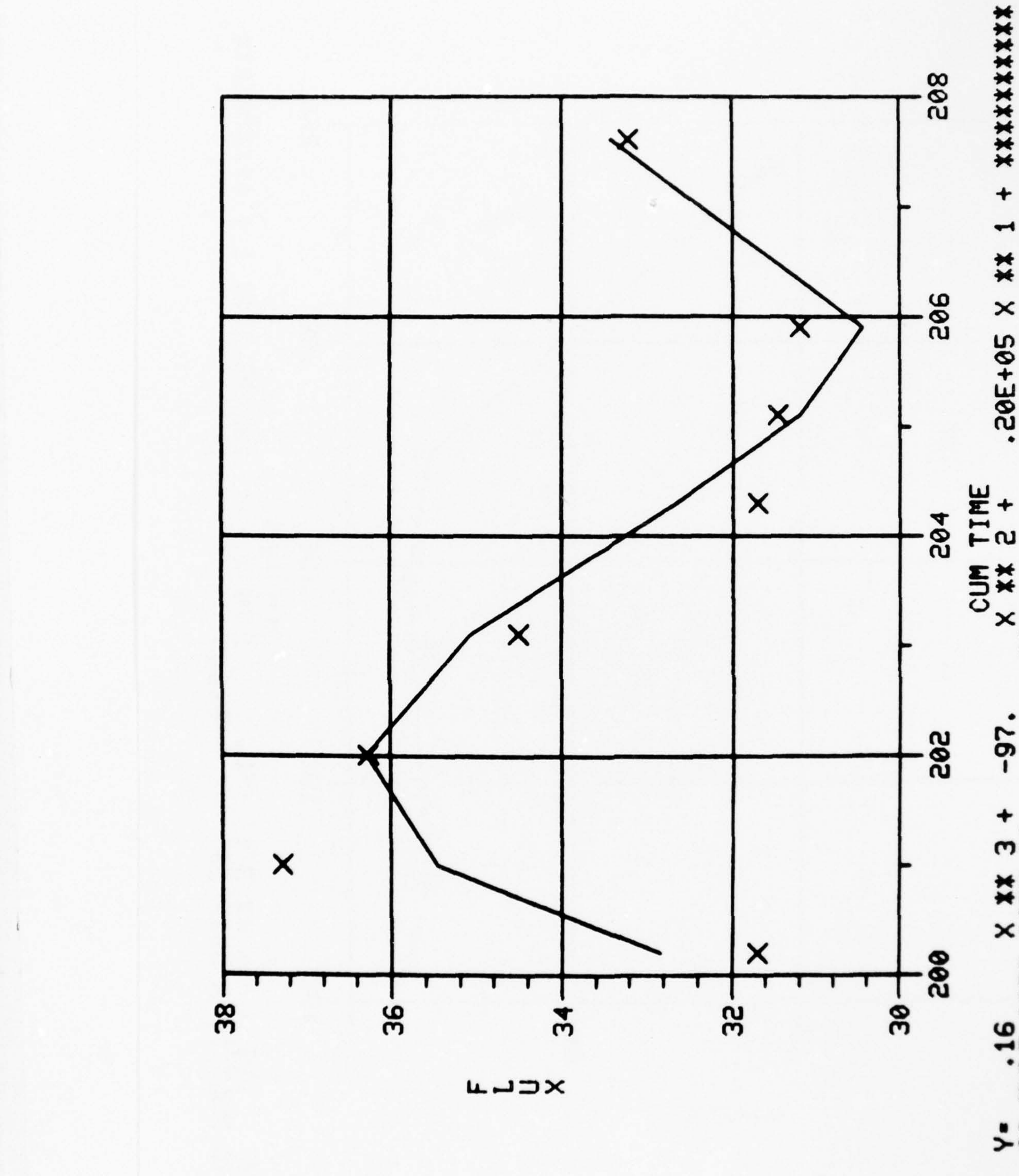
FLUX
38
36
34
32
30
200
202
204
206
208
CUM TIME
Y= .16 X ** 3 + -97. X ** 2 + .20E+05 X ** 1 + ***********
SQ MULT CORR COEF IS .834

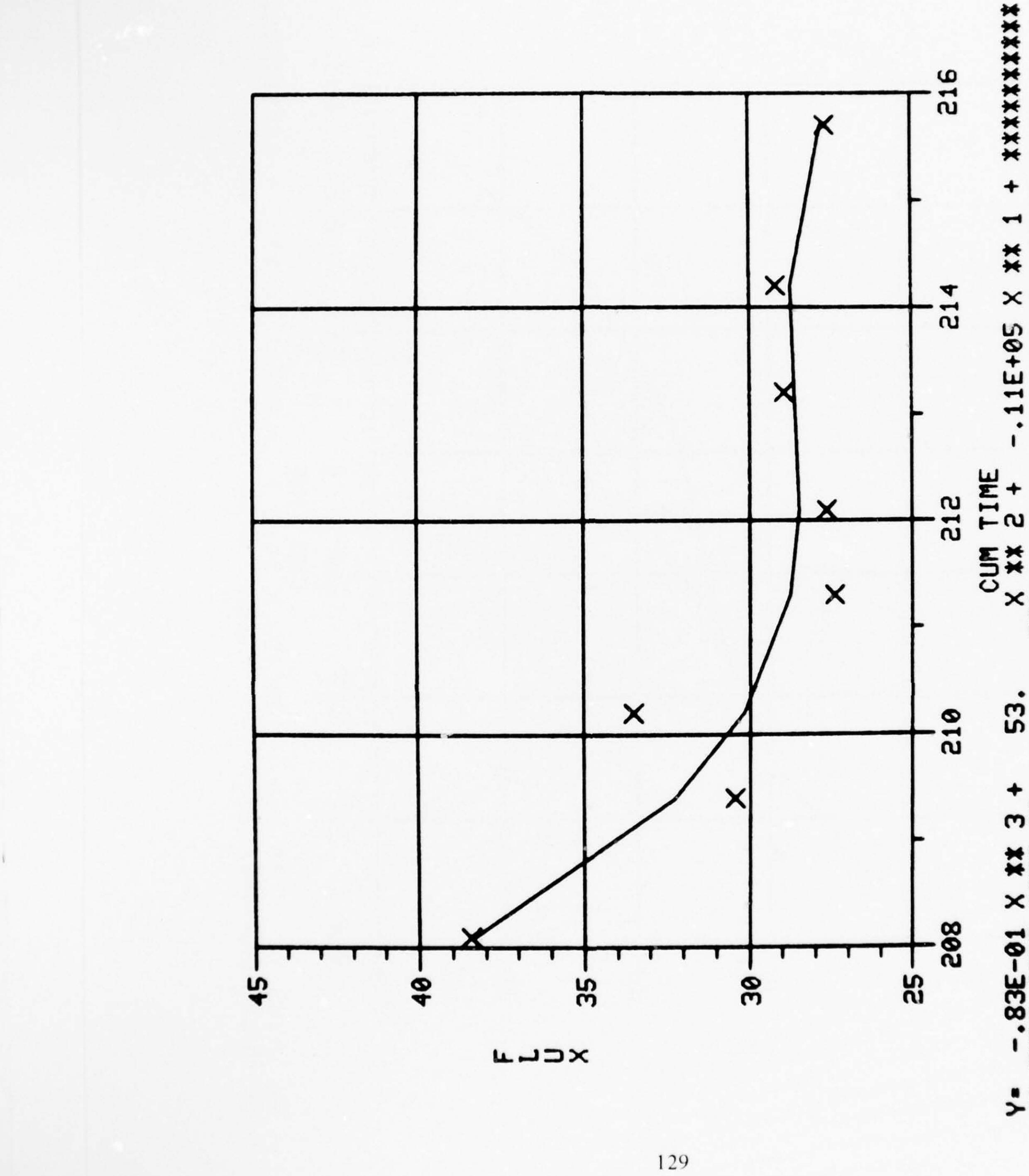

FLUX
45
40
35
30
25
208
210
212
214
216
CUM TIME
Y= -.83E-01 X ** 3 + 53. X ** 2 + -.11E+05 X ** 1 + **********
SQ MULT CORR COEF IS .831

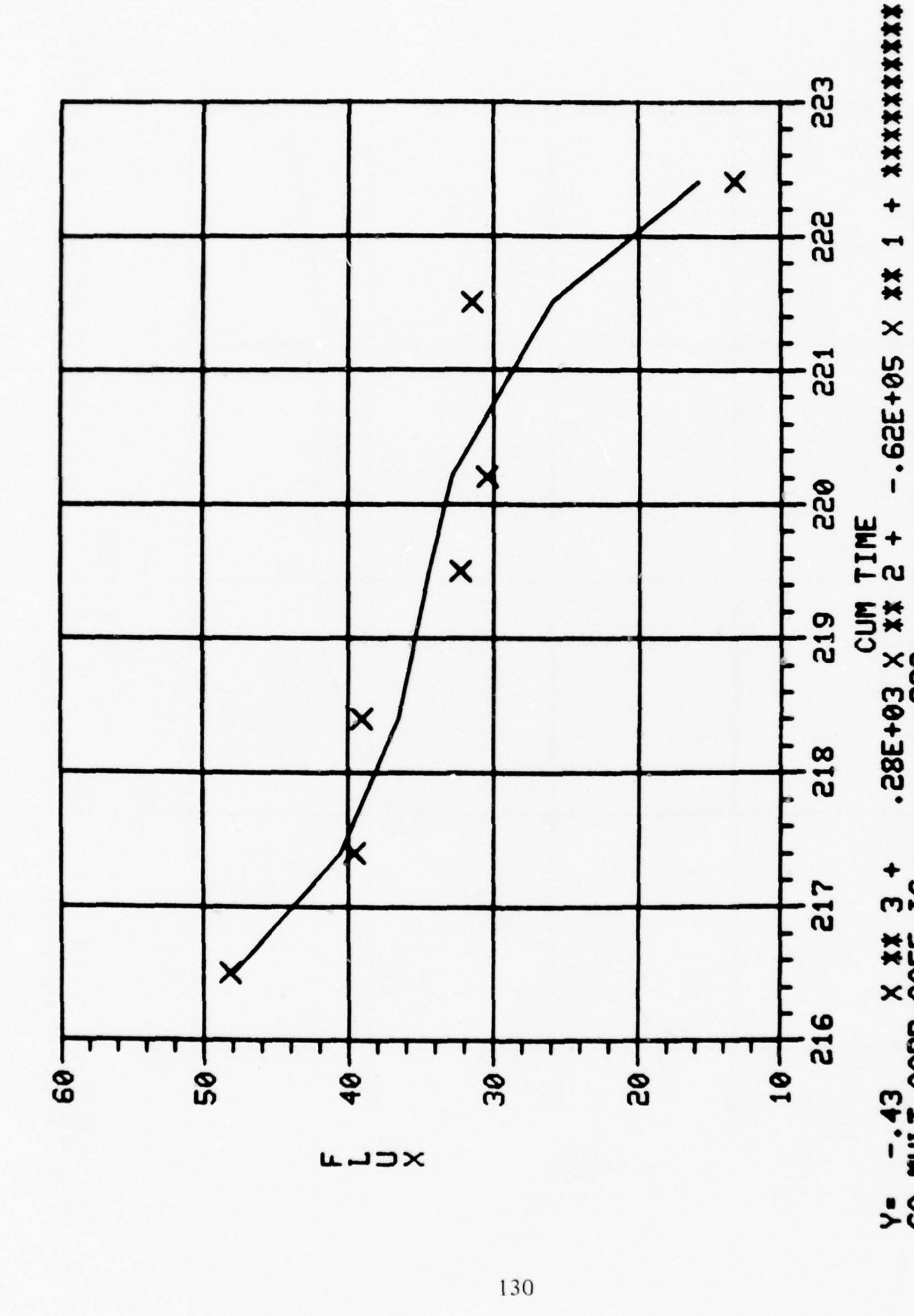
FLUX
60
50
40
30
20
10
216
217
218
219
220
221
222
223
CUM TIME
Y= -.43 X ** 3 + .28E+03 X ** 2 + -.62E+05 X ** 1 + *********
SQ MULT CORR COEF IS .923

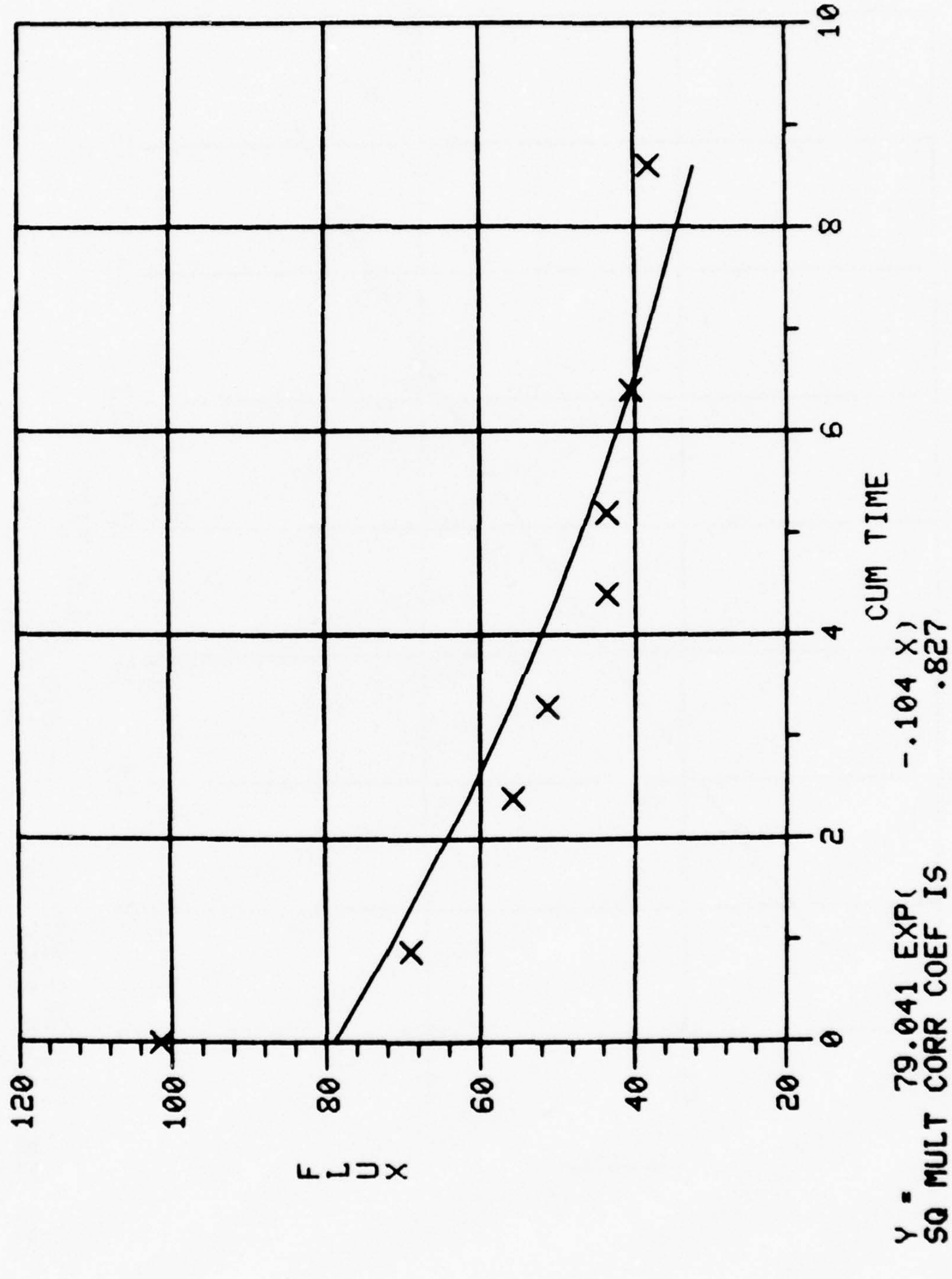
120
100
80
60
40
20
FLUX
0
2
4
6
8
10
CUM TIME
Y = 79.041 EXP( -.104 X)
SQ MULT CORR COEF IS .827

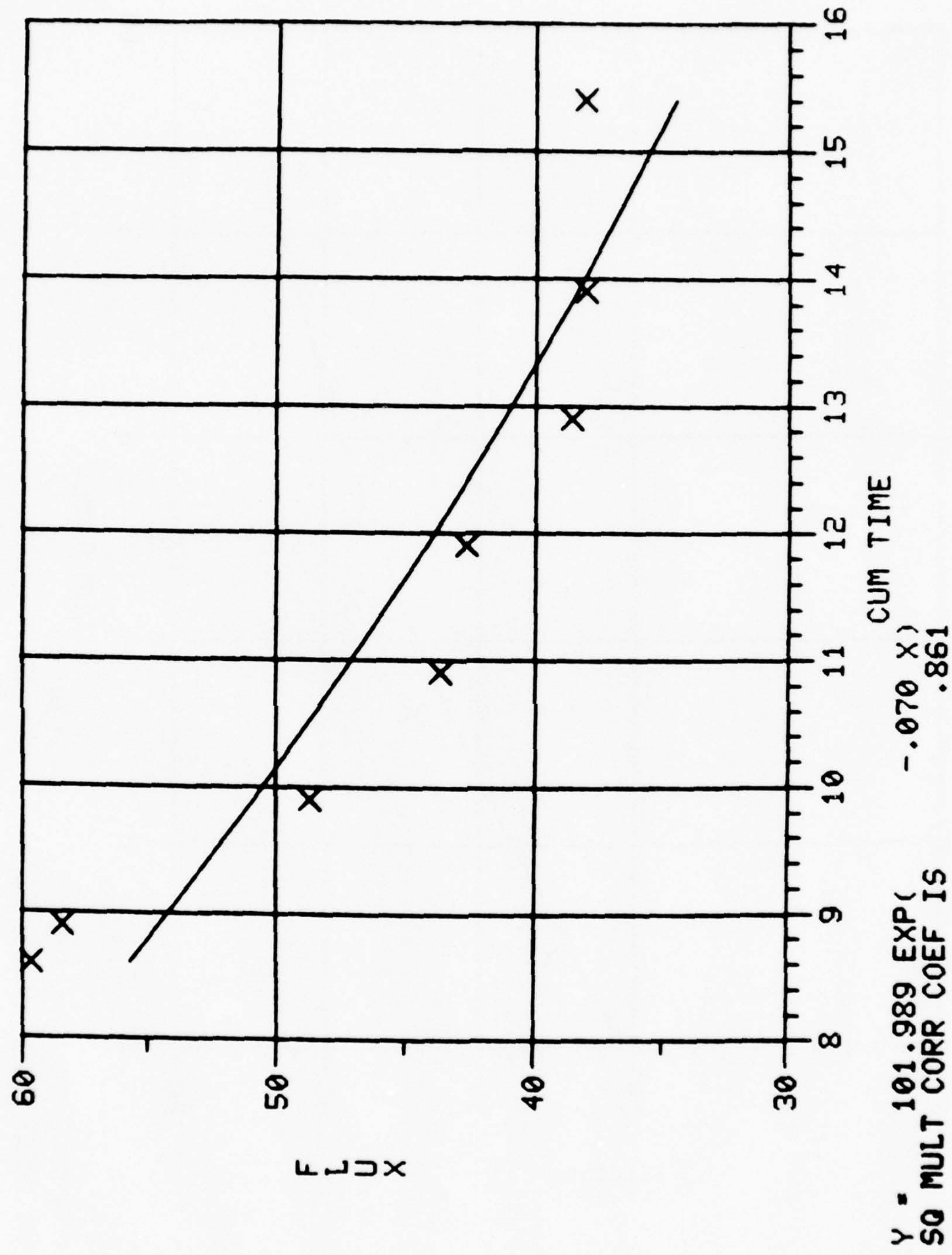
FLUX
60
50
40
30
8
9
10
11
12
13
14
15
16
CUM TIME
Y = 101.989 EXP( -.070 X)
SQ MULT CORR COEF IS .861

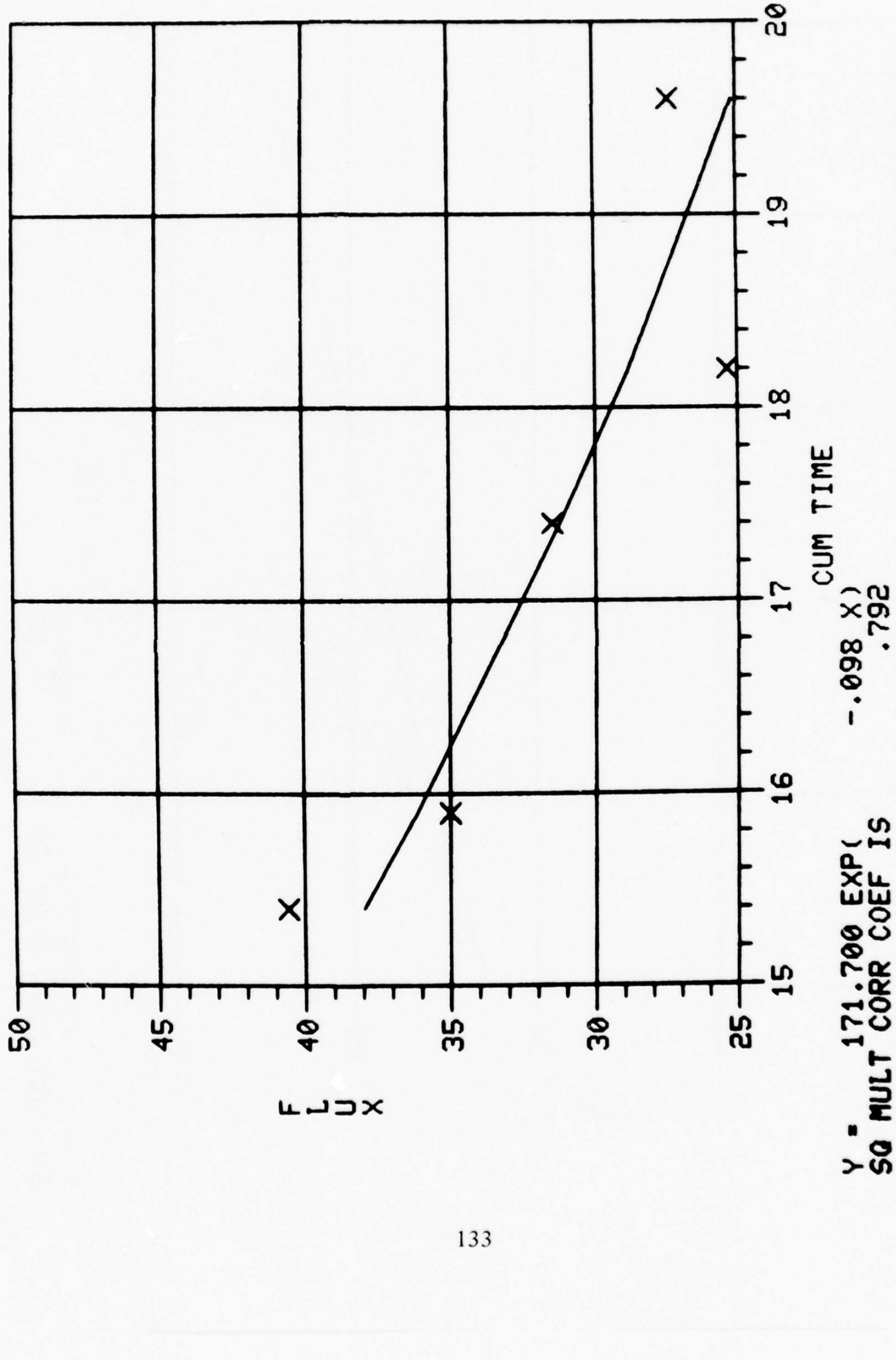
FLUX
50
45
40
35
30
25
15
16
17
18
19
20
CUM TIME
Y = 171.700 EXP( -.098 X)
SQ MULT CORR COEF IS .792

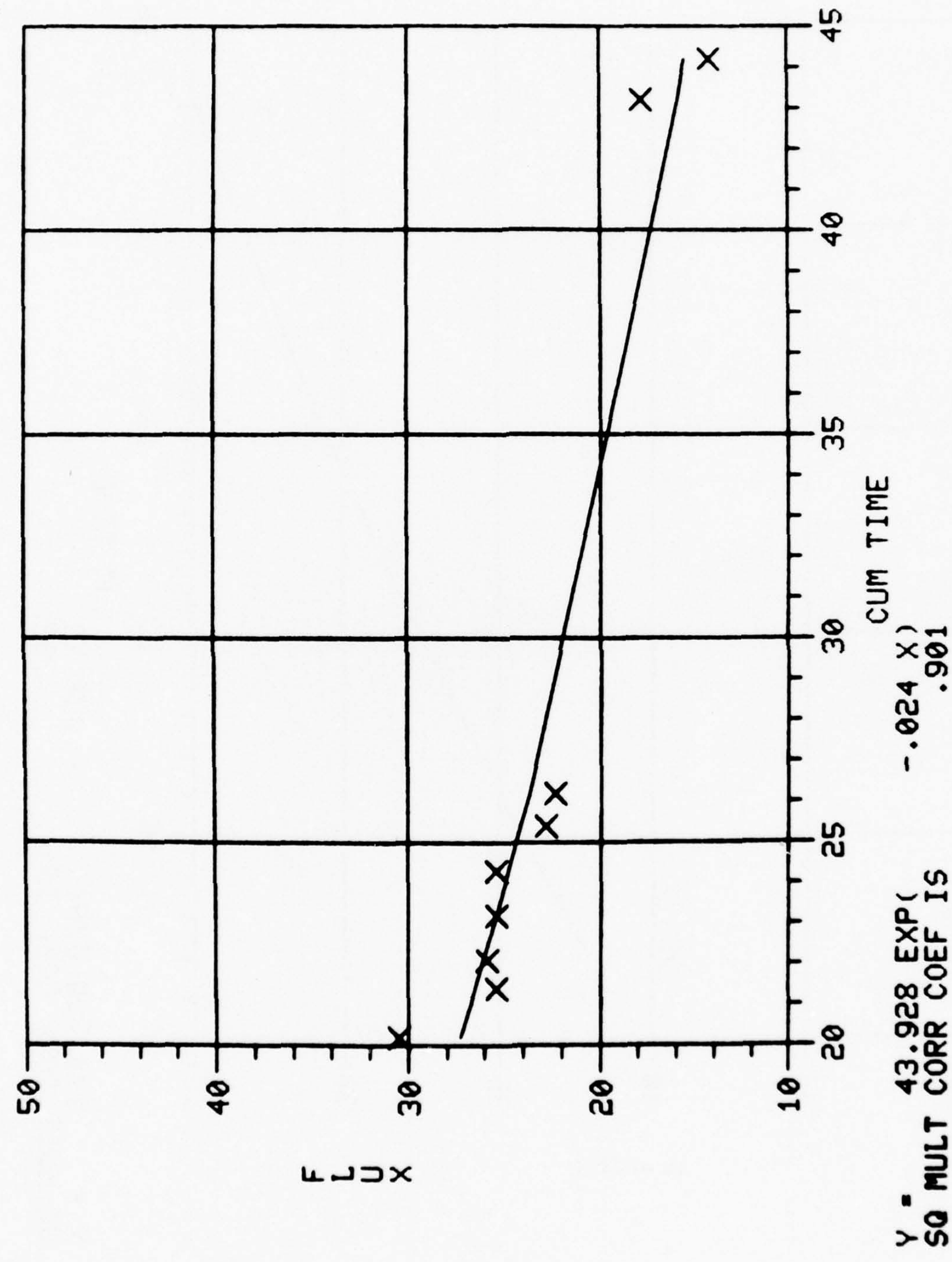
FLUX
50
40
30
20
10
20
25
30
35
40
45
CUM TIME
Y = 43.928 EXP( -.024 X)
SQ MULT CORR COEF IS .901

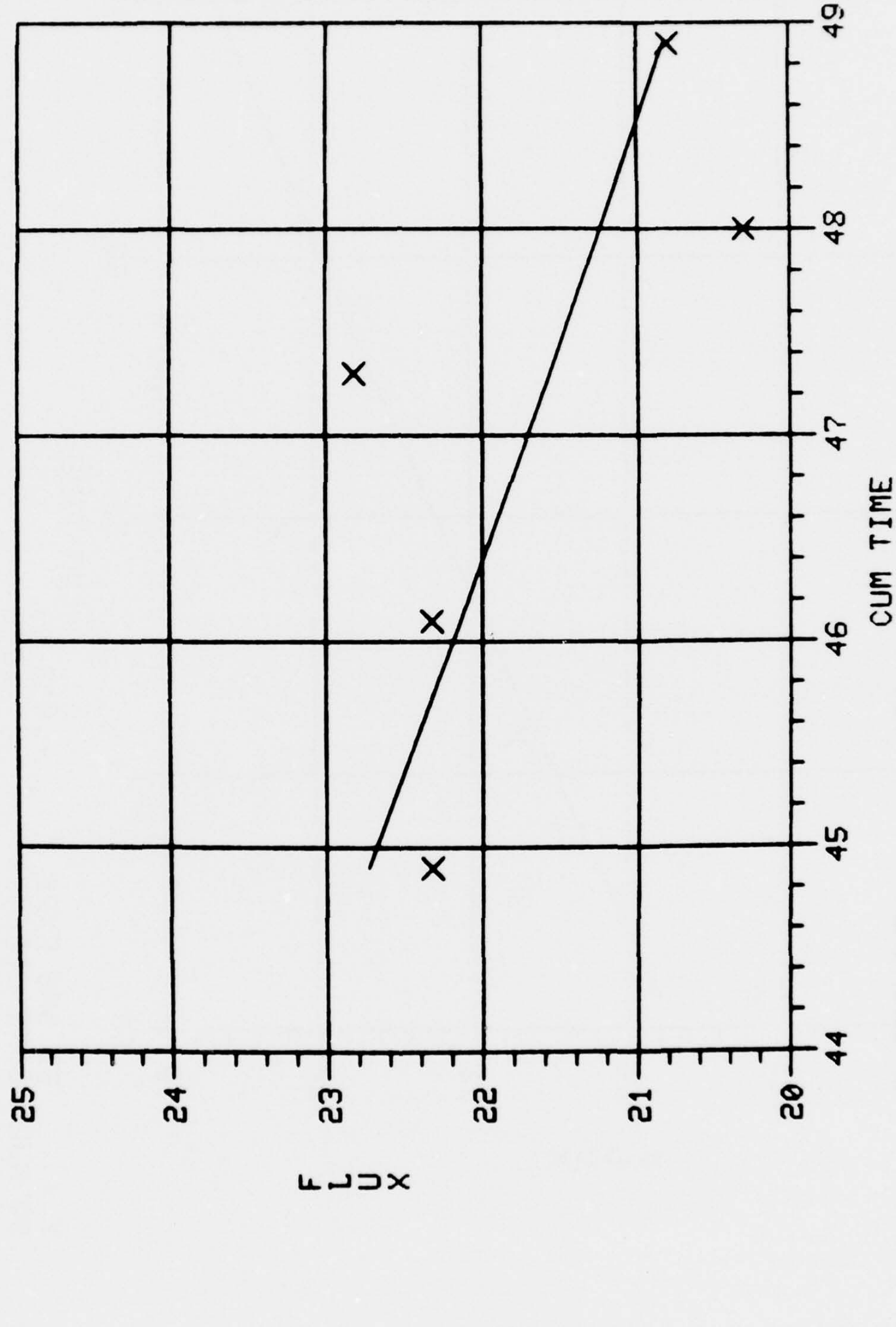
FLUX
25
24
23
22
21
20
44
45
46
47
48
49
CUM TIME
Y = 60.598 EXP( -.022 X)
SQ MULT CORR COEF IS .456

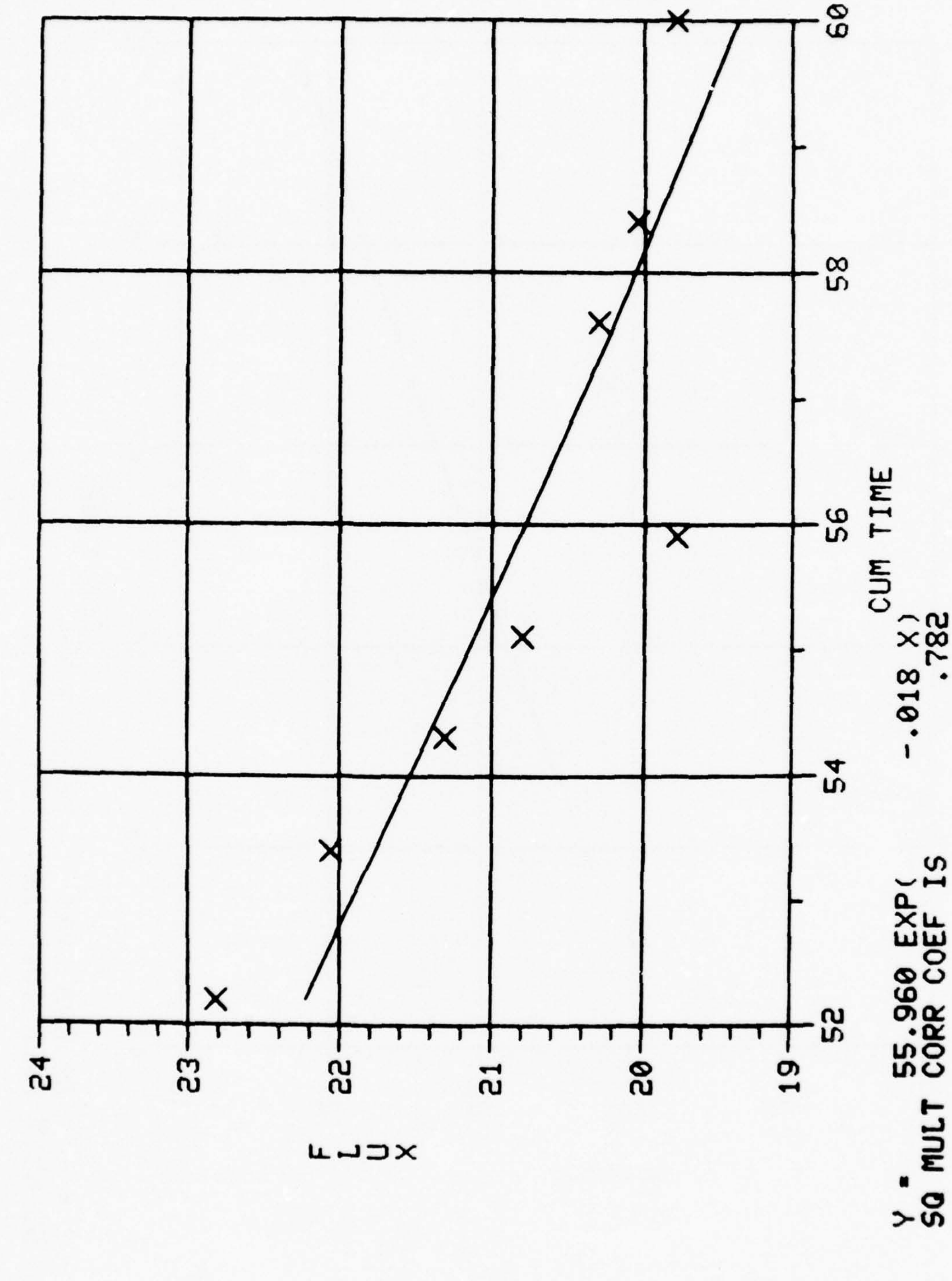
FLUX
24
23
22
21
20
19
52
54
56
58
60
CUM TIME
Y = 55.960 EXP( -.018 X)
SQ MULT CORR COEF IS .782

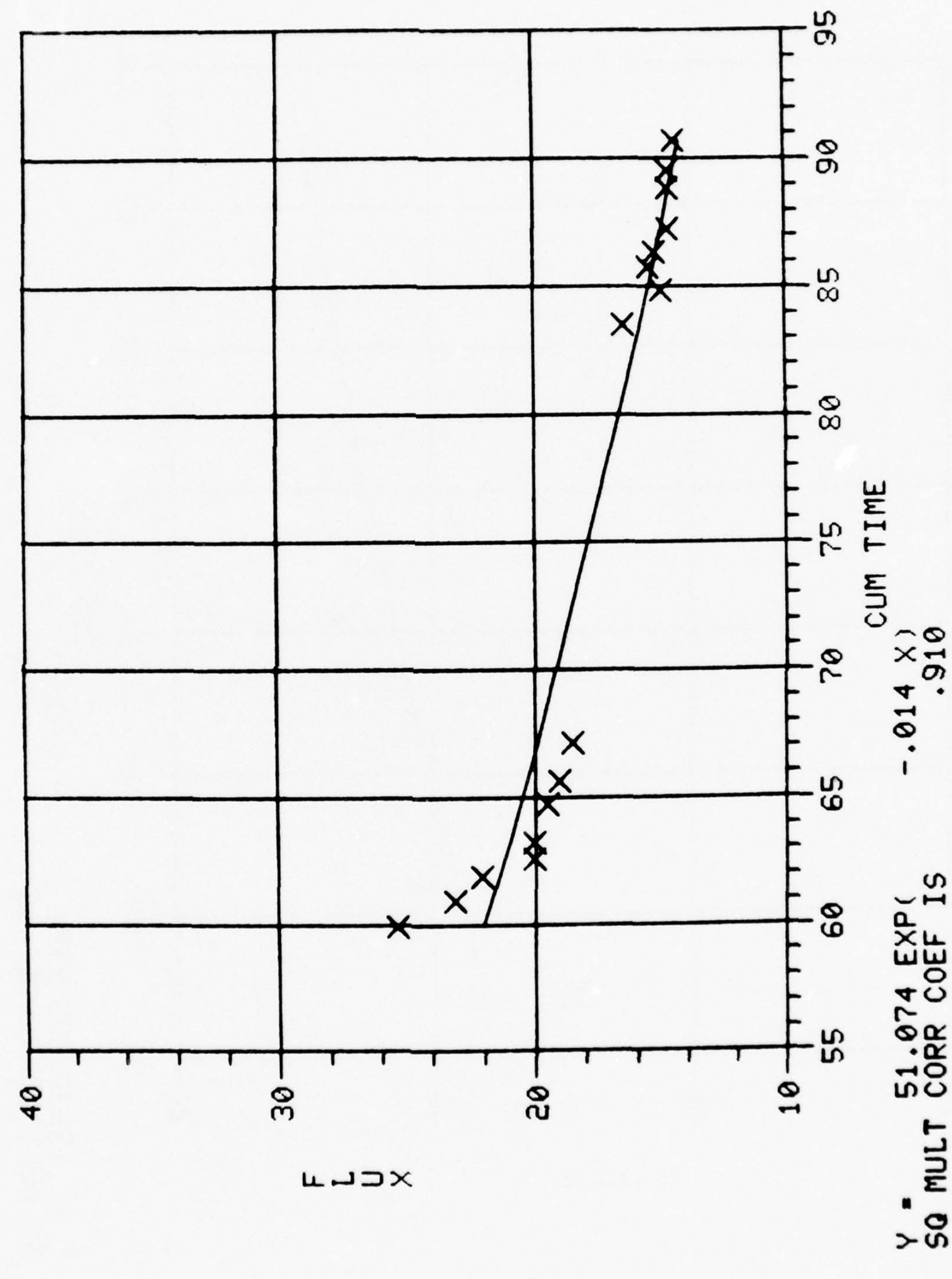
FLUX
40
30
20
10
CUM TIME
55
60
65
70
75
80
85
90
95
Y = 51.074 EXP( -.014 X)
SQ MULT CORR COEF IS .910

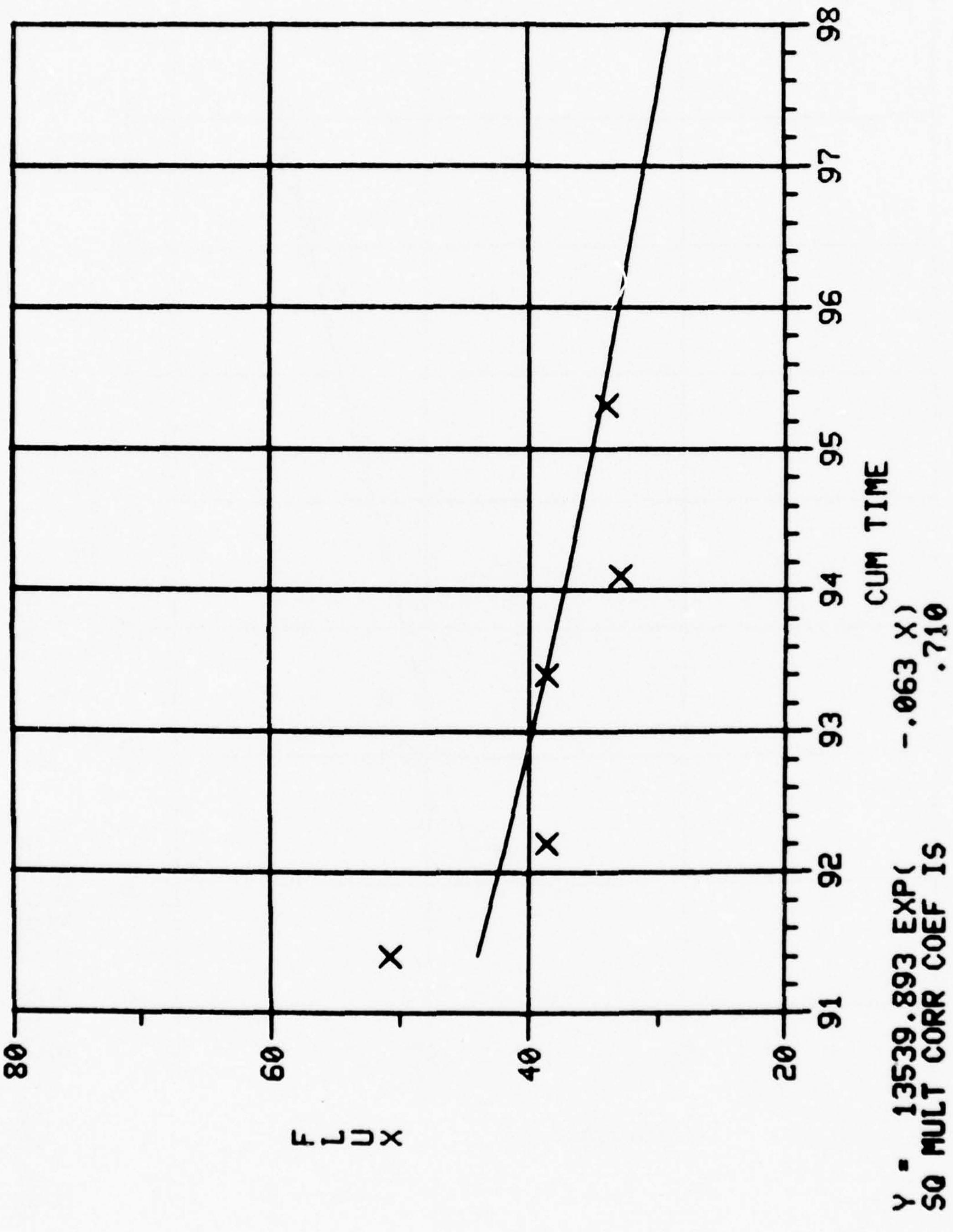

FLUX
CUM TIME
80
60
40
20
91
92
93
94
95
96
97
98
Y = 13539.893 EXP( -.063 X)
SQ MULT CORR COEF IS .710

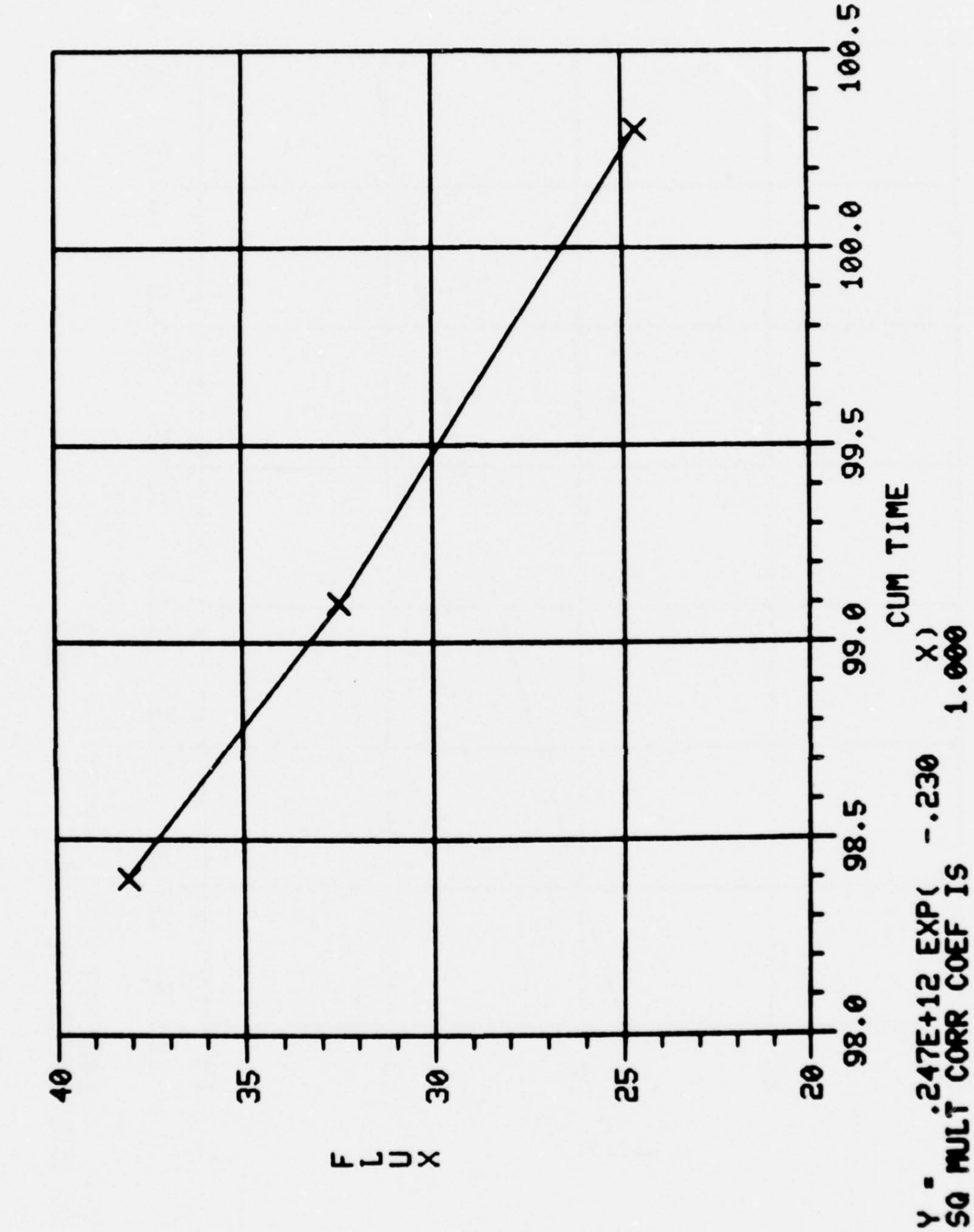
FLUX
CUM TIME
40
35
30
25
20
98.0
98.5
99.0
99.5
100.0
100.5
Y = .247E+12 EXP( -.230 X)
SQ MULT CORR COEF IS 1.000

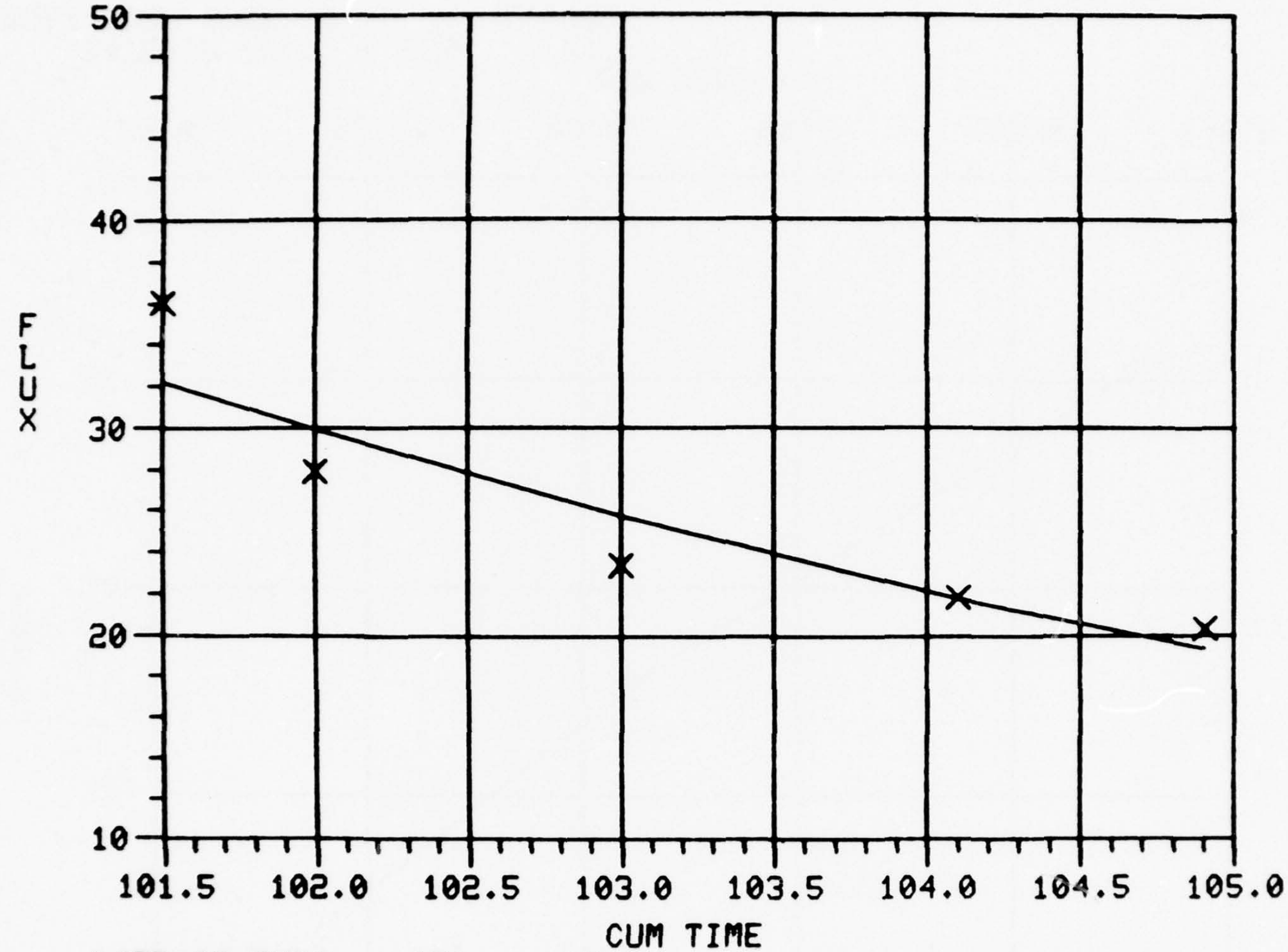


Y = .142E+09 EXP( -.151 X)
SQ MULT CORR COEF IS .863

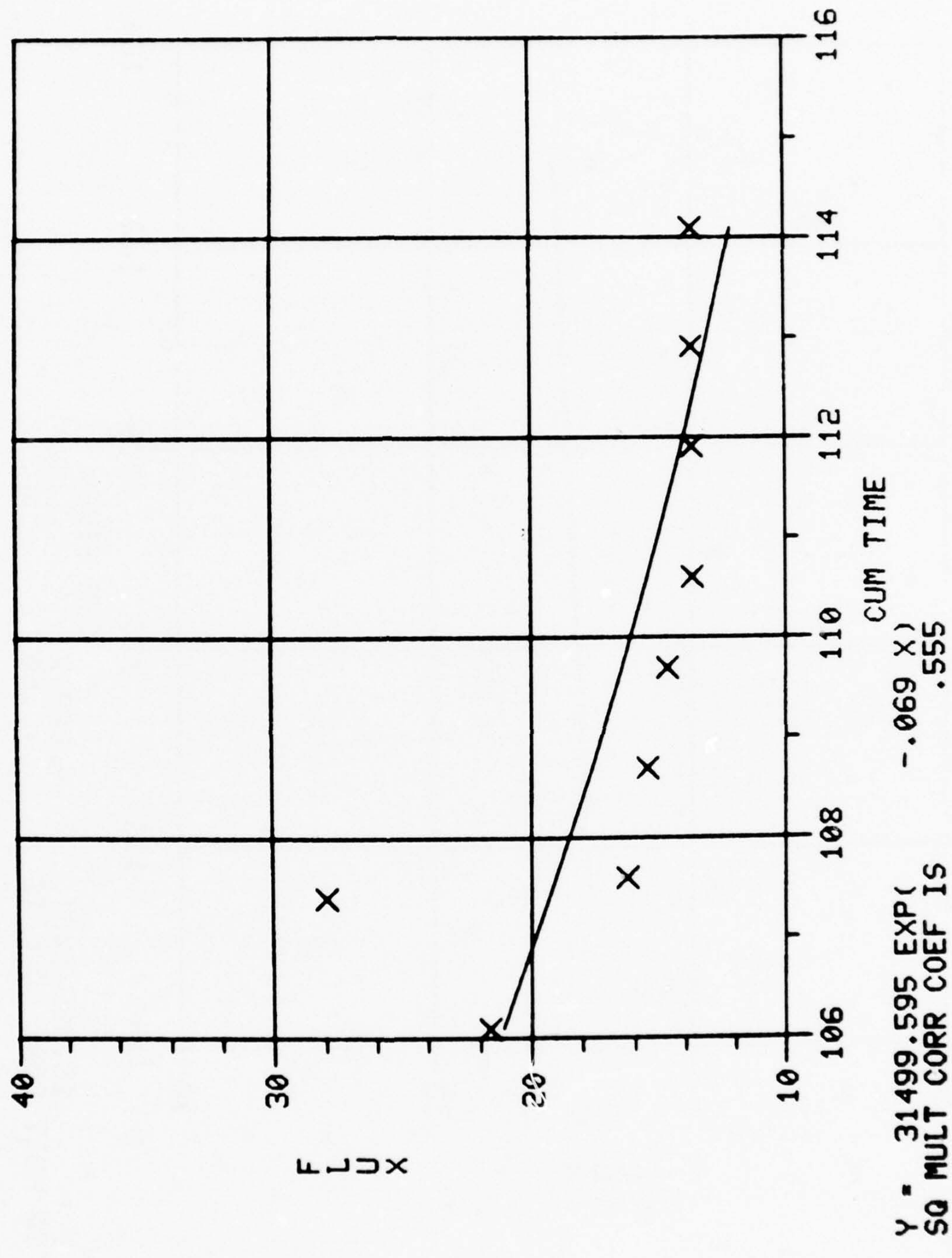

FLUX
40
30
20
10
106
108
110
112
114
116
CUM TIME
Y = 31499.595 EXP( -.069 X)
SQ MULT CORR COEF IS .555

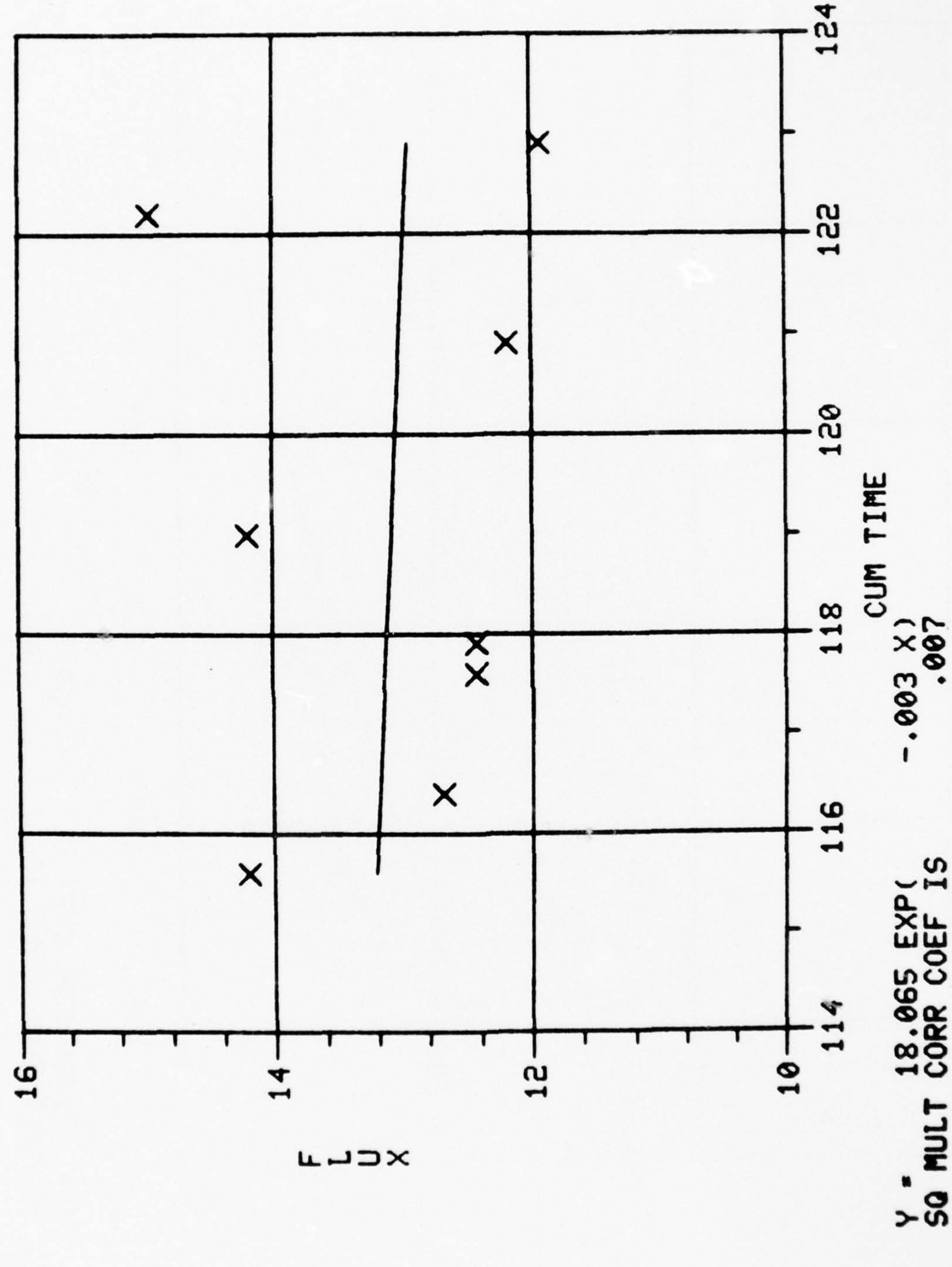
FLUX
16
14
12
10
114
116
118
120
122
124
CUM TIME
Y = 18.065 EXP( -.003 X)
SQ MULT CORR COEF IS .007

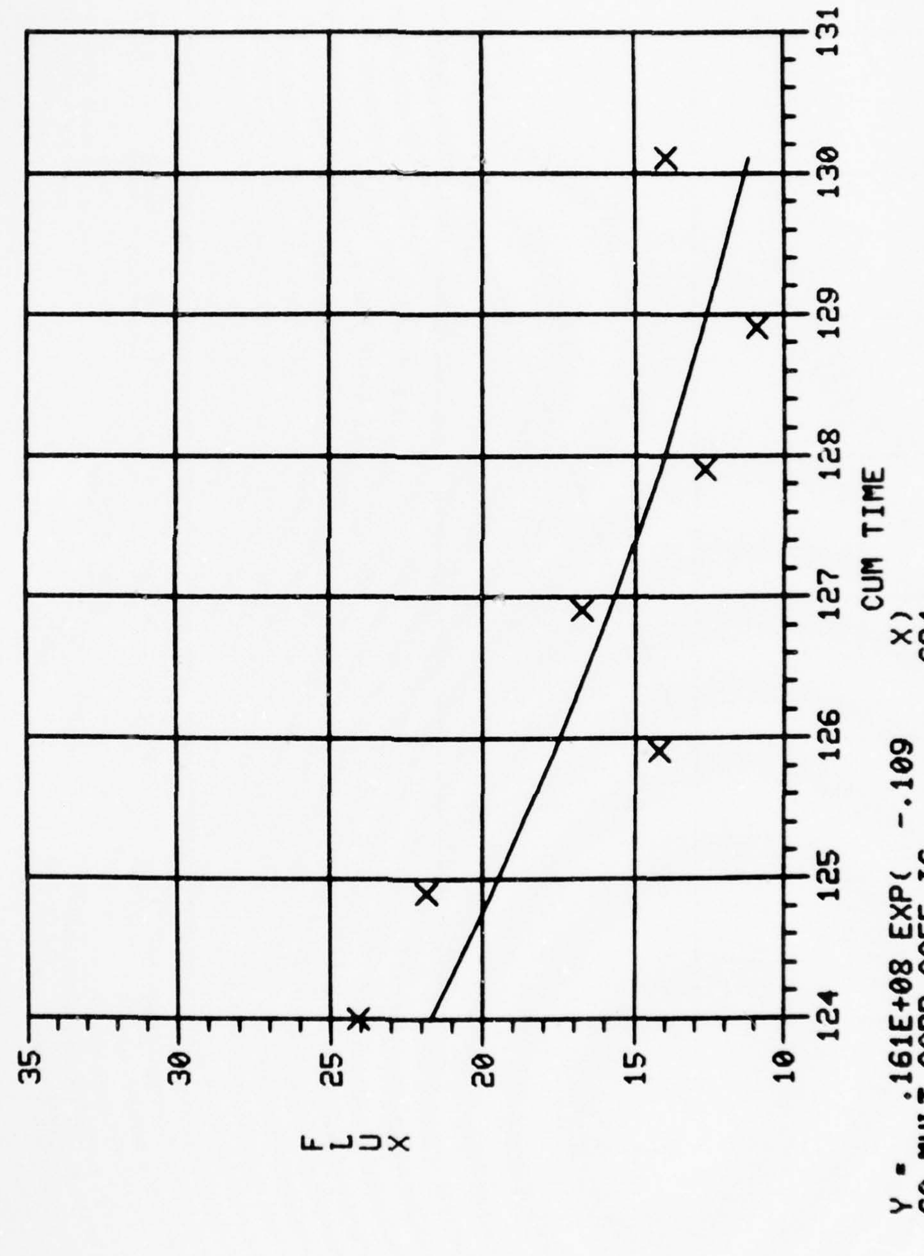

FLUX
CUM TIME
35
30
25
20
15
10
124
125
126
127
128
129
130
131
Y = .161E+08 EXP( -.109 X)
SQ MULT CORR COEF IS .684

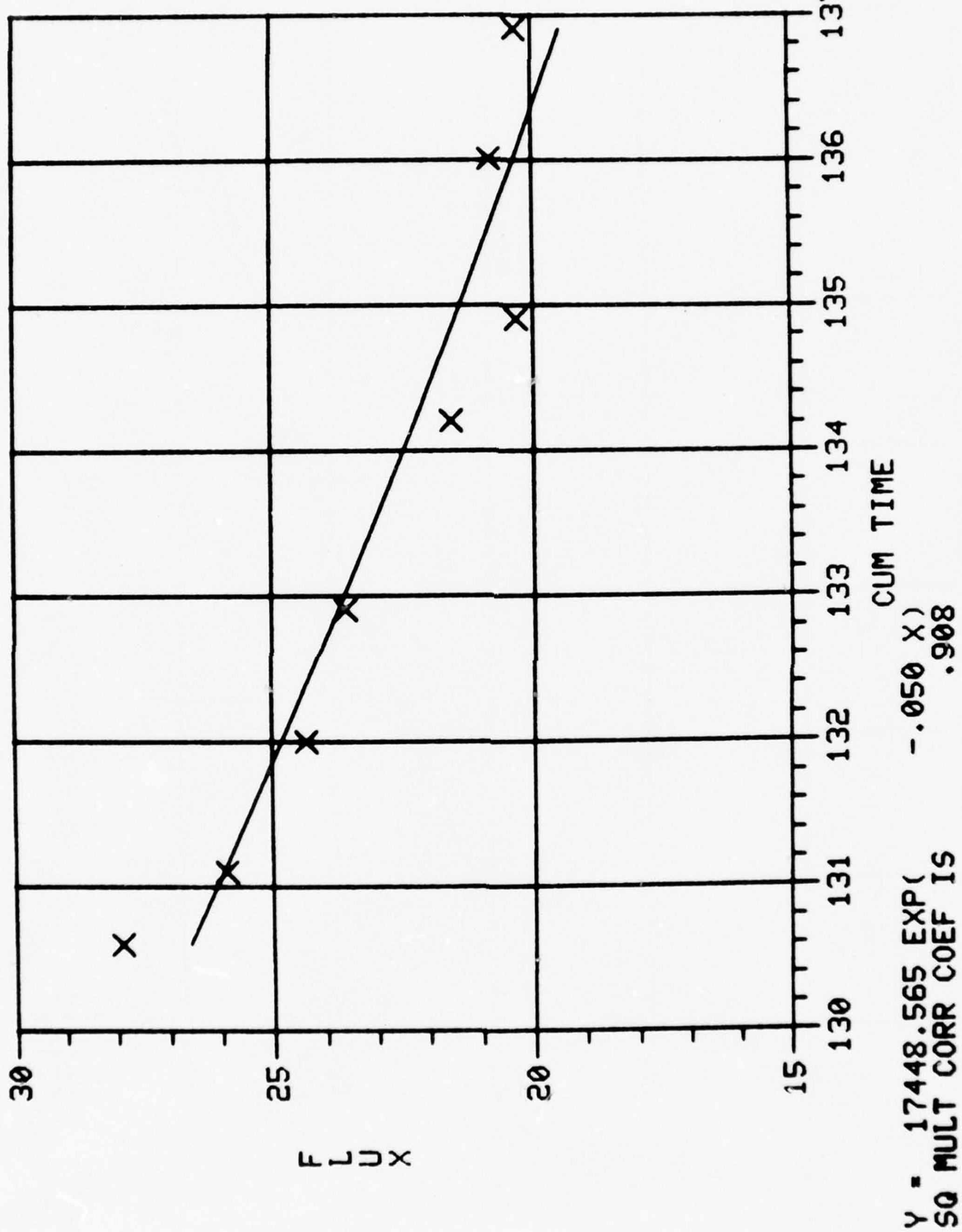
FLUX
CUM TIME
30
25
20
15
130
131
132
133
134
135
136
137
Y = 17448.565 EXP( -.050 X)
SQ MULT CORR COEF IS .908

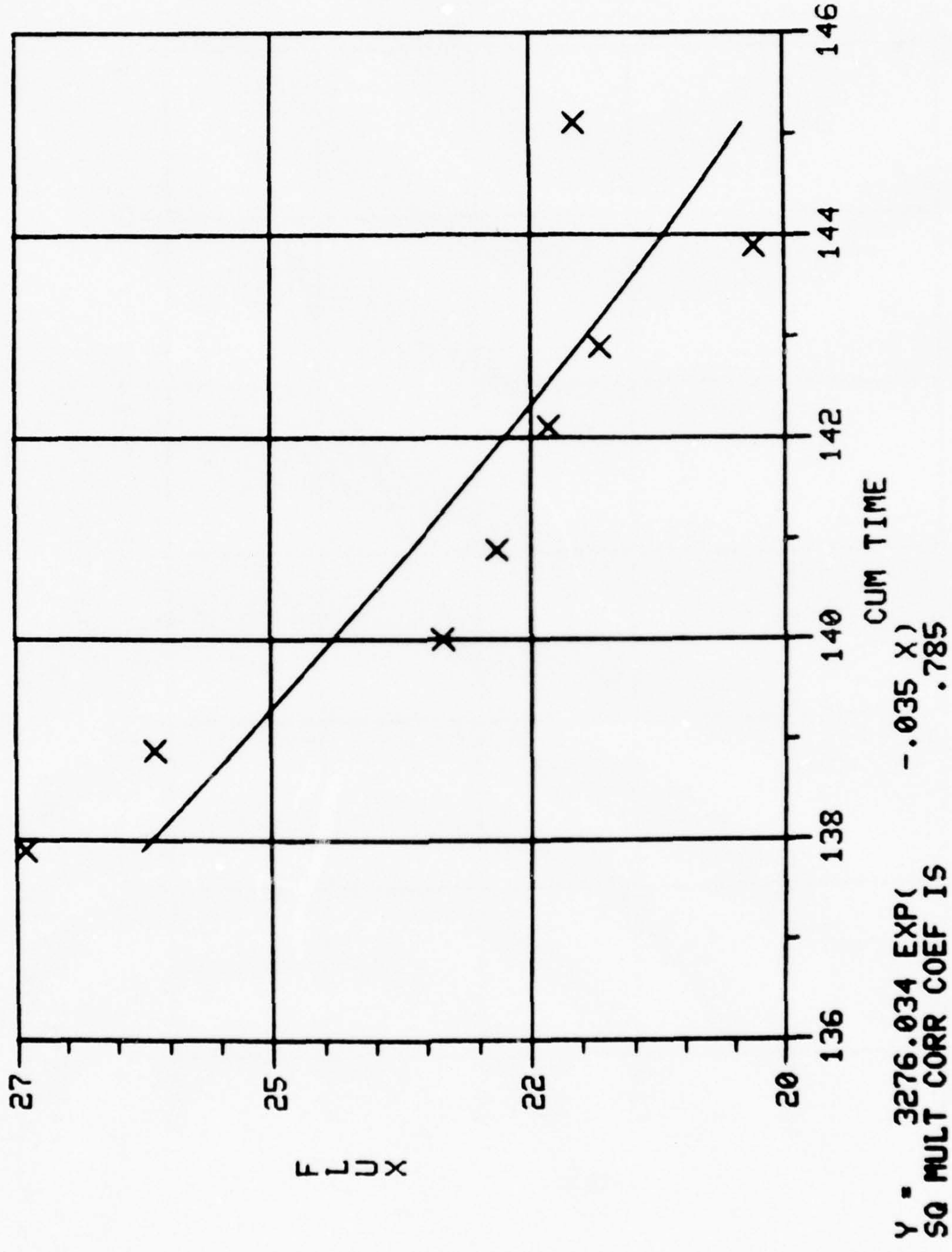

FLUX
27
25
22
20
136
138
140
142
144
146
CUM TIME
Y = 3276.034 EXP( -.035 X)
SQ MULT CORR COEF IS .785

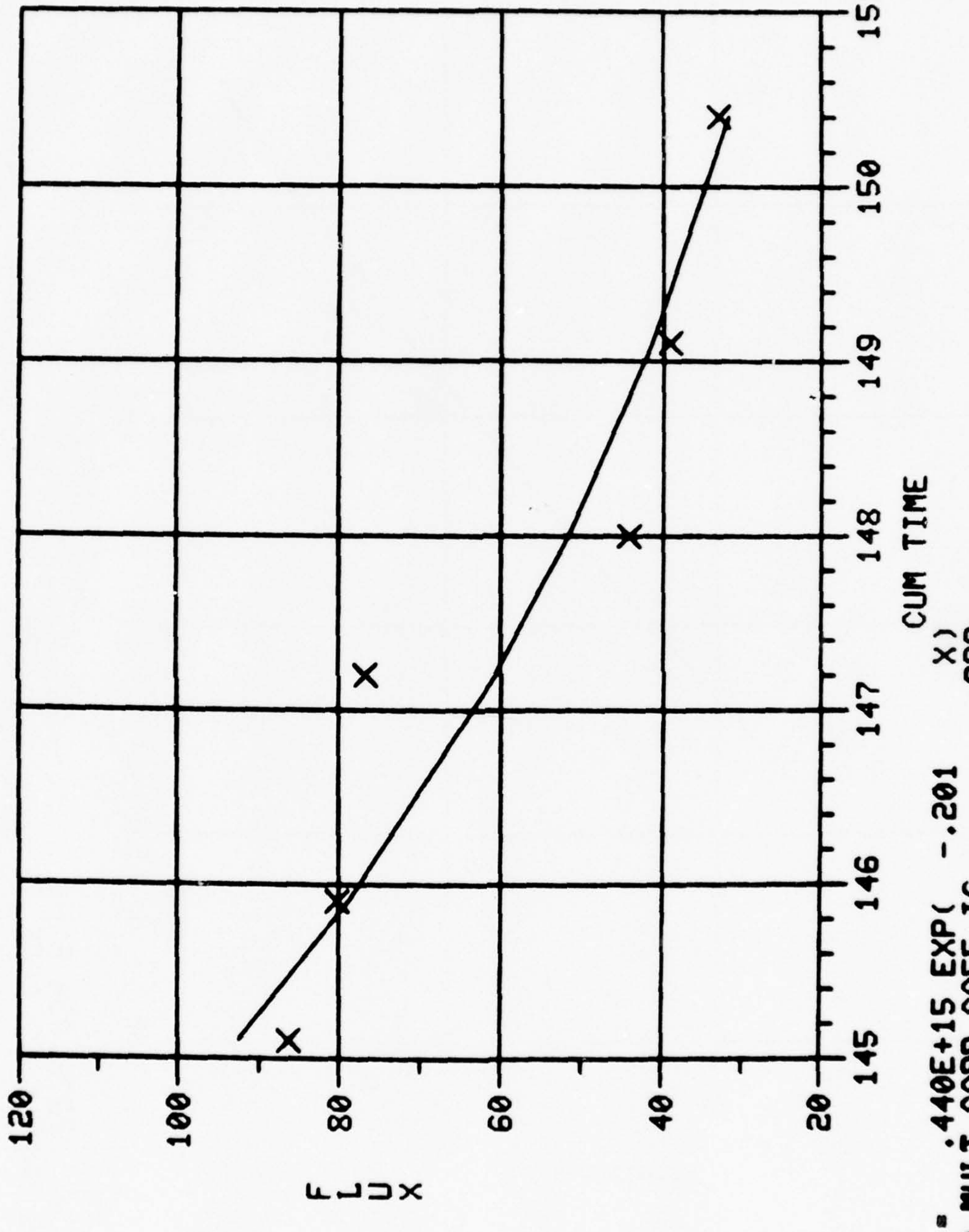
FLUX
120
100
80
60
40
20
145
146
147
148
149
150
151
CUM TIME
Y = .440E+15 EXP( -.201 X)
SQ MULT CORR COEF IS .898

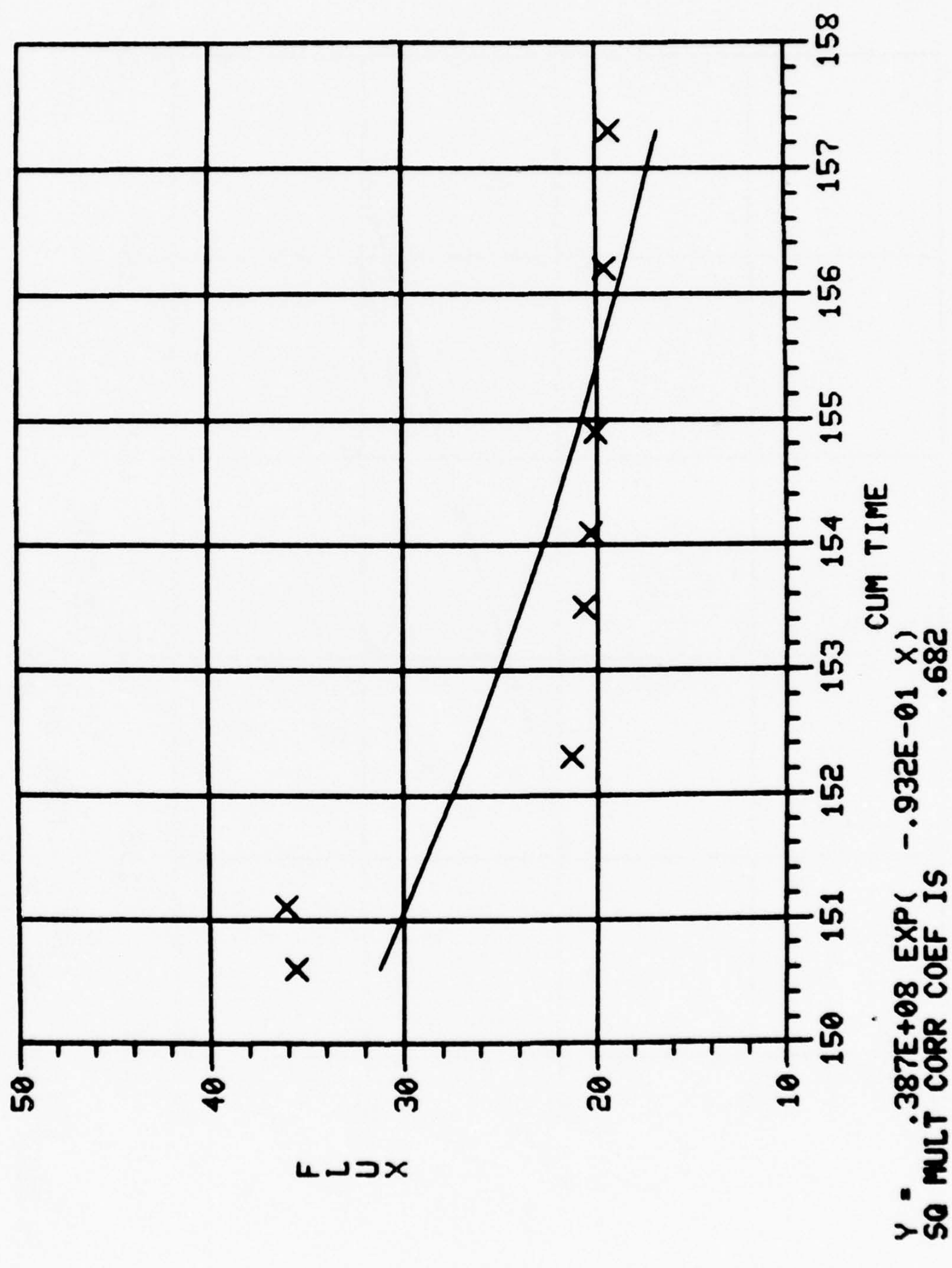

FLUX
CUM TIME
50
40
30
20
10
150
151
152
153
154
155
156
157
158
Y = .387E+08 EXP( -.932E-01 X)
SQ MULT CORR COEF IS .682

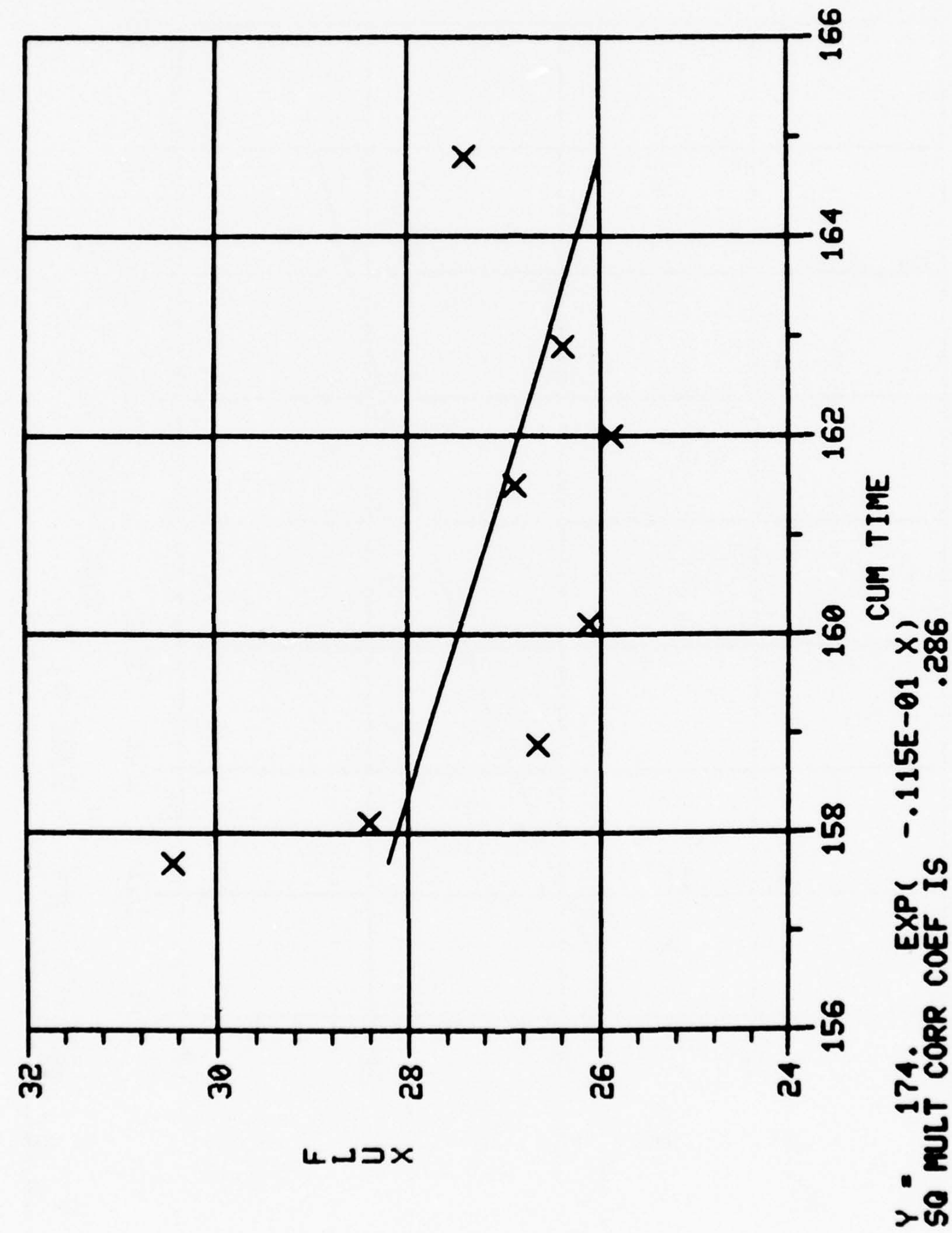

FLUX
32
30
28
26
24
156
158
160
162
164
166
CUM TIME
Y = 174. EXP( -.115E-01 X)
SQ MULT CORR COEF IS .286

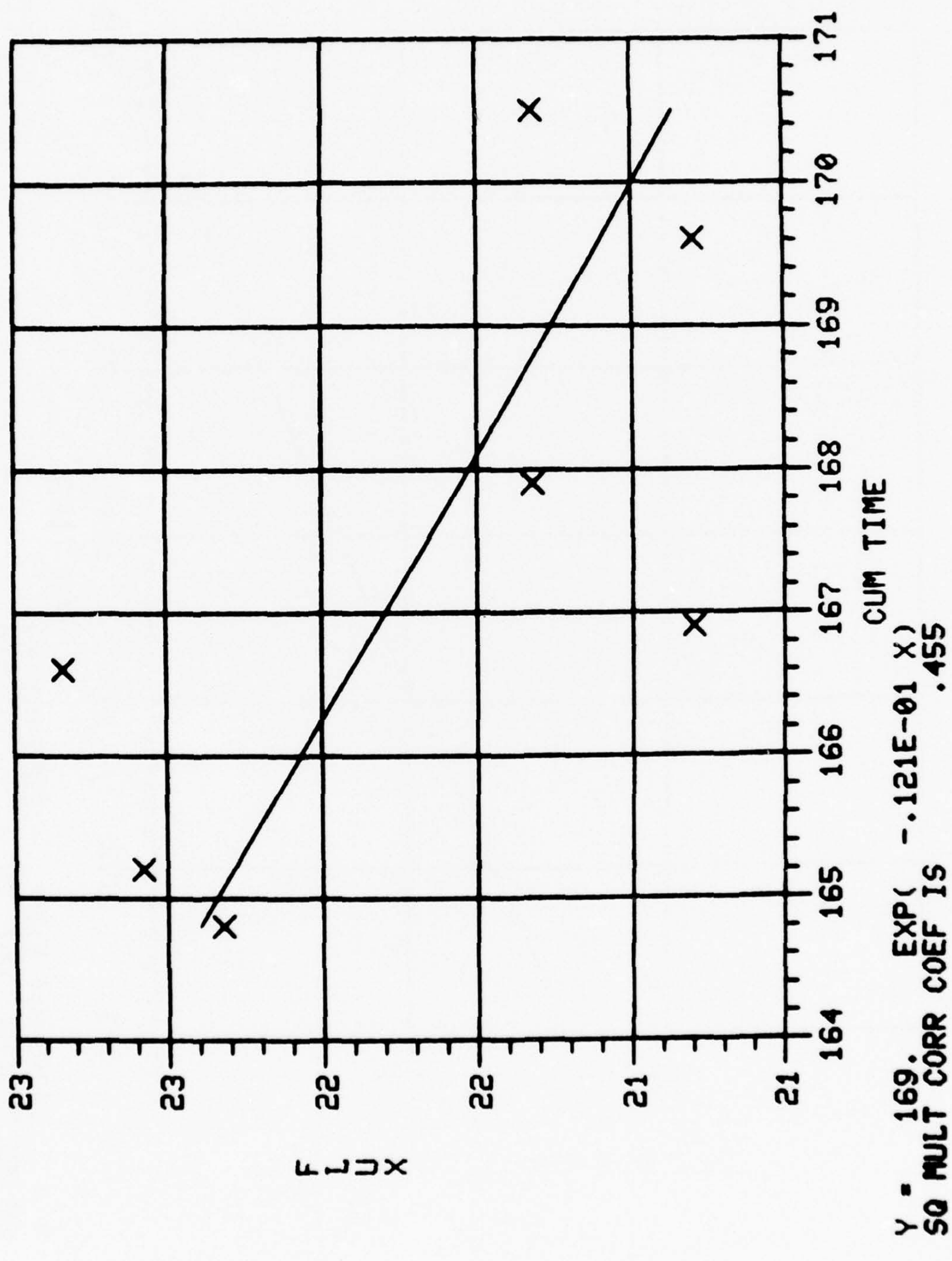

FLUX
CUM TIME
164
165
166
167
168
169
170
171
23
23
22
22
21
21
Y = 169. EXP( -.121E-01 X)
SQ MULT CORR COEF IS .455

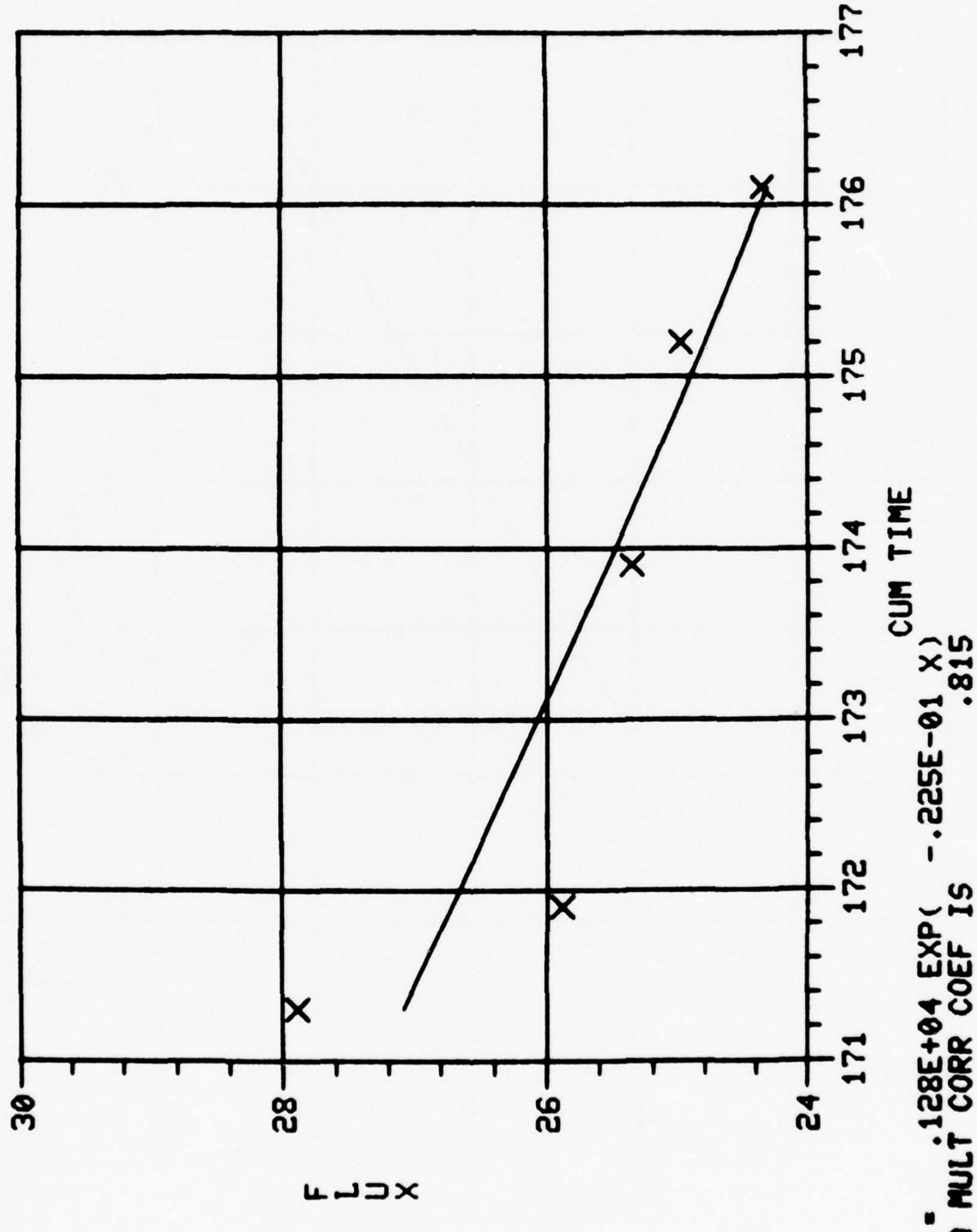
FLUX
30
28
26
24
171
172
173
174
175
176
177
CUM TIME
Y = .128E+04 EXP( -.225E-01 X)
SQ MULT CORR COEF IS .815

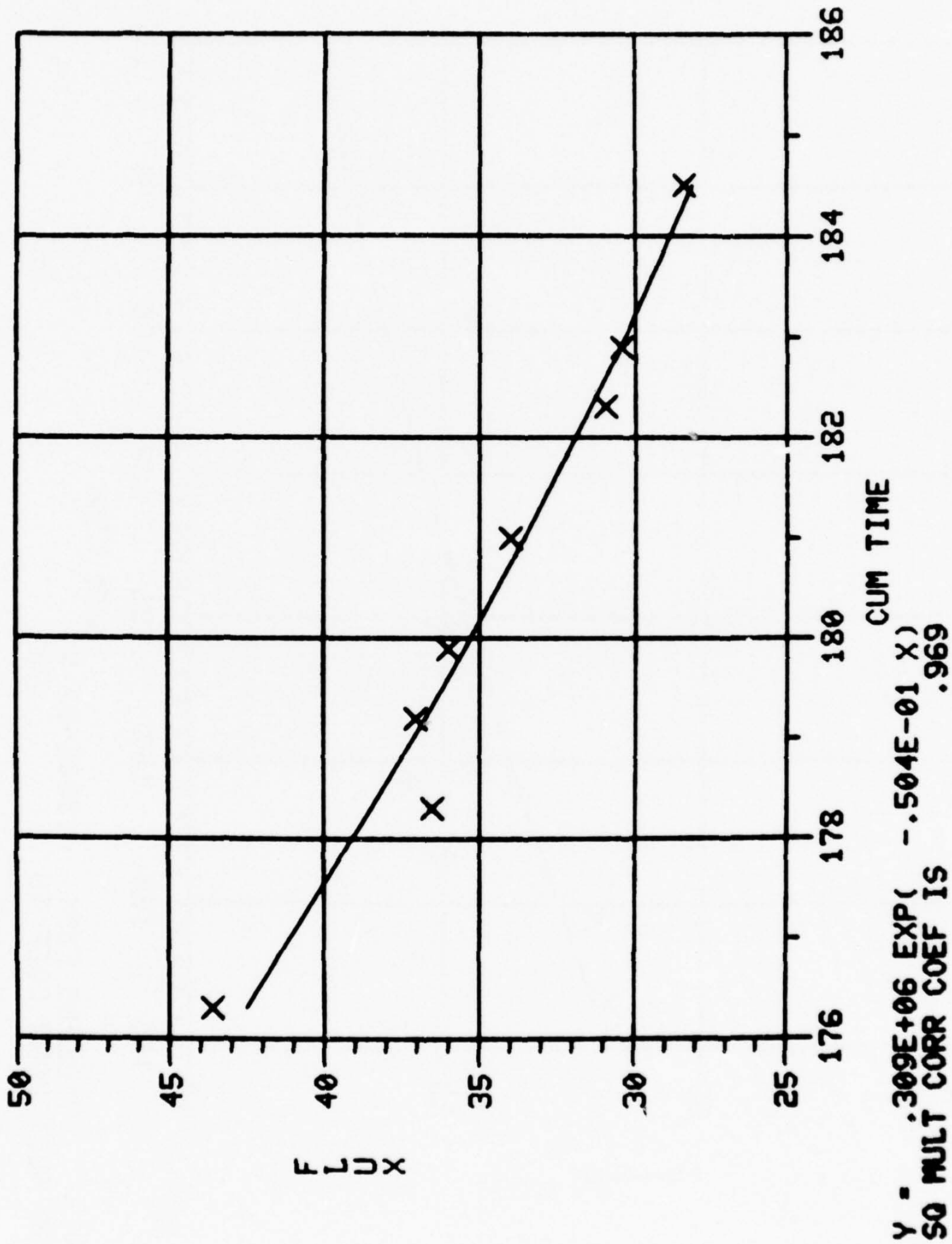
FLUX
50
45
40
35
30
25
176
178
180
182
184
186
CUM TIME
Y = .309E+06 EXP( -.504E-01 X)
SQ MULT CORR COEF IS .969

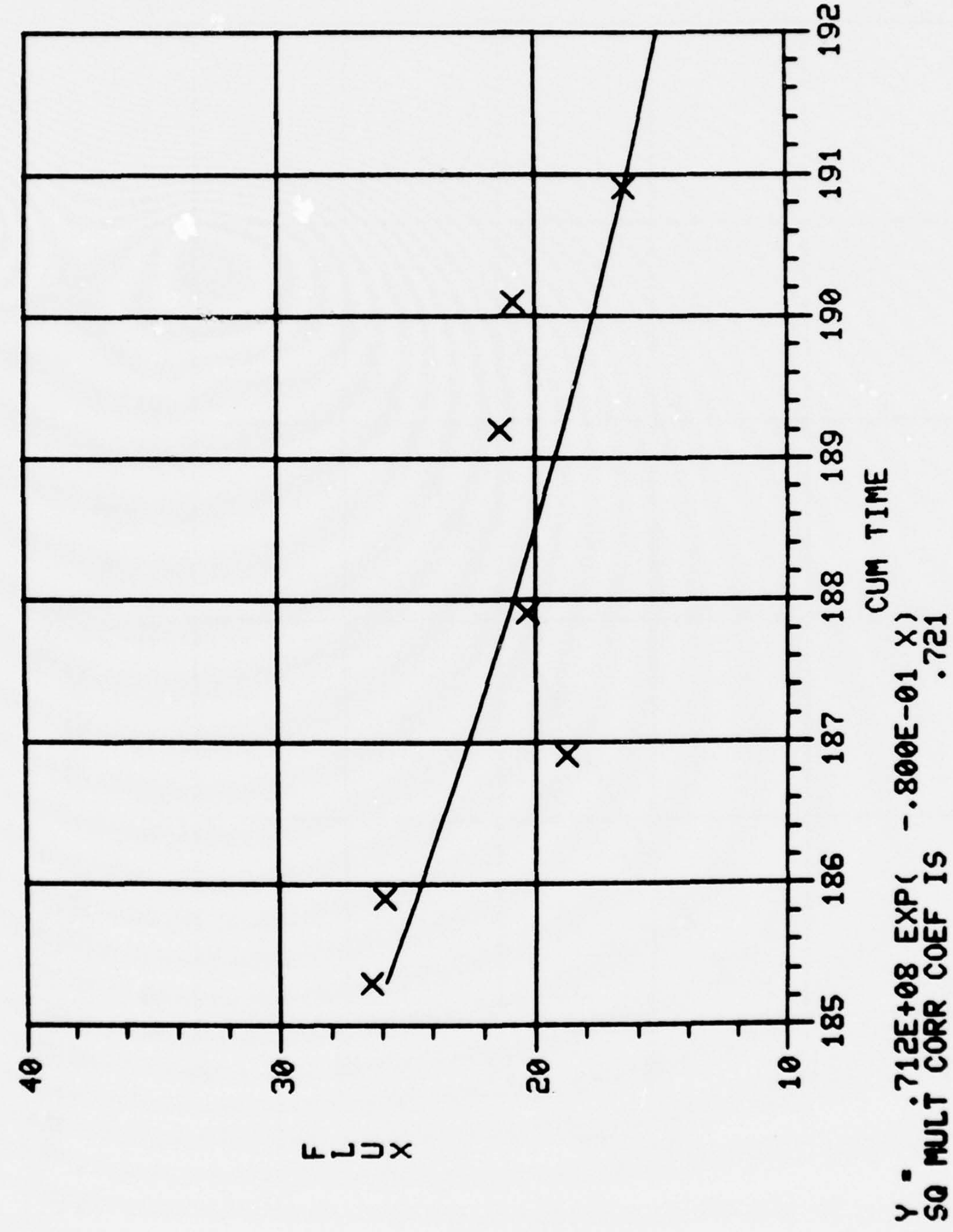
FLUX
40
30
20
10
185
186
187
188
189
190
191
192
CUM TIME
Y = .712E+08 EXP( -.800E-01 X)
SQ MULT CORR COEF IS .721

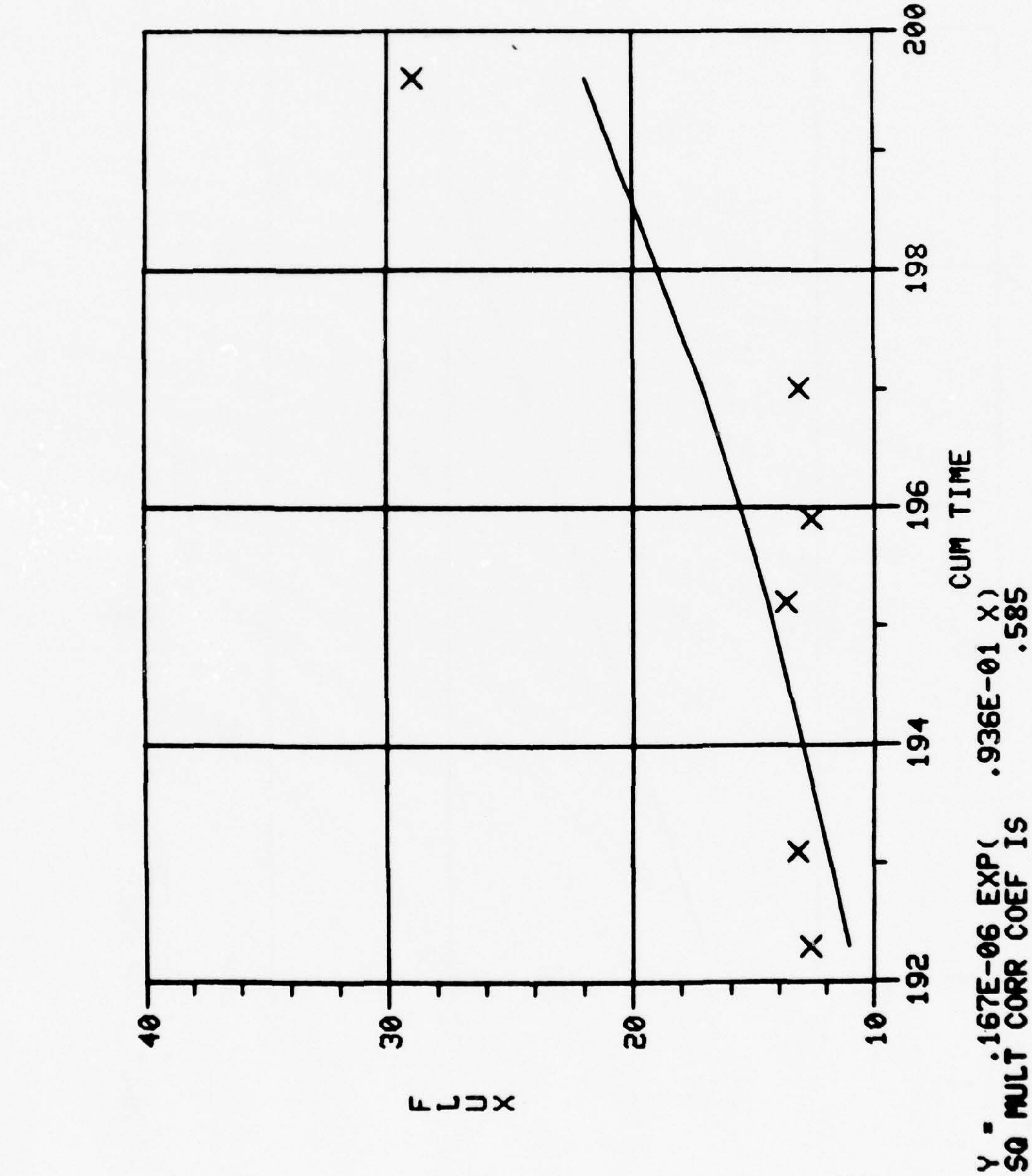
FLUX
40
30
20
10
192
194
196
198
200
CUM TIME
Y = .167E-06 EXP( .936E-01 X)
SQ MULT CORR COEF IS .585

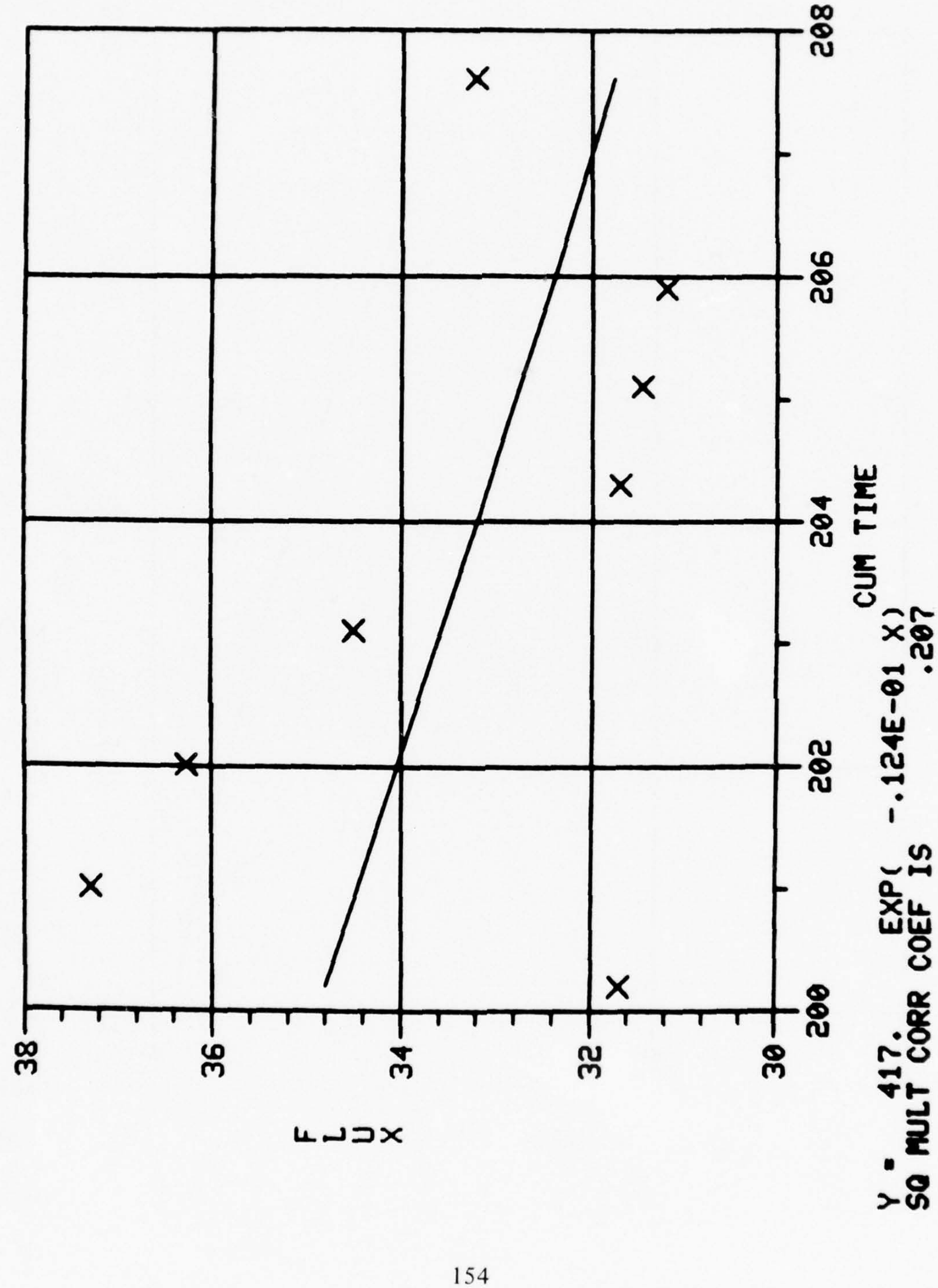
FLUX
CUM TIME
38
36
34
32
30
200
202
204
206
208
Y = 417. EXP( -.124E-01 X)
SQ MULT CORR COEF IS .207

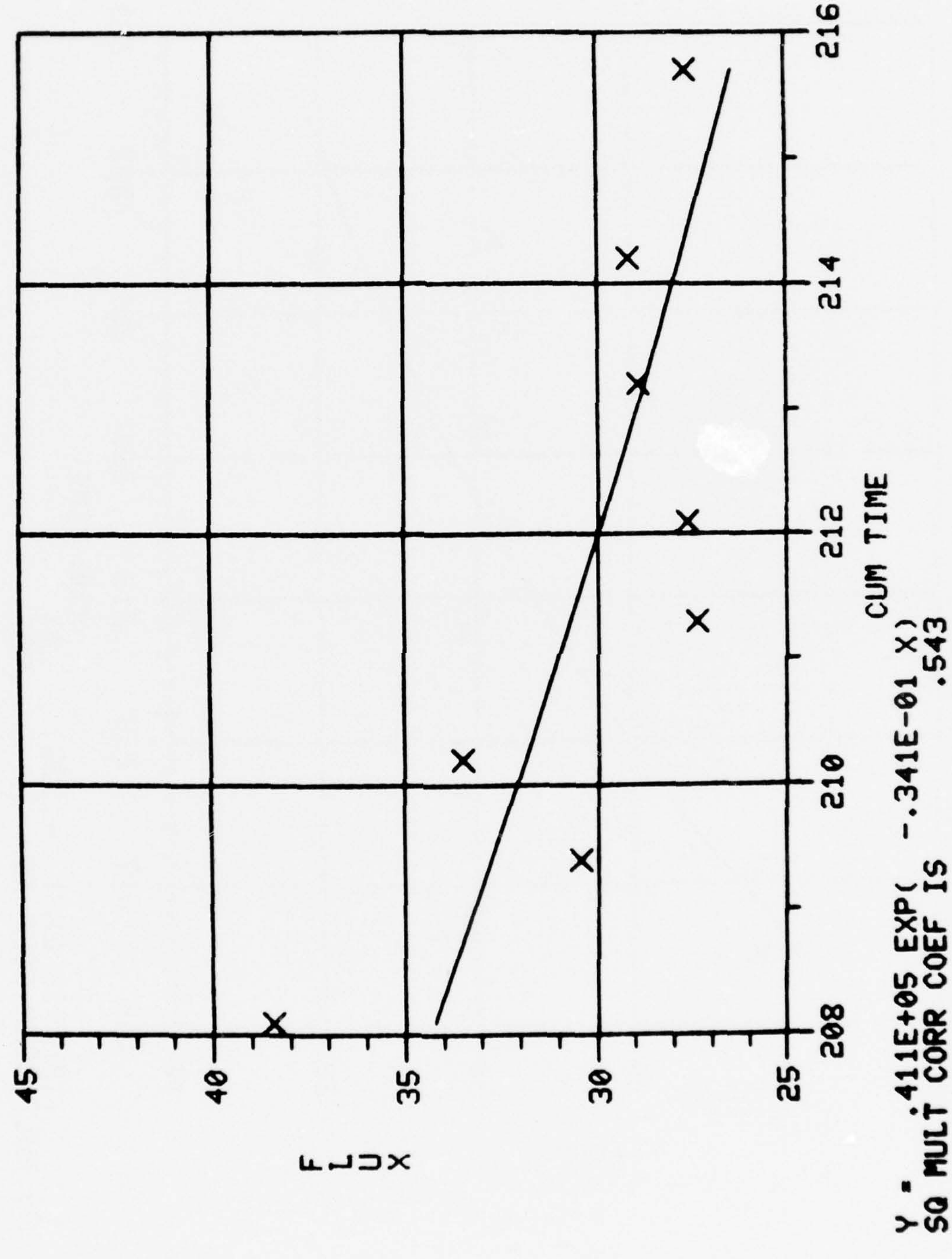
FLUX
45
40
35
30
25
208
210
212
214
216
CUM TIME
Y = .411E+05 EXP( -.341E-01 X)
SQ MULT CORR COEF IS .543

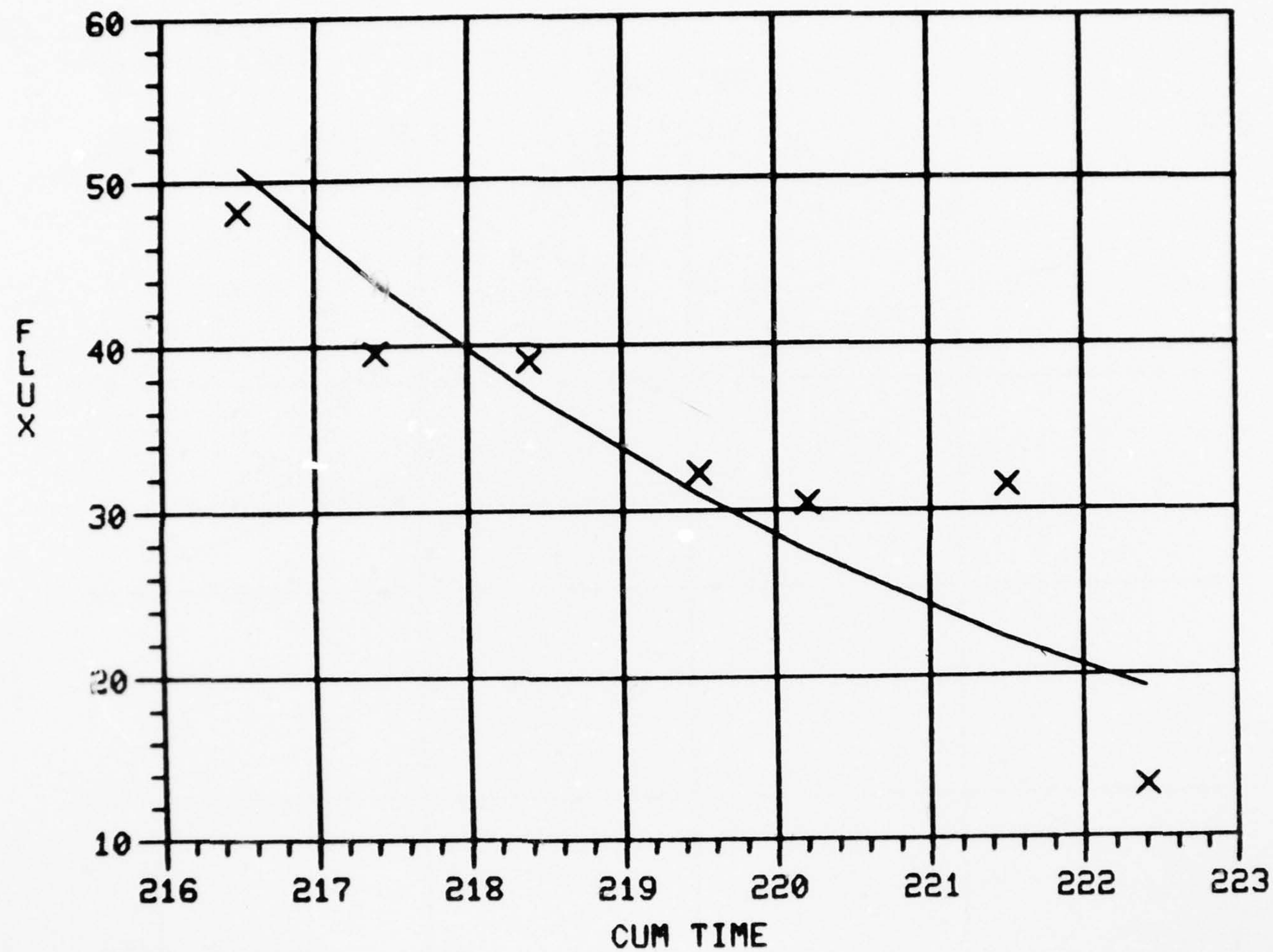


Y = .185E+18 EXP( -.165 X)
SQ MULT CORR COEF IS .723

## APPENDIX E

## CURVE FITS FOR SEGMENTED, SPIRAL-WOUND DATA

The data for the spiral-wound system was segmented at what appeared to be the point where the system reached steady state. Three different points were picked which resulted in three groups of data each containing two segments. The points of division are 555.3, 560.2, and 575. Each group contains four graphs, a first-order and exponential fit for the presumed unsteady state portion of the data and the same two fits for the steady state portion of the data. It should be noted that in the two plots of the steady state for Group 2 there is an erroneous data point at 560 hours. A quirk in the graphics packages made inclusion of this point necessary, and it should have only a negligible effect on the equation and the coefficient of determination.

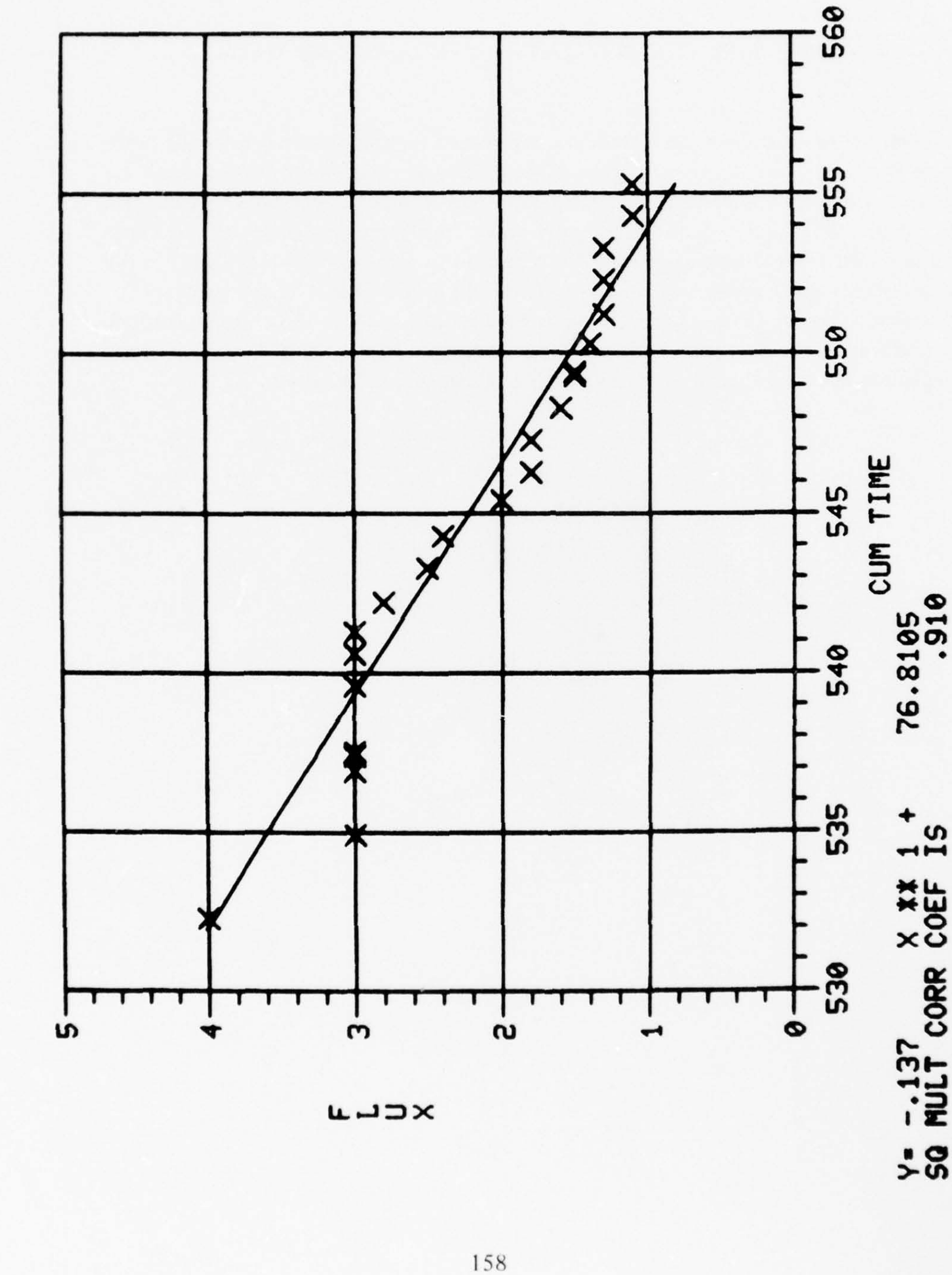

FLUX
0
1
2
3
4
5
530
535
540
545
550
555
560
CUM TIME
Y= -.137 X ** 1 + 76.8105
SQ MULT CORR COEF IS .910

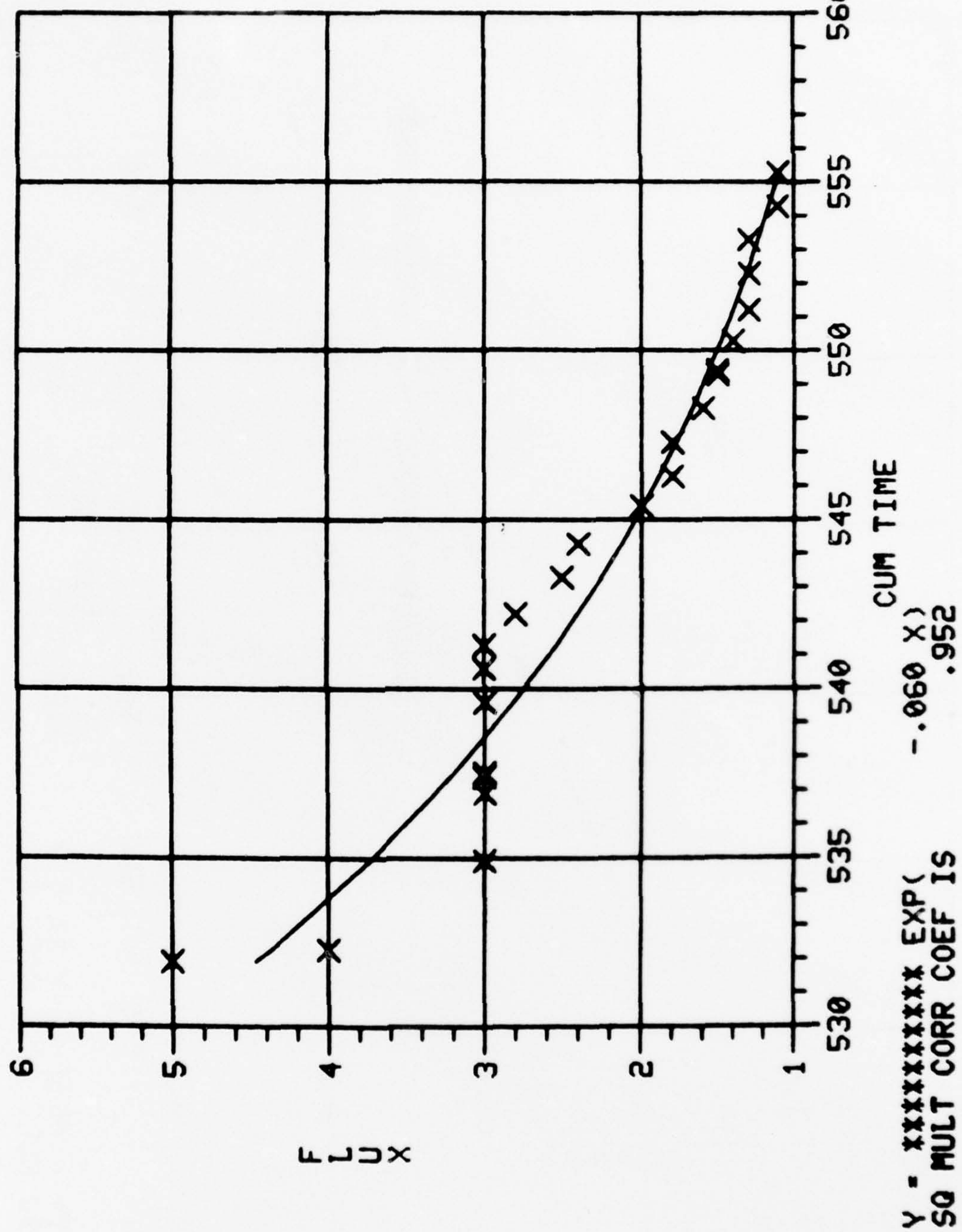
FLUX
CUM TIME
6
5
4
3
2
1
530
535
540
545
550
555
560
Y = XXXXXXXXX EXP( -.060 X)
SQ MULT CORR COEF IS .952

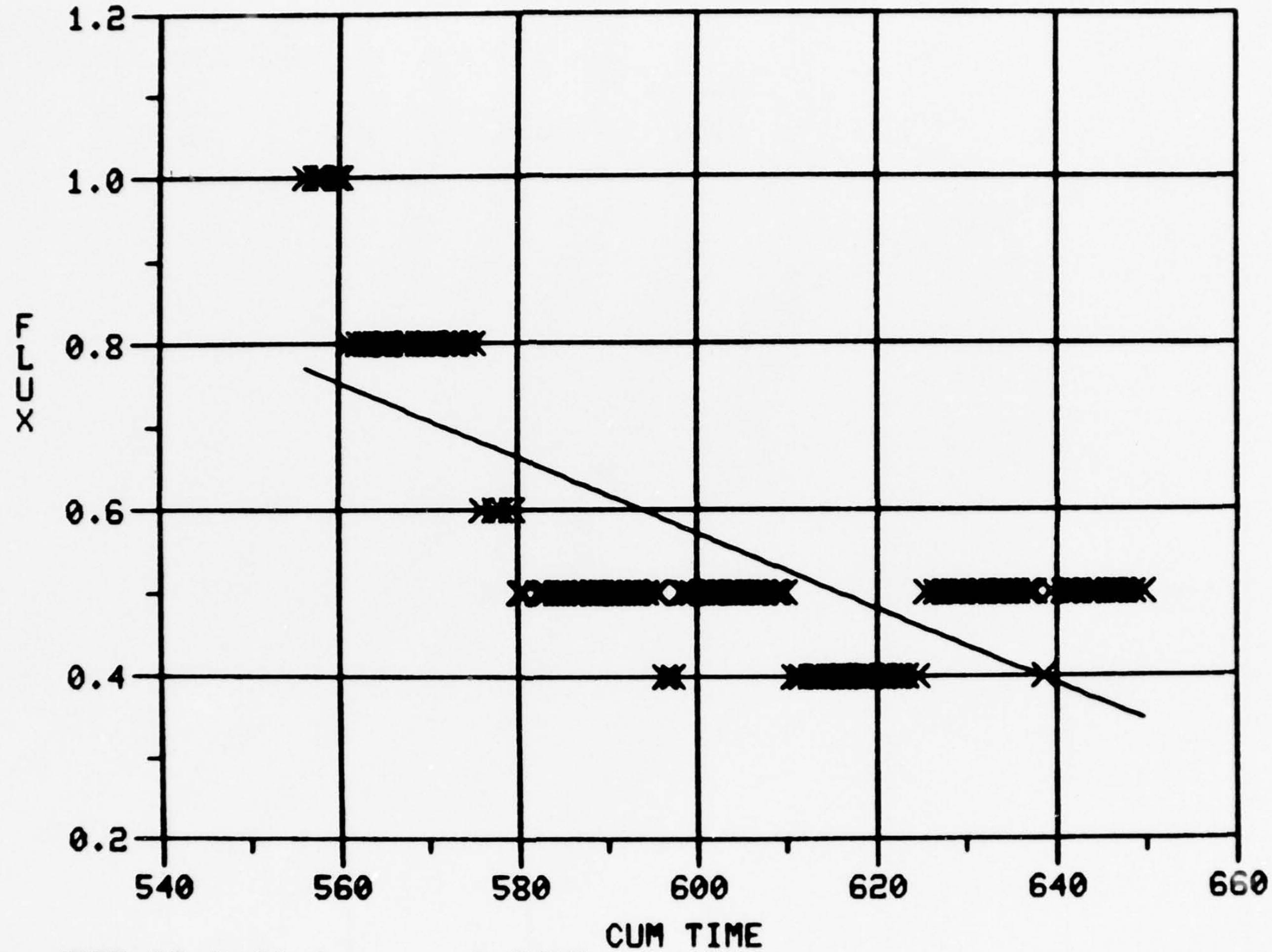


Y= -.452E-02 X ** 1 +      3.2857
SQ MULT CORR COEF IS       .543

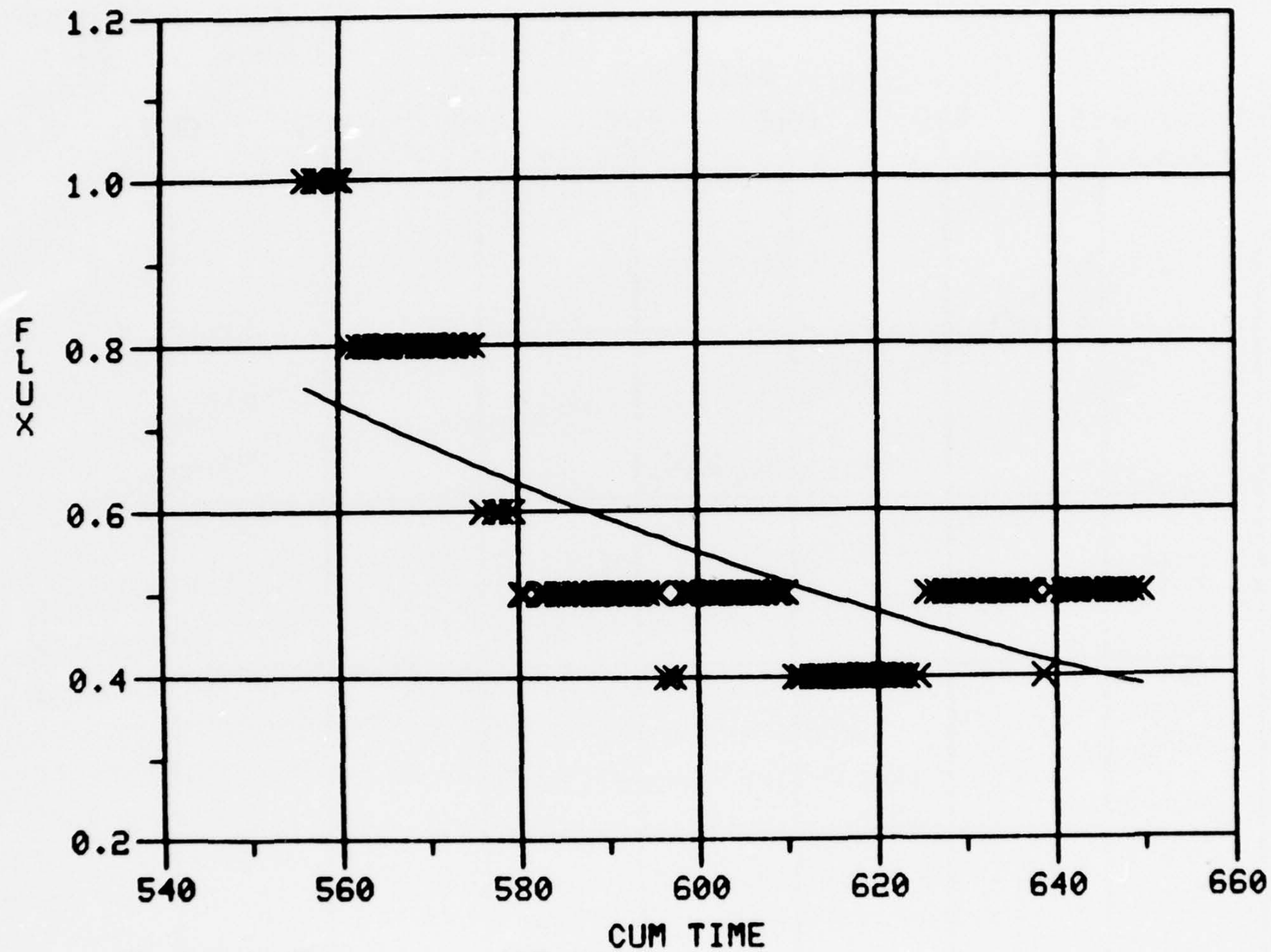


Y = 38.044 EXP( -.007 X)
SQ MULT CORR COEF IS .535

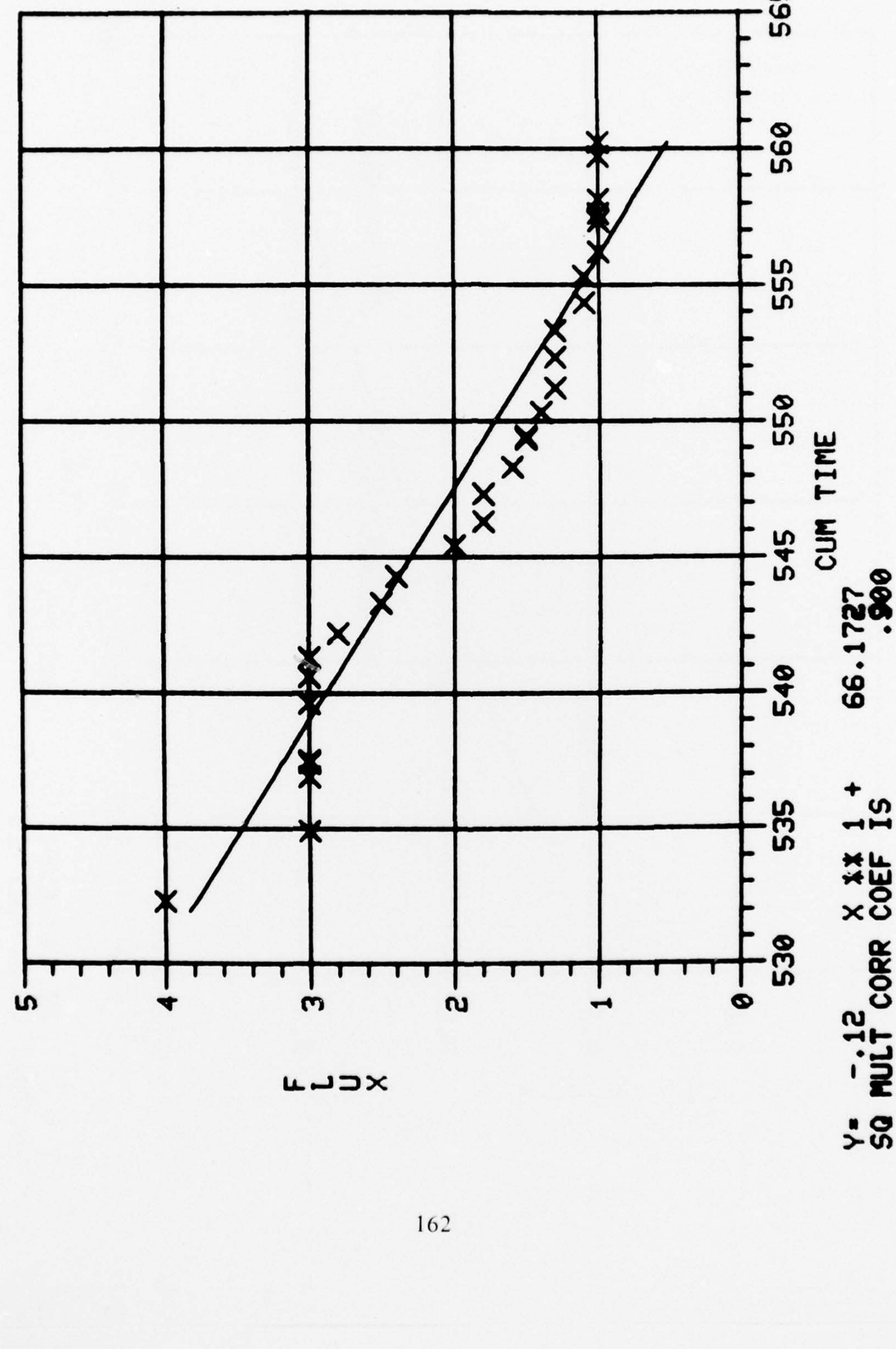

FLUX
CUM TIME
0
1
2
3
4
5
530
535
540
545
550
555
560
565
Y= -.12 X ** 1 + 66.1727
SQ MULT CORR COEF IS .900

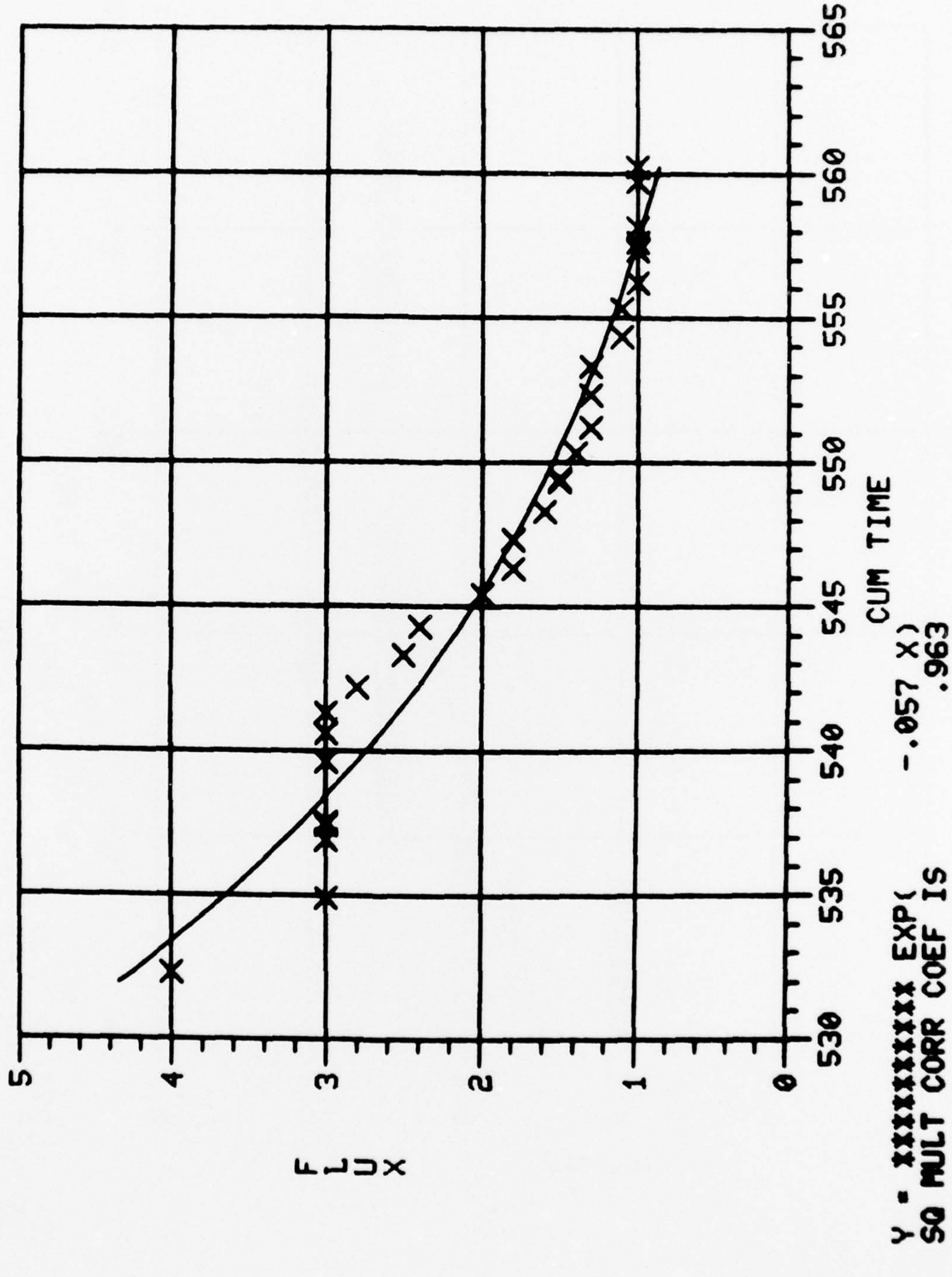
FLUX
5
4
3
2
1
0
530
535
540
545
550
555
560
565
CUM TIME
Y = XXXXXXXXX EXP( -.057 X)
SQ MULT CORR COEF IS .963

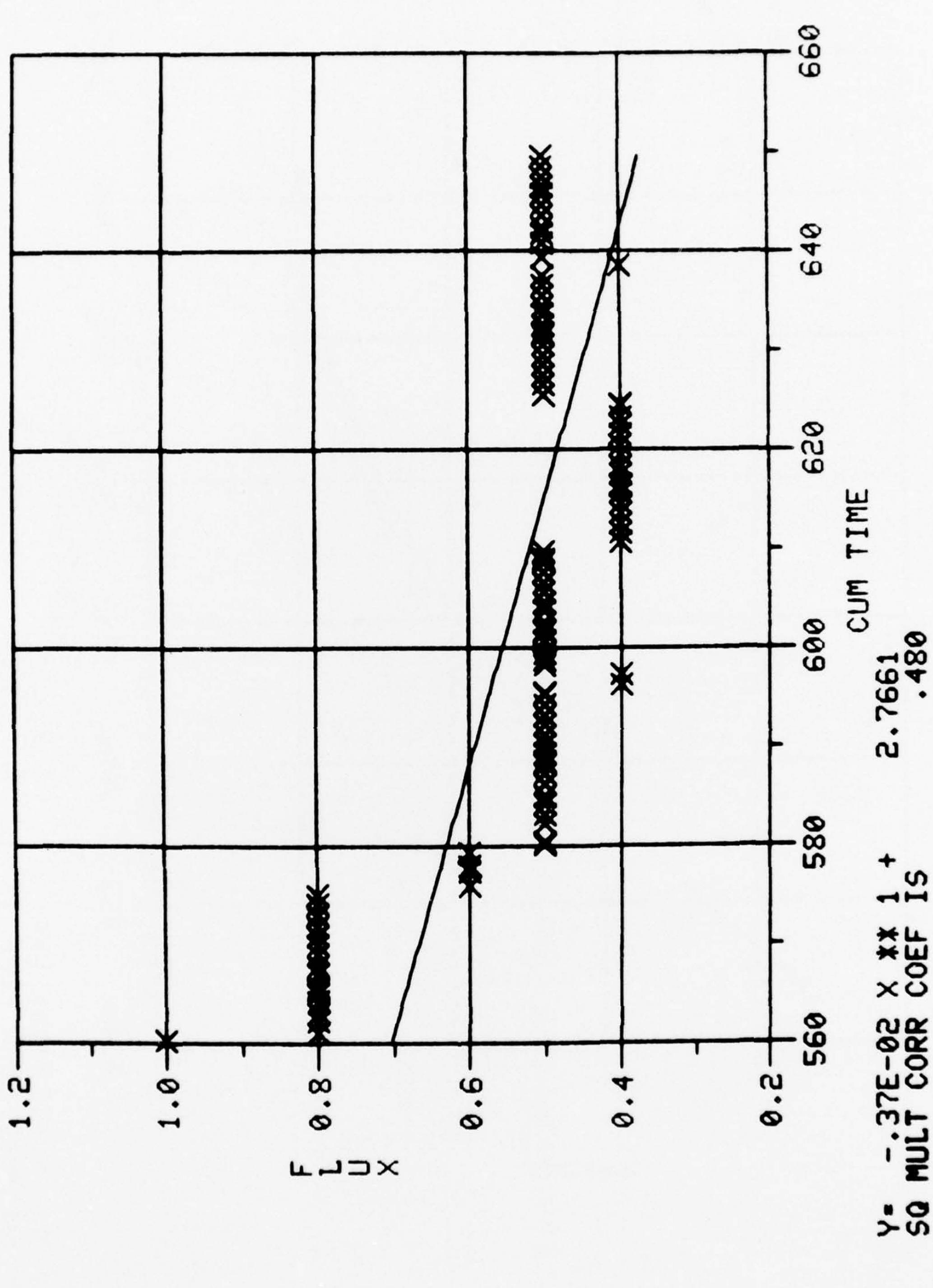
FLUX
1.2
1.0
0.8
0.6
0.4
0.2
560
580
600
620
640
660
CUM TIME
Y= -.37E-02 X ** 1 + 2.7661
SQ MULT CORR COEF IS .480

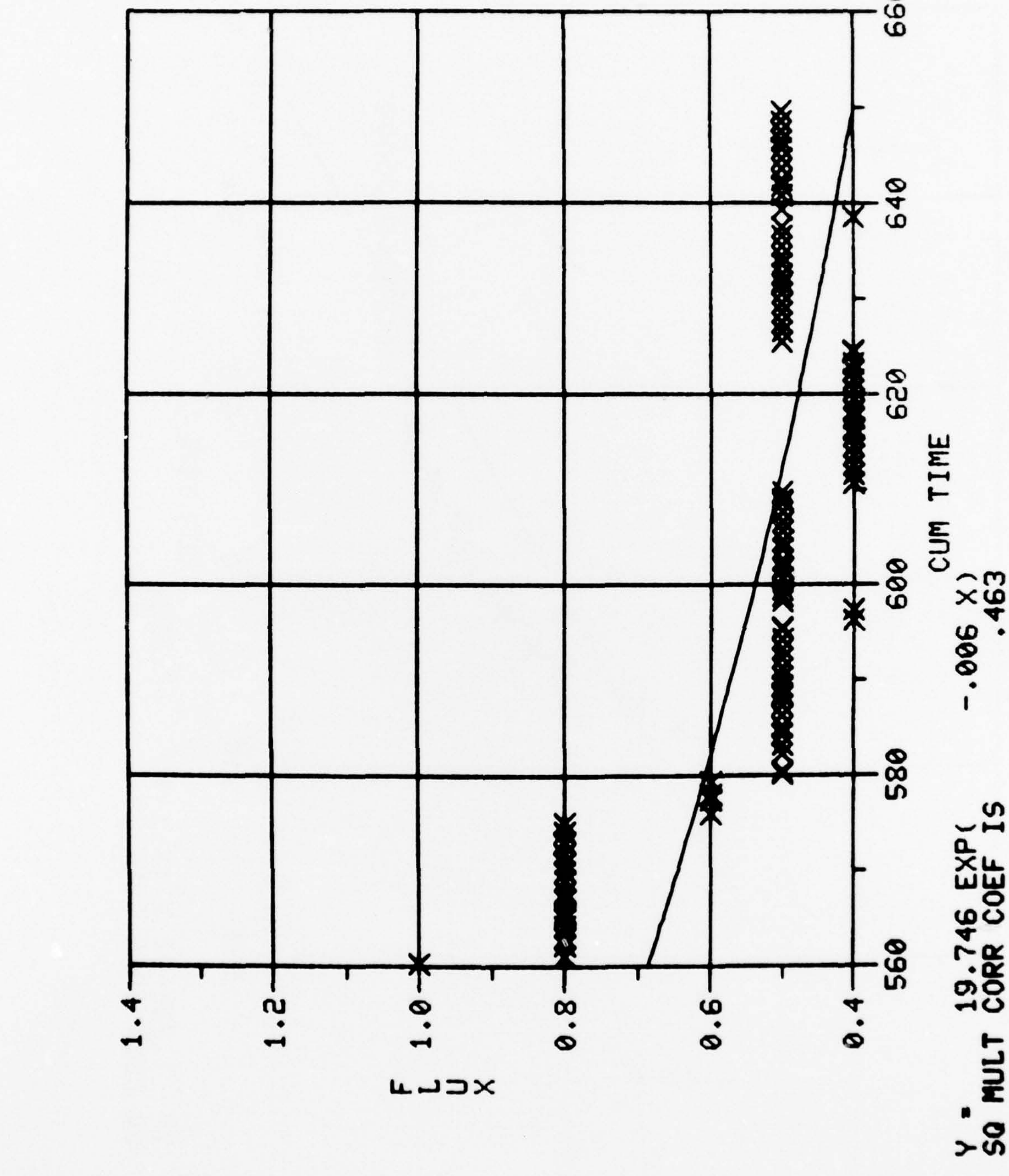

FLUX
1.4
1.2
1.0
0.8
0.6
0.4
560
580
600
620
640
660
CUM TIME
Y = 19.746 EXP( -.006 X)
SQ MULT CORR COEF IS .463

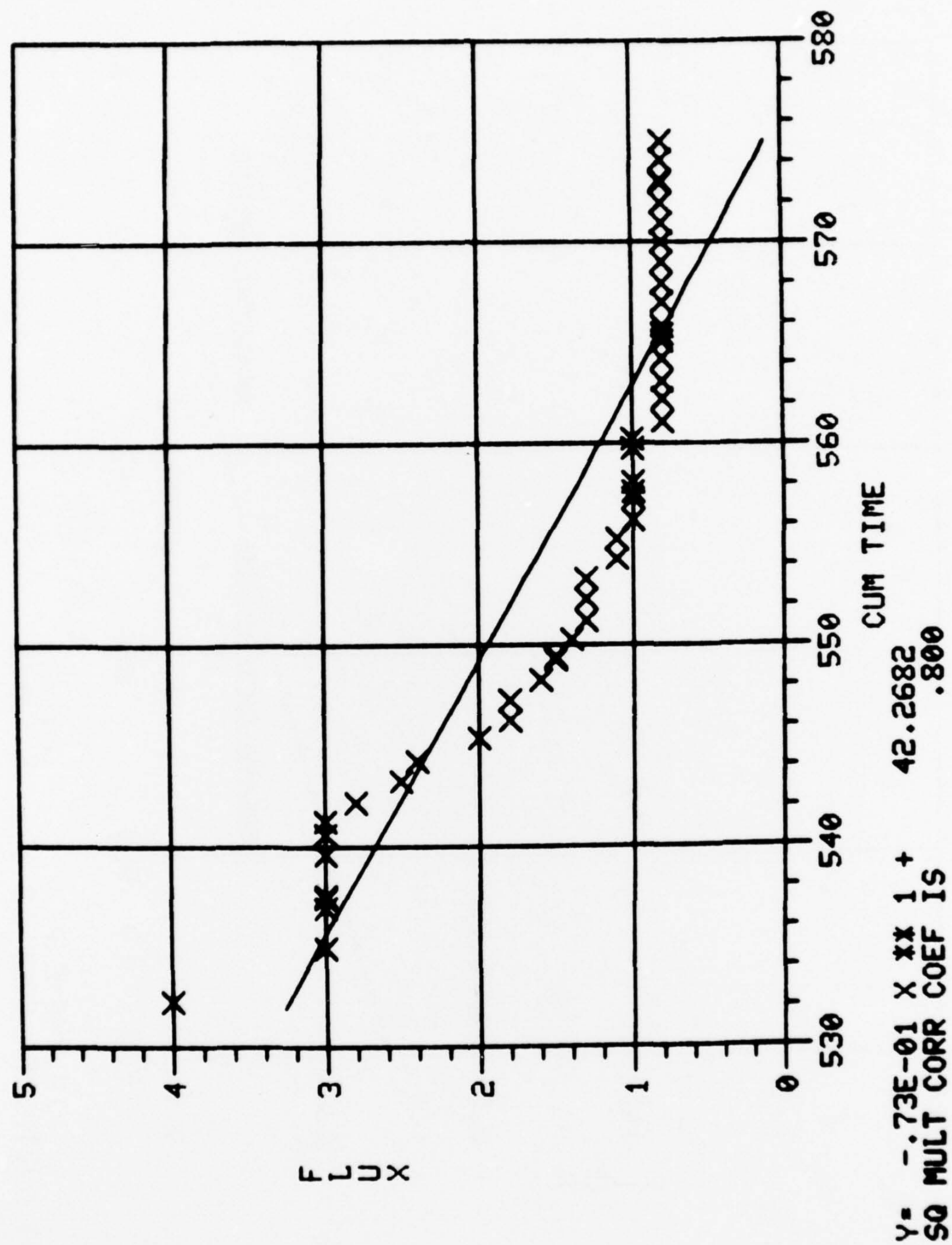
FLUX
CUM TIME
0
1
2
3
4
5
530
540
550
560
570
580
Y= -.73E-01 X XX 1 + 42.2682
SQ MULT CORR COEF IS .800

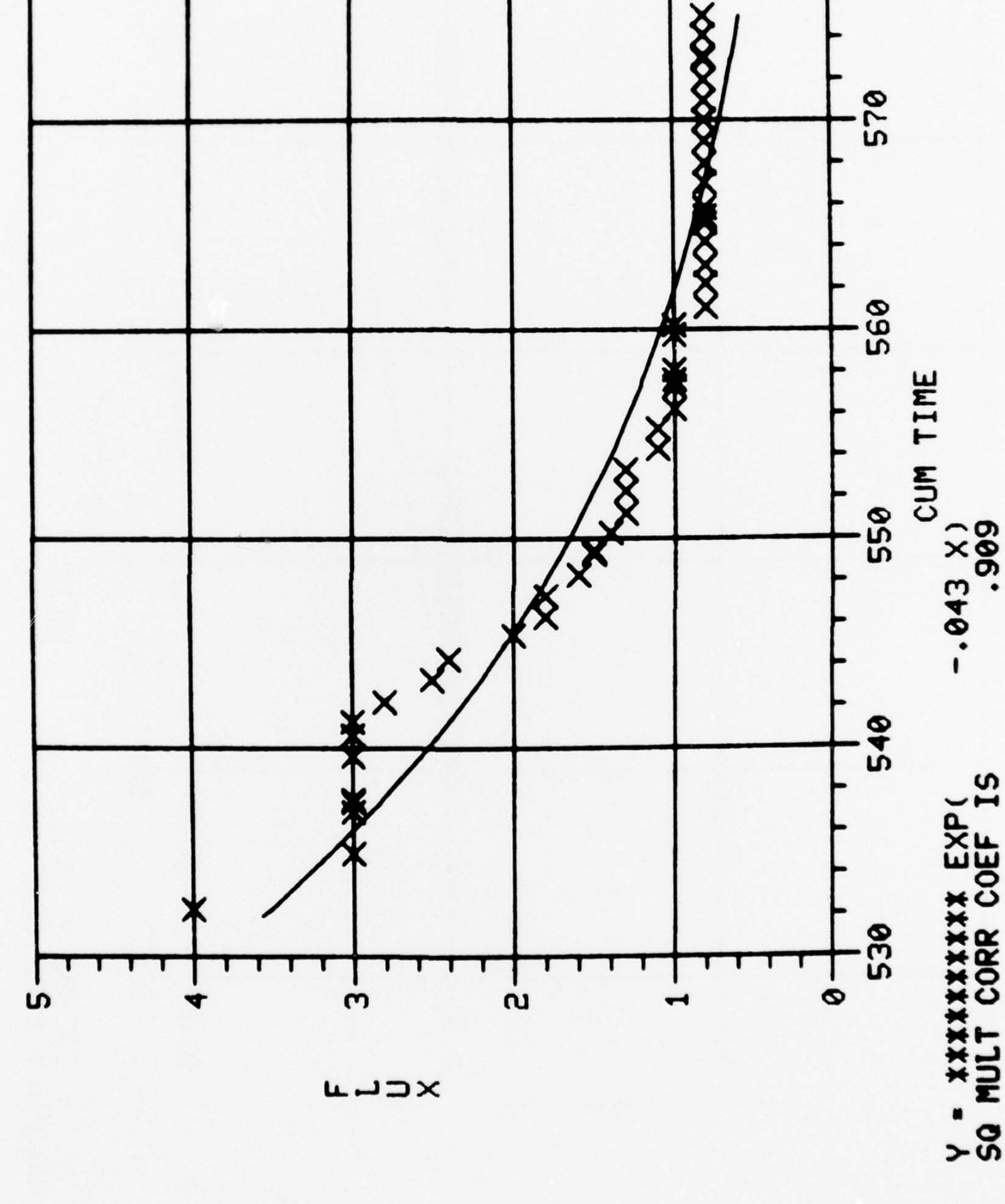
FLUX
CUM TIME
0
1
2
3
4
5
530
540
550
560
570
580
Y = XXXXXXXXX EXP( -.043 X)
SQ MULT CORR COEF IS .909

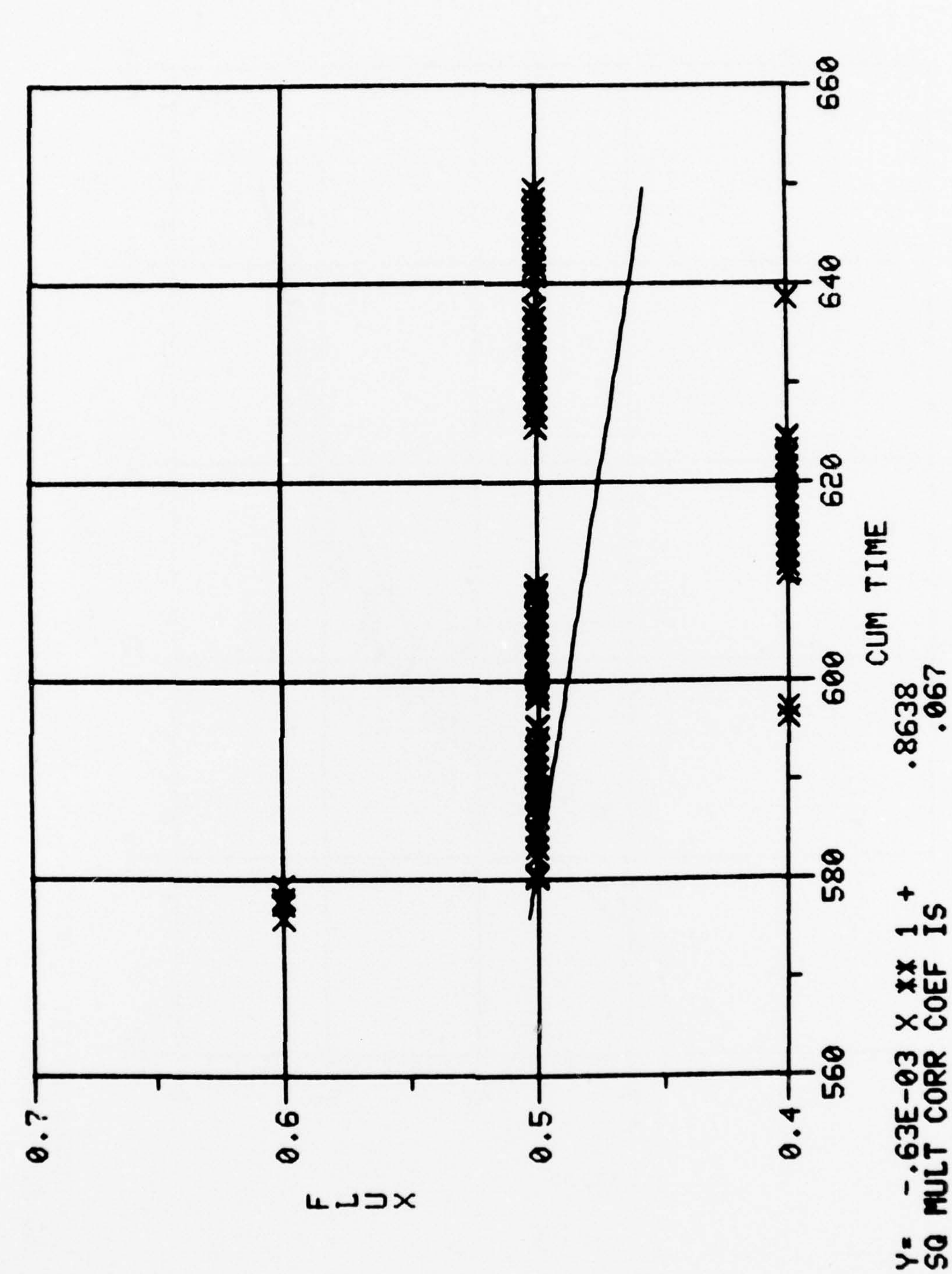
FLUX
0.7
0.6
0.5
0.4
560
580
600
620
640
660
CUM TIME
Y= -.63E-03 X ** 1 + .8638
SQ MULT CORR COEF IS .067

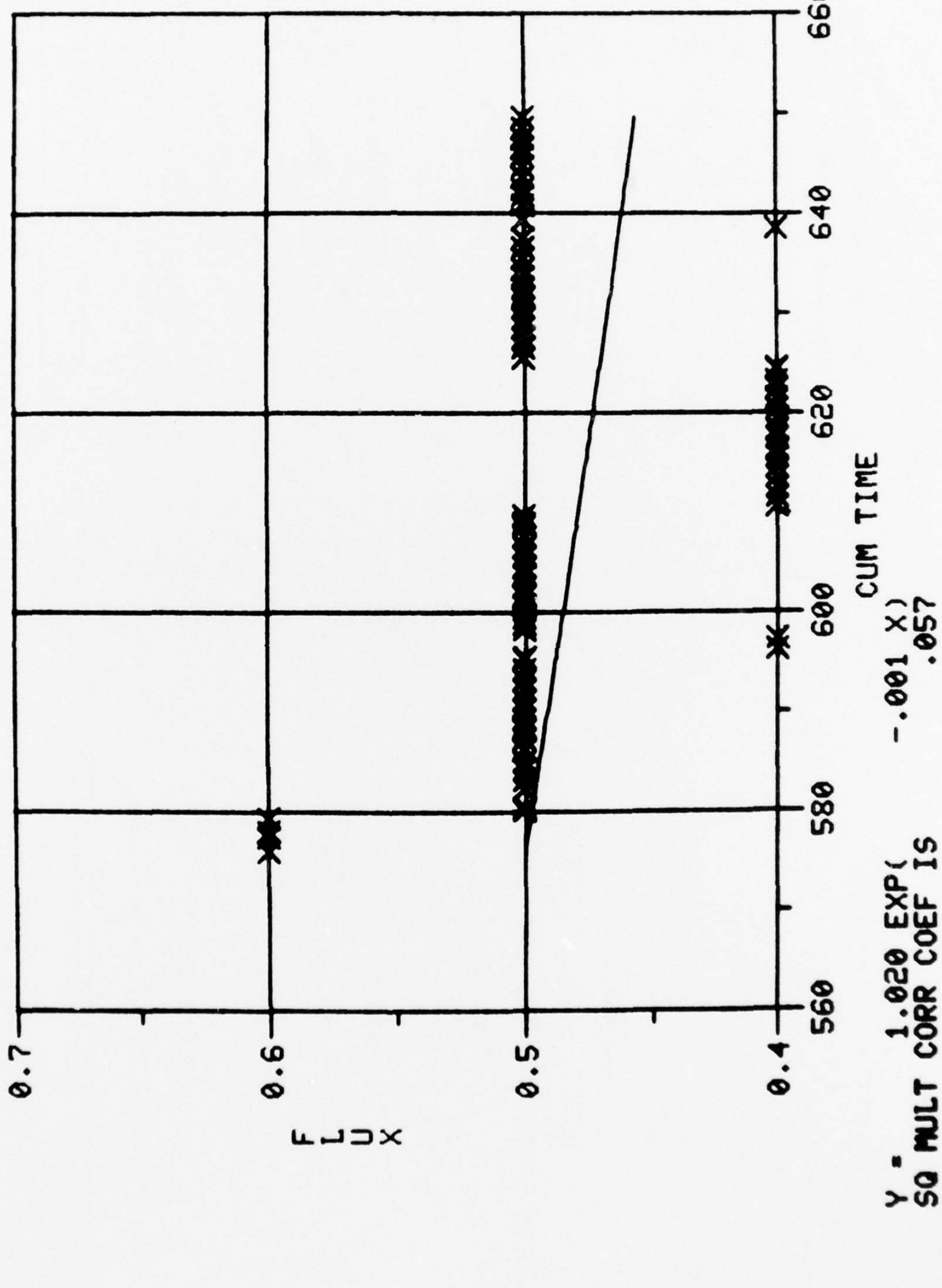
FLUX
0.4
0.5
0.6
0.7
560
580
600
620
640
660
CUM TIME
Y = 1.020 EXP( -.001 X)
SQ MULT CORR COEF IS .057

# METRIC CONVERSION FACTORS

## Approximate Conversions to Metric Measures

| Symbol | When You Know | Multiply by | To Find | Symbol |
|---|---|---|---|---|
| | | **LENGTH** | | |
| in | inches | *2.5 | centimeters | cm |
| ft | feet | 30 | centimeters | cm |
| yd | yards | 0.9 | meters | m |
| mi | miles | 1.6 | kilometers | km |
| | | **AREA** | | |
| $in^2$ | square inches | 6.5 | square centimeters | $cm^2$ |
| $ft^2$ | square feet | 0.09 | square meters | $m^2$ |
| $yd^2$ | square yards | 0.8 | square meters | $m^2$ |
| $mi^2$ | square miles | 2.6 | square kilometers | $km^2$ |
| | acres | 0.4 | hectares | ha |
| | | **MASS (weight)** | | |
| oz | ounces | 28 | grams | g |
| lb | pounds | 0.45 | kilograms | kg |
| | short tons (2000 lb) | 0.9 | tonnes | t |
| | | **VOLUME** | | |
| tsp | teaspoons | 5 | milliliters | ml |
| Tbsp | tablespoons | 15 | milliliters | ml |
| fl oz | fluid ounces | 30 | milliliters | ml |
| c | cups | 0.24 | liters | l |
| pt | pints | 0.47 | liters | l |
| qt | quarts | 0.95 | liters | l |
| gal | gallons | 3.8 | liters | l |
| $ft^3$ | cubic feet | 0.03 | cubic meters | $m^3$ |
| $yd^3$ | cubic yards | 0.76 | cubic meters | $m^3$ |
| | | **TEMPERATURE (exact)** | | |
| °F | Fahrenheit temperature | 5/9 (after subtracting 32) | Celsius temperature | °C |

*1 in ≡ 2.54 (exactly). For other exact conversions and more detailed tables, see NBS Misc. Publ. 286, Units of Weights and Measures, Price $2.25, SD Catalog No. C13.10:286.


## Approximate Conversions from Metric Measures

| Symbol | When You Know | Multiply by | To Find | Symbol |
|---|---|---|---|---|
| | | **LENGTH** | | |
| mm | millimeters | 0.04 | inches | in |
| cm | centimeters | 0.4 | inches | in |
| m | meters | 3.3 | feet | ft |
| m | meters | 1.1 | yards | yd |
| km | kilometers | 0.6 | miles | mi |
| | | **AREA** | | |
| $cm^2$ | square centimeters | 0.16 | square inches | $in^2$ |
| $m^2$ | square meters | 1.2 | square yards | $yd^2$ |
| $km^2$ | square kilometers | 0.4 | square miles | $mi^2$ |
| ha | hectares (10,000 $m^2$) | 2.5 | acres | |
| | | **MASS (weight)** | | |
| g | grams | 0.035 | ounces | oz |
| kg | kilograms | 2.2 | pounds | lb |
| t | tonnes (1000 kg) | 1.1 | short tons | |
| | | **VOLUME** | | |
| ml | milliliters | 0.03 | fluid ounces | fl oz |
| l | liters | 2.1 | pints | pt |
| l | liters | 1.06 | quarts | qt |
| l | liters | 0.26 | gallons | gal |
| $m^3$ | cubic meters | 35 | cubic feet | $ft^3$ |
| $m^3$ | cubic meters | 1.3 | cubic yards | $yd^3$ |
| | | **TEMPERATURE (exact)** | | |
| °C | Celsius temperature | 9/5 (then add 32) | Fahrenheit temperature | °F |

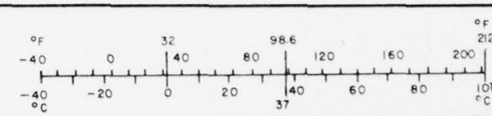

## DISTRIBUTION FOR MERADCOM REPORT 2212

| No. Copies | Addressee |
|---|---|
| | **Department of Defense** |
| 1 | Director, Technical Information<br>Defense Advanced Research<br>Projects Agency<br>1400 Wilson Blvd<br>Arlington, VA 22209 |
| 12 | Defense Documentation Center<br>Cameron Station<br>Alexandria, VA 22314 |
| | **Department of the Army** |
| 1 | Commander, HQ TRADOC<br>ATTN: ATEN-ME<br>Fort Monroe, VA 23651 |
| 1 | HQDA (DAMA-AOA-M)<br>Washington, DC 20310 |
| 1 | HQDA (DAEN-RDL)<br>Washington, DC 20314 |
| 1 | HQDA (DAEN-MCE-D)<br>Washington, DC 20314 |
| 1 | Chief, Engineer Division<br>DCSLOG<br>ATTN: AFKC-LG-E<br>HQ Sixth US Army<br>Presidio of San Francisco, CA<br>94129 |
| 1 | Director<br>Army Materials and Mechanics<br>Research Center<br>ATTN: DRXMR-STL<br>Technical Library<br>Watertown, PA 02172 |
| 1 | U.S. Army Ballistic Res Labs<br>Technical Library<br>ATTN: DRXBR-LB (Bldg 305)<br>Aberdeen Proving Ground, MD<br>21005 |
| 1 | Commander<br>Edgewood Arsenal<br>ATTN: SAREA-TS-L<br>Aberdeen Proving Ground, MD<br>21010 |
| 1 | Director<br>US Army Materiel Systems Analysis<br>Agency<br>ATTN: DRXSY-CM<br>Aberdeen Proving Ground, MD<br>21005 |
| 1 | Director<br>US Army Engineer Waterways<br>Experiment Station<br>ATTN: Chief, Library Branch<br>Tech Information Center<br>Vicksburg, MS 39180 |
| 1 | Commander<br>Picatinny Arsenal<br>ATTN: SARPA-TS-S No. 59<br>Dover, NJ 07801 |
| 1 | Commander<br>US Army Troop Support & Aviation<br>Materiel Readiness Command<br>ATTN: DRSTS-KTE<br>4300 Goodfellow Blvd.<br>St. Louis, MO 63120 |
| 2 | Director<br>Petrol & Fld Svc Dept<br>US Army Quartermaster School<br>Fort Lee, VA 23801 |
| 2 | Engineer Representative<br>US Army Standardization Group, UK<br>Box 65, FPO New York 09510 |
| 1 | Learning Resources Center<br>US Army Engineer School<br>Bldg 270<br>Fort Belvoir, VA 22060 |
| 1 | Commandant<br>US Army Command and General<br>Staff College<br>ATTN: ATSW-RI-L<br>Fort Leavenworth, KS 66027 |
| 1 | Commander and Director<br>USAFESA<br>ATTN: FESA-RTD<br>Fort Belvoir, VA 22060 |

| No. Copies | Addressee |
|---|---|
| | **MERADCOM** |
| 1 | Commander, DRDME-Z<br>Tech Dir, DRDME-ZT<br>Assoc Tech Dir/R&D, DRDME-ZN<br>Assoc Tech Dir/Engrg & Acq, DRDME-ZE<br>Special Asst/Matl Assess, DRDME-ZG<br>Special Asst/Tech Assess, DRDME-ZK<br>CIRCULATE |
| 1 | Chief, Countermine Lab, DRDME-N<br>Chief, Elec Power Lab, DRDME-E<br>Chief, Cam & Topo Lab, DRDME-R<br>Chief, Mar & Br Lab, DRDME-M<br>Chief, Mech & Constr Eqpt Lab, DRDME-H<br>Chief, Counter Intrusion Lab, DRDME-X<br>Director, Product Assur & Testing Directorate, DRDME-T<br>Chief, Material Tech Lab, DRDME-V<br>CIRCULATE |
| 10 | Energy & Water Resources Lab, DRDME-G |
| 50 | Sanitary Sciences Div, DRDME-GS |
| 3 | Tech Reports Ofc, DRDME-WP |
| 3 | Security Ofc, DRDME-S |
| 2 | Tech Library, DRDME-WC |
| 1 | Plans, Programs, & Operations Ofc, DRDME-U |
| 1 | Public Affairs Ofc, DRDME-I |
| 1 | Office of Chief Counsel, DRDME-L |
| | **Department of the Navy** |
| 1 | Director, Physics Program (421)<br>Office of Naval Research<br>Arlington, VA 22217 |
| 1 | Director<br>Naval Research Laboratory<br>ATTN: Code 2627<br>Washington, DC 20375 |
| 1 | Commander, Naval Facilities Engineering Command<br>Department of the Navy<br>ATTN: Code 032-A<br>200 Stovall St.<br>Alexandria, VA 22332 |
| 1 | US Naval Oceanographic Office<br>Library (Code 1600)<br>Washington, DC 20373 |
| 1 | Officer-in-Charge (Code L31)<br>Civil Engineering Laboratory<br>Naval Construction Battalion Center<br>Port Hueneme, CA 93043 |
| | **Department of the Air Force** |
| 1 | HQ USAF/RDPS (Mr. Allan Eaffy)<br>Washington, DC 20330 |
| 1 | Mr. William J. Engle<br>Chief, Utilities Branch<br>HQ USAF/PREEU<br>Washington, DC 20332 |
| 1 | AFSC/INJ<br>Andrews AFB, MD 20334 |
| 1 | AFCEC/XR/21<br>Tyndall AFB, FL 32401 |
| 1 | HQ USAF/PREES<br>ATTN: Mr. Edwin B. Mixon<br>Bolling AFB–Bldg 626<br>Washington, DC 20332 |
| 1 | AFAPL/SFL<br>Wright-Patterson AFB, OH 45433 |
| 1 | Department of Transportation<br>Library, FOB 10A, TAD-494.6<br>800 Independence Ave., SW<br>Washington, DC 20591 |
| | **Others** |
| 1 | Professor Raymond R. Fox<br>School of Engineering and Applied Science<br>The George Washington University<br>Washington, DC 20052 |